SODIUM GRAPHITE REACTORS

by

CHAUNCEY STARR

and

ROBERT W. DICKINSON

Atomics International

A Division of North American Aviation, Inc.

PREPARED UNDER CONTRACT WITH THE
UNITED STATES ATOMIC ENERGY COMMISSION

ADDISON-WESLEY PUBLISHING COMPANY, INC.

READING, MASSACHUSETTS, U.S.A.

Printed in the United States of America

Library of Congress Catalog Card No. 58–12598

First printing, September 1958

FOREWORD

The information presented in this book is the result of work performed by many people associated with the Atomics International Division of North American Aviation, Inc. over the past ten years. Successful culmination of these efforts in the design, construction, and operation of the SRE has demonstrated the Sodium Graphite Reactor concept, using slightly enriched fuel, to be a sound one. At the same time, as with any experimental program to develop a new concept, areas of technical improvement have been pointed out during each stage of development. Some of these areas could be exploited in the SRE, but construction schedules necessitated deferring development areas of less critical importance. The contents of this book describe a basically successful operation, but a conscientious effort has been made to describe both the pitfalls encountered and areas remaining to be developed further in the perfection of Sodium Graphite Reactor Systems. This candid treatment is intended to be an aid to those concerned with reactor technology in general and Sodium Graphite reactors in particular.

The future of this reactor system appears bright because of its ability to produce high-quality steam at costs which appear reasonable, since additional development based on the experience noted in this book can do little but reduce costs. A note of caution is worth while in examining the economics of this reactor system as well as those of any reactor system which has not yet been operated on a full scale for a considerable length of time. Predictions based on pilot plants are superior to those generated by abstract studies, but should still wait for final verification on performance of the final product. A large SGR is now being designed for construction for the AEC by Atomics International and its collaborators; this plant is a significant milestone along an often difficult but always promising road of development.

It is the earnest hope of all the contributors to this book that its contents may prove valuable to those devoted to the generation of electric power for peaceful purposes from nuclear energy.

Canoga Park, California — C. Starr
May, 1958

PREFACE

In the preparation of this book, which represents the result of work performed by Atomics International, its subcontractors, and cooperating business and Government organizations, the authors reviewed a considerable volume of technical information generated by many scientists and engineers during the past decade. However, it was the sole responsibility of the authors to evaluate and select significant data for this book and to organize and present it to the reader.

The references, which include most of the reports reviewed by the authors, constitute a large body of additional information. The Atomic Energy Reports listed as references are available for inspection at the Commission's depository libraries in the United States and abroad and are sold by the Office of Technical Services, U. S. Department of Commerce, Washington 25, D. C.

A large number of the staff at Atomics International gave valuable assistance in the preparation of this book, including J. E. Burress, V. R. DeMaria, L. E. Glasgow, B. H. Hayward, D. H. Johnson, J. E. Owens and W. J. Sanders. We take this means of gratefully acknowledging the efforts of these and the many others. In addition, we express our appreciation to those who represented the U. S. Atomic Energy Commission's Industrial Information Branch, Technical Information Service: Charles D. McKereghan, who was book project officer, Dewitt O. Myatt, who guided the styling of the illustrations; and James R. Aswell and Jefferson D. Bates, who reviewed the manuscript editorially. The Technical Information Services Extension at Oak Ridge, Tennessee, put the references in final form.

Canoga Park, California
June, 1958

Chauncey Starr
Robert W. Dickinson

CONTENTS

CHAPTER 1

SODIUM GRAPHITE REACTORS AND THEIR IMPORTANCE TO THE NUCLEAR INDUSTRY

1–1. Background

In 1949, North American Aviation, Inc. (NAA), under an Atomic Energy Commission contract, initiated the concept of the sodium graphite reactor with a study of various fuel, moderator, and coolant combinations for a reactor which would produce plutonium at minimum cost, and utilize materials and technology used to at least some degree in American industry.

Natural uranium systems were first investigated under this program, but it was found (1950) that use of fuel slightly enriched in U^{235} significantly improved performance. This study indicated that both plutonium and useful electric power could be produced by a thermal, heterogeneous reactor with low enrichment uranium metal as fuel, graphite as moderator, and liquid sodium as coolant. This system was investigated further by NAA, and a more detailed design and engineering study of several promising configurations was initiated. As this study was completed, emphasis on reactor systems in the United States shifted from dual-purpose plutonium producers to reactors for power only. The previous work on the Sodium Graphite Reactor (SGR) systems was reviewed by NAA in the light of this new development, and the SGR appeared attractive for this single objective also.

The reactor configuration decided upon by NAA, during 1952, as best suited for the initial effort in this direction was a single-pass, sodium-cooled reactor with hexagonal graphite *logs* canned in zirconium. Fuel, selected on the basis of the best metallurgical information available in 1953, was unalloyed alpha-rolled, beta heat-treated, metallic uranium slugs enriched to 2.778 a/o (atom percent) U^{235}. Coolant channels were placed in the center of the graphite logs for convenient fabrication. This design was accepted by the Atomic Energy Commission as part of the original five-year reactor development program, and in June of 1954 a joint effort between NAA and the AEC was initiated. Intensive design of the Sodium Reactor Experiment (SRE) was started at that time and in April of 1955 actual construction of the plant began.

Design of the SRE was influenced by two main considerations: (1) desire for a large amount of instrumentation throughout the plant to provide as

complete a record of operating characteristics as possible, and (2) the use of either standard equipment or adaptions of standard equipment wherever possible, to minimize cost.

Major technology development programs included investigations of sodium, graphite, cladding materials, and fuel elements. Component development was limited chiefly to modifying commercial equipment for use in sodium systems. The technology of sodium and of materials in contact with sodium developed by military and civilian sodium-cooled reactor programs was followed closely during the course of design and construction of the SRE. Developments in these programs were incorporated wherever possible. No extensive work was undertaken on the chemistry or thermodynamics of sodium, since efforts along these lines were in progress at other laboratories during the construction period. Materials technology was taken directly from these other programs, since time did not permit extensive investigation of corrosion, erosion, or compatibility of construction materials prior to their selection and fabrication in the SRE.

Initially the SRE was planned solely as an experimental installation, and no effort was made to utilize the power it would produce. Instead, an air-blast heat exchanger was installed to dissipate the 20 Mw of heat generated at full power. Later, in April 1956, the Southern California Edison Company offered to install a steam generator and turbine system, and at present either means of absorbing the reactor heat can be used.

Construction of the SRE was completed in the latter part of February 1957, and the ambient subcritical experiment, without sodium in the core, was performed on March 23, 1957. It should be noted that this initial measurement of the SRE also corresponded to the first criticality experiment, since the nuclear design of this reactor was not fully confirmed in a critical assembly mockup at any time. It was recognized that a critical experiment was most desirable, but neither time nor facilities had been available for performing this experiment. Some confirmation of nuclear design had, however, been derived from exponential experiments using an aqueous homogeneous low-power reactor as a neutron source. This experimental information was integrated into the nuclear design.

The reactor was filled with sodium shortly after the dry subcritical experiment had been completed, and on April 25, 1957, the SRE was brought to criticality with 350°F sodium in the core. Experimental physics measurements to check out reactor characteristics against calculated and predicted behavior then continued at low reactor power until July 12, 1957. At the completion of the low-power experiments, reactor power was increased and steam was generated in the Southern California Edison Facility. At this time, an electrical power output of 2000 kw was produced from about 8 Mw reactor power (40 percent full design thermal

power) and the reactor was operated intermittently at this maximum level for the remainder of the year.

Instrumentation installed throughout the reactor and heat-transfer system permitted excellent measurement of temperature distributions under both steady-state and fast transient conditions. One item of engineering importance, the free convection flow of the reactor coolant, was difficult to calculate during the reactor design period. Temperature and flow instrumentation during power operation indicated that free convection flow of sodium was excessive, and was causing an undesirably fast rate of cooling in certain parts of the reactor and system following a quick shutdown from full power (scram). This rapid cooling would have caused thermal stresses in the area of the core tank nozzles to rise to several times the yield strength of the materials if the reactor were scrammed from full power. Excessive stresses did not occur during either steady-state operation or moderate changes in power, but took place during fast shutdown from full temperature gradient. Power was therefore limited to that available from the maximum permissible temperature gradient from which the reactor could be safely scrammed.

A rapid means of post-scram flow control had not been built into the reactor system, and it was therefore considered desirable to install some form of flow control prior to operating the reactor at full temperature gradient. Eddy-current brakes were designed and installed on the cold legs of the primary and secondary system. Post-scram convection flow could thus be matched to the rate of power decay by energizing these sodium flow brakes, alleviating overcooling and resultant thermal stress problems.

Several other minor engineering changes were made between January and April 1958. The reactor was brought to full power in early May 1958.

The graphite research program, which antedated SRE design and is still being pursued, was continued throughout the design period. The major concerns of this program were thermal conductivity changes, stored energy release, gas evolution, and sodium permeability of reactor-grade graphite. This program, carried out in cooperation with other reactor graphite programs, indicated (1) that graphite should be separated from sodium, although no serious damage other than reactor poisoning should be expected in event of a can rupture, (2) that stored energy release should not be a problem, and (3) that thermal conductivity could be expected to decline somewhat during irradiation.

Unalloyed zirconium was employed for moderator cladding because Zircaloy was not then available. A research program was immediately instituted to determine the suitability of zirconium under reactor operating conditions. Experiments showed a zirconium grain growth above 950°F, indicating that coolant temperature should be held below this

figure so long as the present moderator cans are in use. This grain growth, which tends to decrease the fatigue strength of zirconium, was not indicated, however, in Zircaloy-2 at temperatures below 1200°F.

Oxygen embrittlement of zirconium at high temperatures also appeared to be a problem. Therefore, during construction of the SRE, it was decided that cold trapping was not sufficient to reduce oxygen to an acceptable level for high-temperature operation, and hot traps were designed and installed to reduce oxygen to a negligible concentration. Concurrent studies of carburization of zirconium in contact with graphite in the absence of an electrolyte indicated that no significant problem existed from this source.

Fuel element research and development was conducted in parallel with design and construction of the plant. Fabricating techniques for the selected fuel elements were developed, and capsule irradiations of specimen fuel materials were carried out. Results of these experiments, in accord with those at other installations, indicated that due to swelling, metallic uranium was less than an ideal high-temperature reactor fuel. Consequently, development of improved fuels was begun, with the result that a thorium-uranium alloy fuel showing promise of higher performance will be ready for use in the SRE at the first indication of serious deterioration of the metallic uranium fuel elements.

In June of 1957 the scope of the SGR Program was increased beyond the construction of the SRE. This expanded program includes increased experimental studies of fuels and construction materials, and provides the means for applying information gained from the SRE and its associated programs to large-scale sodium graphite reactor systems, such as the 75,000 kw electrical plant now under design for the Consumers Public Power District of Nebraska.

The primary objective of the advanced SGR program is to produce cheaper and more reliable electric power, and all studies undertaken are examined from this viewpoint. Current efforts include the investigation of less expensive construction metals for sodium systems, e.g., the use of low-alloy ferritic steels rather than the austenitic types now employed. In addition, system simplifications are being developed by analysis, model test, and full-scale component test, in order to ease the problems of thermal stress associated with the excellent heat-transfer properties of liquid metal.

High-temperature fuels are being investigated and developed in the advanced program in order to overcome the difficulties now known to be associated with unalloyed metallic uranium fuel. The first of these fuels to be given an extensive operational trial in the SRE is an alloy of 7.6 w/o (weight percent) highly enriched uranium in thorium. Irradiation experiments have indicated that this fuel has properties superior to metallic uranium, and irradiations of greater than 3500 Mwd/t are expected. It

should be pointed out that the 7.6 w/o of uranium in this SRE fuel alloy is not the optimum for a sodium graphite reactor; in fact it is probably considerably higher than the optimum percentage if a lattice specifically designed for this fuel were used. The weight percent of uranium was set by the necessity for inserting this fuel into a graphite lattice which was originally designed for uranium metal fuel. Irradiation of this loading, which will commence in December 1958, will give statistically significant information on the behavior of thorium-uranium under actual reactor conditions, and postirradiation examination of this fuel will provide large-scale experimental information on the breeding and conversion possibilities of the Th-U^{235} cycle. It is not expected that this SRE fuel load will breed, because of the less-than-optimum lattice parameters, but information gained can be readily converted to optimum configurations.

Oxide and carbide fuels have been fabricated for experimental SRE fuel assemblies. Irradiation of these and of hollow rods of alloyed uranium is proceeding.

Control and safety device mechanisms and schemes are under continuing development, not only to improve reliability but also to take increasing advantage of the inherent flexibility of the SGR concept by speeding refueling. These efforts are aimed at eventually producing a smooth reactor face, with no control mechanisms projecting. This would simplify refueling and perhaps eventually permit refueling through the top shield while the reactor is at power.

Experiments with the SRE indicate that all routine sodium graphite reactor core maintenance operations, such as replacement of coolant channel orifice plates, inspection and repair of radioactive control mechanisms, and external examination of fuel clusters, may be made without using a full-scale, expensive, hot cell. This has been achieved by constructing simple shielding and manipulator assemblies to be used in conjunction with fuel and moderator-can handling casks. Eliminating the hot cell as a necessary adjunct of reactor operations represents a considerable savings. Hot cells will, of course, continue to be required for experimental work.

Alternate core configurations, leading to lower initial capital costs and increased neutron economy, are being designed. One of these, the Calandria Concept, in which graphite is contained in a single low-cost container rather than in many individual cans, is under construction (Article 8-3.2). It offers significantly improved neutron economy, and allows fuel enrichments as low as 1½ percent to be used in sodium graphite reactor configurations. It is planned to install such a core in the SRE sometime in 1960, when all possible useful engineering information has been gained from the current canned moderator installation.

Development work in sodium-heated steam generators, which have been

a source of some difficulty in other reactor programs, is continuing (Section 1–3, this chapter). Configuration and materials experience gained in this field is being applied in both model and large-scale tests, which use the SRE as a heat source at power levels up to 20 Mw.

Continued operation of the SRE as an experimental core, along with advanced studies now in progress, indicates that the sodium graphite reactor is an important and valuable concept for large, economical, reliable plants where high performance of both reactor and steam systems is necessary.

1–2. Technological Aspects of Sodium Graphite Reactors

1–2.1 Advantages. The aim of every power reactor system is, of course, to provide electricity as economically as possible. The sodium graphite reactor system has some unique characteristics which lend themselves to the reduction of capital and operating costs.

First among these is the ability to provide steam at the same conditions now used in modern, efficient, conventional-fuel steam plants. The sodium coolant is liquid from 208° to 1630°F, thus providing a wide operating range of temperatures without requiring system pressurization. Availability of high coolant temperatures permits generation of steam in the thousand degree temperature range, at any pressure found economically desirable. Thus, efficient turbine machinery of current design can be used, which results in reduction of capital costs by eliminating the need for financing the design of a special steam turbine for unique conditions. Properly designed turbo-generator plants with a thermal efficiency approaching 40 percent are possible with current steam technology. This high thermal efficiency serves to reduce both capital costs, and also operating costs, since smaller amounts of uranium are burned to produce a megawatt-hour of electricity. In addition, the high efficiency further reduces operating costs by increasing the operating lifetime of a given fuel loading. The reflection of this increased irradiation time in reduced operating cost is obvious.

Second, sodium, uranium, graphite, zirconium, and steel are all chemically compatible and no violent chemical reactions between fuel, cladding, moderator, or coolant are conceivable. Provided proper precautions are taken during plant design to exclude water from the vicinity of the sodium-bearing system, there has been no incident yet conceived which could cause an accident requiring a pressure-containing building. The heat capacity of sodium graphite systems, combined with the high boiling point of sodium, limits any accident to one which is easily contained within the core vessel and piping galleries themselves, thus obviating the need for large, expensive pressure containers for the entire system.

Third, the wide temperature range in which sodium is liquid also contributes to the relative simplicity of many components of the reactor and system. System pressures of less than 100 psi are usual; therefore heavy-walled vessels are unnecessary. Difficulties associated with fabricating extremely thick-walled components which must be both structurally sound and mechanically precise are avoided. Molten sodium may be handled as a common, low-pressure heat-transfer fluid except for its induced radioactivity (in primary systems only) and its chemical reactivity with oxygen-bearing compounds. Problems of pump cavitation are minimized by the relatively low vapor pressure of sodium. The liquid metal may be readily pumped either mechanically or electromagnetically, depending on the particular situation and system economics involved.

The low-pressure aspect also permits a gratifying degree of flexibility. High pressure seals are not required, and therefore conventional, industrial-type seals perform satisfactorily and permit easy fuel changes. It has been proven feasible to change a fuel element in the SRE in less than two hours from start to finish of the operation. Improvements in this time could be made with equipment especially designed for refueling purposes only. The fuel-handling equipment for the SRE is designed to perform experimental functions as well as fuel handling, and is more complicated than a single-purpose machine. The low-pressure system also permits varied and complete core instrumentation, since the penetration of pressure boundaries is relatively simple. For example, all fuel elements in the SRE are provided with thermocouples, in order to determine power generation at any desired point. In addition, orifice plates attached to fuel elements may be changed readily to optimize coolant flow in each channel as determined by core instrumentation.

The low-pressure system, which allows the use of core thimbles within which control and safety mechanisms may operate without concern for the effects of a flowing coolant stream, also permits full advantage to be taken of reliable forces such as gravity to operate safety rods. The problems associated with contamination of the coolant stream through corrosion of control-rod absorber materials are eliminated, and thimbles may be replaced at will during periods of reactor shutdown.

Fourth, in company with most liquid metals, sodium has a low Prandtl number. The film heat-transfer coefficients attainable with modest fluid velocities, combined with the wide liquid range, permit large temperature rises and drops through reactor and heat-transfer equipment. The specific heat of sodium is such that large coolant flows are unnecessary. The relatively low-flow, high-temperature-rise system significantly reduces the internal load on the final electric generating plant because of the relatively low pumping power required.

Sodium is compatible with ordinary structural materials, and the

fabrication problems of these systems are not too acute. Low-alloy steels appear satisfactory as system materials, and their application is limited only by strength characteristics at operating temperatures. Austenitic steels are used in the system to give high-temperature strength rather than to resist corrosion. At present no special metallurgy is necessary for sodium-cooled systems. However, any advance in the metallurgy of low-alloy steels which raises softening temperatures to about 1200°F will be considered in the design and fabrication of future sodium systems.

Finally, sodium graphite reactors are inherently stable, because of the negative characteristic of the prompt temperature coefficient associated with fuel. A "power" temperature coefficient of reactivity is positive, however, because of longer time constant effects in the graphite moderator. The time constant associated with the strongly negative fuel coefficient is of the order of seconds, while the time constant of the positive coefficient associated with the moderator is of the order of many minutes. The slow positive coefficient is actually an advantage, since less control is needed to compensate for the reactivity of a cold reactor. It is encouraging to observe the slow insertion of a control rod as a sodium graphite reactor is brought to full power and temperature, indicating the additional reactivity available for fuel burnup and equilibrium poison compensation. The relatively rapid transients associated with changes in power demand are easily and, in fact, automatically taken care of by the fast negative temperature coefficient of the fuel. From the standpoint of control, the SRE has proved to be an exceptionally flexible and stable reactor.

1–2.2 Disadvantages. The disadvantages of the sodium graphite system must also be considered. Since sodium is chemically reactive with both air and water, it requires an inert atmosphere wherever it comes into contact with a gas, either inside or outside the reactor system. Stringent (and usually expensive) measures must be taken to reduce the possibility of contact between water and sodium where steam is generated. Also, the 15-hour half-life of sodium-24, and its 2.73-Mev gamma make a sodium heat-transfer system inaccessible for immediate maintenance when sodium has passed through a nuclear reactor. Because temperature changes can be large and sudden in case of fast power changes and shutdown, and these changes may be rapidly reflected as thermal stresses in system and reactor components, the excellent heat-transfer characteristics of sodium are not an unmixed blessing. However, these high thermal stresses can be adequately handled if proper attention is given to the engineering design of the reactor system.

The choice of graphite as a moderator necessitates some means of separating it from the sodium. Although the two are chemically compatible, sodium will penetrate voids in the graphite and thus introduce a weak

absorber into the moderator, where thermal flux would be expected to be the highest. This is undesirable for nuclear reasons, and therefore the graphite is clad. Zirconium and zirconium alloys are entirely suitable for cladding, since they provide both chemical compatibility and a low thermal neutron absorption cross section. Steel may also be used, provided a proper geometry of the reactor is chosen to minimize the effects of the higher thermal neutron absorption. In any case, these materials will perform satisfactorily and introduce no additional hazards.

The above problems, although restrictive, present no insurmountable engineering barriers to the construction of sodium-cooled reactor power plants. Careful attention to system and component design, and full appreciation of both the advantages and disadvantages of liquid sodium as a coolant, can provide a successful engineering basis for high-performance nuclear power plants. A sodium graphite nuclear power plant can produce steam at costs completely competitive to those of other nuclear power plants and approaching those of conventionally fueled power plants.

1–3. Power Conversion Problems

1–3.1 Steam generators and superheaters. One of the largest single problems that has faced designers and builders of sodium-cooled nuclear power plants, including sodium graphite reactors, is not associated with the reactor itself. The area of difficulty is the steam-generating equipment used to convert the heat contained in sodium to steam of a quality usable in modern steam turbines.

A prime advantage of sodium as a coolant is the possibility of achieving temperatures high enough to produce highly superheated steam; consequently, steam generators for conversion of feed water to superheated steam are of the utmost importance. The history of sodium-heated steam generators has indicated many novel design problems. One steam generator, of rather small capacity, was used successfully on the Experimental Breeder Reactor (EBR-1). This unit, which was extremely large in proportion to its steam-generating capacity, was designed with stainless steel double-walled tube with a copper layer between the walls and a gas tracer leak detection system in the copper layer, and with headers rather than tube sheets. It operated quite successfully over a period of about three years.

Concurrent with this successful operation, sodium-heated steam generator projects were undertaken as military reactor projects, with limited success. Numerous configurations have been proposed and tried, in an attempt to produce satisfactory and reasonably compact steam-generating and superheating units. Unfortunately, designs are inevitably complicated by the necessity for reasonable assurance that sodium and water

will not come in contact in such a fashion as to create either an explosion hazard or corrosion due to the caustic formed in sodium-water reactions.

1–3.2 "Once-through" steam generators. As noted later in Section 7–2, the Southern California Edison Company employs a once-through unit, which is actually a combined feedwater heater, evaporator, and superheater in a single unit. Sodium surrounds double-walled tubes containing water or steam, and mercury, the leak detector fluid, fills the annulus between tubes. This concept has been simplified to some extent in experimental units tested by Atomic Power Development Associates. In their development of equipment for the Enrico Fermi Fast Breeder Power Plant, single-wall tube construction was used, as opposed to the double-wall and mercury intermediate fluid leak detectors of the Edison equipment. The APDA unit of austenitic steel operated satisfactorily for a period of about a year at a thermal capacity of 1 Mw. Some difficulty was encountered on the sodium side of the horizontal unit because of stratification of sodium in temperature layers; thermocouples indicated that steam of different quality was produced by tubes at different elevations. Evidence of similar stratification at moderate power has been observed in the horizontal unit Edison installed at the SRE.

Use of a once-through steam generator requires a rather elaborate water purification system, since most impurities introduced into the steam generator in feedwater remain in the evaporating section. A maximum amount of about $\frac{1}{10}$ ppm total solids, a general feedwater purity requirement, is inherent in once-through boilers generally, and is not restricted to those heated by sodium. The once-through type of steam generator has functioned satisfactorily to date in the SRE with these water conditions, but from this limited experience a prediction of service over an extended period of time is not warranted.

Control of once-through steam generators is quite sensitive because of the small amount of water storage within the unit. Fluctuations in feedwater flow are rapidly reflected back to the reactor, since there is no thermal capacity of the magnitude provided by the steam drum of natural circulation units. In summary, the simplicity of this configuration is attractive, but its long-term performance remains unproven.

1–3.3 Tube-sheet natural circulation units. Several configurations of shell and tube natural circulation steam generators, with separate superheaters, have been constructed during the development of other sodium-cooled reactor systems. Early models were constructed of austenitic stainless steel, were usually of U-tube or bent-tube configuration, and were all of double-wall construction, with either mercury or an inert gas filling the space between inner and outer tubes. The presence of a leak in either boundary was detected by pressure monitoring this "third fluid." Chloride stress corrosion, particularly in crevices between tube and tube sheet, was encountered in these stainless steel units. Feedwater bearing minute quantities (of the order of $\frac{1}{2}$ ppm) of chloride ion and dissolved oxygen found its way into the small annulus formed by the outside of the tube and the tube sheet. Because one face of the tube sheet was invariably at a temperature higher than the saturation temperature of the boiler water, boiling is presumed to have occurred in this annulus, resulting in a concentration of salts which attacked the thin-walled tubing and in some instances the heavier tube sheet. Laboratory tests have indicated that stress levels as low as 5000 psi and oxygen and chloride concentrations as low as $\frac{1}{10}$ ppm are sufficient to initiate stress corrosion cracking in austenitic stainless steels.

In an attempt to overcome stress corrosion cracking, ferritic steel was used as a construction material in an experimental heat exchanger. Accelerated laboratory tests indicated that, from a corrosion standpoint, $2\frac{1}{2}$ chrome-1 molybdenum steel was satisfactory for use in contact with flowing sodium, and this material was selected. In order to reduce stress caused by thermal expansion, the U-tube designs previously employed were replaced by a re-entrant tube type, in which the tubes were restrained at one end only. The double wall and gas tracer leak detection concept was maintained in this design; the outer thimble, which was in contact with sodium on the inner side and water (or steam) on the outer side, contained an inert gas monitoring space. Gas-containing grooves were knurled into the inner tube, and the two tubes then were roller expanded together. This scheme provided a heat-transfer path with 95 percent the efficiency of a single-walled tube of comparable thickness. Crevices between tube and tube sheet were eliminated by an ingenious attachment of the water-side tube to the inner face of the water-side tube sheet in which the tube was butt welded to an upset lip on the inner face of the tube sheet. Inert arc welding by automatic machines produced a weld of very high quality.

This 3-Mw model is being tested in an experimental facility capable of reproducing all anticipated temperature and flow transient conditions. A failure in the superheating section of this unit, caused by a manufacturing error in which overrolling of a tube had eliminated a clearance provided for thermal expansion, occurred after 250 hours of full-power steady-state operation. However, the unit was repaired over a weekend, and operation was resumed immediately.

1–3.4 Header-type natural circulation steam generators. An approach to sodium-heated steam generator design in which abrupt changes in the cross section of structural material in contact with liquid metal were

minimized has been attempted. The equipment was designed so that the cylindrical steam pressure container also serves as a tube sheet, with sodium introduced into the unit from vertical headers external to the vessel. The molten liquid metal is contained in double-walled tubing *pancakes*, which are in turn contained in the cylindrical pressure vessel in which feedwater is evaporated. Inlet and outlet penetrations made through the pressure vessel wall by means of stress-relieving nipples are connected to the external sodium headers. Superheating is accomplished in similarly constructed units, except that steam is contained within double-walled tubing pancakes and the low-pressure, high-temperature sodium flows within the cylindrical outer shell.

This design appears to have considerable merit in overcoming calculated thermal stresses in equipment containing one or more thick tube sheets. The particular unit constructed uses double-walled tubing; the outside tube is $1\frac{1}{4}$ inch OD. Mercury is contained within the annulus between tubes, and is monitored by pressure indicators so that each individual pancake is sensed for leaks either to water or to sodium. Carbon steel is used on the water side of evaporator tubes to minimize possibility of stress corrosion from chloride ion impurities in feed water. Type 347 stainless steel is used for the inner tube, in contact with sodium and mercury. The superheater is all austenitic (Type 347) steel.

This steam generator configuration is not necessarily ideal for central station application, but numerous improvements based on individual plant requirements are conceivable. Chief among these is a replacement of the mercury-filled annulus type of double tube with a gas tracer system contained between double tube walls. This change would eliminate an expensive mercury inventory and expensive manufacturing method. Selection of other materials for both pressure vessels and tubing could be made to suit the temperature and feedwater requirements of a particular system.

A test unit of this type is now installed at the SRE, and performance testing and evaluation is continuing. Cross-sectional drawings of the evaporator section of this unit are pictured in the Sodium-NaK Supplement to the *Liquid Metals Handbook*, 1955.

CHAPTER 2

SODIUM REACTOR EXPERIMENT

2–1. General Description

The SRE, Fig. 2–1, was designed and constructed by Atomics International, a division of North American Aviation, Inc., as part of a program with the Atomic Energy Commission to develop a sodium-cooled, thermal power reactor for civilian application. Construction was largely by subcontract, under the supervision and direction of Atomics International, who also designed and manufactured special components for the SRE, notably the fuel elements, moderator cans, freeze-seal modifications to pumps and valves, cold traps, and some of the nuclear and liquid-metal instruments. The Southern California Edison Company installed and is operating the steam electric power generating plant.

Site location and general descriptions are given in Section 7–2.

The SRE is designed as a flexible experimental facility to take maximum advantage of the benefits of the coolant and moderator chosen. It is a fully thermal reactor; the mean energy of neutrons causing fission is 0.030 ev. A low U^{235} inventory is possible and desirable because of the very slight temperature coefficient of reactivity attendant on the use of a solid moderator. The *equilibrium* temperature coefficient of reactivity in the SRE is slightly positive up to 700°F; at this temperature, the coefficient passes through a node and then becomes slightly negative at higher temperatures. The *prompt* temperature coefficient is always negative, because of Doppler effects in the fuel. At equilibrium, the positive temperature coefficient associated with the moderator comes into play. There is a considerable time delay, however, before equilibrium temperature is reached within the large, solid graphite mass. Operational experience has shown that the slight positive temperature coefficient of reactivity does not make the reactor more difficult to control; actually it eases reactor startup.

2–2. The Reactor

The reactor, Fig. 2–2, is cooled by liquid sodium in the primary loop. Induced Na^{24} activity in the primary loops introduces the need for an intermediate heat exchanger in which reactor heat is transferred to the secondary loop containing nonradioactive sodium. The secondary system dissipates reactor heat either in air-blast heat exchangers or in the steam generator of the Southern California Edison Company's installation.

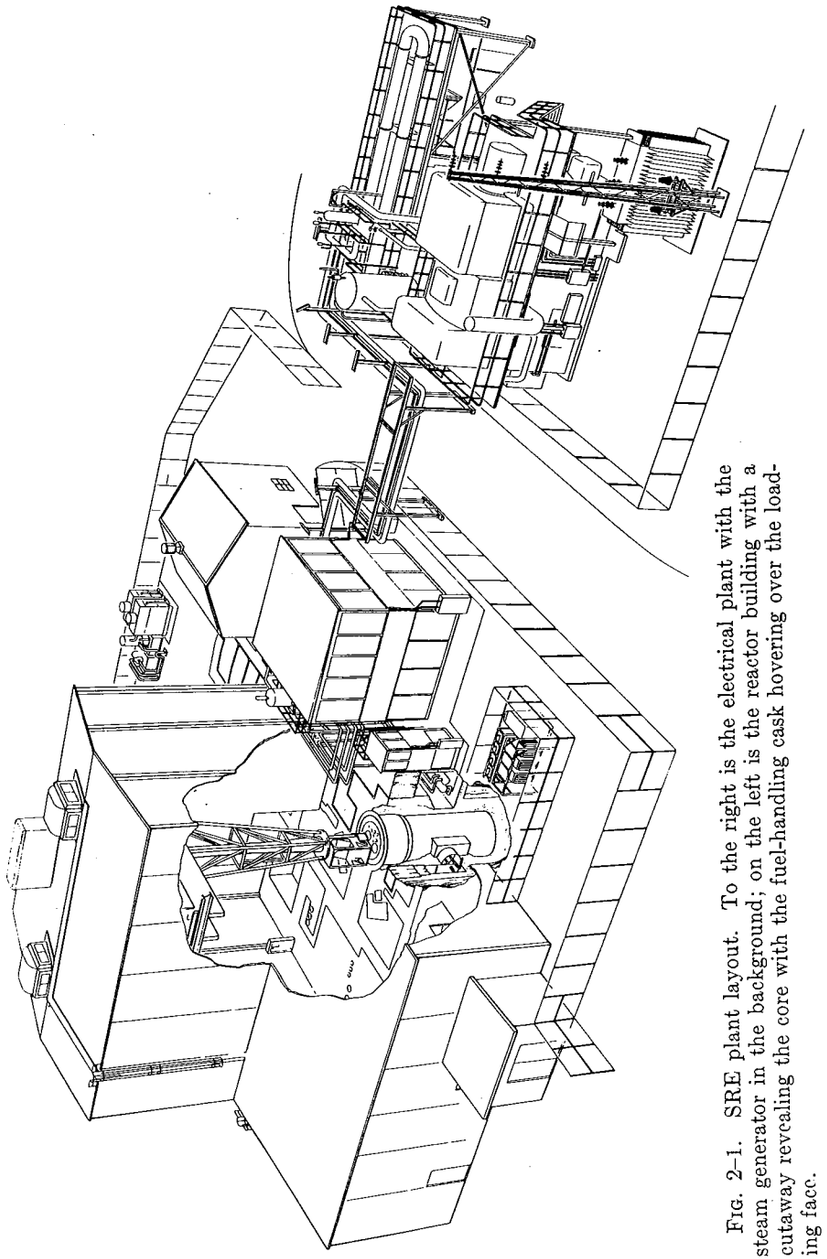

FIG. 2–1. SRE plant layout. To the right is the electrical plant with the steam generator in the background; on the left is the reactor building with a cutaway revealing the core with the fuel-handling cask hovering over the loading face.

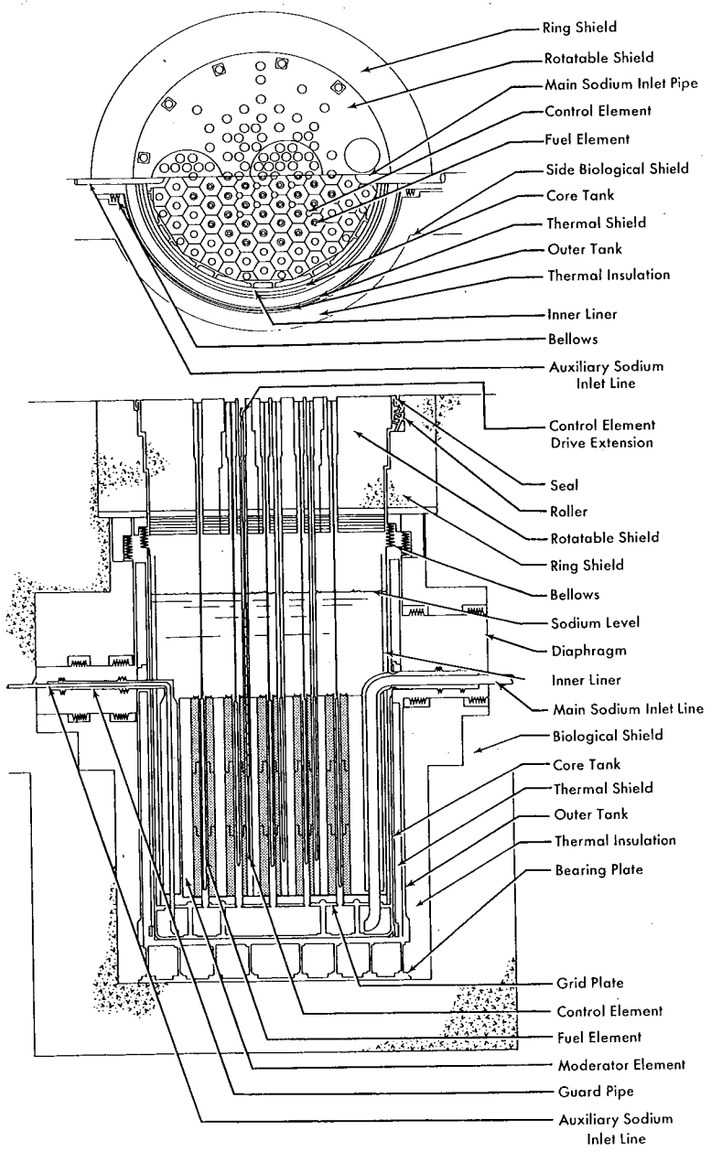

FIG. 2–2. SRE core section and top shield layout with cutaway.

2–2.1 Coolant. Reactor coolant flow is single pass, with sodium flowing up through the core and collecting above it in a top pool maintained at slightly above atmospheric pressure. This pressure prevents cavitation in the suction of circulating pumps which draw heated sodium from the reactor top pool and force it through the heat-transfer apparatus. The entire reactor system is maintained at relatively low pressure; the maximum pressure is 55 psig.

High-temperature characteristics of sodium are exploited by heating it from 500 to 950°F in the reactor, and cooling it from 950 to 500°F in associated heat-transfer apparatus. This high-temperature gradient permits sodium flow to be reduced, thus lessening pumping requirements, but it also increases thermal stress problems. One important objective of the SRE development program is to establish the best means of alleviating thermal stresses created by steady-state and transient power operation.

2–2.2 Moderator and reflector assemblies. The moderator is (National Carbon Company) grade TSP graphite in hexagonal prisms measuring 11 inches across flats. Each prism, 10 feet high, is made up of 3 logs stacked vertically, machined as a unit, and keyed together with cylindrical graphite plugs.

The graphite logs are clad with zirconium sheet 0.035-inch thick at the sides and 0.10-inch thick at top and bottom. The can is completely welded and leaktight. Stainless-steel spacer plates are mechanically fastened to the zirconium cladding at the top and bottom of the elements. The cans are prevented from lateral displacement by a stainless steel grid plate on the bottom of the can area and a clamping ring securing the stainless steel spacer plates at the tops of the cans.

The spacer plates provide bearing surfaces for the clamping ring and bottom support pedestal, but their primary function is to maintain proper clearance for moderator cooling. Clearance is held at an average of 0.170 inch at operating temperature (950°F). Through this gap a by-pass stream of inlet sodium flows, cooling the graphite and assuring a uniform temperature gradient up the can by removing heat generated within the graphite. The 10-foot height of the can includes 6 feet for moderator in the active core section and 2 feet each at the top and bottom of the core section for reflector.

A fuel channel is located in the center of each of the 43 graphite assemblies which make up the core region. Each is a 2.8-inch ID zirconium tube, welded to the zirconium end cladding of the graphite. In addition to these fuel channels, 17 corner channels are provided for control and safety rods and experimental assemblies, as desired. These channels are formed by shaping the corners of selected adjacent cans to form circular passages. The reflector is comprised of other hexagonal graphite assemblies with

dimensions similar to those of the moderator cans. The reflector assemblies contain no central channels and are clad in stainless steel.

2–2.3 Fuel elements. The fuel elements are fabricated in clusters of 7 rods, each consisting of a 6-foot high column of 6-inch uranium slugs in a thin-walled stainless steel jacket tube. The slugs are thermally bonded to the jacket by a mixture of sodium and potassium (NaK). Above the column of slugs is a space containing helium. This gas-filled space allows expansion of the bonding NaK and also serves as a reservoir for any fission gases that may be driven off the surface of the slugs. The 6 outside rods are spirally wrapped with stainless steel wire, which prevents fuel rods from touching each other or the process channel within the moderator can. A locating guide and an orifice plate for controlling sodium flow for each fuel channel are fastened to the bottom of the cluster assembly.

The cluster is supported by a wall hanger tube attached to a stepped shield plug. This shield plug rests in the rotatable top shield when the fuel element is inserted in its process channel. Thermocouple wires can be passed up the hollow center of the hanger rod to indicate temperatures at selected locations along the fuel cluster.

During normal operation, there is a pressure drop of 2.5 psi across the central fuel element and 1.5 psi across its orifice plate. The flow past the central fuel element is 17,500 lb/hr of sodium, at a velocity of 5 ft/sec. Outer fuel clusters are orificed to pass lesser amounts of sodium, in accordance with power generation distribution within the core. This maintains approximately equal temperature of the sodium discharging from each process channel into the top sodium pool.

2–2.4 Control elements. There are four control elements, capable of regulating a total of 7.8 percent reactivity. Each element is contained in a stainless steel thimble assembly extending from the top surface of the rotatable plug to a point just below the active section of the core. This assembly prevents contact between flowing sodium and the poison element which is operated within the thimble.

The poison column of the control element is made up of a series of 18 rings of boron-nickel alloy suspended on a *pull tube*. The boron concentration in the alloy is approximately 2 percent by weight. This poison column is essentially black to thermal neutrons.

The control rods, inserted in the core much of the time the reactor is critical, are cooled by conduction through an atmosphere of helium at 16 psig introduced into the top of the thimble.

Control rod motion is obtained by a ball-nut screw arrangement in which the pull tube is attached to the nut and a drive mechanism (above the top shield) turns the screw. The nut is prevented from rotating by

guides moving in flutes machined on the inside of the heavy wall portion of the thimble above the core. Control rods have dual speed drives that produce 0.29 ft/min motion for shim action, and 3.75 ft/min for regulating action. To avoid removal of a large amount of negative reactivity at any single time the high-speed drives are mechanically limited to a travel range of ±7 inches. The motion-limiting stops can be reset if travel through a different range of insertion is required. The control rods cannot be disengaged or dropped for scram purposes. A detailed description is contained in Article 6–1.3.

2–2.5 Safety elements. Four safety elements may also be inserted in the core. These elements, which can control approximately 5.7 percent reactivity, are contained in thimbles similar to those of the control elements. However, safety elements are operated only by a high-speed drive of 3.75 ft/min for withdrawal, and have a latch mechanism which can release the rod at any time during withdrawal from the core or when in the fully withdrawn (cocked) position. When the latch is disengaged by a scram signal, the poison rod assembly falls freely within the thimble by gravity. The safety rods (not normally inserted in the core during operation) are maintained in a helium atmosphere. Dimensions of the thimble and poison column need not be held closely for heat transfer reasons, as is necessary with the control rods.

2–2.6 Experimental facilities. Six corner channels in the reactor core are available for experimental purposes. Of small diameter ($3\frac{1}{2}$ inches), they extend from the top of the core to the lower sodium plenum and can be used for the full 6-foot height of the active core. Removable plugs in the top shield provide access to these core channels.

Three central channel locations in graphite assemblies are also available, at successively greater radii from the core center. Center channel openings are similar to those of the corner channels except that they do not connect with the lower sodium plenum.

2–2.7 Reactor vessel. The reactor core, consisting of the moderator assembly, fuel rods, and control and safety rods discussed above, is within a stainless steel core tank, 19 feet deep and 11 feet in diameter. A stainless steel liner, supported near midpoint by brackets on the core tank, provides a $2\frac{1}{2}$-inch annulus at the inner surface of the tank. The liner, open at both ends and pierced by the coolant circulating pipes, projects above the upper sodium pool. This liner minimizes thermal stresses up the core tank wall by providing a stagnant sodium layer that reduces the effect of mismatches in the temperature of the flowing sodium.

Surrounding the core tank is a thermal shield composed of a vertical series of 7 low carbon steel rings with interlocking joints. Immediately

outside the thermal shield rings is the outer tank, also fabricated of low-carbon steel. This tank is an emergency means of containing sodium if a leak develops in the core tank. Both the core tank and the outer tank have bellows attached between the top of the tanks and the shield structure directly above them. These bellows allow vertical thermal expansion of the tanks and serve as seals for the inert gas atmosphere maintained between the tanks (for more details see Article 6–1.1).

A cavity liner of low-carbon steel surrounds the outer tank. The annulus between the cavity liner and the outer tank is filled with a 1-foot layer of calcined diatomaceous silica and asbestos thermal insulation under an inert atmosphere. This cavity liner, which prevents ground water from permeating the thermal insulation, is cooled by circulating tetralin through steel pipes located outside the liner.

Four concentric cylinders of low-carbon steel support the flat bottom of the outer tank. These cylinders rest on circular bearing plates which are attached to the bottom of the cavity liner by anchor bolts extending into the concrete foundation.

2–3. Shielding

A 4-foot thick, reinforced-concrete pad poured on a limestone base supports the cavity liner. An annular cylinder of reinforced concrete about 3 feet thick surrounds the cavity liner.

The biological shield at floor level is made of magnetite iron ore aggregate set in concrete. It is a ring-shaped shield supported on a ledge at the top of the cavity liner. The 70-ton ring shield has three steps to prevent radiation streaming. A circular rotatable shield is supported on these steps and a gas seal between the rotatable shield and the ring shield is made by a lip and trough arrangement filled with low-melting-temperature alloy. Both the ring shield and the rotatable shield are of dense concrete (3.7 g/cm^3), $5\frac{1}{2}$ feet thick.

The rotatable top shield is a stainless steel shell filled with magnetite iron ore and dense concrete grout. It weighs approximately 82 tons when all of its internal plugs are in place. Eighty-one small plugs, two 40-inch diameter plugs and one 20-inch diameter plug extend through the shield. The large plugs are located so that any graphite assembly within the core tank can be removed when the shield is rotated to a proper position. The small plugs provide access to the core for hanging fuel rods, control- and safety-rod thimbles, neutron sources, and experimental assemblies. Attached to the underside of the concrete in the top shield is a plate of low-carbon steel whose lower surface is in contact with a layer of lead in which tubing is embedded (through which tetralin coolant circulates). Immediately below the lead is a stainless steel seal plate. The periphery of this

seal plate is welded to the side steel shell of the rotatable shield. Suspended horizontally from this seal plate are thin, stainless steel plates, separated from each other by about $\frac{1}{2}$ inch. These plates serve as a thermal radiation shield and are encased to prevent the formation of sodium frost which might cause a thermal short circuit. The thermal radiation shield volume is vented by a small weep hole. Each plug in the top shield is stepped to prevent radiation streaming, and is filled with concrete and aggregate or lead to provide the same degree of shielding as the rotatable shield.

Five $1\frac{3}{4}$-inch ID radial tubes embedded in the concrete outside the reactor extend from floor level downward, ending just within the cavity liner and below the core center. These tubes contain instruments used to take thermal neutron and gamma flux measurements during reactor startup and power operation.

2–4. The Cooling System

The coolant system, as previously mentioned, is subdivided into a primary and secondary loop to minimize shielding requirements of the radioactive reactor coolant. The primary and secondary systems each have two separate circulating loops, a main loop designed for transferring 20,000 kw of heat and an auxiliary loop for transferring 1000 kw of heat (Fig. 2–3).

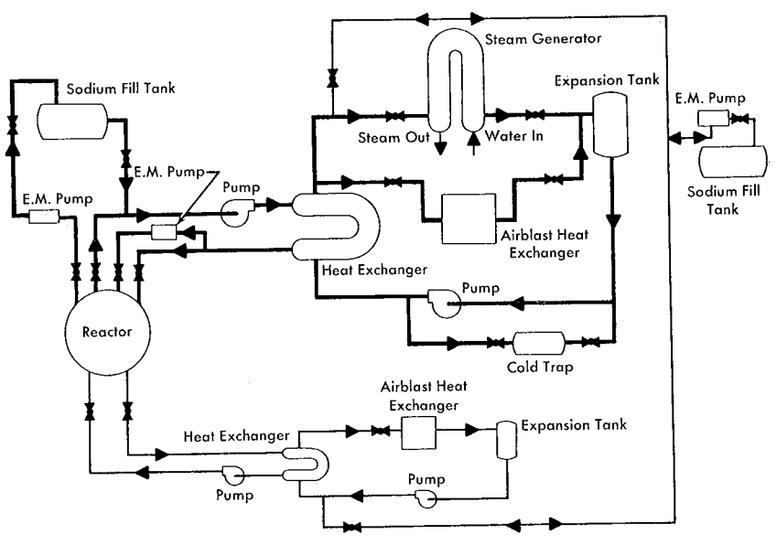

Fig. 2–3. SRE coolant flow diagram.

Sodium flows through 6-inch stainless steel pipe in the main primary and secondary circuits at a velocity of 13 ft/sec. Pressure drop is 15 psi in the primary circuit and 42 psi in the secondary circuit. The auxiliary sodium velocity is $5\frac{1}{2}$ ft/sec through 2-inch stainless piping, with a total pressure drop of 11 psi in the primary loop and 6 psi in the secondary loop. An air-blast heat exchanger is the only means for dissipating heat provided in the auxiliary secondary loop, while the main secondary loop is provided with both an air-blast heat exchanger and a steam generator.

Inlet lines from the main and auxiliary primary coolant loops enter the core tank above the graphite assemblies and extend vertically downward in double-walled, stainless steel pipes into a plenum between the bottom of the core tank and the grid plate. An inert atmosphere is maintained between the walls of the double-walled pipe to prevent excessive heat transfer.

The sodium, at a temperature of 500°F, passes from the lower plenum up through the fuel channels, absorbing heat from the fuel elements, and discharges into an upper pool 6 feet deep at a mixed mean temperature of 950°F. Separate outlet pipes for the main and auxiliary primary loops are located in the core tank above the graphite assemblies.

The coolant pipes are double-walled, with an inert atmosphere in the annulus between pipes, for a distance of about 6 feet outside the reactor core. This prevents gross leakage of sodium if the inner pipe containing sodium should fail.

Bellows are provided around the pipe nozzles at the interface between the cavity liner and the piping gallery. These bellows permit thermal expansion of the piping while maintaining a seal for the inert atmosphere within the tank annulus.

Sodium pumps are modified hot-oil process pumps similar to those used in refinery services. Principal modifications are vertical mounting, and the addition of frozen sodium seals at the pump casing and the pump shaft. The conventional stuffing box around the shaft is replaced with a narrow cooled annulus that provides a continuously shearing film of frozen sodium to seal the impeller space within the pump. Main primary and secondary pumps are driven by electric motors. The main primary pump can deliver 1480 gpm against a 60-foot sodium head. The main secondary pump can deliver 1240 gpm against a 140-foot sodium head. Low-power electric motors serve the two auxiliary pumps. All pumps are controlled at the reactor control station.

Piping and vessels containing sodium are heated by rod and strip heaters. These heaters provide system preheating and keep sodium molten during filling and when reactor heat is not being generated. Thermocouples are attached to piping and vessels to indicate temperatures. Control of heaters, to maintain uniform temperatures, is effected by switch gear located

throughout the reactor building. Temperature readout instruments and automatic controls are located as close as feasible to the associated switch gear. Sodium leak-detecting cable is attached to the underside of piping and vessels and leads to instruments located in the control room. Thermal insulation is strapped to all sodium-containing surfaces. Electrical terminals projecting through the insulation are protected by metal tubes plugged with thermal insulation.

Hot and cold traps maintain sodium oxide content at specified low levels in the sodium cooling systems. The main primary loop has two circulating, disposable-filler hot traps which can be used alternately, and one circulating cold trap. The hot traps are maintained at about 1200°F by electric heaters and employ the principle of *gettering* oxygen on a large area of zirconium foil. Regenerative heat exchangers attached to the hot traps reduce the heat loss in this system. The main secondary and auxiliary primary coolant loops also contain circulating cold traps. The auxiliary secondary loop is fitted with a tetralin-cooled diffusion cold trap because of the low quantity of sodium being circulated.

Twelve small-diameter holes, which can be used for gamma irradiation, open into the main and auxiliary galleries and are fitted with shielding plugs. Four similar openings into the cold trap and sodium service vaults are also available for gamma irradiation.

One-inch pipes, welded into the inlet and discharge lines of the main intermediate heat exchanger, carry sodium to two vertical standpipes. This permits insertion of material samples from the reactor room floor into the standpipes, one normally containing flowing sodium at 500°F and the other flowing sodium at 950°F. The outlets from these two standpipes are connected to the flowing sodium streams through thermal-sleeved, stress-relieving nozzles. Samples of construction materials are inserted into this facility to study corrosion and mass-transfer effects in radioactive flowing sodium under reactor conditions.

Component cooling in the SRE is accomplished by a circulating liquid-tetralin system. Tetralin is used because it has low vapor pressure and is relatively inert to sodium. Cool tetralin is circulated from a reservoir by two parallel, electrically driven process pumps. The returned, heated tetralin is cooled in two evaporative cooler units operated in parallel. Total cooling load can be maintained by either pump and either evaporative cooler. In the event of complete electrical failure, coolant may be circulated by a remote-starting gasoline engine attached to one of the tetralin pumps.

2–5. Fuel Handling

A shielded cask about 35 feet high and weighing approximately 50 tons is used to remove and replace SRE fuel elements. Heat generated in the cask by radioactive fuel elements is removed by a blower system which circulates air between the cask body and the lead biological shield. Mechanical motion within the cask is from externally mounted motors that rotate shafts sealed at the cask wall with lubricated O-rings. Fuel element removal is detailed in Article 6–3.3.

After removal from the reactor, the fuel element is placed in one of three cleaning cells. These cells, which open to the reactor floor, can be flooded with water; the products of reaction between cleaning water and residual sodium are disposed of in the liquid and gas radioactive storage facilities. After cleaning, fuel rods are transported by the cask to storage holes in the reactor floor. A hot cell is located below the reactor floor, and elements can be lowered into the cell directly from the fuel-handling cask through access ports.

2–6. Inert Gas System

An inert gas system, which supplies both helium and nitrogen to the SRE installation, furnishes nonreactive gas blankets for contact with sodium. Helium is supplied to parts of the system requiring direct contact between gas blankets and sodium, and nitrogen is supplied to regions (not normally containing sodium) into which sodium might leak. Individual regulators reduce helium and nitrogen to appropriate pressures throughout the system. These systems are protected by relief valves, and flow is monitored by in-line flow meters. Helium is used in the fuel-handling cask, cleaning and storage facilities, seals for sodium pumps and valves, core tank, and all system components with a free sodium surface. Nitrogen is used to maintain a low oxygen atmosphere in the primary piping galleries and in the cavity containing reactor thermal insulation.

2–7. Waste Disposal System

Operation of the SRE may generate both gaseous and liquid radioactive wastes. Vent lines are connected to the systems containing potentially radioactive gases. These gases are discharged from the building vent line to a stack on the roof of the reactor building. Gases are continuously monitored, and if activity rises above a preset, safe level, the gases are automatically diverted to one of two shielded storage tanks. Gases diverted into the storage tanks are first passed through one of two low-pressure, piston-type compressors to reduce their volume. Compressors and controls are in a shielded vault some distance from the reactor building proper. Radioactivity in gases stems from sodium vapor and impurities in cover gases exposed to a neutron field.

Liquid wastes, generated primarily from washing reactor components that have been in contact with primary coolant, are normally directed to a sump from which they are pumped into one of a series of holdup tanks

for sampling. Highly radioactive wastes are transferred from the holdup tank into shielded storage tanks. Low-activity wastes go to portable, disposable, containers. Controls and valves for the liquid-waste system are manipulated entirely outside the shielding barriers.

Waste-disposal storage facilities are sufficient for normal waste accumulations, but are not sized to accommodate the quantities that a severe reactor incident might generate.

2–8. Emergency Electrical System

There are several sources of emergency power for the SRE if normal electric power fails. The emergency load, which approaches 50 kw, is required to maintain operation of the instrumentation and heat-removal equipment.

Two sets of battery-motor alternators are provided to supply continuous emergency power and are supplied by lead-acid storage batteries rated for one hour at full discharge. In addition, there is a 300-kw diesel-driven alternator that starts automatically on failure of the main electric power.

Operation of the tetralin cooling system is vital to the plant, because pump and valve freeze seals depend on this coolant system for their integrity. Therefore, if all the previously noted standby systems fail to operate, a remote-starting gasoline engine connected to one of the tetralin pumps by belting ensures coolant circulation.

2–9. The Reactor Building

The reactor building is not designed as a containment pressure vessel, since the maximum credible accident would not release enough gas volume to require pressure containment. It is designed, however, to retain gases at about atmospheric pressure, and to reduce diffusion leakage of potentially contaminated gas to a daily rate of not more than 10 percent of building volume. Aside from this, the building is designed simply to provide reactor shelter, office space, and support for a 75-ton bridge crane.

The building is of preformed tilt-up concrete slabs, and the exterior shield is fireproof throughout. Nonradioactive sodium systems, as well as shielded concrete vaults for primary fill tanks and service systems that are not in constant use, are outside the reactor building.

Electricity is supplied by a substation capable of furnishing 1000 kw of electric power. Water, for other than drinking purposes, is supplied from local wells.

2–10. Steam-Electric Facilities

The steam plant is a conventional steam electric installation. A 7500-kw turbine generator is supplied with steam from a once-through, liquid-metal to water steam generator, providing a plant capacity in excess of

rated reactor output. With the exception of the steam generator, the high-purity water conditioning system necessary for the steam generator, and the interconnections between the reactor and the steam plant, all components are conventional (Section 7–2).

As a summary of the general introduction presented in this chapter, a design data table (Table 2–1) provides ready reference to SRE design. Detailed development is discussed in the following chapters.

Table 2–1

Reactor Project Data

Power	
Thermal power	20,000 kw
Electrical power	6000 kw (gross)
Thermal efficiency	28.6% Net
Core heat flux, maximum	340,000 Btu/ft^2·hr
Core heat flux, average	209,000 Btu/ft^2·hr
Core specific power, maximum	340 kw/kg of U^{235}
Core specific power, average	240 kw/kg of U^{235}
Fuel and materials	
Fuel material	Alpha-rolled, beta heat-treated uranium
Percent enrichment	2.778 weight percent
Amount of fuel	3000 kg (for 43 fuel elements)
Geometry of fuel	Cylindrical, 7 rod clusters
Dimensions	2.73 in. diam. by 6 ft long, each rod 0.75 in. diam.
Fuel element spacing	11.0 in. on triangular lattice
No. of rods/cluster	7
No. of clusters	43
No. of fuel channels	43
Fuel element cladding material	Type 304 stainless steel
Cladding thickness	0.010 inch
Fuel bonding material	NaK alloy
Bond thickness	0.010 inch average
Sheath temperature	
Maximum	1000°F
Average	740°F
Fuel temperature	
Maximum	1200°F
Average	750°F
Reactor inventory	83 kg of U^{235} (43 clusters)
Fuel coolant channel material	Zirconium
Diameter	2.80 inches ID
Wall thickness	0.035 inch

(*cont.*)

Fuel consumption	20 g/day
Moderator/reflector	
Material	Graphite (type TSP)
Amount	~45 ton
Operating temperature	550 to 1000°F
Coolant	Sodium
Side shielding	
Material	Low-carbon steel
Arrangement	Rings with interlocking joints
Coolant	Tetralin (outside cavity liner)
Top shielding	
Material	Steel and lead
Arrangement	Flat plates
Coolant	Tetralin (inside top shield plug)
Biological shielding	
Material	Magnetite ore concrete
Arrangement	Cast block
Coolant	Tetralin
Reactor vessel material	Type 304 stainless steel
Fuel loading and unloading system	Lead-shielded, air-cooled, fuel-handling cask, including inert gas system
Heat removal and operating data	
Flow path in core	Upward, once-through
Reactor coolant system	
Number of primary loops	One main and one auxiliary
Coolant	Sodium
Operating pressure	3 psi at free sodium surface in reactor core tank
Design pressure	14 psi
Inlet temperature	500°F
Outlet temperature	950°F
Specific activity	0.32 curie/cc at 20 Mw
Maximum coolant velocity in core	5 ft/sec
Flow rate	1180 gpm
Primary system pressure drop	15 psi main, 11 psi auxiliary
Type of circulation	Forced
Pumping power required	18 kw
Number of pumps	One main, one auxiliary
Pump type	Centrifugal, mechanical
Type of heat exchanger	Shell and tube type, U-tube configuration
Intermediate heat exchange loop	
Coolant	Sodium
Operating pressure	3 psi at free sodium surface in secondary expansion tank
Design pressure	~100 psi

Inlet temperature (at primary loop heat exchanger)	440°F
Outlet temperature (at primary loop heat exchanger)	900°F
Flow rate	1080 gpm
Secondary system pressure drop	42 psi main, 6 psi auxiliary
Type of circulation	Forced
Pumping power required	37 kw
Number of pumps	One main, one auxiliary
Pump type	Centrifugal, mechanical
Type of steam generator	Once-through type, double U-tube with mercury monitoring fluid
Power conversion loop	
Coolant	Water
Operating pressure	600 psig
Design pressure	750 psig
Inlet temperature (steam generator, feed water)	284°F at 6000-kw load
Outlet temperature (steam generator, superheated steam)	825°F
Flow rate	60,000 lb/hr
Degrees superheat	335°F
Source of superheat	Superheater integral with evaporator
System pressure drop	50 psi through steam generator
Turbine inlet temperature	825°F
Turbine inlet pressure	600 psig
Turbine generator	
Type of turbine	Straight condensing, non-reheat
Turbine specifications	7500 kw, 3600 rpm, 13 stage, 2 pt. extraction
Generator specifications	7500 kva, 3600 rpm, 2400/4160 volt 1.0 p.f. air-cooled, with direct connected exciter
Condenser type	2-pass, nondivided water box
Condenser pressure	2 inches mercury absolute
Condenser coolant flow rate	7000 gpm
Type of heat sink	Cooling tower, counterflow, induced draft type
Physics data	
Thermal neutron flux density (in moderator)	
Maximum	6×10^{13} n/cm^2·sec
Average	4×10^{13} n/cm^2·sec
Intermediate neutron flux density	
Maximum	1.5×10^{13}

(*cont.*)

Average	1×10^{13}
Fast neutron flux density	
Maximum	10^{13} n/cm^2·sec
Average	10^{12} n/cm^2·sec
Leakage	Leakage probability = 0.26
Flattening	None
Reactivity balance	
Fuel depletion	0 to 0.4%
Temperature reactivity	
Fuel	−0.2%
Moderator	+0.5 to 1.0%
Xenon and samarium poisoning	−1.9%
Total reactivity to control	3.0%
Control system strength	7.8%
Safety system strength	5.7%
Conversion ratio	0.5 (initial)
Average neutron energy	kT = 0.06 ev
Neutron lifetime	0.50×10^{-3} sec
Principal dimensions	
Core	6 ft high by 6 ft diameter
Reflector	2-ft thickness
Reactor core tank	19 ft high by 11 ft diameter
Height of sodium pool above reflector	$65\frac{7}{8}$ in. at operating temperatures
Side thermal shield	$5\frac{1}{2}$ in. thick in addition to $1\frac{1}{2}$ in. thickness of core tank
Top thermal shield	2 in. of steel and $1\frac{1}{4}$ in. of lead
Top biological shield	$65\frac{7}{16}$ in. of concrete, $1\frac{13}{16}$ in. steel shot, and $\frac{1}{2}$-in. steel plate
Controls and containment	
Controls	
Number of rods	4 control, 4 safety
Shape	Cylindrical
Poison material	Boron-nickel alloy
Location of drive mechanism	Above top biological shield
Type of drive mechanism	Electric motor drive
Operating control method	Automatic flux control and manual
Scram control method	Magnetic latch release
Other safety features	(a) Negative prompt temp. coeff. (b) High heat capacity
Type of containment	Frozen metal seals, O-ring seals
Maximum credible accident	Unrestrained withdrawal of control rods during startup. Result: no release of radioactivity

CHAPTER 3

NUCLEAR AND DESIGN CHARACTERISTICS

3–1. Reactor Physics

The nuclear analysis required in the design of a heterogeneous reactor such as the SRE basically involves the evaluation of cell or module characteristics of the fundamental lattice. A major source of uncertainty in the nuclear characteristics of the SRE lattice was the use of fuel elements that were constructed as seven-rod clusters. The resonance escape probability and the intracell thermal neutron flux distribution could not be accurately predicted for a lattice with this type of fuel element. The nuclear characteristics are best determined by an integrated theoretical and experimental program.

Therefore, exponential experiments were performed to investigate these parameters. The experimentally determined resonance escape probabilities and intracell flux distributions were compared with theoretical calculations based on various constants and models. In addition, experimental values for the critical mass of the SRE as well as values of the uniform temperature coefficient and the control-rod effectiveness were obtained and compared with the theoretical values. These comparisons were used as a guide for the theoretical analysis and all final SRE calculations were performed on a basis consistent with the exponential experiments.

3–1.1 Theory. The method of analysis employed was the standard two-group diffusion theory. Table 3–1 presents the major formulas used to calculate the lattice parameters. For the development and definitions of quantities used reference is made to the book by Glasstone and Edlund, *Elements of Nuclear Reactor Theory* [1].*

The calculation of η is straightforward, because it does not depend on fuel cluster geometry. The cross sections are averaged over the proper Maxwellian neutron spectrum and η obtained directly from the formula in Table 3–1. Most of the remaining quantities, however, depend on fuel cluster geometry, hence special attention is given to this treatment. Figure 3–1 is a diagram of the fuel cluster and lattice cell for the exponential experiment. It is required to calculate each of the lattice parameters for this configuration in a manner consistent with the two-group diffusion theory model.

*See references at the end of the chapter.

TABLE 3–1

TWO-GROUP LATTICE FORMULAS

(1) $$\eta = \frac{\nu\sigma_f(25)}{\sigma_a(25) + (N_{28}/N_{25})\sigma_a(28)},$$

where N_i = number of atoms of the ith species per unit volume.

(2) $$\epsilon = 1 + \frac{(\nu\sigma_f - \sigma_f - \sigma_e)P}{\sigma - (\nu\sigma_f + \sigma_e)P},$$

where P = the first collision probability of fission neutrons in the fuel clusters.

(3) $$p = e^{-1/G},$$

where $$G = \frac{V_m\xi\Sigma_s(\text{mod})}{V_u\Sigma_{\text{res}}} + (E - 1),$$

V_i = volume-fraction of the ith material in a lattice cell,

$$\Sigma_{\text{res}} = N_u\left(\int\sigma_{\text{res}}\frac{dE}{E}\right)_{\text{eff}},$$

$$E - 1 = \frac{\mathcal{K}_m(r_e^2 - r_i^2)}{2r_i}\left[\frac{I_0(\mathcal{K}_m r_i)K_1(\mathcal{K}_m r_e) + K_0(\mathcal{K}_m r_i)I_1(\mathcal{K}_m r_e)}{I_1(\mathcal{K}_m r_e)K_1(\mathcal{K}_m r_i) - K_1(\mathcal{K}_m r_e)I_1(\mathcal{K}_m r_i)}\right].$$

(4) $$f = \frac{\Sigma_a(\text{fuel})V_{\text{fuel}}\bar{\phi}_{\text{fuel}}}{\Sigma_a(\text{fuel})V_{\text{fuel}}\bar{\phi}_{\text{fuel}} + \Sigma_a(\text{mod})V_{\text{mod}}\bar{\phi}_{\text{mod}}},$$

where $\bar{\phi}$ = average thermal neutron flux.

(5) $$\tau = \left[\tau_f - (\tau_f - \tau_{\text{in}})\frac{\sigma_{\text{in}}}{\sigma_{\text{tot}}}P + \frac{D}{\xi\Sigma_s}\ln\frac{1.44}{5kT}\right]\left(\frac{\rho_0}{\rho}\right)^2\frac{1}{V_m(1 - V_0)}.$$

(6) $$L^2 = \frac{1}{3\bar{\Sigma}_a\bar{\Sigma}_{\text{tr}}},$$

$$\bar{\Sigma} = \frac{\sum_i \Sigma_i V_i\bar{\phi}_i}{\sum_i V_i\bar{\phi}_i}$$

r_i = radius of the process tube hole in the moderator.

r_e = outer radius of a moderator cell.

$\mathcal{K}_m$ = inverse diffusion length for resonance neutrons in the moderator.

τ_f = age of fission neutrons to the indium resonance in graphite of density 1.60 g/cm^3.

(*cont.*)

τ_{in} = age of inelastically scattered fission neutrons to the indium resonance.

V_0 = volume-fraction of the lattice cell which is void.

T = moderator temperature in degrees Kelvin.

k = Boltzmann's constant.

All cross sections are averaged over an appropriate neutron energy spectrum.

Fast fission factor. The essential quantity to calculate in consideration of the fast effect, ϵ, is the first collision probability, P. This factor P is defined as the probability that a fission neutron will make a collision within the uranium fuel before escaping into the moderator. For this calculation the fuel is imagined to be a hollow cylinder, centered on the circle of centers of the outer six rods in the fuel clusters, with a cross-sectional area equal to that of all the fuel rods in the cluster. When the fission spectrum cross section and the dimensions are known, P may then be calculated by the usual methods [1]. Although this gives only a rough approximation for P, it should be noted that a highly accurate value is not required because P enters only into terms which are small compared with other more accurately known terms.

Resonance escape probability. The most troublesome quantity to evaluate in regard to the resonance escape probability, p, is the effective resonance integral,

$$\left(\int\sigma_{\text{res}}\frac{dE}{E}\right)_{\text{eff}} = A\left[\frac{1}{F} + \mu\frac{S}{M}\right]\text{barns},$$

where A and μ are experimentally determined parameters that depend on the fuel material but not on geometry. It is assumed that, for low enrichment uranium, the product $A\mu$ is 26 [2]. This fixes the slope of the line asymptotic to a plot of the effective resonance integral versus S/M. The

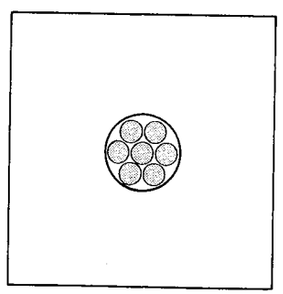

FIG. 3–1. Fuel cluster and lattice cell for the exponential experiments.

coefficient A can thus be treated as a parameter to be determined by a fit to the exponential experiments. The disadvantage factor for resonance neutrons, F, for a rod of radius R, is given by the expression

$$F = \frac{\mathfrak{K}R}{2} \frac{I_0(\mathfrak{K}R)}{I_1(\mathfrak{K}R)},$$

where $\mathfrak{K}$ is the inverse diffusion length for resonance neutrons in the fuel and is taken to be 0.42 cm^{-1} for uranium. The effective radius R is found by imagining a single, solid uranium rod that replaces the fuel element cluster and has a cross-sectional area equal to that of all the fuel rods in the cluster.

The surface-to-mass term, S/M, is evaluated for unit length of the cluster by imagining the surface S to be that described by a rubber band stretched tightly around the fuel rods. The fuel rods are closely packed, so that a straight line drawn through the cluster must intersect uranium at some point. The mean free path for resonance neutrons in the material between the rods is quite long compared with the space between fuel rods. Therefore, a resonance neutron which crosses this surface usually strikes uranium. Hence this "rubber band surface" is a valid one to consider for the cluster.

The excess absorption for resonance neutrons ($E - 1$) depends only on the dimensions of the moderator and the inverse diffusion length $\mathfrak{K}_m$ for resonance neutrons in the moderator. $\mathfrak{K}_m$ is treated as a parameter which is to be determined by a fit to the exponential experiment.

Thermal utilization. Consider next the thermal utilization, f. The cross sections appearing in this formula are Maxwellian averages. The calculation of f is straightforward in the case of the exponential experiments,

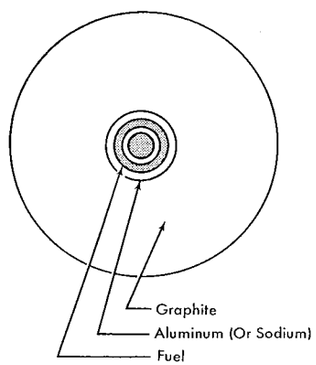

FIG. 3–2. Five-region model of the lattice cell.

since the volume-averaged fluxes, $\bar{\phi}$, are measured directly. For the SRE lattice, however, no experimental measurements were available and a flux calculation was necessary. A one-velocity diffusion theory was applied to the five-region cylinderized model of the lattice cell (Fig. 3–2). The results of these calculations were then empirically adjusted so as to render them consistent with the flux measured in the exponential lattices. The adjusted flux was then used to calculate f.

Migration area. In a completely analogous manner the absorption and transport cross sections were averaged over a lattice cell. The thermal diffusion length, L, was then calculated from these cell-averaged cross sections.

The calculation of the age, τ, is based on the experimentally determined value, τ_f, of 311 cm^2, the age to the 1.44-ev indium resonance for fission neutrons in graphite of density 1.60 g/cm^3. This experimental age is modified by the inclusion of the effects of inelastic scattering in the fuel and additional aging from the indium resonance to thermal energy (taken to be 5 kT, following the work of E. R. Cohen [3]). The age in graphite of inelastically scattered neutrons to the indium resonance, τ_{in}, 221 cm^2, was obtained from a separate calculation [4]. Corrections for graphite density, moderator, and void volume fractions are then applied to the modified age.

3–1.2 Exponential experiments. The exponential experiments were conducted in an assembly consisting of large vertical graphite stringers with suitable vertical holes for insertion of the fuel elements. A water boiler reactor, located below the assembly, was used as a source of neutrons for the experiments. Figure 3–3 shows the composite arrangement of reactor and assembly used in this experimental program. Lattice spacings of 7, $9\frac{1}{2}$, or 12 inches could be assembled with the use of spacer blocks. The fuel elements that simulated a seven-rod cluster fuel element were aluminum cylinders with seven holes provided for insertion of $\frac{3}{4}$-inch diameter uranium slugs. Aluminum was used as a substitute for sodium in the construction of the exponential experiment fuel element, since the low-energy macroscopic scattering and absorption cross sections of aluminum are nearly identical to those of sodium. The uranium used for most of the experiments was that intended for the SRE, and contained 2.78 percent U^{235}. However, natural uranium fuel elements were utilized in some of the experiments. In addition, a six-rod cluster, made by replacing the central uranium rod of the seven-rod element with aluminum or graphite, was studied. Measurements were also made with a four-rod fuel cluster made up of 1-inch diameter rods of uranium enriched to 0.9 percent.

Figure 3–4 shows the results of the buckling measurements of nine different lattice systems. Curves are shown for fuel elements of natural uranium and uranium enriched to 2.78 percent U^{235} in a seven-rod

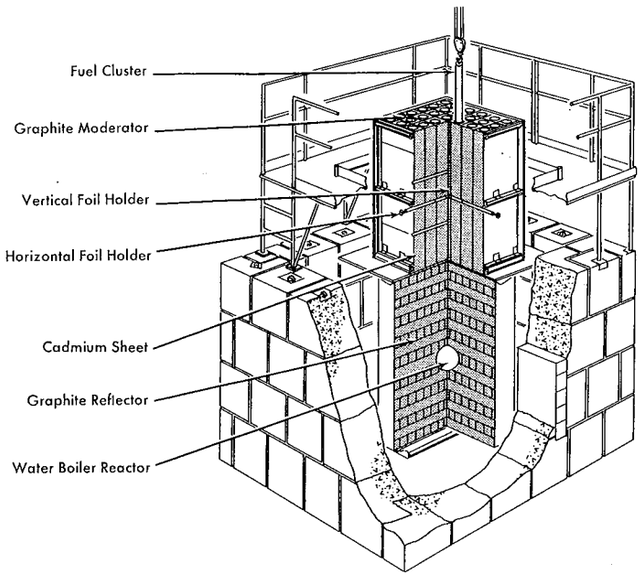

FIG. 3–3. Sodium graphite exponential experiment.

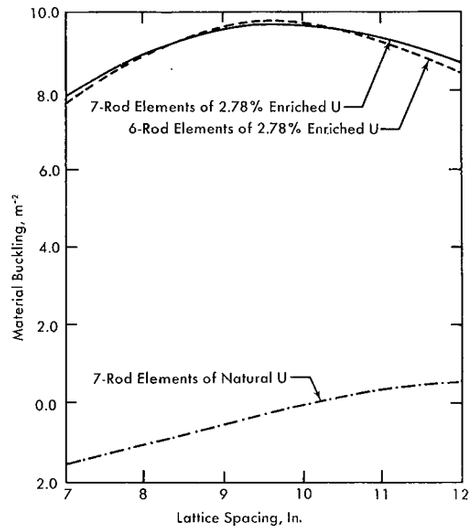

FIG. 3–4. Lattice bucklings measured in the sodium graphite exponential experiment.

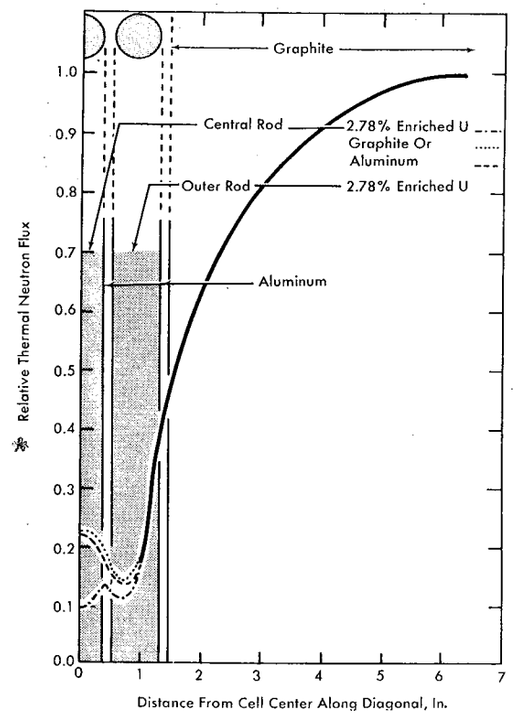

FIG. 3–5. Flux distribution measurements.

cluster as well as a curve for 2.78 percent enriched uranium in a six-rod cluster. Details of the results and type of assemblies used are given in Table 3–2.

Detailed flux distribution measurements within a lattice cell were obtained as typified by the flux distribution curves in Fig. 3–5. These measurements were made by neutron activation techniques, using small foils containing dysprosium oxide. From the intracell flux distribution data, the relative average thermal neutron density in each of the components of the lattice cell was calculated. These data are tabulated as Table 3–3 and were used in calculating the thermal utilization factors and the thermal neutron diffusion lengths of the lattices.

The formula used to relate the lattice constants to the experimentally measured buckling; B^2, is

$$1 + L^2B^2 = \eta\epsilon pfe^{-\tau B^2}.$$

TABLE 3–2

MATERIAL BUCKLING OF GRAPHITE LATTICES

Fuel element			Assembly dimensions			Buckling, m^{-2}
No. of rods of fuel	Rod size, inches	Fuel enrichment, w/o	No. of cells	Width, inches	Lattice spacing, inches	
7	0.75	2.78	36	42	7	7.81 ± 0.21
7	0.75	2.78	25	47.5	9.5	9.67 ± 0.17
7	0.75	2.78	16	48	12	8.65 ± 0.09
6*	0.75	2.78	36	42	7	7.69 ± 0.25
6*	0.75	2.78	25	47.5	9.5	9.76 ± 0.16
6*	0.75	2.78	16	48	12	8.37 ± 0.11
7	0.75	Natural	36	42	7	−1.51 ± 0.15
7	0.75	Natural	36	57	9.5	−0.35 ± 0.15
7	0.75	Natural	16	48	12	0.526 ± 0.15
4	1.00	0.91	36	42	7	−0.77 ± 0.64
4	1.00	0.91	36	57	9.5	1.67 ± 0.28
4	1.00	0.91	16	48	12	2.24 ± 0.14

* ¾-inch graphite rod filling central channel of element.

TABLE 3–3

RESULTS OF INTRACELL FLUX DISTRIBUTION MEASUREMENTS

Fuel elements			Lattice spacing, inches	Average relative thermal flux				
No. fuel rods	Rod diam., inches	Fuel enr., %		Central rod	Outside rod	Center rod / Outer rod	Alum.	Graph.†
7	0.75	2.78	7	1.20	1.98	0.61	3.20	7.06
			9.5	1.22	2.15	0.57	3.57	9.63
			12	1.24	2.27	0.55	3.93	11.96
6*	0.75	2.78	7	2.23	2.13		3.27	7.02
			9.5	2.35	2.24		3.69	9.41
			12	2.56	2.41		4.04	12.02
7	0.75	Natural	7	1.07	1.36		1.66	2.84
			9.5	1.06	1.36		1.72	3.35
			12	1.09	1.39		1.77	3.80
4	1.00	0.91	7		1.26		1.68	3.01
			9.5		1.20		1.67	3.38
			12		1.29		1.81	3.99

* ¾-inch graphite rod filling central channel of element.
† Includes flux in central rod if of graphite.

An examination of the uncertainty connected with the calculation of each of the lattice parameters and the effect of this uncertainty upon the buckling indicated that the quantity contributing the greatest uncertainty to the analysis was the resonance escape probability. This is due not only to the semiempirical nature of the theory used to calculate p, but also to the uncertainty of the value to assign to the data involved; namely, the effective resonance integral and $\mathcal{K}_m$. It was therefore decided to treat these two quantities as parameters in this analysis and attempt to find values for them which would enable calculation of reliable bucklings for all the exponential assemblies. The values so determined were then to be used to calculate the critical mass of the SRE. Therefore, p was calculated for each lattice by means of the above equation, using the experimentally determined value for B^2 and calculated values for the remaining lattice constants. Experimental intracell thermal neutron flux distributions were used, however, in the calculation of f and L^2. The nuclear data used in these calculations are given in Table 3–4.

Since the major dependence of the effective resonance integral is upon the coefficient A, and the S/M term is approximately constant for all the fuel clusters considered, there is only one parameter of concern in the effective resonance integral. The problem is then reduced to determining the relationship between A and $\mathcal{K}_m$. To this end, a curve of A versus $\mathcal{K}_m$ was constructed for each lattice system.

To illustrate the uncertainty which should be attached to the value thus obtained for the effective resonance integral and to construct a plot from which A and $\mathcal{K}_m$ may be determined, a study was undertaken to assign reasonable uncertainties to each of the quantities used for the determination of p in the buckling equation. The calculation of p was repeated, using values which give a reasonable upper and lower bound. A plot of A versus $\mathcal{K}_m$ was then made. The result is shown in Fig. 3–6, and it is apparent that the value of A which this indicates is fairly insensitive to the value chosen for $\mathcal{K}_m$. The value of 5.6 for the lethargy width of

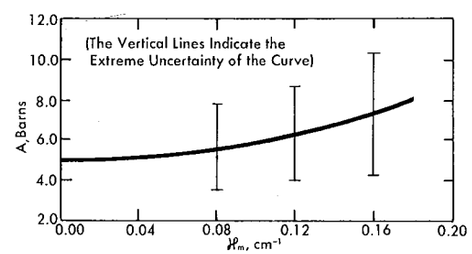

FIG. 3–6. Fit of data for A and $\mathcal{K}_m$ used in calculating resonance escape probability.

TABLE 3–4

NUCLEAR DATA

Material	σ_a(2200) barns	σ_s, barns	$\overline{\cos\theta}$	Atomic weight
Graphite	5.14×10^{-3}	4.8	0.0555	12.00
U^{238}	2.75	8.3	0.0028	238.1
U^{235}	687	10	0.0028	235.1
Sodium	0.50	3.5	0.0290	23.0
Zirconium	0.192	8	0.0073	91.22
Stainless steel	2.94	9.76	0.0117	55.85
Potassium	1.97	1.5	——	39.10

For U^{235}

$\bar{\sigma}_f(20°C) = 504.0$ barns $\quad f(20°C) = 0.981$
$\bar{\sigma}_f(190°C) = 396.8$ barns $\quad f(180°C) = 0.980$
$\bar{\sigma}_f(425°C) = 316.0$ barns $\quad f(425°C) = 1.002$
$\alpha = 0.184$
$\nu = 2.47$

Enrichment $= N_{25}/N_{28} = 0.02893$ for SRE fuel

Poisons

$\bar{\sigma}_a$(Xe-135) $= 2.14 \times 10^6$ barns at 425°C
λ(Xe) $= 2.09 \times 10^{-5}$ sec^{-1}

Total xenon fission yield $= 0.059$
Samarium fission yield $= 0.014$

Uranium cross sections averaged over the fission spectrum, barns

$\sigma_t(28) = 7.10$ $\quad \sigma_t(25) = 7.1$
$\sigma_f(28) = 0.28$ $\quad \sigma_f(25) = 1.2$
$\sigma_{in}(28) = 1.85$ $\quad \sigma_{in}(25) = 1.5$
$\sigma_c(28) = 0.09$ $\quad \sigma_c(25) = 0.2$
$\nu_{28} = 2.5$ $\quad \nu_{25} = 3.0$

Average scattering cross sections for fast neutrons

$\bar{\sigma}_s$(uranium) $= 7.4$ barns
$\bar{\sigma}_s$(graphite) $= 4.40$ barns
$\bar{\sigma}_s$(sodium) $= 3.7$ barns
$\bar{\sigma}_s$(stainless steel) $= 7.7$ barns
$\bar{\sigma}_s$(zirconium) $= 8.6$ barns
$\bar{\Sigma}_s$(NaK) $= 0.050$ cm^{-1}

the resonance neutron group leads to the value 0.12 cm^{-1} for $\mathcal{K}_m$. This is the value chosen for use in the SRE critical mass calculations. The value of A is in turn found to be 6.1 barns, which is considerably less than the value obtained by activation measurements cited in the literature [5]. However, the empirical approach to the calculation of the SRE critical masses requires the use of the value obtained by this analysis, in order to retain consistency.

3–1.3 SRE critical mass. The second part of the experimental program involved measurements of the nuclear characteristics of the Sodium Reactor Experiment during the startup and early phases of the operation of this reactor. The geometry of the SRE is slightly different from that of the exponential assemblies, but the same lattice theory applies. The moderator is in the form of hexagonal blocks of graphite which are enclosed in thin-walled zirconium cans. Sodium is circulated upward between these cans as well as along the fuel in the process tube at the axis of each moderator block. The fuel cluster consists of seven rods of uranium each enriched to 2.78 w/o U^{235}. Each fuel rod is enclosed in thin-walled stainless-steel tubing. NaK bond provides good heat transfer between the uranium and the stainless-steel tubing. A total of 43 process tubes can be loaded with fuel. With this core loading the reflector thickness will be at least 2 feet in all directions. Control and safety rod thimbles are located in the corners of several lattice cells, as shown in Fig. 3–7. There are four control rods, four safety rods, and seven additional thimbles for experiments.

The critical mass of the SRE was determined both with and without sodium in the reactor core. In the dry reactor, that is, without sodium in the core, the reactor was loaded only to the point where the addition of two fuel elements would make the assembly critical. This loading was sufficiently high so that the critical mass could be determined accurately

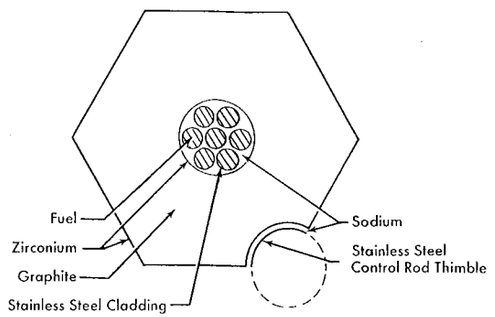

FIG. 3–7. SRE lattice cell.

by extrapolation. With sodium in the core, the reactor was loaded to the critical condition. The volume fractions of materials in the SRE core during the critical experiments were as follows:

	SRE dry core (without sodium coolant)	*SRE wet core (with sodium coolant)*
	68°F	356°F
Uranium	0.0294	0.0297
Graphite	0.8702	0.8696
Stainless steel	0.0038	0.0034
Zirconium	0.0173	0.0173
NaK	0.0015	0.0013
Void	0.0778	0.0161
Sodium	—	0.0626

Critical experiments were performed using standard techniques. An antimony-beryllium source was inserted near the center of the reactor core. Neutron counters located in the reflector were used to determine the neutron density as a function of the number of fuel elements loaded. Curves of inverse neutron multiplication were plotted as a function of the number of fuel elements in the reactor. Because of the limited size of the reactor and reflector, it was necessary to locate the neutron counters so close to the reactor core that shadowing effects caused by insertion of fuel elements close to one counter could strongly influence the behavior of the inverse multiplication curve for that counter. Three neutron counters were symmetrically located in the reflector and the average multiplication obtained from these three counters was used to determine the loading curve. It was found that by averaging the multiplication obtained in this fashion, a relatively smooth loading curve could be obtained and the critical mass could be predicted with improved accuracy. These results indicate that the dry critical mass is 22.2 fuel elements or 42.4 kg of U^{235} and the wet critical mass at a temperature of 400°F is about 32.7 fuel elements or 62.2 kg of U^{235}. This gives a critical mass of about 32.8 fuel clusters when corrected to 352°F. The loading configuration of the reactor core when the wet critical condition was first achieved is shown in Fig. 3–8.

The requirement of 400°F operation during the wet critical experiment uncovered an instrumentation difficulty. Commercial neutron counters which were tested for use in this experiment were found to perform unsatisfactorily at this temperature, and hence special fission counters had to be constructed for the critical experiments. A stainless-steel tube 4 inches long and $\frac{1}{2}$ inch in diameter was used for the body of the new counters.

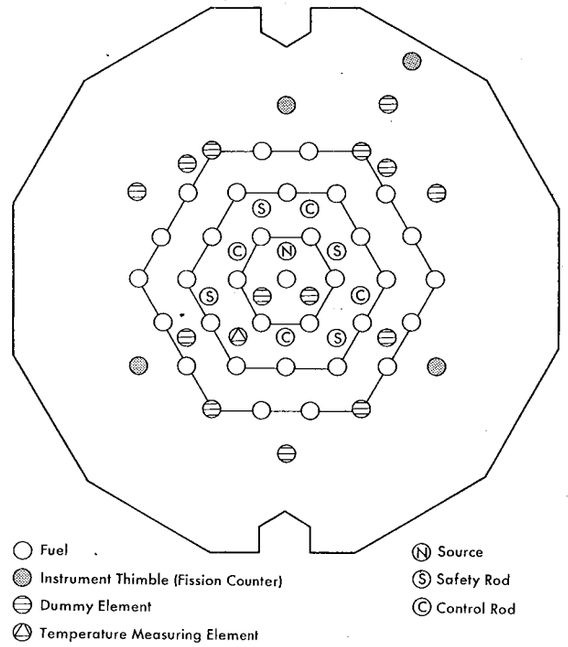

FIG. 3–8. SRE core configuration at end of wet critical test.

Enriched uranium, used as the sensitive material, was plated on a piece of shim stock that was then rolled into cylindrical form and slid inside the counter body. A 30-mil center wire was supported by a ceramic seal at one end. After assembly, the counter was baked out at about 750°F during evacuation and then filled with argon at about 1 atmosphere pressure before sealing. The process of baking the counter during evacuation was found to be an important step in the fabrication process. Counters that were not baked out were found to be unsatisfactory following exposure to high temperatures. This failure was most likely caused by contamination of the filling gas with oxygen that was driven out of the counter walls. Counters that were properly fabricated were operated successfully at 400°F.

Critical mass calculations for SRE had been performed prior to the actual experiments. The two-group reactor formulas and all nuclear data were consistent with those used in the analysis of the exponential experiments. The calculation of the two-group lattice parameters followed the same procedure as that used in the exponential experiments, except that the thermal flux was estimated in the manner previously described. The

calculations of the thermal utilization and thermal diffusion length were further complicated because of fairly large amounts of stainless steel in the fuel clusters and control rod thimbles. However, these corrections were taken into account in the final calculations.

The resonance escape probability was calculated by using the empirically

TABLE 3–5

TWO-GROUP CORE AND REFLECTOR DATA

	Dry	*Wet*	*Hot-poisoned*
	SRE lattice constants		
η	1.827	1.823	1.753
ϵ	1.043	1.043	1.043
p	0.855	0.854	0.848
f	0.8523	0.8144	0.8403
k	1.389	1.321	1.302
L^2	173 cm^2	167	195
D_2	1.021 cm	0.960	0.973
τ	425 cm^2	371	370
D_1	1.14 cm	1.07	1.08
	Axial reflector		
L^2	606 cm^2	553	670
D_2	1.08 cm	0.979	0.991
τ	479 cm^2	384	378
D_1	1.20 cm	1.11	1.12
	Radial reflector		
L^2	2160 cm^2	1470	1840
D_2	0.985 cm	0.930	0.940
τ	367 cm^2	338	336
D_1	1.06 cm	1.01	1.02
	Critical loading		
Theoretical	21.1 fuel clusters	28.4	33.2
Experimental	22.2	32.7	—

determined values for A and $\mathfrak{C}_m$. In the case of the dry reactor (i.e., no sodium present and the reactor at room temperature), a correction for the effect of the streaming of neutrons through the empty channels was applied. (When sodium is introduced into the system, this streaming effect is quite small.)

Two-group data for the radial and axial reflectors were also computed by means of the standard formulas. The main difficulty here occurred in the case of the axial reflectors, which are quite heterogeneous in their structure. It was decided to divide these reflectors into several thin layers and calculate an average cross section for each layer. Composite reflector constants were then constructed by weighing the average cross sections in each layer according to the square of the flux.

Table 3–5 summarizes the two-group core and reflector data. Three reactor cases are considered. The dry case has the reactor without sodium and the entire reactor at 70°F. The wet case has sodium in the reactor and the entire reactor at 356°F. The hot-poisoned case has the reactor operating at full power with equilibrium xenon and samarium poison, the temperatures in each portion of the system being estimated by heat transfer analysis.

Critical mass calculations for a reflected reactor are carried out for these three cases. These results are also given in Table 3–5, together with the experimentally determined critical mass for the dry and wet cases. The critical mass for the hot-poisoned case has not yet been measured.

Flux distribution measurements were made in the dry subcritical reactor by placing both bare and cadmium-covered gold foils either in special experimental thimbles or in small envelopes made of steel shim stock which could be attached to fuel elements. The experimental thimbles could be inserted through the top shield of the reactor into either empty fuel channels or the normal experimental channels provided between moderator cans. Figures 3–9 and 3–10 show a comparison of experimental and theoretical flux distribution in the axial and radial directions through the reactor core and reflector.

As an additional check on the correlation of theory and experiment, the reactivity worth of additional fuel clusters was calculated by assuming an arbitrary change in η and recomputing the critical mass of the reactor. The reactivity ascribed to the change in critical mass is then $\rho = \Delta\eta/\eta$. Figure 3–11 shows the results of this calculation and a comparison with measured values. From the figure we see that the calibrated worth of the thirty-fourth fuel cluster, which is one in excess of the wet critical loading, is 0.37 percent. The experimental value, determined by a stepwise calibration of one of the reactor control rods using period measurements, was found to be 0.43 percent.

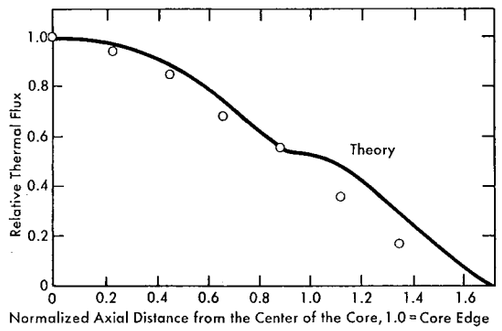

FIG. 3–9. Average axial thermal flux of dry SRE compared with theory.

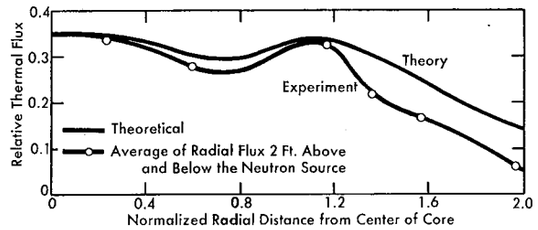

FIG. 3–10. Radial thermal flux plot of dry SRE.

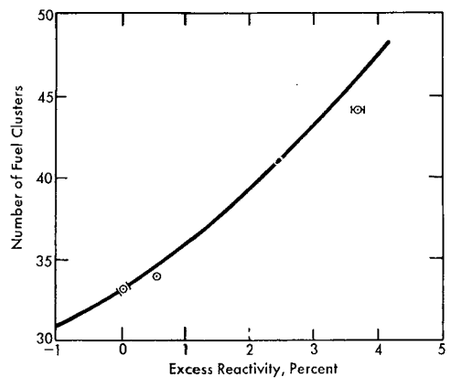

FIG. 3–11. Reactivity versus fuel loading for SRE, wet.

3–1.4 Control rods. Two control rods were calibrated by means of period measurements, giving the results 2.2 and 1.7 percent reactivity. The reactivity values of the other control and safety rods were then determined by intercomparison with a calibrated rod. The total reactivity worths of the control and safety rods (neglecting shadowing) were found to be 7.8 and 7.0 percent respectively.

The reactivity controlled by the control rods is calculated by means of perturbation theory. H. L. Garabedian [6] developed the two-group perturbation theory formula for the reactivity ρ which forms the basis of these calculations. It was found that the reactivity is given by

$$\rho = \frac{\displaystyle\int_{\text{reactor}} \left[-\phi_1^* \, \delta\Sigma_1 \tilde{\phi}_1 + \phi_1^* \, \delta(\epsilon\nu\Sigma_f)\tilde{\phi}_2 + \phi_2^* \, \delta(p\Sigma_1)\tilde{\phi}_1 - \phi_2^* \, \delta\Sigma_2 \tilde{\phi}_2 - \nabla\phi_1^* \cdot \delta D_1 \nabla\tilde{\phi}_1 - \nabla\phi_2^* \cdot \delta D_2 \nabla\tilde{\phi}_2 \right] dV}{\displaystyle\int_{\text{core}} \phi_1^* \epsilon\nu\Sigma_f \tilde{\phi}_2 \, dV} \tag{3–1}$$

where $\tilde{\phi}$ represents the perturbed flux and ϕ^* the adjoint function. The subscripts 1 and 2 refer to fast and thermal neutrons respectively. The symbol δ denotes the perturbation in the quantity which follows it. Thus, $\delta\Sigma_1$ denotes the perturbation in Σ_1, where Σ_1 is the "slowing down" cross section. Figure 3–12 presents the unperturbed flux and adjoint function.

Each term in the numerator of Eq. (3–1) is associated with a process which is taking place within the reactor. The first term is associated with

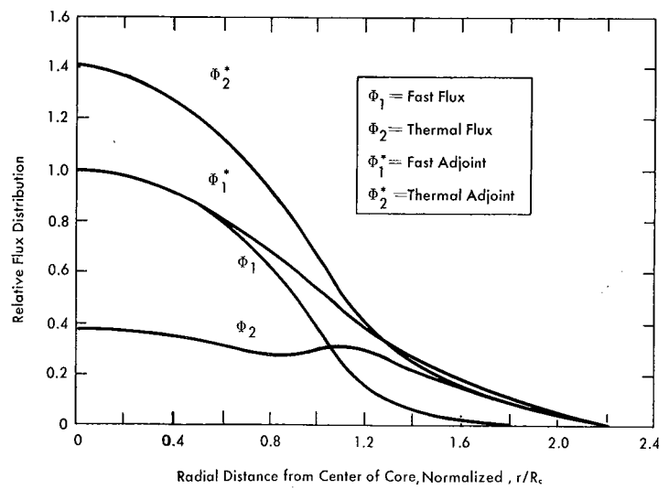

FIG. 3–12. Neutron flux for SRE, wet case.

the removal of neutrons from the fast group, the second term with the source of neutrons in the fast group, the third term with the source of neutrons in the thermal group, the fourth term with the removal of neutrons from the thermal group and the fifth and sixth terms with the fast and thermal neutron currents respectively. The adjoint function which is associated with each term signifies the weight or importance to be associated with the process which that term represents. The denominator of Eq. (3–1) is the value of the source of fast neutrons weighted over the core of the perturbed reactor. The perturbed value of $\epsilon\nu\Sigma_f$ is used in evaluating this quantity.

Equation (3–1) must be developed into a form appropriate to a strong absorber of thermal neutrons. A method for evaluating each perturbation must also be obtained.

In order to use Eq. (3–1) to evaluate the reactivity change caused by inserting a control rod into a hole in the core of a reactor, a suitable model for this process must be developed in terms of the homogeneous reactor model upon which Eq. (3–1) is based. The insertion of a control rod does not displace material from the reactor; therefore the model must accomplish this without displacing material, by imagining the rod to slide into the homogeneous solid core without pushing aside material as it enters. Thus the proper values for the perturbations of the cross sections are equal to the values of corresponding cross sections for the rod. This model leads to the following formulas for the perturbations to be used in Eq. (3–1):

$$\begin{aligned}
\delta\Sigma_1 &= \Sigma_1 \text{ (rod)},\\
\delta\Sigma_2 &= \Sigma_a \text{ (rod)},\\
\delta D &= \frac{1}{3}\left[\frac{1}{\Sigma_{tr} + \Sigma_{tr}\text{ (rod)}} - \frac{1}{\Sigma_{tr}}\right],\\
\delta(\epsilon\nu\Sigma_f) &= \epsilon\nu\,\delta\Sigma_f = 0\\
\delta(p\Sigma_1) &= p\Sigma_1 \text{ (rod)}.
\end{aligned}$$

Since all these quantities are assumed to be independent of position, they can be removed from under the integral signs. Σ_{tr}, p, and ϵ are the values for the unperturbed core.

A control rod of the type being considered will not appreciably perturb the fast flux, so it can be assumed that $\tilde{\phi}_1$ is equal to the unperturbed fast flux ϕ_1. However, a means of obtaining a reasonable approximation for the perturbed thermal flux must be developed. This can be done as follows. With a black control rod assumed to be located on the axis of the reactor, a two-group bare reactor calculation is made, and a curve of the thermal flux is constructed. The thermal flux in the reflected reactor

without the rod is obtained from Fig. 3–12. The addition of a reflector to the reactor will not appreciably disturb the flux in the neighborhood of the control rod, nor will the presence of the control rod in the reflected reactor appreciably disturb the flux in the reflector. Therefore, a reasonable approximation to the thermal flux in the reflected reactor when the rod is present can be obtained by smoothly joining these two curves.

The equations for the flux in the bare reactor are

$$\begin{aligned}
\tilde{\phi}_1 &= \left[J_0(\alpha r) - \frac{J_0(\alpha R)}{Y_0(\alpha R)}\,Y_0(\alpha r)\right] - \frac{2}{\pi}\,\frac{J_0(\alpha R)}{Y_0(\alpha R)}\\
&\qquad\times\left[K_0(\beta r) - \frac{K_0(\beta R)}{I_0(\beta R)}\,I_0(\beta r)\right],\\
\tilde{\phi}_2 &= S_1\left[J_0(\alpha r) - \frac{J_0(\alpha R)}{Y_0(\alpha R)}\,Y_0(\alpha r)\right] - \frac{2}{\pi}\,S_2\,\frac{J_0(\alpha R)}{Y_0(\alpha R)}\\
&\qquad\times\left[K_0(\beta r) - \frac{K_0(\beta R)}{I_0(\beta R)}\,I_0(\beta r)\right],
\end{aligned} \tag{3–2}$$

where

$$S_1 = \frac{p\Sigma_1}{\Sigma_2 + D_2\mu^2}, \qquad S_2 = \frac{p\Sigma_1}{\Sigma_2 - D_2\nu^2},$$

$$\alpha^2 = \mu^2 - \left(\frac{\pi}{H}\right)^2, \qquad \beta^2 = \nu^2 + \left(\frac{\pi}{H}\right)^2;$$

μ^2 and $-\nu^2$ are roots of the characteristic equation

$$(1 + L^2B^2)(1 + \tau B^2) = k_\infty;$$

H is the unreflected height of the reactor, which is assumed to be known; R is the radius of the bare reactor and must satisfy the criticality equation

$$N_0(\alpha r_e) - \frac{Y_0(\alpha R)}{J_0(\alpha R)}\,J_0(\alpha r_e) = -\frac{S_2}{S_1}\,\frac{2}{\pi}\left[K_0(\beta r_e) - \frac{K_0(\beta R)}{I_0(\beta R)}\,I_0(\beta r_e)\right], \tag{3–3}$$

where r_e is the effective radius of the control rod.

Using the value of R obtained from Eq. (3–3), the flux can then be determined from Eq. (3–2). The current into the rod is given by

$$\mathbf{J} = -D\nabla\phi = -D\,\frac{d\phi}{dr}.$$

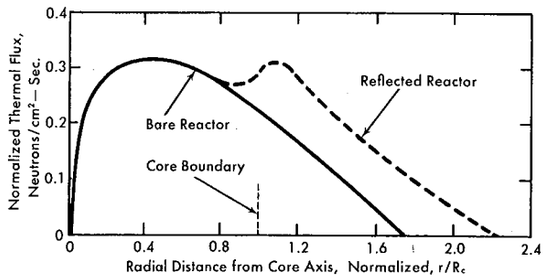

FIG. 3–13. Radial flux (wet) with black control rod on axis.

Figure 3–13 shows a curve for the radial flux in the wet reactor. The dotted curve is the thermal flux in the reflector, which is obtained from Fig. 3–12. This curve is used in evaluating the integral in the denominator of Eq. (3–1).

The integrals in the numerator of Eq. (3–1) are considered next. Since the perturbation is zero except over the volume of the rod, these integrals extend only over the rod. It has been assumed that the flux separates into axial and radial functions,

$$\phi(r, z) = R(r)Z(z),$$

so the volume integral becomes the product of two simple integrals:

$$\int_{\text{rod}} \phi^* \tilde{\phi}\, dV = 2\pi \int_0^{h_c/2} Z^*(z)\tilde{Z}(z)\, dz \int_{\text{rod}} R^*(r)\tilde{R}(r) r\, dr. \qquad (3\text{–}4)$$

Because of symmetry about the midplane, the axial integrals are taken over only the upper half of the reactor. Since the rod does not appreciably perturb the fast flux, we replace $\tilde{\phi}_1$ by ϕ_1 in these integrals. Moreover, it is assumed that the radial fast flux and the adjoint function can be replaced by their average values $\overline{R_1}$ and $\overline{R^*}$ over the rod. Then, for the fast flux, Eq. (3–4) becomes

$$\int_{\text{rod}} \phi_i^* \tilde{\phi}_1\, dV = \overline{R_i^* R_1}(\pi r_0^2) \int_0^{h_c/2} Z_i^*(z) Z_1(z)\, dz, \qquad (3\text{–}5)$$

where $i = 1$ or 2 and r_0 is the radius of the rod.

Of the thermal flux integrals, the one involving $(\epsilon\nu\Sigma_f)$ vanishes, because $\delta\Sigma_f = 0$. To evaluate the term involving $\delta\Sigma_a$, the fact that $\delta\Sigma_a = \Sigma_a$ (rod) is used. [Σ_a (rod) $\tilde{\phi}_2$], therefore, is the absorption by the rod, which must equal the total current into the rod. If R_2^* is taken to be a constant, $\overline{R_2^*}$,

over the rod, it can be removed from the integral, giving

$$\int_{\text{rod}} R_2^*\, \delta\Sigma_2 \tilde{R}_2\, dV = \overline{R_2^*} \oint_{\text{rod}} \tilde{\mathbf{J}}_2 \cdot \mathbf{dS}. \qquad (3\text{–}6)$$

This is valid for a unit length of the rod. When the axial integration is performed, we obtain

$$\int_{\text{rod}} \phi_2^*\, \delta\Sigma_2 \tilde{\phi}_2\, dV = 2\pi r_0 \tilde{J}_2 \text{ (midplane) } \overline{R_2^*}(r) \int_0^{h_c/2} Z_2^*(z)\tilde{Z}_2(z)\, dz.$$

The axial integral is evaluated by replacing $\tilde{Z}_2(z)$ by the unperturbed axial flux $Z_2(z)$, which is valid if the reactor is bare on the top and bottom and the rod extends over the entire height. However, if the reactor is reflected top and bottom, it is not evident that this substitution is valid. Nevertheless, it will still be used because, as will be shown, the only important terms in Eq. (3–1) are those involving $\tilde{\phi}_2$, and if the other terms are neglected an integral involving $\tilde{Z}_2(z)$ is a factor of both numerator and denominator. Since the adjoint functions Z_1^* and Z_2^* which appear in these integrals have approximately the same shape, an error in one will nearly cancel an error in the other.

To evaluate the integrals involving flux gradients, an expression for $\nabla\phi$ within the rod is needed. A simple approximation is made for the flux within the rod and the size of the integrals is estimated. Consider a rod located off the axis of the reactor. Let (ρ, θ) be the coordinates of a point within the rod, referred to the center of the rod, and let the thermal flux within the rod be represented by the expression

$$\tilde{\phi}_2 = \tilde{Z}_2(z)\left[A I_0(\mathfrak{K}\rho) + B \frac{I_0(\mathfrak{K}r_0)}{I_1(\mathfrak{K}r_0)} I_1(\mathfrak{K}\rho)\cos\theta\right]. \qquad (3\text{–}7)$$

The constant A can be related to the average flux at the rod's surface in the midplane of the reactor by $\bar{\phi}_s = A I_0(\mathfrak{K}r_0)$; B is the amplitude of the variation of the flux around the surface and must be less than A. The scalar product of the two gradients is

$$\nabla\phi_2^* \cdot \nabla\tilde{\phi}_2 = \frac{\partial\phi_2^*}{\partial r}\left(\frac{\partial\tilde{\phi}_2}{\partial\rho}\cos\theta - \frac{\sin\theta}{\rho}\frac{\partial\tilde{\phi}_2}{\partial\theta}\right) + \frac{\partial Z_2^*}{\partial z}\frac{\partial\tilde{Z}_2}{\partial z}.$$

The thermal neutron integral is

$$\int_{\text{rod}} \nabla\phi_2^* \cdot \nabla\tilde{\phi}_2\, dV = \int_0^{h_c/2} \int_0^{r_0} \int_0^{2\pi} \nabla\phi_2^* \cdot \nabla\tilde{\phi}_2\, d\theta\, \rho d\rho\, dz.$$

If we now replace ϕ_2^* and $d\phi_2^*/dr$ by their average values over the rod and replace $\tilde{Z}_2(z)$ by $Z_2(z)$, we obtain, after some manipulation,

$$\int_{\text{rod}} \nabla\phi_2^* \cdot \nabla\tilde{\phi}_2 \, dV = \pi r_0 \left[BI_0(\mathfrak{C}r_0) \frac{\overline{d\phi_2^*}}{dr} \int_0^{h_c/2} Z_2^*(z)Z_2(z) \, dz + \frac{2A}{\mathfrak{C}} I_1(\mathfrak{C}r_0)\overline{\phi_2^*} \int_0^{h_c/2} \frac{dZ_2^*}{dz}\frac{dZ_2}{dz} \, dz \right]. \quad (3\text{-}8)$$

When reasonable numerical values for the SRE are substituted in Eq. (3–8), the value of the volume integral over the rod is found to be about 0.25 cm^{-3}. Moreover, since δD_2 cannot be very large (usually less than 1 cm), it is evident that $\int \nabla\phi_2^* \cdot \delta D_2 \nabla\tilde{\phi}_2 \, dr$ will always be considerably less than 1 cm^{-2}. We are justified in neglecting this term since, as will be seen in the next section, the dominant term in the numerator of Eq. (3–1) is about 90 cm^{-2}.

The term involving the gradients of the fast neutron flux will be still smaller because the rod does not perturb the fast flux appreciably. It also can be neglected.

A black absorber captures every thermal neutron which enters it. If the scattering cross section of the control rod is appreciable, some of the thermal neutrons incident upon the rod will be reflected, so the rod is no longer black. To investigate this effect, the absorption in the rod when scattering is present must be examined. Although diffusion theory is not accurate in strong absorbers where the flux is changing rapidly, it will nevertheless be used to calculate a first-order correction to the absorption by the rod when scattering is not negligible. If the control rod is a strong absorber, it will make very little difference whether it is solid or hollow. For simplicity, therefore, consideration is limited to a solid cylinder.

If the flux at the surface of the rod is denoted by ϕ_s, then the flux within the rod may be represented by

$$\phi = \phi_s \frac{I_0(\mathfrak{C}r)}{I_0(\mathfrak{C}r_0)},$$

where r_0 is the radius of the rod and $\mathfrak{C}$ is the inverse diffusion length for thermal neutrons in the rod and is given approximately for heavy elements by the relation

$$\frac{\mathfrak{C}}{\Sigma_s + \Sigma_a} = \tanh \frac{\mathfrak{C}}{\Sigma_s}.$$

The absorption per unit length in the rod is given by

$$\int_{\text{rod}} \phi\Sigma_a \, dV = 2\pi \int_0^{r_0} \Sigma_a\phi_s \frac{I_0(\mathfrak{C}r)}{I_0(\mathfrak{C}r_0)} r \, dr = 2\pi\Sigma_a\phi_s \frac{r_0}{\mathfrak{C}} \frac{I_1(\mathfrak{C}r_0)}{I_0(\mathfrak{C}r_0)}. \quad (3\text{-}9)$$

A black rod is characterized by the conditions $\mathfrak{C}r_0 \gg 1$ and $\Sigma_a \gg \Sigma_s$. In this event, $\mathfrak{C} \simeq \Sigma_a$ and $I_0(\mathfrak{C}r_0) \simeq I_1(\mathfrak{C}r_0)$, so Eq. (3–9) becomes

$$\int_{\text{rod}} \phi\Sigma_a \, dV = 2\pi r_0\phi_s.$$

The quantity

$$\frac{\Sigma_a}{\mathfrak{C}} \frac{I_1(\mathfrak{C}r_0)}{I_0(\mathfrak{C}r_0)} \quad (3\text{-}10)$$

can be used as a measure of the blackness of the rod. It has the value unity for a black rod, and a value between zero and unity if the conditions characterizing a black rod are not satisfied. In the latter case, the reactivity calculated for a black rod should be multiplied by this factor, to correct for semi-blackness.

For the boron-nickel SRE rods we have $\Sigma_a = 3.52$ cm^{-1}, $\Sigma_s = 1.20$ cm^{-1}, $r_0 = 3.18$ cm, and $\mathfrak{C} = 4.72$ cm^{-1}. The value of the blackness factor is

$$\frac{\Sigma_a}{\mathfrak{C}} \frac{I_1(\mathfrak{C}r_0)}{I_0(\mathfrak{C}r_0)} \simeq \frac{\Sigma_a}{\Sigma_a + \Sigma_s} = 0.75.$$

The values of reactivity calculated by the perturbation theory formula should be multiplied by this number.

The four control rods in the SRE reactor are not located on the axis of the reactor but are placed on a circle whose approximate radius is 40 cm. Hence ϕ_2^* in Eq. (3–6) should be evaluated at $r = 40$ cm instead of at $r = 0$. The current $\tilde{J}_2$ into the rod will not be greatly affected by the location of the rod so long as it is placed far from boundaries and strong absorbers. Since the migration length in the SRE core is about 25 cm, this condition is met. It will therefore be assumed that $\tilde{J}_2$ is approximately the same for the actual rod location as it is for a central rod. Hence the reactivity of each rod should be multiplied by the factor $\phi_2^*(40)/\phi_2^*(0)$.

The shadowing effect between rods is neglected. This could be evaluated by replacing the flux calculation in Eq. (3–2) by the solution for a ring of rods.

Table 3–6 shows the results of perturbation theory calculations for the SRE wet case, together with some experimentally measured reactivities for comparison.

TABLE 3–6

CONTROL AND SAFETY-ROD REACTIVITIES

Element	Reactivity	
	Theoretical, %	Experimental, %
1 Safety rod	1.5	1.3–1.7
4 Safety rods (no shadowing)	—	5.7
1 Control rod	1.6	1.7–2.1
4 Control rods (no shadowing)	6.6	7.8

3–1.5 Temperature coefficient. Temperature coefficient of reactivity experiments were carried out using the electric heaters that are provided on the core tank and piping. By using these heaters together with immersion heaters which were inserted into the sodium pool through plugs in the top shield, it was possible to heat the reactor electrically and thereby determine the isothermal temperature coefficient of reactivity.

The temperature coefficient for the reactor was calculated by evaluating each of the lattice parameters at several temperatures over a range from 356 to 1122°F. In this calculation the entire reactor was assumed to be at uniform temperature. A theoretical curve of the temperature coefficient of reactivity is shown in Fig. 3–14.

The experimental value of the temperature coefficient at 500°F was about 8×10^{-4}%/°F, which is lower than the calculated value. Further

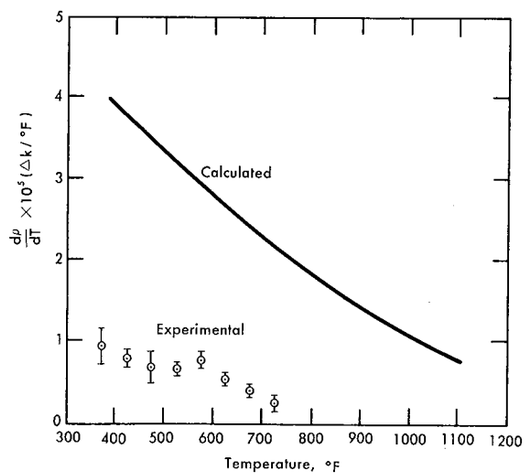

FIG. 3–14. SRE temperature coefficient of reactivity.

experimental work on the temperature coefficient measurements is planned. Since the calculations were done nearly two years prior to operation of the SRE, using a somewhat primitive reactor concept, good accuracy is not to be expected. The important thing is that the positive coefficient predicted by theory is actually observed, at least over the region of lower temperature. The reason for this positive coefficient is that the thermal flux distribution throughout a lattice cell changes drastically as the temperature rises, the flux in the fuel increasing relative to that in the moderator. This means that the thermal utilization increases considerably with increase in temperature. Although the resonance escape probability decreases due to Doppler broadening, the decrease is insufficient to override the thermal flux flattening effect. Hence, a positive temperature coefficient results [7].

Another experiment which was performed to obtain nuclear information on the Sodium Graphite Reactor was a measurement of the temperature coefficient of the effective resonance integral in uranium and in thorium rods. By the use of activation techniques, the resonance neutron absorption in cylinders of uranium and thorium was determined as a function of the temperature of the uranium or thorium metal [8]. The information obtained has been used to predict the metal, or prompt, temperature coefficient of reactivity and, from this, to predict the behavior of the reactor under transient conditions. Thus, this measurement is of particular importance to the safety of the reactor when loaded with either uranium or thorium base fuel. The temperature coefficient of the volume component of the effective resonance integral in uranium was found to be 7.2×10^{-5}/°F after correcting for the effect of the absorptions in the $1/v$ cross section region which extends above the cadmium cutoff. The metal temperature coefficient for SRE was calculated using a slightly higher value, namely, 7.8×10^{-5}/°F. The result was

$$\frac{d\rho}{dT_{\text{metal}}} = -7.9 \times 10^{-6}/°\text{F}.$$

3–2. REACTOR STATICS

3–2.1 Shielding. Shielding for the SRE was calculated prior to the development of methods [9–11] which are currently in use for design of advanced reactor systems. These newer methods can be utilized to establish with less uncertainty shielding requirements of the type described.

The shielding for the SRE is divided into two functional systems, thermal and biological. The thermal shield, which directly surrounds the reactor, is designed to reduce the radiation heating in the biological shield to a tolerable design limit. The biological shield then reduces the remain-

ing radiation level to the permissible operating limit. The main reactor shield complex, which is described in Chapter 6, consists of a fixed side and bottom installation and a rotatable top shield.

Side shield. The side shield, opposite the core and reflector portion of the reactor, consists of a $\frac{1}{4}$-inch 304 stainless-steel inner liner (which assures a stagnant layer of about $2\frac{1}{2}$ inches of sodium adjacent to the core tank, thus minimizing thermal stresses); a $1\frac{1}{2}$-inch 304 stainless-steel core tank; a $5\frac{1}{2}$-inch low carbon steel thermal shield; a $\frac{1}{4}$-inch steel outer tank; 12 inches of calcined diatomaceous silica and asbestos block insulation, a $\frac{1}{4}$-inch low carbon steel cavity liner (serving as a liner for the concrete, an aid in heat removal from the concrete region, and a means of attaching the tetralin shield coolant pipes); followed by 4 feet of structural concrete.

Since the reactor is buried, the choice of ordinary concrete was strictly for structural considerations. The concrete had a density of 145 lb/ft^3.

Thermal shield thickness was established by the limitation placed on the maximum temperature rise in the concrete, taken to be about 35°F. The maximum heat generation in the concrete was therefore limited to 50 Btu/ft^2·hr, (because of its relative conservatism, this limit could be exceeded somewhat without deleterious effect). The major contribution to the heat generation in the steel is from capture gammas generated in this region, amounting to 2500 Btu/ft^2·hr, and comprising over 85 percent of the total incident radiation heat flux. The thermal shield reduces the maximum radiation heat flux on the concrete to 50 Btu/ft^2·hr, 70 percent of which is from capture gammas generated in the steel region.

The thickness of the side concrete shield was established by structural considerations, but it should also be noted that an evaluation of the maximum possible amount of activation of the earth surrounding this shield was made. This calculation was necessary in order to establish whether a possible hazard existed due to activity pickup in ground waters by drainage of rain water. It was concluded that the amount of activity formed [estimated to be 23 curies) would not present a problem with regard to contamination of either the local reservoir or the laboratory water supply.

Bottom shield. The bottom shield consists of a $4\frac{1}{2}$-inch steel thermal shield (i.e., the core tank and the bottom of the outer tank), about $1\frac{1}{2}$ feet of thermal insulation, a 1-inch cavity liner, and 4 feet of structural concrete. The concrete had a density of 145 lb/ft^3; its nuclear characteristics are the same as for the side shield concrete.

Thickness of the thermal shield was established by the limitation placed on heat generation in the concrete; again a conservative limit of 50 Btu/ft^2·hr was used. In the analysis of heat generation in the thermal shield, it was found that the major contribution was from capture gammas generated in the grid plate. This amounted to about 35 percent of the total of 1000 Btu/ft^2·hr, whereas sodium decay and thermal shield capture gammas contributed an additional 20 percent each. Maximum radiation heat generation in the concrete was 41 Btu/ft^2·hr, the major contribution coming from capture gamma rays generated in the concrete and grid plate (about 25 percent each), and from sodium decay and thermal shield capture gammas (about 20 percent each).

Although the thickness of the concrete shield was established by structural considerations, evaluation of the maximum possible amount of activation of the sandstone and earth below this shield indicated that 4 curies of activity could be formed. As before, it was concluded that this amount of activity would not present a problem with regard to contamination of local water supply.

Top shield. The lower part of the SRE top shield consists of a series of 13 stainless-steel insulation plates (total thickness 0.5 inch) followed by two 1-inch thick steel plates which surround a $1\frac{1}{4}$-inch layer of lead in which the thermal shield coolant (tetralin) tubing is contained. This constitutes the top thermal shield. Above this is 5 feet 7 inches of magnetite concrete plus 2 inches of steel. The steel region actually consists of a 2-inch region containing steel shot covered by a $\frac{1}{2}$-inch thick steel plate, the shot region being added to facilitate installation and maintenance of control and thermocouple cables below the loading-face surface.

Magnetite concrete was stipulated for the top shield because the magnetite ore was a low-cost aggregate capable of yielding a relatively dense concrete (i.e., in excess of 200 lb/ft^3), and was readily available. Use of heavy concrete was economically justified in this case because a lighter concrete, although cheaper, would result in added costs because of the larger volume requirements. These additional costs would include such items as increased excavation for both the reactor and fuel storage areas, as well as the necessity for additional concrete around the reactor, increased fuel-handling cask height, and increased building height (the building height is set by the length of the fuel rod and associated assembly, including hanger rod and shield plug).

A minimum aggregate density was specified at 4.6 g/cm^3, and by using a dry aggregate intrusion grouting method of placement, a cured concrete density of 230 lb/ft^3 was obtained. This method of placement was found desirable, in spite of the added costs involved, because of space limitations between the many sleeves penetrating the top shield. Prepacking of the aggregate ensures uniformity of the shield concrete, thus eliminating voids and regions of low density, especially in confined regions. The chief constituents of the resultant concrete (in weight percent) were: iron 56.6, oxygen 33.2, calcium 5.6, silicon 2.45, and hydrogen 0.62.

Thermal shield thickness was designed so that no more than 50 Btu/ft^2·hr of nuclear radiation heat would be incident on the concrete, thus permit-

ting a maximum temperature rise of 20°F (in the magnetite concrete). Although this would be considered excessively conservative for present-day design, the use of this specification did not involve any significant increase in cost in the SRE shield. The major contribution to the nuclear radiation heat flux incident on the top thermal shield is from the sodium decay gammas originating in the pool just below the shield; this source amounted to about 230 Btu/ft^2·hr, or approximately 75 percent of the total incident nuclear radiation heat flux. It should be noted that the nuclear radiation heat flux is only about 27 percent of the 1160 Btu/ft^2·hr total heat flux incident on the underside of the thermal shield. With the thermal shield arrangement as described above, maximum calculated heat flux incident on the concrete was 16 Btu/ft^2·hr, which presented a reasonable safety factor. In this case, the major single contribution was still from sodium decay gammas; capture gammas from the sodium pool and thermal and biological shields contributed a total of about 50 percent of the nuclear radiation heat flux.

Concrete shield thickness was designed so that the leakage dose rate would not exceed 0.1 of the maximum permissible dose, or 0.75 mr/hr. Several design changes (resulting in the shield design as described above) instituted after the original dose-rate calculations had been completed improved the shielding. The resultant calculated dose rate at the shield surface was 0.10 mr/hr, with major contribution coming from concrete capture gammas. Although these figures might appear to indicate that the use of a boron additive would have helped reduce the shield thickness, this would not have been the case. The over-all shield density would have been reduced to the point where the contribution from fast neutrons (not affected by boron addition, but only by the density reduction) would have increased to a level corresponding to that originally due to the concrete capture gammas.

There are 81 small ($4\frac{1}{2}$-inch top diameter) plugs penetrating the top shield, plus three larger plugs, two of these 40 inches in diameter, the other 20 inches in diameter. It was considered that radiation streaming up the annuli between plugs and shield might present a serious problem in regard to top shield accessibility during reactor operation and would increase the radiation level above that calculated for the bulk shield. To overcome this, the width of these annuli were kept to the very minimum, in general, $\frac{1}{32}$ inch on the small plugs and $\frac{1}{16}$ inch on the large plugs. These tolerances were maintained down to the step in the shield plugs (occurring about midway into the concrete portion of the shield). Below this point the sizes of the annuli were permitted to increase by a factor of two.

Results of measurements made thus far, which were taken at a reactor power of 8 Mw, indicate that the radiation level at the shield surface will, in general, be less than 0.3 mr/hr at full power (20 Mw). However, some evidence of gamma-ray streaming was apparent in the control-rod regions.

Even this radiation, when extrapolated to full power, was less than the maximum permissible dose rate.

Primary coolant system shielding. To determine the required shield thicknesses for the primary coolant system, the specific activity of the sodium and the piping layout are most important. A preliminary calculation of the specific activity was obtained by assuming that all the sodium in the primary system is stationary; computing the total number of neutrons absorbed per second would then permit determination of the specific activity. The volume of sodium in each region was computed (e.g., in the process channels, between moderator cans, between reflector cans, etc.), its temperature and cross section determined, and from this the total number of neutron captures per unit time in each region was obtained. Division of the total number of captures per second by the total sodium volume in the primary system gave the specific activity, for this case 0.10 curie/cm^3.

The thickness of the shielding over the entire main and auxiliary primary coolant circuits was designed so that the surface dose rate would not exceed 0.75 mr/hr or 0.1 of the maximum permissible dose rate.

A choice of magnetite concrete for this shielding was again based upon relative low cost and compactness compared with ordinary concrete. This shielding was poured by conventional means into prefabricated forms which were stripped when the concrete had been cured. The aggregate density was specified to be a minimum of 4.5, which resulted in a cured concrete density of 224 lb/ft^3.

Using the above value for the specific activity, the shielding calculations indicated that 4 feet of concrete were required over the main primary gallery except in the region of the heat exchanger, where 4 feet 3 inches were found necessary. In the auxiliary primary gallery, 3 feet 6 inches of concrete were required except over the heat exchanger, where 4 feet were necessary. However, to avoid the complication of changing the distance from the shield surface to the support ledge and the design problems which would be encountered in using different thicknesses of blocks, it was decided to use a single shield thickness of 4 feet 3 inches in both galleries. This shielding is in the form of 13 removable blocks over both galleries. The total weight of these blocks is about 750,000 pounds. Removal of blocks permits after-shutdown maintenance of the piping system and its associated components.

Later calculations, using the same method as the original calculations, indicated that the specific activity of the sodium would be 0.28 curie/cm^3. The increase was brought about by changes in the core design. The effect of this new value is included in the following description of radiation levels over the shield blocks.

In laying out piping in the galleries, it was found that a rather severe

space limitation existed in the building, eliminating the possibility of providing adequate steps between the shield blocks and the foundation walls. As a result, the bottom of the shield blocks rest on a 4- to 8-inch ledge of ordinary structural concrete. Foundation walls above the ledge were made of magnetite concrete. To facilitate removal of the blocks, which were quite large (from 10 to 50 tons each), it was necessary to provide a nominal $\frac{1}{2}$-inch gap between them and the foundation walls. Since the main primary loop, containing sodium with a saturated activity of 0.28 curie/cm^3, represented a source strength of about 1600 curies of sodium-24 per foot of piping, there existed the possibility of a serious scattering and streaming problem, particularly through gaps between shield blocks and between blocks and foundation. Several schemes, such as pouring lead shot or inserting lead sheet in the interstices between blocks, were considered to alleviate this problem. The lead sheet approach, because of its relative simplicity, was the one finally adopted.

Results of measurements performed at a power level of 8 Mw, when extrapolated to full power, indicated streaming dose rates of up to 300 mr/hr. These readings were undoubtedly low, since the size of the beam was less than the size of the detector chamber used in the measurements. As a result of this streaming, it was difficult to determine the general radiation levels directly over the shield blocks. Analysis using the more recently calculated sodium specific activity, however, had indicated that the radiation level directly above the main intermediate heat exchanger would be about 4.0 mr/hr, while the radiation levels over the remainder of the main primary and auxiliary loops would be less than 0.75 mr/hr. This high level over the heat exchanger resulted from the new value for specific activity of the coolant plus the fact that the original shield calculations were based on a concrete density of 230 lb/ft^3, whereas a density of only 224 lb/ft^3 was achieved. This did not reflect in an increased dose rate over the rest of the primary circuit however, since the shielding provided was at least 3 inches more than originally specified.

Fuel storage area. The fuel storage area in the SRE is a 16 by 6 vertical array of 25-foot tubes, capped at the lower end. The tubes are on 1-foot centers; their upper ends, which are open at reactor room floor level, are set in a 2-foot thick layer of magnetite concrete. Shield plugs attached to the fuel elements serve as additional shielding, whereas in empty storage tubes it is necessary to provide special shield plugs to prevent excessive levels of scattered radiation in the reactor room.

Magnetite concrete was used for the shielding pad, i.e. the reactor floor area surrounding the tops of the fuel storage tubes. The choice of magnetite concrete was dictated primarily by space limitations in connection with the adjacent trench carrying coolant piping for storage tubes and the proximity of a hot cell. Also, with the use of ordinary concrete a transient high dose rate could occur in the room when a fuel element is

partially inserted into the storage tube during transfer from the fuel-handling cask. An additional lead shielding skirt for the cask could have been provided, but its width would have become excessive, resulting in severe stress problems. The use of magnetite concrete around a tube, however, in an area equivalent to the lower portion of the cask skirt, would shield a spent fuel element to about the maximum permissible dose rate. Again, the low cost of magnetite concrete made it quite attractive for this purpose. The density achieved for this concrete pour was the same as that for the gallery shield blocks, i.e., 224 lb/ft^3.

Concrete pad thickness was determined by two criteria: that, during the transfer operation, the shielding would be sufficient so that the maximum transient radiation levels around the cask would not exceed 7.5 mr/hr, and that a shield plug matching the thickness of the concrete pad would provide sufficient attenuation to reduce the dose rate from a stored element to 0.75 mr/hr.* A 2-foot thick magnetite concrete pad was calculated to be sufficient to accomplish this.

When a fuel element is located in a storage tube and the shield plug over an adjacent tube is removed, a high scattered dose rate will exist. Calculations indicate that this level would be in the range of about 1.0 r/hr, but that it would be highly collimated.

Since the reactor fuel has not as yet achieved a substantial burnup, radiation measurements above the storage area have not indicated any levels in excess of background. No measurements of scattered radiation have been made.

3–2.2 Coolant flow and heat transfer in SRE core. The SRE core is cooled by two separate coolant streams, both flowing upward in the core.

The main coolant stream, which removes heat generated in the fuel elements, flows through coolant tubes containing the fuel elements. Coolant enters the coolant tubes from the lower plenum and discharges into an upper plenum. The relative flow rate through each coolant tube is controlled by an orifice plate attached to the lower end of each fuel element. Orifices are sized to obtain a flow distribution in the core which will result in approximately the same coolant outlet temperature for all tubes. At full power, the coolant velocity varies from about 5 ft/sec in the central coolant tube to about 2.5 ft/sec in the outermost coolant tubes.

The second coolant stream, which removes heat generated in the moderator, reflector, control rods, and thermal shield, flows in the passages between the moderator (and reflector) cans. This coolant enters the core from the intermediate plenum, which is located between the lower plenum and the core, and discharges from the core into the upper plenum, where it mixes with the main coolant stream. Proper flow distribution of this

* In fact, the attached top shield plug which is transferred with a fuel element exceeds this requirement.

coolant in the core is obtained by virtue of the low friction pressure drop through the reactor, which makes the buoyancy force predominant. In passages having higher heat loads, the coolant tends to be hotter and therefore less dense. Hence, the flow rate automatically increases in these passages. In channels where the heat load varies, such as control rod channels, the coolant flow rate automatically adjusts itself to the heat load. The total flow rate of this second coolant stream is adjusted externally, either manually or automatically, so that its mean outlet temperature matches the outlet temperature of the main coolant stream.

The limitation on thermal power of the seven-rod fuel element, and therefore on the thermal power of the reactor, is imposed by the maximum permissible uranium temperature. In the case of alpha-rolled beta heat-treated uranium, this temperature is 1220°F, the alpha-to-beta phase transition temperature.

The SRE fuel element consists of seven fuel rods arranged in a triangular lattice. A cross-sectional view of the fuel element in the coolant tube is shown in Fig. 3–15. The fuel elements and their construction are described in detail in Chapter 5, but are illustrated here for proper orientation in the heat-transfer discussion. A partial longitudinal view of the fuel element is shown in Fig. 3–16.

Thermal neutron flux distribution in the seven-rod fuel element has been measured in an exponential lattice (Fig. 3–5). The results show that the center rod power will be about 57 percent of a peripheral rod power for 2.78 w/o enriched uranium (Table 3–3).

Despite the fact that the center rod power is substantially less than the power of a peripheral rod, an inadequate mixing of (1) the coolant flowing between the center rod and the peripheral rods with (2) the coolant flowing between the peripheral rods and the coolant tube wall would result in an overheated center rod. This overheating would be due to the higher heat load on the coolant flowing between center and peripheral rods. For this reason, the degree of coolant mixing was experimentally deter-

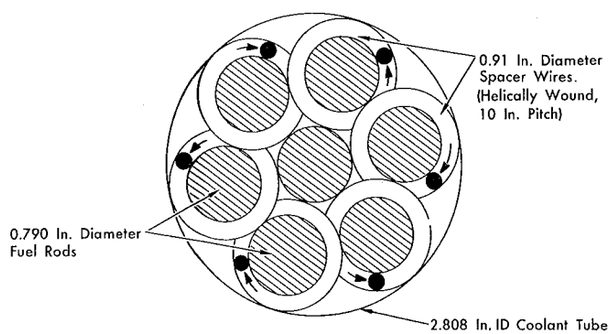

FIG. 3–15. Cross section of SRE fuel element.

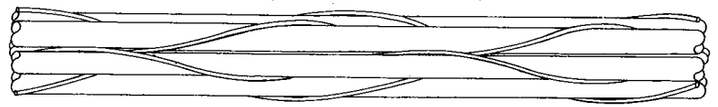

FIG. 3–16. Side view of section of seven-rod fuel cluster, illustrating wire wrap.

mined [12,13]. For purposes of experimentation, water was substituted as a coolant mockup. A chemical solution was injected at the upstream end of the fuel element into the water-substitute coolant flowing between center rod and peripheral rods. Measurements were then taken, at various distances downstream, of the chemical concentration in the coolant flowing between peripheral rods and the coolant tube wall. Results indicated adequate coolant mixing, and further indicated that this mixing is induced largely by the spacer wire wound helically around each peripheral rod.

No experimental or analytical heat transfer coefficient for liquid metals flowing through a lattice of rods in the complex manner (spiral flow) described above is available in the literature. However, it can be expected that the heat transfer coefficient for spiral flow would be greater than for pure axial flow; consequently use of a heat transfer coefficient for axial flow should be conservative. For flow in channels between rods, heat is transferred to sodium from all surfaces seen by the sodium. For flow in channels between the coolant tube and peripheral rods, heat is transferred to the sodium essentially only from the peripheral rod surfaces seen by the sodium, since there is very little heat flow through the coolant tube wall. Hence the flow in the channels between the coolant tube and the peripheral rods is similar to flow between parallel plates with heat from one surface only. It has been shown [14,15] that the liquid metal heat-transfer coefficient for this case is less than for the case of heat from both surfaces.

The mean heat-transfer coefficient for the sodium flowing through the SRE seven-rod fuel element was assumed to be given by the Seban equation [14] for flow between parallel plates with heat from one surface only, namely,

$$\mathrm{Nu} = 5.3 + 0.02\,\mathrm{Pe}^{0.8},$$

where Nu = Nusselt number and Pe = Peclet number. The equivalent diameter was calculated using the conventional definition of equivalent diameter, namely, 4 × flow area/wetted perimeter.

The hot channel factors used in the calculations are listed in Table 3–7. A general description of the method used to determine the hot channel factors is as follows:

F^a, variation in coolant tube diameter. The change in flow rate in a coolant tube due to variation in coolant tube diameter was calculated, taking into account the change in equivalent diameter in the fuel element section and

the change in the annular flow area between the orifice plate and the coolant tube wall. The reason for the variation of $F^a_{\Delta t}$ with radial position of the coolant tube is that as the orifices decrease in size, the percentage of flow through the space between the orifice plate and the coolant tube wall increases. Consequently, any variation in coolant tube diameter has greater effect on the flow rate as the orifice diameter becomes smaller.

F^b, *variation in orifice diameter.* The change in flow rate in a coolant tube due to a variation of ±0.003 inch in the orifice diameter was used to determine F^b.

F^c, *eccentricity of fuel element in coolant tube.* Calculations show that if a seven-rod fuel element is offset in the coolant tube to the extreme eccentric position in the same direction over its entire length, the velocity and weight rate of flow in the smallest outer channel will be 6 and 17 percent less, respectively, than in an outer channel of a centered fuel element. Since it is unlikely that a fuel element will be extremely positioned as described above, and since there will be some coolant "mixing" between channels, the effective decrease in the weight rate of flow in the smallest outer channel was assumed to be 5 percent, which is the basis for $F^c_{\Delta t} = 1.05$.

F^d, *heat generation asymmetry in fuel element due to radial position in core.* The ratio of maximum peripheral rod power to mean peripheral rod power for a seven-rod fuel element, which is also $F^d_{\Delta t}$, F^d_θ, and F^d_ϕ, was determined from the gradient, at the fuel element, of the radial thermal neutron flux distribution for the core.

F^e, *deviations from estimated radial power distribution for the core.* An arbitrary allowance of 5 percent deviation from the estimated radial power distribution was made.

For a maximum permissible zirconium temperature of 950°F, the permissible nominal coolant outlet temperature is given by

$$t_2 = t_1 + \frac{950 - t_1}{F_{\Delta t}},$$

where t_1 = coolant inlet temperature, and t_2 = maximum permissible nominal coolant outlet temperature. For a coolant inlet temperature of 500°F, this expression becomes

$$t_2 = 500 + \frac{450}{F_{\Delta t}};$$

t_2 has been calculated by substituting $F_{\Delta t}$ from Table 3–7 into the above expression. The results are tabulated in Table 3–8.

Also shown in Table 3–8 is the estimated radial power distribution for a 43-element core. This estimated radial power distribution was obtained

by extrapolating the measured radial power distribution for a 36-element core. In addition, Table 3–8 lists the power output of individual coolant tubes for a reactor power output of approximately 20 Mw and the flow distribution in the core.

The axial, maximum fuel temperature distribution for a peripheral fuel rod is given by

$$t_f = t_1 + \frac{Q}{wc}\left[\frac{wc}{\alpha U A(1+\gamma)(6+\beta)}\,\frac{\phi_z}{\bar{\phi}} + \frac{q_{pz}}{q_p}\right]$$

for a nominal channel, and

$$t_f(\text{h.c.}) = t_1 + \frac{QF_{\Delta t}}{wc}\left[\frac{wcF_\theta}{F_{\Delta t}\alpha U' A(1+\gamma)(6+\beta)}\,\frac{\phi_z}{\bar{\phi}} + \frac{q_{pz}}{q_p}\right]$$

for a hot channel, where

A = heat transfer area of fuel element = 1.24 ft^2,
c = specific heat of coolant,
Q = thermal power of coolant tube with fuel element,
q_p = mean thermal power of a peripheral rod in a seven-rod fuel element,
q_{pz} = mean thermal power in distance z of a peripheral rod in a seven-rod fuel element,
U = over-all heat transfer coefficient $\left(\frac{1}{(1/h)+R}\right)$,
U' = over-all heat transfer coefficient with hot channel factor for film temperature difference $\left(\frac{1}{(F_{\theta(h)}/h)+R}\right)$,
h = heat transfer coefficient,
R = thermal resistance between fuel axis and cladding-coolant interface,
z = axial distance downstream from upstream end of fuel element,
α = factor applied to U to allow for asymmetric power and coolant flow distribution associated with a peripheral fuel rod (the calculated value of α is 1.04),
β = ratio of center rod power to a peripheral rod power (0.57, calculated from measured thermal flux distribution in a seven-rod fuel element),
γ = ratio of heat generated in fuel element coolant plus heat entering through coolant tube wall to heat generated in fuel element (0.01, assumed),
ϕ_z = mean heat flux through peripheral rod surface at z,
$\bar{\phi}$ = mean heat flux through peripheral fuel rod surface.

TABLE 3–7

HOT CHANNEL FACTORS FOR COOLANT TUBES WITH SEVEN-ROD FUEL ELEMENTS

Thermal parameter affected	Distance of coolant tube from core axis, cm	Variation in coolant tube diameter, F^a	Variation in orifice diameter, F^b	Eccentricity of fuel element in coolant tube, F^c	Heat generation asymmetry in fuel element due to radial position in core, F^d	Deviations from estimated radial power distribution, F^e	Total hot channel factors, F
Coolant temperature rise, Δt	0	1.02	1.00	1.05	1.00	1.05	1.12
	27.9	1.03	1.00	1.05	1.01	1.05	1.15
	48.4	1.04	1.01	1.05	1.01	1.05	1.17
	55.9	1.05	1.01	1.05	1.02	1.05	1.19
	74.0	1.06	1.01	1.05	1.02	1.05	1.20
	83.8	1.06	1.01	1.05	1.02	1.05	1.20
	96.8	1.07	1.01	1.05	1.02	1.05	1.21
Radial temperature drop in rod, θ	0	—	—	—	1.00	1.05	1.05
	27.9	—	—	—	1.01	1.05	1.06
	48.4	—	—	—	1.01	1.05	1.06
	55.9	—	—	—	1.02	1.05	1.07
	74.0	—	—	—	1.02	1.05	1.07
	83.8	—	—	—	1.02	1.05	1.07
	96.8	—	—	—	1.02	1.05	1.07
Film drop, $\theta(h)$	0	1.01	1.00	1.01	—	—	1.02
	27.9	1.01	1.00	1.01	—	—	1.02
	48.4	1.01	1.00	1.01	—	—	1.02
	55.9	1.01	1.00	1.01	—	—	1.02
	74.0	1.01	1.00	1.01	—	—	1.02
	83.8	1.01	1.00	1.01	—	—	1.02
	96.8	1.01	1.00	1.01	—	—	1.02
Heat flux, ϕ	0	—	—	—	1.00	1.05	1.05
	27.9	—	—	—	1.01	1.05	1.06
	48.4	—	—	—	1.01	1.05	1.06
	55.9	—	—	—	1.02	1.05	1.07
	74.0	—	—	—	1.02	1.05	1.07
	83.8	—	—	—	1.02	1.05	1.07
	96.8	—	—	—	1.02	1.05	1.07

TABLE 3–8

SUMMARY OF RESULTS FOR 43 FUEL ELEMENT CORE*

Radial position of coolant tube, r, cm	Nominal coolant outlet temperature, °F	Radial power distribution	Coolant tube power, q, kw	No. of coolant tubes at r, n	nq, kw	Flow rate in coolant tubes	
						w, lb/sec	nw, lb/sec
0	900	1.0	605	1	605	4.62	4.62
27.9	892	0.915	553.5	6	3,321	4.31	25.86
48.4	885	0.834	505	6	3,030	4.00	24.00
55.9	878	0.811	491	6	2,946	3.96	23.76
74.0	875	0.671	406	12	4,872	3.30	39.60
83.8	875	0.584	353.5	6	2,120	2.87	17.22
96.8	872	0.500	302.5	6	1,815	2.48	14.88
				Total power from fuel element coolant	18,709		
				Power from moderator coolant (10%)	1,871		
				Total reactor power	20,580 kw		
				Total fuel element coolant flow rate			149.9
				Moderator coolant flow rate (10%)			15.0
				Total coolant flow rate			164.9 lb/sec

* Reactor power, 20 Mw; coolant inlet temperature, 500°F; mixed mean coolant outlet temperature, 880°F.

The following thermal conductivities were used in evaluating U, U', and h:

Material	*Thermal conductivity* Btu/hr·ft·°F
Uranium	18
304 S. S. Jacket	11
NaK bond	15
Na	42

The axial coolant temperature distribution is given by

$$t_c = t_1 + \frac{Q}{wc}\frac{q_{pz}}{q_p}$$

for a nominal channel, and

$$t_c(\text{h.c.}) = t_1 + \frac{QF_{\Delta t}}{wc}\frac{q_{pz}}{q_p}$$

for a hot channel.

Figure 3–17 shows the axial temperature distributions for the fuel and coolant in the coolant tube located at the axis of the core. The fuel temperature will be lower in fuel elements located in all other coolant tubes.

3–3. TRANSIENT AND SAFETY CHARACTERISTICS

3–3.1 Features affecting transient and safety performance. Information concerning the transient and safety features of the SRE has been accumulated over a period of time using analytical, analog, digital, and,

FIG. 3–17. Axial temperature distributions for fuel and coolant at axis of the core.

more recently, experimental techniques to determine the influence of reactor design features on transient behavior. The results are summarized first by outlining these reactor features and then by showing results of transient analysis.

The following features and characteristics have been built into or are inherent in the SRE design. These are instrumental in determining the transient and safety performance of the reactor.

Neutron lifetime: 5.0×10^{-4} sec (calculated).

Effective delayed neutron fraction: 0.00729 (calculated).

Prompt temperature coefficient: A preliminary measurement of this coefficient yields $-(1.3 \pm 0.6) \times 10^{-5}$/°F. The fuel-element thermal time constant is about 2 sec. Since the moderator time constant is about 3 min, this temperature coefficient also determines the prompt power coefficient.

Isothermal temperature coefficient: The experimental data are fitted by this expression: $[12 - 2.2(T - 300)/100] \times 10^{-6}$/°F $\pm$ 20%, where T = moderator temperature in °F. Note that this coefficient is positive over much of the normal temperature range; however, the associated time constant is 3 min.

Slow power coefficient: The prompt power coefficient is, of course, negative, as mentioned above. The slow power coefficient might be thought to be similar to the isothermal temperature coefficient, but actually temperature gradients within the core tend to accent the fuel temperature effect. As a result, this slow power coefficient is determined to be about $(9.4 - 3.9P) \times 10^{-6}$/Mw, where P is power in megawatts. Note that this coefficient is negative for all power above 2.4 Mw.

Control rods: The SRE contains eight safety and control rods which give about 11 percent reactivity control, including the effect of shadowing. These rods are divided in function as follows:

- Four rods are interlocked as safety rods and must be fully withdrawn at startup. These rods have a full travel drop time of 600 msec.
- Four rods are interlocked as shim rods. These rods can be operated individually or ganged, at which time they have a maximum reactivity rate of 0.012%/sec.
- A dual drive mechanism permits either one of two shim rods to be used in the regulating mode. The high-speed drive can change reactivity at speeds up to 0.03%/sec, but the maximum change is limited to 0.5% by mechanical stops.

Safety circuit response time: When reactor power exceeds the safety circuit set point, a scram signal is initiated with a 20-msec delay. This causes the rod magnets to release with a 50-msec delay.

Period circuit response time: If the reactor period is less than the scram set point, the scram is initiated with a 200-msec delay.

Neutron source: The neutron source is an antimony-beryllium source producing 9.6×10^7 neutrons/sec.

Fission product poisoning: Equilibrium xenon, 1.3%; xenon override, 0.3%; equilibrium samarium, 0.6%.

System transients have been studied in detail for the SRE, using an analog computer. These studies covered transients initiated by simulated withdrawal of control rods, or by simulated changes in sodium flow and temperature.

Two general types of rod withdrawal accidents are possible. The first would be a continuous rod withdrawal with the reactor at full power and operating temperature conditions. Withdrawal of all shim rods at these conditions, combined with simultaneous failure of both the protective system and operator to correct this situation, will result in the transient illustrated in Fig. 3-18. In general, the rate of reactivity addition associated with this transient is limited by the maximum speed of rod withdrawal. If no scram occurs, melting of a portion of the fuel elements would be the shutdown mechanism.

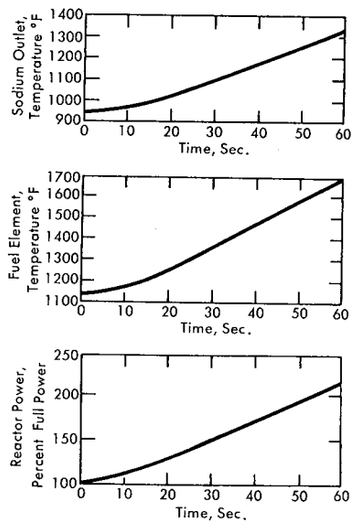

FIG. 3-18. SRE rod withdrawal transient (simultaneous withdrawal of all shim rods with no corrective action).

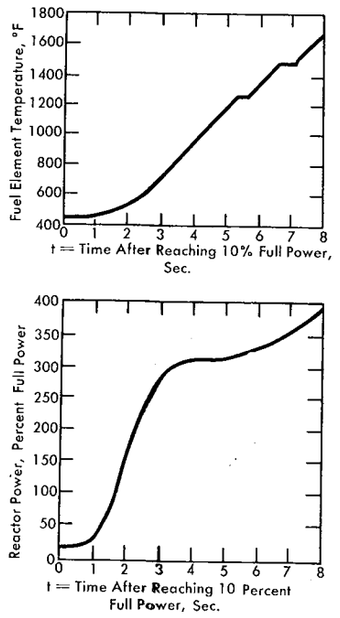

FIG. 3-19. SRE startup accident (simultaneous withdrawal of all shim rods from shutdown condition with no corrective action).

The second type would be a continuous rod withdrawal from a shutdown power level, such as may conceivably occur when the reactor is being brought to a critical condition from source level. This is commonly called a "startup accident." The protective system parameters are sized so as to prevent damage to the reactor during this kind of accident. However, if protective system action should not occur and the rods were continuously withdrawn with no operator action to stop the withdrawal or initiate a scram, the reactor would be on a short period when it reached the normal operating power range. The magnitude of the reactor transients which would occur during this type of uncorrected accident in the SRE is shown in Fig. 3–19. If no scram occurs, melting of a portion of the fuel elements would be the shutdown mechanism.

During operation at full power and full temperature, a change in coolant flow rate changes reactor temperatures rapidly. A failure of a coolant pump or a misoperation of the sodium flow controls (from either manual or automatic malfunction) could produce significant changes in fuel element and sodium coolant temperatures in the fuel channels. Such changes

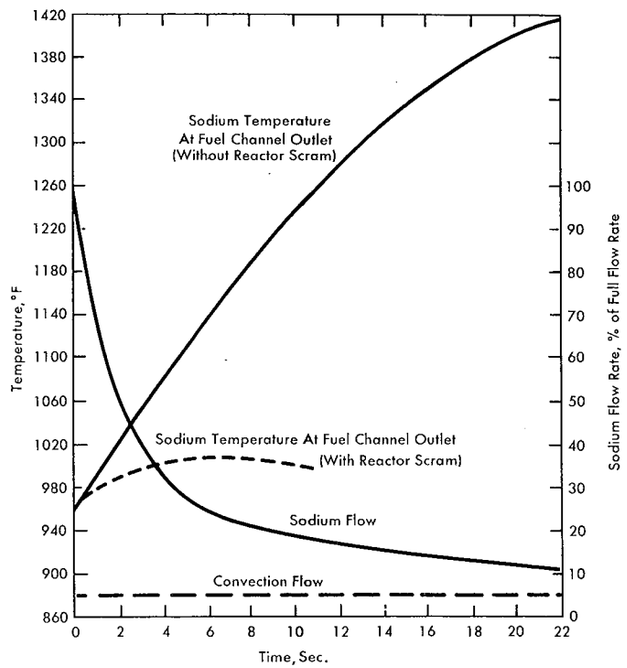

FIG. 3–20. SRE loss of sodium flow accident (with and without corrective action).

may occur rapidly, as in the case of a complete loss of a pump, or slowly, as from improper operation of a flow controller. The protective system is designed to prevent such occurrences from causing serious damage.

In the case of a sudden decrease in flow rate caused by the failure of a coolant pump, the fuel element and sodium temperatures in the fuel channels increase. Sodium temperature at the outlet of an average fuel channel in the SRE is illustrated by a solid line in Fig. 3–20, for the case of no corrective action being taken. Sodium mixing in the large upper plenum would effectively reduce the sodium temperatures above the channel outlet. The effectiveness of a scram in stopping the sodium temperature upsurge at the fuel channel outlet is illustrated by the dotted line. If no scram occurs, melting of a portion of the fuel elements would be the shutdown mechanism.

Because the rate of change of sodium flow is limited, improper operation of the sodium flow controller would produce a much slower transient than a complete loss of the sodium pumps.

Transients may result from either a sudden increase or decrease in sodium flow rate at the maximum rate of change as limited by the design. These two types of transients, with no corrective action being taken in either case, are illustrated in Fig. 3–21.

The effect of such changing flow rates is to change the fuel element and sodium outlet temperatures as shown in the two upper graphs of Fig. 3–18.

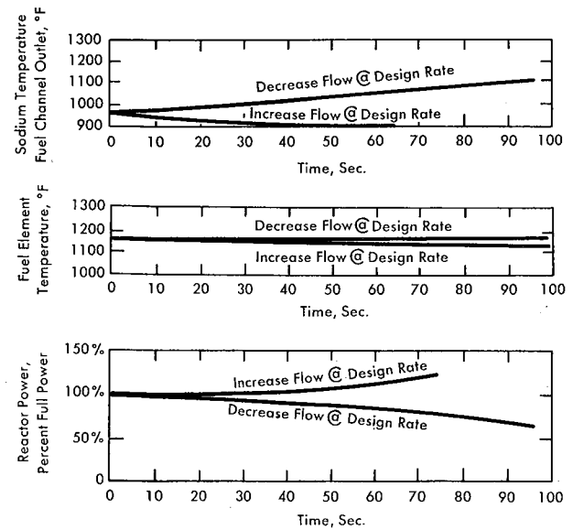

FIG. 3–21. SRE sodium flow transients (no corrective action).

An increase in sodium flow rate increases reactivity because of the decrease in fuel-element temperature, and results in a power level increase as shown in the lower graph of Fig. 3–21. Conversely, a decrease in sodium flow rate results in a decrease in power level. In either case there are no hazardous effects.

If a failure should occur in the external heat-removal system, inlet temperature transients to the reactor would result in causing both the reactor power level and temperature to change. This is illustrated in Fig. 3–22 for a sudden 100°F inlet sodium temperature increase in the SRE. There would be no hazardous effects from this type of transient.

3–3.2 Safety characteristics. Although the conventional steam plant portion of the SRE contains high-pressure steam, the reactor and its coolant system are a separate installation which operates at low pressure. This is an important characteristic of the reactor design, as no "boiler explosion" type accident can occur as a result of system malfunction.

Within the reactor there is no releasable potential energy from pressurization or chemical reaction because the reactor operates under low pressure and all materials used in the reactor are chemically compatible. There is no necessity for a gas-tight pressure shell surrounding the reactor. A typical industrial building structure is used.

The reactor and its associated radioactive components are located in shielded areas below the reactor floor level, reducing radiation levels in

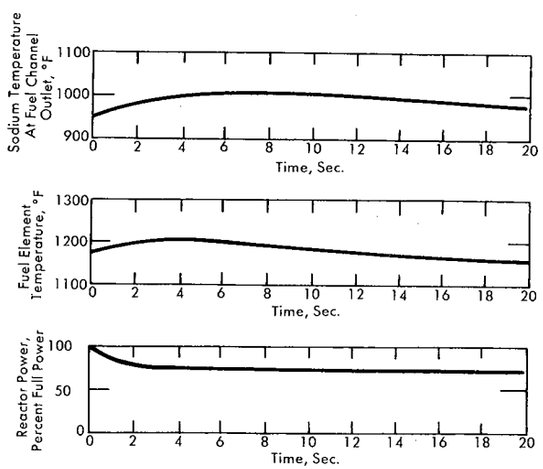

FIG. 3–22. SRE sodium inlet temperature transient (rapid 100°F increase in sodium inlet temperature with no corrective action).

all working areas to well below normal standards of permissible radiation. Secondary nonradioactive sodium coolant circuits transfer heat from the radioactive primary sodium coolant to the air-blast heat exchanger or the steam-generator portion of the plant.

Reactor fuel is contained in steel cladding, preventing contact between the fuel and coolant. Containment of all radioactive fluids is provided by welded steel containers and piping, steel liners on the concrete shielding, and sealed joints. In the steam generator there are double-walled tubes for containing sodium. An inert gas atmosphere is used in all areas containing primary system piping and components, thereby preventing chemical reaction between radioactive sodium and air.

During plant shutdown the sodium heat-transfer circuits may be used for forced cooling of the reactor to remove stored and after-glow heat. An emergency power system employing storage batteries and a diesel driven generator ensures that shutdown coolant flow is maintained during electric power failure.

If loss of all forced sodium flow occurs, natural convection flow within the reactor and in the sodium coolant loops would provide continuous cooling of the reactor after shutdown. Even without flow in the coolant loops, a slow rise in over-all reactor temperature after shutdown is ensured by the large heat capacity of the reactor structure. The upper limit of the reactor temperature is established at a safe level by the heat-removal capacity of organic coolant for biological shielding.

An automatic plant control system provides for safe normal operation of the reactor power plant. A plant protective system provides additional automatic control of the reactor systems for safety against failure or improper operation of any component. The protective system is designed for reliability, with reactor scrams reduced to a minimum. Reactor setback (fast rod insertion) and alarms are used wherever possible. Scram, setbacks, and alarm signals are described in detail in Section 6–5.

The regulating and shim rods, which serve to control reactor power level during normal operation, have a rate which is limited to ensure that excessive reactivity cannot quickly be inserted by erroneous action. Safety rods which fall by gravity into the reactor core provide scramming action in the event other protective system action cannot adequately assure plant safety.

A strong negative prompt fuel temperature coefficient of reactivity provides automatic reactivity control over power surges. The negative over-all steady-state reactor power coefficient at full temperature gradient (460°F) further ensures that an increase in power is counteracted by a decrease in reactivity.

Primary containment for the sodium and inert gas atmosphere in the core tank is obtained by the combination of the core tank, core tank

bellows, linings of the loading face shield and ring shield, and by a cast low-melting alloy seal between the loading face shield and the ring shield.

The outer tank serves as secondary containment for sodium which may leak from the core tank. Outer walls of the double-walled inlet and outlet downcomer sodium piping attached to the outer tank also serve as secondary containment. In the event of a sodium leak from the core tank or downcomer piping the outer tank is sized so that the sodium level within the core tank would remain above the outlet nozzles. The cavity liner, which covers the concrete biological shielding surrounding the reactor cavity, provides additional containment for sodium and for the core tank atmosphere.

Concrete biological shielding adjacent to the reactor is continuously cooled by an organic coolant system to prevent excess thermal gradients and high temperatures.

The primary (radioactive) piping and equipment are located in concrete galleries which are below reactor floor level. These galleries form an integral part of the substructure and are lined with steel plate on the bottom and sufficiently high up the sides to serve as secondary containment in the event of any sodium leakage into the cells.

A nitrogen atmosphere is continuously maintained in the galleries. Use of inert gas reduces the oxygen content in the gallery atmosphere below that which will support sodium combustion and eliminates chemical reactions in the event of a sodium liquid or vapor leak into the cells. The nitrogen pressure is held slightly above atmospheric. The positive pressure minimizes oxygen in-leakage, while the low pressure differential minimizes nitrogen loss. Gallery oxygen content is continuously monitored.

Access to galleries is through stepped concrete hatches entered from the reactor floor level. These hatches are sealed to minimize vapor or gas leakage. The external surfaces of the galleries exposed to subsurface water are completely covered with a waterproof membrane. Steel gallery floor liners serve as an additional barrier to prevent leakage. The substructure is capable of withstanding earthquake loads and external water pressure.

Piping in contact with liquid sodium and sodium vapor is stainless steel and serves as the primary containment for these components. It is designed to withstand thermal stresses from normal and casualty operation of the reactor. Pressures in the system are sufficiently low that they are not critical in establishing pipe wall thicknesses. All joints are welded. Leak detectors are located on inaccessible sodium piping to indicate sodium leakage.

The elevation of the core tank suction nozzle is above the top of the moderator cans, so that the reactor core and reflector cannot be uncovered by pumping down the sodium level.

The reactor atmosphere relief valve is set to provide a minimum pressure differential between this atmosphere and that of the piping and equipment cells. The low pressure differential provides additional assurance that sodium cannot be forced out of the core tank below the level of the top of the moderator cans.

Sodium in the primary pumps is contained in the pump case and is prevented from reaching the pump bearings by the use of frozen sodium seals. These seals are backed up with an inert gas atmosphere in the pump, maintained at a slightly higher pressure than the liquid sodium. The inert gas atmosphere is in turn contained by mechanical seals.

All areas containing radioactive gas or contaminants are provided with gas seals to ensure against leakage to the reactor room or the routinely occupied areas. All systems are operated at low pressures, thereby minimizing both causes and effects of leakage to adjacent areas.

Gases which are normally radioactive are piped directly to shielded gas holdup tanks. Gases which are normally not radioactive are monitored before release to the atmosphere or to the gas holdup tanks as determined by the radiation level.

In addition to the gas-handling systems, the reactor area of the building is equipped with automatic air and gas monitoring devices which actuate an alarm system in the event abnormal radiation levels are detected. The building ventilation system is designed to cope with eventualities such as a leaky gas line, rupture of a gallery seal, or spillage of small quantities of radioactive sodium. Pressure differentials between areas are designed to minimize the spread of contamination and facilitate the control of any possible leakage of radioactive material to the building atmosphere.

Radioactive liquid waste is piped to a series of liquid holdup tanks. After adequate radioactive decay, it is concentrated to reduce volume. Final disposal is made at sea.

Instrumentation and control is provided for the purpose of rapidly detecting an off-normal condition in the reactor plant and, when necessary, to reduce reactor power level and coolant flow. This instrumentation and control system constitutes the reactor plant protective system. It is in addition to the plant control system, which serves to automatically regulate power generation during normal operation.

Off-normal conditions could originate from any of several causes, including failure of the plant control system, improper operation of a component while on manual control, and failure of a system component.

Some of the important safety features incorporated into the protective system are fail-safe circuits and equipment wherever possible, duplication of circuitry, so that failure of any one circuit leaves one or more other circuits intact and operable, and backup circuits using entirely different types of sensing elements.

Types of protective system action taken in the event of off-normal conditions include alarms, setbacks, and scrams. By combination of these various types of protective action, reliability is ensured while maintaining maximum practicable safety level.

Alarm annunciators which do not initiate automatic corrective action are provided to warn the operator whenever an important reactor variable reaches an off-normal condition. They include warnings from reactor auxiliary systems as well as from the principal reactor systems.

An off-normal condition arising within the reactor as a result of changes in reactor power level, coolant temperature, or coolant flow must be corrected before reactor temperatures or rates of change of temperatures become excessively high. Setback in reactor power level is the first automatic action to correct such conditions within the reactor. The setback is intended to correct any off-normal conditions in the reactor itself without a complete shutdown and without introducing further rapid temperature transients associated with scram.

If a power setback does not successfully correct off-normal conditions, a scram will be automatically initiated. One safety-rod drop and four safety-rod drop scrams may be initiated, depending on the condition. The four-rod drop causes the most severe transient; its use is limited to conditions which are potentially most hazardous (see Section 6–5).

The protective system is designed throughout to permit all possible action which could prevent a scram, when such alternatives are available, without endangering the reactor and personnel. A scram causes greater power loss, time delay, and thermal shock than other operator and protective system actions.

The neutron-absorbing rods include four safety rods which are used only for complete reactor shutdown, and four control rods, of which two can be used for shim or regulating control, depending on which drive speed range is selected, and two for shim control.

Separate safety rods are always withdrawn above the reactor core prior to operation of the reactor. In the event of a scram they fall into the core by gravity. These safety rods always have sufficient reactivity control to shut the reactor down, regardless of the position of the shim rods. Electrical interlocks are provided to ensure that control rods are not withdrawn until the safety rods are fully withdrawn and ready to scram. The safety rod latches are held in position by means of an electromagnet forcing against a spring. In case of electrical failure the safety rods fall into the core, regardless of the position of motion of the regulating and shim rods.

During a reactor scram, in addition to the safety rods being released to permit gravity fall into the reactor core, control rods are automatically

driven down at fast speed. This provides a backup which rapidly shuts the reactor down in case the safety rods should fail to drop by gravity.

Shim and safety-rod withdrawal speeds are limited absolutely by the use of induction motors whose speed cannot exceed synchronous speed. This limits the rate at which reactivity can be added due to shim and safety rod withdrawal, thereby eliminating the possibility of obtaining a short reactor period during rod withdrawal.

The total length of upward travel during fast motion of the regulating rod is limited both mechanically and electrically to substantially less than the amount which could put the reactor on a dangerously short period. When the automatic control system tends to drive the regulating rod beyond its normal operating range, the shim rods are slowly adjusted to permit the regulating rod to move back into its operating range through action of the automatic control system.

A strong regenerative neutron source ensures that a substantial neutron flux is always present for safe and controlled startup of the reactor. The source level neutron flux is registered by the instrumentation, providing assurance that the protective system receives signals at all power levels during startup. Startup is impossible if the source should be removed or if the low level neutron instrumentation should be inoperative.

Interlocks are provided wherever necessary to prevent improper manual action which could damage the plant.

Electric power for normal plant operation is available from both the external power supply and the generator in the reactor plant. An alternate power supply is thus provided whenever either an internal or external power outage occurs. In the event that both these normal sources of power should fail simultaneously, electricity would be supplied by the emergency power system (batteries and diesel) for vital loads only.

The upper reactor plenum contains a large quantity of liquid sodium which mixes with sodium flowing out of the fuel channels before discharge into the heat-transfer circuits. In event of overheating of sodium in any of the fuel channels, the upper plenum mixing ensures that localized or transient high temperatures would be reduced. If any sodium vapor should be formed in a fuel channel, which could possibly happen with the formation of a severe restriction, the vapor would be condensed in the upper plenum and there would be no significant pressure rise. During full-power operation the upper plenum sodium temperature is approximately 700°F below the sodium boiling point.

Natural convection flow in the sodium coolant loops is sufficient to remove after-glow heat from the reactor after shutdown in the unlikely event of the simultaneous loss of power to all coolant pumps. Natural sodium convection flow also occurs within the reactor to provide distri-

bution of heat and prevent excessive localized temperatures. An eddy-current brake is provided to match sodium coolant flow with power generation, to maintain constant fuel-channel outlet temperature during the most severe transient period.

If the sodium coolant loops should fail in their heat-removal function after a shutdown, the large heat capacity of the core structure, and particularly of the graphite moderator, would ensure a slow reactor temperature rise. In such an event sodium convection flow within the core tank would provide distribution of fuel after-glow heat within the reactor, transferring heat to the graphite and to outer elements of the reactor structure, from which it would eventually be carried away by the organic biological shield coolant.

The SRE thus exemplifies the safety possible in sodium graphite reactors. Chief areas of safety are in control design and in taking advantage of the naturally occurring favorable factors in this moderator-coolant combination.

References

1. S. Glasstone and M. C. Edlund, *The Elements of Nuclear Reactor Theory*. New York: D. Van Nostrand Company, Inc., 1952.

2. J. R. Risser et al., *Surface to Mass Dependence of Effective Resonance Integrals for Uranium 238 Cylinders*, USAEC Report ORNL-958, Oak Ridge National Laboratory, March 1951.

3. E. Richard Cohen, The Neutron Velocity Spectrum in a Heavy Moderator, *Nuclear Sci. and Eng.* **2,** 227 (1957).

4. F. L. Fillmore, North American Aviation, Inc. Unpublished.

5. Eric Hellstrand, Measurements of the Effective Resonance Integral in Uranium Metal and Oxide in Different Geometries, *J. Appl. Phys.* **28,** 1493 (1957).

6. H. L. Garabedian, *Theory of Homogeneous Control of a Cylindrical Reactor*, USAEC Report AECD-3667, Westinghouse Atomic Power Division, June 1954.

7. W. T. Hayes and F. L. Fillmore, North American Aviation, Inc. Unpublished.

8. G. W. Rodeback, *Temperature Coefficients of Uranium and Thorium Resonance Integrals*, USAEC Report NAA-SR-1641, North American Aviation, Inc., September 1956.

9. R. L. Ashley and D. S. Duncan, *The Theoretical Calculation of the Attenuation of Gamma Radiation from a Swimming Pool Type Reactor*, USAEC Report NAA-SR-1921, North American Aviation, Inc., August 1957.

10. A. R. Vernon, *Analysis of the Biological Shield of the Sodium Reactor Experiment*, USAEC Report NAA-SR-1949, North American Aviation, Inc., June 1957.

11. D. S. Duncan, *The Calculation of Gamma Ray Heating in Target Samples Located in the BSR Shield*, USAEC Report NAA-SR-2557, North American Aviation, Inc., 1958.

12. W. J. Freede and T. T. Shimazaki, Determining Coolant Flow in SRE Fuel Elements, *Nucleonics* **15**(2), 64–67 (February 1957).

13. W. J. Freede and T. T. Shimazaki, Heat Transfer and Hydraulic Characteristics of the SRE Fuel Element, in *Reactor Heat Transfer Conference of 1956*, USAEC Report TID-7529, Nuclear Development Corporation of America, November 1957. (Book 1, Part 1)

14. R. A. Seban, Heat Transfer to a Fluid Flowing Turbulently Between Parallel Walls with Asymmetric Wall Temperatures, *Trans. Am. Soc. Mech. Engrs.* **72,** 789 (1950).

15. W. B. Harrison and J. R. Menke, Heat Transfer to Liquid Metals Flowing in Asymmetrically Heated Channels, *Trans. Am. Soc. Mech. Engrs.* **71,** 797–803 (1949).

CHAPTER 4

MATERIALS REQUIREMENTS

4–1. Sodium Technology

Liquid sodium is no longer considered an exotic material in industrial applications. Its use as a heat-transfer medium at high temperature has become relatively common. General technology of sodium systems has been described in a Liquid Metals Handbook and a subsequent sodium supplement to this handbook [1].

Certain aspects of sodium technology are unique to the sodium-graphite reactor system, however, and those specifically applicable to the SRE are discussed here.

Liquid sodium below 1000°F, when highly purified, is inert towards most structural metals. Stainless steel and zirconium show no reaction toward sodium in this temperature region. The constituents of stainless steel exhibit solubility in sodium, but this phenomenon is too minor to be important at temperatures present in the SRE. Beryllium has shown some apparent penetration by sodium, but since the beryllium present in the SRE is not a structural material and this penetration is small, it is not a problem.

Impurities are always present in sodium, and the problems of materials compatibility with sodium arise from the reactions of reactor metals with these impurities. Integrity of reactor components in sodium depends on adequate control of certain of these impurities during operation. Other impurities present in sodium are subject to activation in a strong neutron field and must be eliminated so that later accessibility and component handling in the reactor will not be hindered. Still others are nuclear poisons, whose presence requires excess fissionable material in reactor fuel.

Control of the latter two types of undesirable impurities, i.e., elements with long-lived isotopes and nuclear poisons, must be accomplished during manufacture of the sodium. Purchasing specifications limit the increase in thermal neutron absorption cross section of the sodium caused by the presence of nuclear poisons to no more than the equivalent of 20 ppm of boron. Examples of the concentration of various elements which cause an increase in cross section equivalent to 20 ppm of boron are shown in the following list.

Element	*ppm maximum*
Boron	20
Lithium	150
Cadmium	4.5
Gadolinium	0.5
Samarium	1.0
Europium	3.0
Mercury	40

Effective neutron absorption cross section for sodium loaded into the SRE, as determined by danger coefficient measurements in the AE-6,* confirmed that these specifications were met.

Specifications for the allowable limits of concentration of elements that may give rise to long-lived activated species under neutron irradiation require that radiation from impurities in 1 gram of sodium be less than 10 r/hr at 1 centimeter, after eleven days cooling from an irradiation of 1 year in a flux of 10^{14} neutrons/cm^2·sec. The maximum concentrations of several impurities which, if present alone, would fulfill this requirement are shown in the following list.

Impurities	*ppm*
Cobalt	2
Cesium	6
Iron	300
Rubidium	100
Scandium	0.5

Neutron activation analysis of the sodium for the SRE has shown conformity with this requirement.

Another class of undesirable impurities in sodium that enter into chemical reaction with structural materials are the nonmetals oxygen, hydrogen, nitrogen, and carbon. Oxygen is the most troublesome of these. In amounts approaching saturation concentration, which varies with temperature, oxygen is likely to precipitate as Na_2O in cold regions of the sodium system. If permitted to continue, such precipitation causes plugging and stoppage of coolant flow. Smaller amounts of oxygen, in the neighborhood of 100 ppm, will react with stainless steel components of a sodium system in areas in which the temperature exceeds 1000°F. For massive structural members the rate of this oxidation is too low to cause concern, but if the proper combination of oxide level and temperature is present at a thin membrane, as in a bellows, failure can occur.

* An Atomics International homogeneous, solution-type reactor.

At any measurable concentration oxygen will react with zirconium above 750°F, with the rate dependent on the temperature. Zirconium, therefore, becomes the limiting material so far as the permissible oxygen level is concerned. This subject is discussed further in Section 4–3.

Oxygen in sodium also causes problems due to transport of matter on a microscopic scale, as compared with the relatively macroscopic nature of corrosion reactions. Even though the original sodium may have been purified to remove elements vulnerable to long-lived activation, high oxygen levels in the sodium facilitate the solution and subsequent deposition of activated species formed in core structural materials. Distribution of these isotopes throughout the sodium system external to the core causes problems of accessibility and renders maintenance operations difficult.

Hydrogen is present in liquid sodium as the hydride, NaH, which will react with metals whose hydrides are more stable than that of sodium. In the SRE, the only such metal present is zirconium, which reacts readily with hydrogen or sodium hydride to form a solid solution of hydrogen in the metal. On further reaction with hydrogen, a second phase of zirconium hydride needles precipitates at zirconium grain boundaries. This second phase imparts impact sensitivity and lower fatigue life to the zirconium (Section 4–3). The presence of hydrogen in the system has no noticeable effect on stainless steel under SRE operating conditions.

The effect of carbon on steel must be mentioned. The means by which carbon is transported in sodium and the species in which it is present are unknown, but experiments have shown that carbon redistribution does take place under proper conditions in a sodium system. Carburization of 18-8 stainless steel does not begin at temperatures below 1050°F, so it is not anticipated that embrittlement or fatigue failure from this cause will be a factor in the life of SRE components.

Since the presence of the impurities mentioned has been found to be detrimental to the operation of a sodium system such as that in the SRE, control measures must be taken to ensure adequate purity of the sodium on loading and to maintain purity during operation. Adequate purchasing specifications provide sufficiently low levels of metallic impurities in the as-loaded sodium. The first SRE sodium loading has shown this to be practical. For nonmetallic impurities, manufacturing control is not sufficient, since contamination during handling and operation is inevitable.

The presence of oxygen in the sodium system is potentially the cause of most problems. Consequently, more effort is expended in removing oxygen than on other purification operations. Removal of large amounts of oxygen is achieved by means of a *cold trap*, a bypass line on the sodium system which contains a cooling section and a filter to collect sodium oxide precipitated in the cooled sodium. (Article 6–2.9). This equipment,

if properly designed, will lower the oxide concentration of the sodium system from several hundred parts per million to about 20 ppm, which is adequate for protection of steel components from gross corrosion. However, because radioactivity transfer might still be troublesome, and oxidation of zirconium will definitely take place (Section 4–3), a more intensive means of oxygen removal is necessary. For the SRE, a *hot trap* consisting of zirconium foil in a configuration maximizing surface area exposed to sodium was chosen to reduce further the oxygen content from the 20 ppm level to less than 5 ppm (Article 6–2.9). The hot trap is operated at a temperature about 200°F above that of the sodium in the core, or at about 1200°F, thus providing a marked increase in rate of oxidation over that for the zirconium moderator cans.

No specific measures have been taken for the removal of hydrogen from SRE sodium, but much of it will be removed with the zirconium hot-trap filler. The rapid rate of the zirconium-hydrogen reaction at hot-trap temperature will result in a hydrogen concentration in the hot-trap zirconium that is far higher than would be reached if equilibrium were attained with the zirconium in the core.

Because carburization of stainless steel components will not take place at reactor core temperatures, no special measures have been taken for removing carbon from the sodium. However, the steel jacket of the zirconium hot trap will be well above the carburization threshold temperature and will provide a *sink* for carbon in the system. Since the walls of this steel jacket are quite thick, no failure is expected from carburization.

Effectiveness of impurity control measures must be determined, and analysis procedures are in effect at the SRE. Quantitative analysis by conventional wet chemistry and spectrographic methods on as-received sodium has shown that the specification values for metallic impurities were not exceeded. Previously mentioned reactivity value determinations and subsequent effective cross-section calculations demonstrated adequate purity with respect to nuclear characteristics.

A Materials Evaluation Facility is incorporated into the SRE to provide a means of obtaining samples of sodium, stainless steel, and zirconium which have been exposed to primary system sodium coolant at core outlet and core inlet temperatures. This facility consists of two vertical $2\frac{1}{2}$-inch pipes in parallel with the reactor core. The inlet of one pipe is connected to the discharge side of the core, the inlet of the other to the inlet piping. Access to these hot and cold legs is through conventional liners and shield plugs equipped with freeze seals to limit the rise of sodium. Within each leg is a spindle containing a sodium sampler and sample holders for specimens of structural metals. With the primary system pump operating, sodium flows through both legs, exposing the metal samples and the sodium sampler to continuously circulating sodium. Operations involving

the removal and replacing of components in the Materials Evaluation Facility are carried out with the fuel-handling cask.

Samples of sodium taken from this facility after various periods of reactor operation are analyzed to determine changes in impurity level as a consequence of reactor operation. As mentioned earlier, the most important aspect is determination of metallic impurities that are nuclear poisons or accessibility hazards. Analysis for oxygen in sodium removed from the primary system supplements information from plugging meters. This latter device determines the temperature at which precipitation begins by means of an orifice plate introduced into the flowing sodium. Comparison of the precipitation ("plugging") temperature with the solubility curve for oxygen in sodium gives a measure of the oxygen concentration.

Exposed coupons of zirconium and stainless steel are removed after various intervals of reactor operation. Radiochemical analysis of the steel specimens indicate to what extent the transport of radioactive species has occurred in the primary sodium system. From determination of the extent of oxidation and hydriding of zirconium specimens, the condition of moderator cans and the zirconium hot-trap filler may be deduced. These data will determine the life of the hot trap, so that it can be removed before the filler has become oxidized to the point of physical degradation.

4–2. Graphite Technology and Development

Artificial graphite has long been one of the mainstays of reactor technology. As a neutron energy absorber (moderator), it combines the very low absorption cross section and good thermalizing power of carbon with excellent mechanical and refractory qualities and chemical stability. It has the added advantage of being a standard commercial product of well-advanced technology and modest cost.

Graphite from good to extreme purity is required for reactor use. Increase in density above that of ordinary commercial grades is also desirable, to the greatest degree consistent with reasonably unimpaired mechanical properties. In the United States the graphite manufacturing industry has consistently worked to meet these demands, and today it is possible to procure graphite consistently of 1.70 to 1.75 g/cm^3 apparent density, and with absorption cross section for thermal neutrons of 0.0036 to 0.0038 barn.

Maximum purity and maximum density are to a degree mutually exclusive. Density is raised by repeated reimpregnations with pitch, which both directly and indirectly raises the impurity level. Maximum purity is achieved by volatilization processes which both require and increase porosity. Furthermore, these extra steps in the graphite manufacturing process add to the cost. In the United States a highly purified graphite of

density near 1.75 costs approximately twice as much per pound as ordinary chemical grade graphite of density 1.65 and cross section 0.0055 barn.

Utilization of graphite in the SRE was restricted to products of standard manufacturing methods, about which sufficient knowledge of physical, mechanical, and irradiation properties was available to permit reasonable design calculations. The core configuration chosen, of hexagonal graphite members approximately 11 inches across the flats, exploited standard graphite extrusions of circular cross section, shaped by standard machining and boring operations. The core height, approximately 10 feet, was accomplished by joining three graphite sections end-to-end instead of attempting extra long extrusions. The reactor was designed assuming a graphite density considered attainable with assurance in 1954, 1.65 g/cm^3.

For neutron economy, graphite of exceptional purity was selected for the SRE. While this might not be most economical for a large power installation, it is clearly so for an experimental reactor whose entire fuel loading may be changed several times in as many years. An equally important reason for selecting purified graphite was the problem of outgassing during service. The earliest SRE design called for hermetically sealed cans to protect the moderator elements; gas evolution from the graphite must then be minimized in order not to exceed the external pressure and bulge the jackets. Even though the final design specified *schnorkels* (breathing tubes) on the moderator cans, the philosophy of minimum outgassing of the graphite was adhered to from the point of view of minimizing corrosion damage to the zirconium cans.

These and other considerations led to the following set of specifications for SRE moderator/reflector graphite:

(1) Raw materials were to be selected by the supplier specifically to avoid chemical impurities of high cross section; processing, machining, handling, and shipping procedures were to be controlled so as to avoid chemical contamination.

(2) Graphitization was to be complete.

(3) Density of the product was to be not less than 1.65 g/cm^3 average, nor less than 1.63 g/cm^3 for any individual piece.

(4) Ash content was to be not more than 0.05 percent for any sample.

(5) Total gas evolution when heated in vacuo at 1832°F was to be not more than 0.15 times the apparent volume for any sample, the gas volume being computed at normal temperature and pressure.

(6) Specimens were to be submitted for nuclear evaluation in the Hanford 305 Test Pile; no sample was to show less than −0.25 d.i.h. when compared with the Hanford standard.*

* The "difference in inverse hours" between a test bar of graphite and the Hanford standard material is an experimental measure of the cross section of the graphite. The specification given corresponds to an effective cross section of approximately 0.0046 barn.

(7) The product was to be machined to specified tolerances, of uniform strength, and free from tears, voids, breaks, or other defects.

(8) Each piece of graphite was to be identified as to its manufacturing history, so that this might be correlated with conformity to specifications and with performance in the reactor.

The graphite purchased for the SRE under these specifications was supplied by National Carbon Company, the grade designated by the vendor as "TSP." Raw materials were selected for low ash content and, in particular, for low boron impurity. The relatively coarse grain size permitted effective chlorine purification, and the double pitch-reimpregnation employed in manufacture met the density requirement. The product was cooled in helium from the graphitization step in order to minimize reaction or chemisorption of atmospheric gases.

Graphite of this quality has a microscopic absorption cross section for thermal neutrons of approximately 0.004 barn and a diffusion length of approximately 53 cm. Fission neutrons are thermalized in a root mean square distance of 19 cm. The unirradiated material has a thermal conductivity of approximately 100 Btu/ft^2·hr per °F/ft at 950°F. Coefficients of thermal expansion are 8×10^{-7}/°F and 15×10^{-7}/°F, respectively, in directions parallel to and perpendicular to the axis of extrusion. Compressive strength is of the order of 6000 lb/in^2, and tensile strength is about 1400 lb/in^2.

Study of the interaction of liquid sodium and graphite indicates that all types of graphite require protection of the sort provided in the SRE design. Beyond the neutron "poisoning" effect of sodium absorbed in the graphite pores, another engineering problem may arise out of the swelling that attends the absorption of sodium. Figure 4–1 illustrates the dilation encountered; spalling and cracking accompany this phenomenon in large graphite bodies. The problem of protection is basically no different from

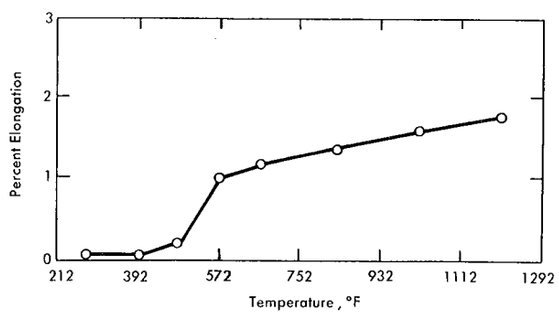

FIG. 4–1. Dilation of TSP grade graphite due to absorption of sodium.

that of isolating the fuel from the coolant, however, and in the SRE the solution was essentially the same, i.e., to encase the graphite elements in close-fitting metal cans.

The choice of zirconium for the moderator/reflector element cans represented a pioneering venture, since the service characteristics of this metal in the anticipated SRE environment were not as yet fully detailed. This design decision was followed by intensive study of forming, fabricating, welding, and testing procedures, stress analysis, and investigation of chemical and metallurgical properties. Progress in some of these studies is related in Section 4–3. Final design of the zirconium cans specified 0.035-inch rolled sheet side walls, formed individually and butt-welded down the center of each face of the hexagonal prism; 0.100-inch-thick end caps with reinforced welds to the side walls; and the schnorkel vent tubes previously mentioned. Lined center bores and corner scallops (three mating scalloped corners creating a cylindrical opening) accommodated the numerous fuel, coolant, and control tubes. "Dimpling" of the side walls provided inter-can spacing for the flow of coolant among the moderator elements. Complete details of design, as well as illustration of finished moderator elements, will be found in Chapter 6.

Two moderator elements and two graphite-filled corner-channel tubes were instrumented to continuously measure the temperature at numerous points within the graphite, as well as the gas liberated by the graphite during reactor operation. As of this writing, the SRE has undergone an extended period of operation at about one-third of designed thermal output; during this period the instruments indicated a maximum temperature gradient within the graphite of about 3°F/inch. No detectable outgassing has occurred, nor has any significant change in composition of the graphite pore atmosphere been observed. These measurements will be continued during future operation of the reactor.

Other graphite studies in progress in the SRE core include the effect of high-temperature irradiation on physical dimensions and thermal conductivity. Preirradiation measurements have been completed; after reactor operation of approximately one year, postirradiation comparisons will be conducted. Meanwhile, parallel studies indicate an irradiation-induced drop in thermal conductivity at room temperature to about one-fourth the original value, and irradiation-induced dilation of less than 0.1 percent.

A study of the nature of the attack of sodium on graphite has been started. One of its objectives is to evaluate new, novel, or experimental graphite-base materials for resistance to sodium. None so far studied has been significantly superior to ordinary graphite. Methods of coating graphite with metals to replace or supplement the zirconium can of the SRE are being explored.

The outgassing behavior of graphite has been the subject of another study only recently initiated, as a result of renewed interest in the use of sealed moderator cans. Thermal and simulated irradiation outgassing experiments are in progress using several grades of graphite; these will supplement the in-pile experiment already described. Limited studies are also being conducted of radiation damage and annealing mechanisms in graphite at elevated temperatures.

Economic evaluation of several graphite grades in power-station reactor situations has been attempted. With the graphite contribution to capital costs as one index and the expense of fuel quantity or enrichment as the other (and assuming there is a known relationship of each variable to graphite nuclear quality), ordinary and premium grades of graphite were compared. Estimates of net power cost contributions for a 100,000-kw plant were remarkably close, within 0.2 mil/kwh, with "ordinary" mold-grade graphite having the apparent advantage.

The continued support and cooperation of graphite manufacturing concerns in the United States must be acknowledged here. Significant contributions to scientific literature, advancements in the art of production, improvements in properties of the product, and adventures into experimental materials radically different from conventional graphite, are attributable to an enlightened and technically expert industry.

The reader interested in details of graphite science will find a comprehensive treatment of the physical properties of this material in a book to be published in 1958, by R. L. Carter [2]. Also available is a publication by S. C. Carniglia [3] which includes a review and interpretation of work on sodium-graphite interactions.

4–3. Zirconium Technology

Compared with stainless steel, zirconium has a significant technical advantage for use in the core of a nuclear reactor. It has an absorption cross section for thermal neutrons of only 0.18 barn, as compared with over 3 barns for stainless steel. The high-temperature strength of zirconium is not particularly great, but proper design of components permits its use at temperatures up to 1000°F. At this temperature the 0.2 percent offset yield stress is over 10,000 psi. Since the addition of small amounts of alloying elements more than doubles the tensile properties of zirconium, future high-temperature reactors may use zirconium alloys instead of the pure metal. Fabrication difficulties with zirconium have been minor, and present technology permits forming any shapes required. The starting materials for fabrication—sheets, plates, and tubes—are easily formed. Inert gas welding techniques with proper torch and fixture design have made zirconium welding a routine operation.

Balanced against these favorable factors are some undesirable features, including: high cost of obtaining reactor grade metal, extreme reactivity of zirconium toward oxygen and hydrogen, and the tendency of zirconium to form exaggerated grains at high temperature.

Mass production techniques and constantly advancing technology are bringing the cost of zirconium down rapidly. For example, the cost per pound has been lowered from $150 in 1948 to $7 in less than ten years.

Reactivity with gases cannot be easily dismissed; it is necessary to understand the reactions of zirconium with oxygen and hydrogen in various media so that adequate measures may be taken to minimize undesirable effects. Since the SRE involves contact between zirconium and molten sodium, research has centered on the reactions of zirconium with impurities dissolved in sodium. Pure sodium is inert with respect to zirconium but, as the discussion in Section 4–1 of this chapter indicated, *pure* sodium is practically unobtainable for reactor use. Consequently, reactions of zirconium with gaseous impurities are of major importance. Oxygen dissolved in sodium will react with zirconium in the system according to the equation $\frac{1}{2}\,\mathrm{Zr} + \mathrm{O} \rightarrow \frac{1}{2}\,\mathrm{ZrO_2}$. The large free energy of formation of zirconium oxide provides a powerful driving force for the reaction, with concentration of oxygen being of little importance. Since oxygen is present in liquid sodium as oxide anions, the combination of dissolved oxygen with zirconium does not involve a change in state of the oxygen.

When oxygen is present in sodium in detectable amounts (the present lower limit of detection is about 5 ppm), it reacts with zirconium to form an adherent layer of zirconium oxide. The oxide then diffuses inward from the oxide-metal interface, driven by a concentration gradient. The rates for both oxidation and diffusion of oxygen in zirconium are strongly temperature dependent.

The rate of oxidation of zirconium in oxide-containing sodium has been studied in dynamic sodium systems at temperatures between 700 and 1200°F, with oxygen levels from essentially zero to about 65 ppm. Oxidation rate, as measured by weight gain attributable to oxygen, can be described by the equation

$$w = kt^{1/2}, \tag{4–1}$$

where w is oxidative weight gain per unit area in time t, and k is the rate constant for a given temperature. The rate constant k may be expressed as a function of temperature by

$$k = Ae^{-\Delta E/RT}, \tag{4–2}$$

where ΔE is energy of activation for the oxidation, R is the molar gas constant, T is the absolute temperature, and A is a constant. Equation 4–1

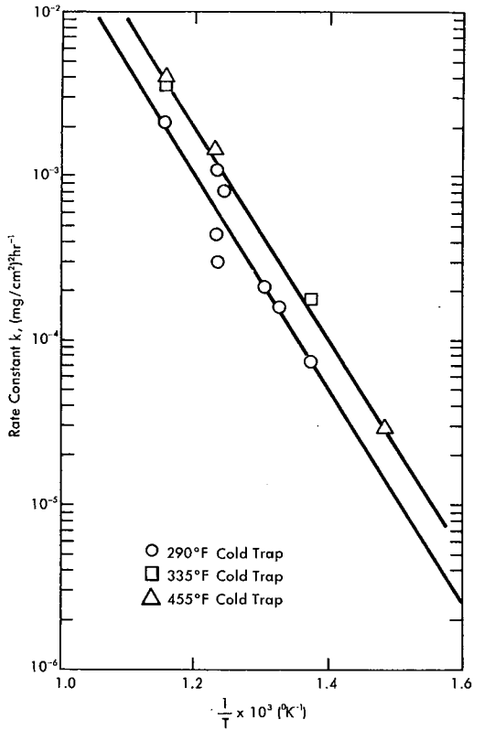

FIG. 4–2. Weight-gain rate data for reactor-grade zirconium in liquid sodium.

for weight gain as a function of time holds well over the 700 to 1000°F temperature range, with some decrease in the exponent of t (to about $\frac{1}{3}$) above 1000°F.

When rate constants k derived from isothermal weight-gain data are plotted against reciprocal absolute temperature in a conventional Arrhenius plot, the data fall in a good line. From the slope of this line, shown in Fig. 4–2, the activation energy for oxidation, ΔE, is found to be 29.2 kcal/mole, with an estimated uncertainty of about 1 kcal. Dependence of the oxidation rate on oxygen level in the sodium is small above 20 ppm. At lower concentrations the rate drops off with decreasing oxygen level until no oxidation is detectable in sodium with unmeasurable oxygen.

Diffusion constant D for the concentration gradient diffusion of oxygen in zirconium may be expressed as a function of the absolute temperature T by the equation [4,5]

$$D = 9.4e^{-51,780/RT}, \qquad (4\text{–}3)$$

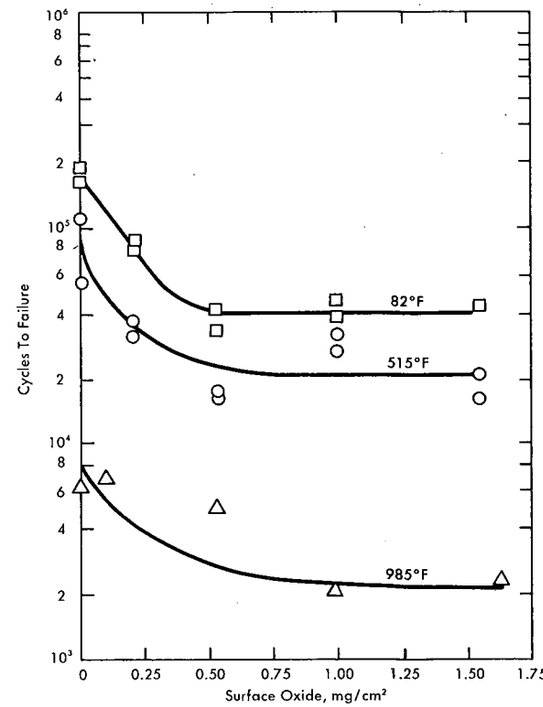

FIG. 4–3. Fatigue cycles to failure.

which, at 1100°F, gives a value for D of about 10^{-12} cm²/sec. Using the approximation that the square of the penetration is equal to the product of D and the time, at 1100°F a depth of oxygen penetration of 0.05 cm would occur in one year.

The presence of oxide films on zirconium is important in sodium graphite reactor technology because of marked decrease in fatigue life and increased sensitivity toward impact failure [6]. A surface oxide layer equivalent to a weight gain of 0.5 mg/cm² on 0.035-inch sheet causes a decrease in number of fatigue cycles to failure to about one-fourth that shown by unoxidized material (Fig. 4–3). This decrease in fatigue life occurs at temperatures up to the highest studied, 985°F. Surface oxide acts as a crack initiator in a fatigue situation. Since the oxide is extremely adherent to the substrate metal, cracks formed in the oxide readily propagate into the metal and result in failure.

Hydrogen is present in sodium as dissolved NaH. Therefore any elements whose hydrides are more stable than NaH will react to form the

more stable product. Zirconium reacts readily with dissolved hydrogen in sodium to form ZrH_x, zirconium hydride, which has appreciable solubility in zirconium at high temperature. Since the rate of reaction with hydrogen and the equilibrium concentration in zirconium are influenced oppositely by increasing temperature, the situation at any given time is difficult to predict. Such other variables as oxide film present on the metal and hydrogen pressure over the sodium add uncertainty to any prediction.

Hydrogen dissolved in zirconium has little effect on its mechanical properties and gives no reason for concern, although a second phase of zirconium hydride needles precipitated along metal grain boundaries does impart impact sensitivity and brittleness. These hydride needles will precipitate any time the hydrogen solubility is exceeded at any temperature. For example, at 300°F as little as 10 ppm of hydrogen will form significant grain-boundary hydride on slow cooling from higher temperature.

Another phenomenon which can occur in zirconium in a sodium reactor environment is strain-nucleated grain growth [7]. In a thermal environment above 950°F recrystallization occurs if nuclei are present on which new grains can form. Very coarse-grained structures are developed if the metal has been plastically strained a critical amount and later annealed. When the metal is work-hardened, as in manufacturing processes, local microscopic areas of high peak stresses are formed. These regions of high energy are caused by slip, bending of atomic planes, twinning, and grain-boundary movement during deformation. They constitute potential nuclei for recrystallization. The greater the strain, the more potential nuclei are formed and the higher the microscopic peak stresses. Annealing the metal in its recrystallization range results in the growth of these nuclei into new stress-free grains.

The new grain size formed on recrystallization is determined by the rate of nucleation of new grains and the rate at which they grow. Low nucleation rate and high growth rate lead to a coarse-grained structure. This situation exists in zirconium which has been strained a critical amount and annealed at a temperature above 950°F. Figure 4–4 shows the critical strain for germinative grain growth as a function of temperature for zirconium strained at different temperatures. The effect of exaggerated grains as a result of germinative grain growth is to lower the fatigue life. Data are scattered, but a reduction in fatigue life by a factor of two to six is found whenever any germinative grain growth is seen.

In spite of the undesirable features of zirconium in a liquid sodium reactor environment, its advantages are such that it is worth while to take measures to minimize the extent to which unfavorable phenomena occur. Reduction of the sodium oxide level in sodium is a major effort in this

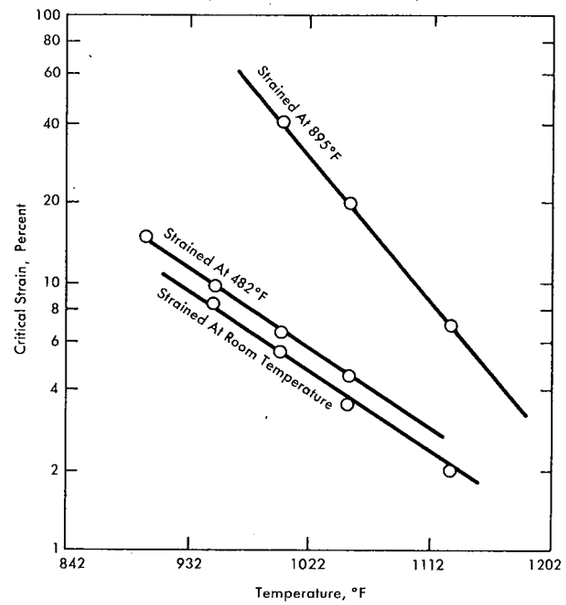

FIG. 4–4. Grain growth of zirconium.

direction (Section 4–1). Inclusion of a hot trap in the SRE is required only because of the presence of zirconium in the system.

To minimize the possibility of fatigue failure, an eddy-current brake has been installed in the SRE to control sodium flow during transient periods of reactor operation. This will alleviate rapid temperature changes, which give rise to repeated flexing of zirconium cladding material.

Control of germinative grain growth in unalloyed zirconium is not feasible by any means other than placing a temperature limitation on zirconium members in the reactor. In the SRE an upper temperature limit of 950°F has been set for zirconium moderator cans and process channels.

Future sodium-graphite reactors will not suffer from the many limitations imposed by zirconium, since present research on alloys is providing materials with lower oxidation rates and less susceptibility to germinative grain growth.

REFERENCES

1. C. B. JACKSON (Ed.), *Liquid-Metals Handbook—Sodium (NaK) Supplement*, U. S. Atomic Energy Commission and U. S. Navy. 3rd ed. Washington, D. C.: U. S. Government Printing Office, 1955.

2. R. L. CARTER, *Graphite and Carbonaceous Moderator Materials.* New York: Prentice-Hall, Inc., 1958.

3. S. C. CARNIGLIA, Interactions of Graphite with Liquid Sodium, in *Proceedings of the French-American Conference on Graphite Reactors, Nov. 12–15, 1957*, USAEC Report BNL-489, North American Aviation, Inc. (Session V, Paper C-27).

4. J. PAUL PEMSLER, *The Diffusion of Oxygen in Zirconium and Its Relation to Oxidation and Corrosion*, USAEC Report NMI-1177, Nuclear Metals, Inc., May 31, 1957.

5. A. W. LEMMON, JR., *Studies Relating to the Reaction Between Zirconium and Water at High Temperatures*, USAEC Report BMI-1154, Battelle Memorial Institute, January 1957.

6. J. C. BOKROS, *Effect of Sodium on the Mechanical Properties of Zirconium*, USAEC Report NAA-SR-1867, North American Aviation, Inc., June 15, 1957.

7. J. C. BOKROS, *Germinative Grain Growth Characteristics of Zirconium*, USAEC Report NAA-SR-1926, North American Aviation, Inc., June 15, 1957.

CHAPTER 5

FUEL ELEMENT DEVELOPMENT

5–1. BASIC CONCEPT

The fuel element is probably the most important item in the reactor in terms of total cost. Economic studies indicate fuel costs represent from 25 to 50 percent of the long-term total cost. The choice of fuel design and material is affected by four main aspects: the general reactor concept, the method of manufacture, performance in the reactor, and reprocessing. It is necessary during the choice of a fuel material to evaluate the over-all process flow of these materials. Even after almost ten years of intensive reactor development this is a most difficult task. Evaluation is naturally based on cost. The basis for economic studies is constantly changing, and as the U. S. atomic energy effort changes more from government-sponsored to commercial enterprise, a constant reappraisal is required. Only recently have commercial prices been available on such processing operations as UF_6 to U ingot, and scrap recovery. Reprocessing itself is completely an AEC-sponsored activity, and quotations have only recently been available. This is merely a brief reference to the importance of fuel material economics and to the large topic of the relation of fuel cost to the choice of a specific material.

Technical problems involved with fuel materials are outlined as follows:

Stresses due to elevated temperature, radiation damage, and accumulation of fission products.
Reactions between the clad and the fuel.
Reactions between the fuel and the coolant in case of rupture of the clad.
Reaction between the clad and the coolant.

Of these factors, the most predominant is radiation damage at elevated temperature. There have been no civilian reactors operating under the temperature conditions anticipated in the present SRE type. It is true that some reactors have a greater temperature difference across a fuel slug, but none has both a high central temperature and a high surface temperature. The general configuration of the SRE fuel element is shown in Fig. 5–1.

Fuel elements are fabricated in the form of seven-rod clusters. Each rod consists of a column of 6-inch uranium slugs in a thin-walled stainless

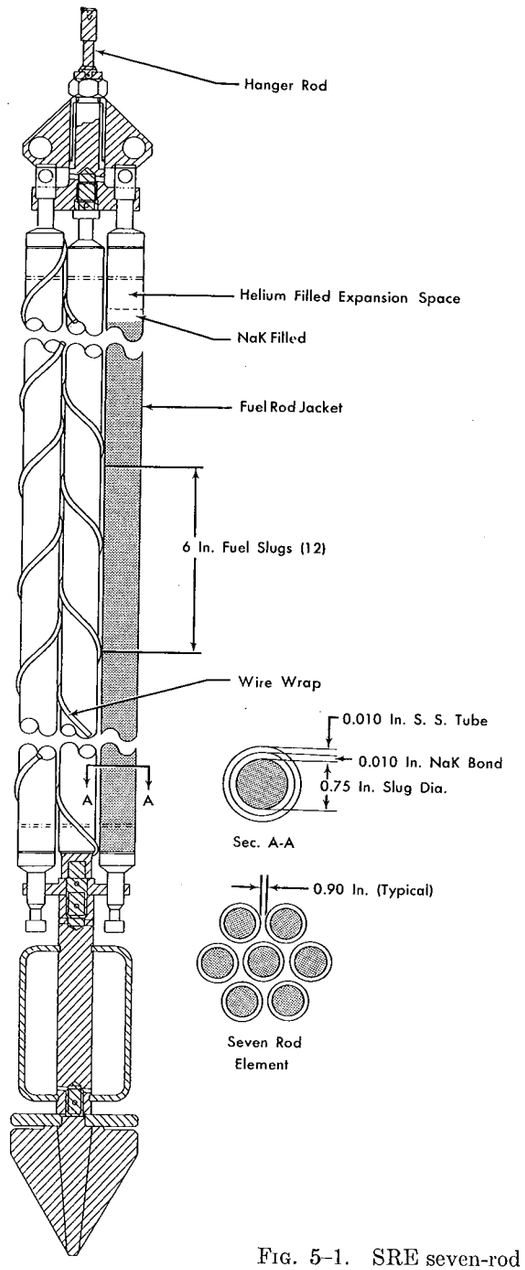

FIG. 5–1. SRE seven-rod fuel element.

steel tube, thermally bonded by NaK alloy. The slugs are 0.750 inch in diameter; the jacket tube is 0.010 inch in wall thickness, and the NaK annulus is 0.010 inch thick. The jacket, of Type 304 stainless steel, is closed at each end with a welded plug. The NaK bonding alloy extends a few inches above the slug column to a free surface. The space above the NaK provides for the thermal expansion of the NaK, and for the accumulation of gaseous fission products during irradiation. A spiral wire wrap around each of the outer six stainless steel tubes separates the fuel rods. This permits the sodium to cool the center rod and the inner surfaces of the peripheral rods, and serves to improve heat transfer by providing a more turbulent flow.

Surface temperature of the fuel is essentially set by the sodium temperature, allowing for a small temperature drop across the stainless steel clad and the NaK bond. Along the rod length, sodium temperature varies from 500 to 950°F. The fuel center temperature has been set by the alpha-beta phase transformation at 1200°F. This upper limit was based on consideration of the change in volume resulting from the phase change and on thermal-cycling results that indicated gross distortion effects.

Dynamic variation in temperature conditions within a single rod further complicates the problem. Self-shielding in the fuel material creates a nonuniform flux distribution within the fuel slugs, with a resultant nonuniform heat generation and nonuniform fission product buildup. Because of the resulting nonsymmetry of temperature, stresses, and physical property change, warping of the slugs is likely, and for this reason, short (6 inch) slugs are used. An alternative fuel element design which uses a series of single hollow slugs each 4 inches in length (Fig. 5–2) eliminates the probability of warping.

Timing of the fabrication of the fuel was another prime factor in the choice of the main fuel material. The choice had to be made in the summer of 1954. At that time, the initial cast uranium-zirconium alloys made by Argonne National Laboratory were showing generally excellent radiation stability. However, use of this alloy required large-scale development of homogeneous ingots and subsequent processing. Some of this development was accomplished at Fernald over a period of a few months, and subsequently there were a few inconsistencies in the early irradiation results. A decision was therefore made to use as the main fuel in the first core loading a standard, off-the-shelf material, i.e., alpha-rolled, beta heat-treated uranium.

As the fuel program will indicate, there was considerable flexibility, to allow for improvement.

The major problems of operating metal fuels at high surface temperature have only recently been known. Under the SRE conditions four aspects may be listed:

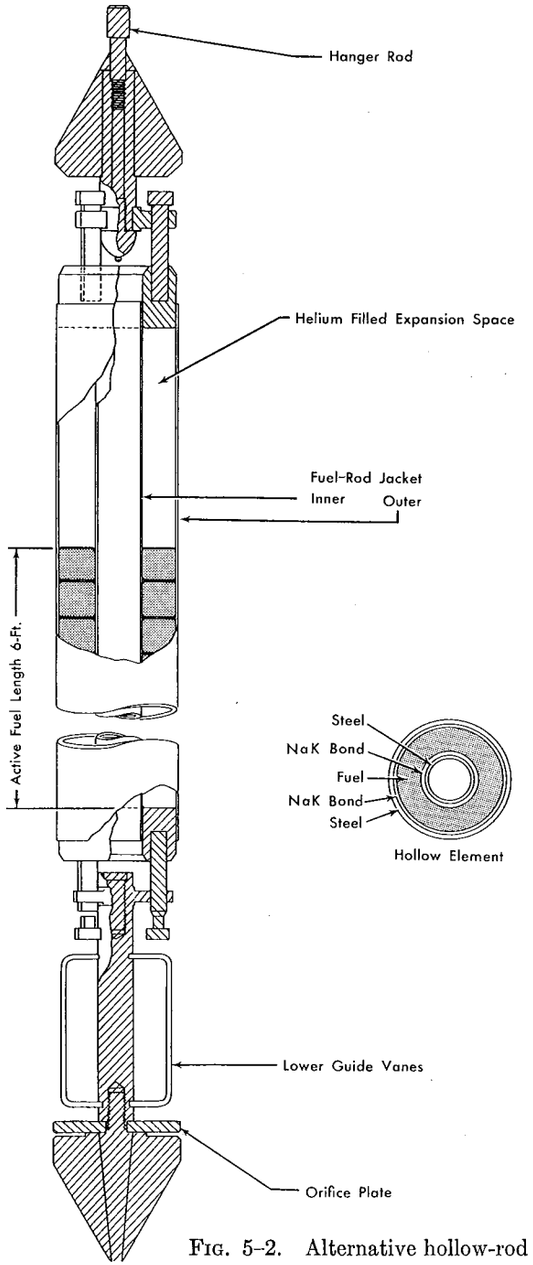

FIG. 5–2. Alternative hollow-rod fuel element.

Cottrell creep at relatively low temperature.
Distortion due to thermal cycling.
Swelling due to fission-gas pressure (a severe problem).
Wrinkling (a relatively minor problem).

This last effect, due to grain size and orientation, is expected to be small because of the flexible NaK bond, and it can easily be further reduced by adding a small amount of alloying agent such as silicon. The Cottrell creep effect, which has been observed in the operation of the Calder Hall reactor [1], is largely dependent on the structural load of the fuel supporting itself on long columns. As the temperature of the fuel increases up to 750°F, this effect reduces to zero. Although this somewhat contradicts the usual interpretation of creep phenomena, the effect appears quite real. Thermal-cycling phenomena associated with the anisotropy of uranium can be greatly reduced by using a randomly oriented grain structure. "Swelling" is the term used to describe the decrease in density of fuel material under irradiation. Experimental results in Great Britain have indicated changes in density in both unalloyed and alloyed uranium. An example of this phenomenon is given in Table 5–1.

TABLE 5–1 [2]

CHANGES IN DENSITY OF FUEL MATERIALS

Material	Temperature, °F	Burnup, %	Approximate density decrease, %
U	70	1.0	2.0
U	570	1.0	5.0–10.0
U	930	1.0	30.0
U	1470	1.0	100
Th-U (40%)	Same as above.		
U-Mo (14%)	Improved by factor of 2 to 3.		

These data have been further substantiated by American results at Argonne and other sites. Paine and Kittel of Argonne National Laboratory have indicated a rather sharp increase in swelling of unalloyed uranium in the 800°F range [3]. There are now under consideration five general techniques to minimize or eliminate this fuel material problem: direct restraint using a strong can, use of a dispersion type fuel in a nonfissionable matrix, internal restraint using a cermet such as uranium in uranium carbide, high-strength alloys, and a design such as a cored slug to permit internal stress relief. Each of these methods has advantages and dis-

advantages which will be resolved only by extensive fuel-cycle analysis, over-all economic analysis, and numerous experimental statistics.

As the other fuel element material problems are examined, rather standard engineering problems are encountered. Reactions between the clad or jacket and the fuel are temperature dependent. Two chemical reactions may occur: solid state diffusion of uranium into steel above 930°F, resulting in a brittle interface, and eutectic formation (m.p. 1390°F) between the uranium and the iron in the stainless steel. For these reasons cans made of steel cannot be considered where extended fuel temperature excursions exceeding 930 to 1020°F may occur. Zirconium and zirconium alloys are being examined for the higher temperature application, but there are few data presently available. In addition, there is a possibility that mechanical interaction between the can and the fuel may result from repeated thermal cycling. There are no major problems with other chemical reactions between fuel element materials and the sodium coolant. All the metallic fuels are essentially nonreactive with sodium or NaK (dependent, of course, on the oxygen content of the sodium). The fuel can retains fission products and also confines any small quantities of non-adherent fuel oxides which otherwise would be free to migrate in the sodium coolant. Finally, the reaction between the sodium coolant and the Type 304 stainless steel can is minor.

5–2. SRE Fuel Program

One of the prime objectives of the fuel element program for sodium graphite reactors has been to develop both a uranium base fuel and a thorium base fuel for long burnup at elevated temperatures. This has taken the form of an experimental fuel program in which various types of potentially improved fuel materials and designs are being tested and evaluated.

The present program is illustrated in Fig. 5–3 and Table 5–2. Major types being studied are:

Uranium alloys which minimize the effects of the alpha-beta phase transformation and provide increased strength.

Cored slugs to provide a free-volume for internal expansion.

Large hollow slugs for economy, and symmetry of stresses and temperature.

Thorium alloy to provide a radiation-stable matrix material and eliminate low temperature phase transformations.

Uranium oxides that allow high burnup at high temperatures.

In each case a complete chemical and metallurgical history was obtained during the fabrication in order to interpret results of hot-cell examination of the irradiated fuel. The powder-compacted slugs being considered are

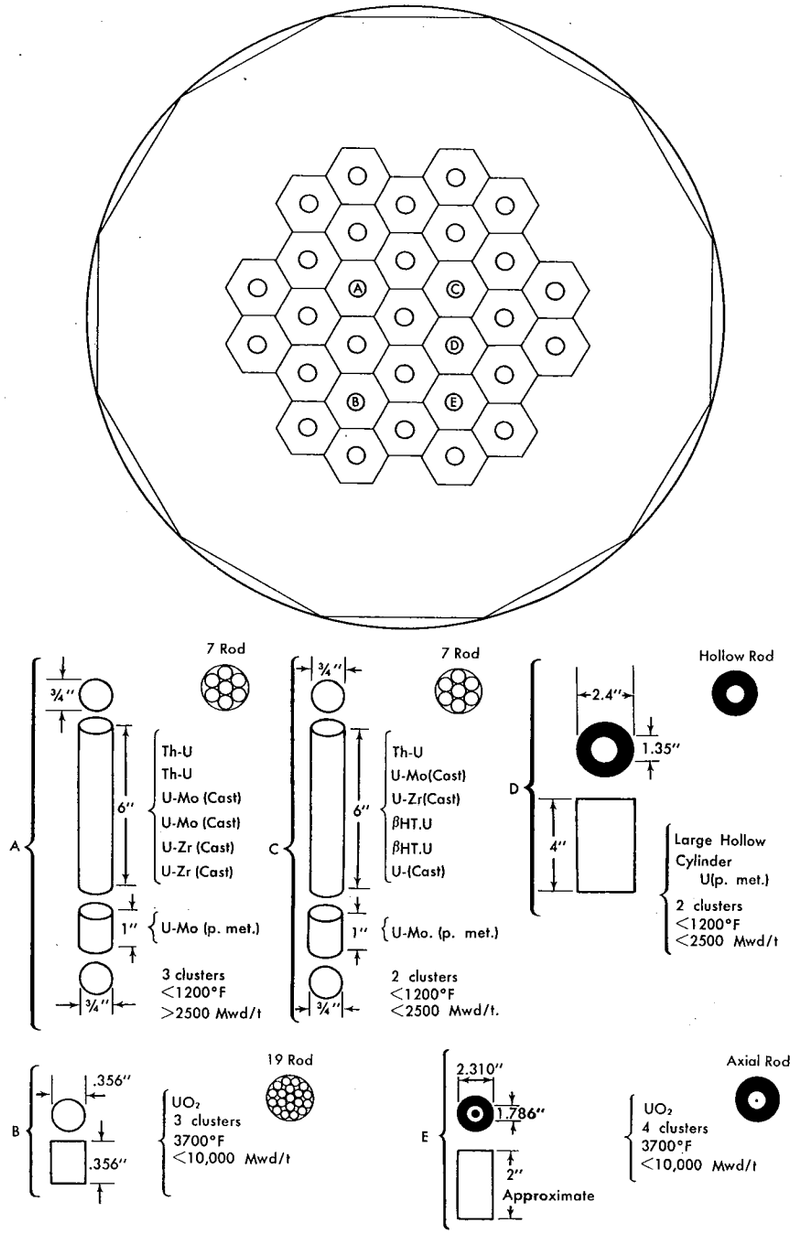

FIG. 5–3. SRE experimental program.

TABLE 5–2

EXPERIMENTAL SRE FUEL PROCUREMENT

Technique	Material	Pieces fabricated	U enrichment
Powder compacted	U-1.2 w/o Mo	515	
	U-large hollow	36	
Cast	U-2 w/o Zr	215	2.78%
	U-1.5 w/o Mo	60	
	U	25	
Cast	U-3.0 w/o Mo	60	3.1%
	U-3.0 w/o Mo large hollow	40	
Extruded	Th-5.4 w/o U	450	Above 90%
	Th-7.6 w/o U	3800	
Pressed and sintered	UO_2 pellets	5000	8%
	UO_2 rings	600	

the U-Mo (1.2 w/o Mo)* compacts ($\frac{3}{4}$-inch diameter, 1-inch length) and the unalloyed large hollow slug. There were 36 unalloyed large hollow slugs and 515 U-Mo alloy slugs fabricated with enriched material. Samples for process control purposes were taken at each major phase of fabrication. The other fuels presently planned for irradiation in the SRE are the uranium-molybdenum (1.5 w/o Mo), cast; uranium-molybdenum (3.0 w/o Mo), cast; uranium-zirconium (2 w/o Zr), cast; unalloyed uranium, cast; thorium-uranium (5.4 w/o U), thorium-uranium (7.6 w/o U), extruded; UO_2; and the alpha-rolled beta-treated fuel.

Swelling is the primary problem with metallic fuels operating at high surface temperatures. This dimensional change results in a decrease in density. The phenomenon is not yet fully explored, but the principal general factors believed to affect swelling in metal fuels are:

Surface temperature.
Temperature difference (surface to center).
Total burnup.
Burnup rate.
Metallurgical structure of the fuel material.
Strength of fuel material.

* Compositions are expressed in weight percent using the symbol w/o, unless otherwise noted.

TABLE 5–3

TYPICAL QUALITY SPECIFICATIONS OF SRE MAIN FUEL

Element	Amount, ppm	Element	Amount, ppm
Carbon	50–250	Chromium	Trace
Iron	20–60	Boron	"
Nitrogen	10–20	Silver	"
Nickel	40–90	Cadmium	"
Manganese	10	Cobalt	"
Silicon dioxide	20	Lead	"
Copper	20	Phosphorus	"
Magnesium	5–15	Zinc	"

To date, only a few widely scattered experimental data are available on the problem of swelling. From these observations, it appears that each fuel material has a threshold temperature or temperature range beyond which swelling increases at a rapid rate. This temperature range varies between 660 and 1200°F and depends, among other things, on the fuel composition and geometry. Plate-type specimens swell more rapidly than cylindrical shapes. It does not appear feasible to extrapolate irradiation data, for example, from plate to cylindrical geometry. Similarly, extrapolation from small cylinders to large cylinders is not recommended. Each fuel design and each fuel material (see Table 5–3) must be evaluated under the intended operating conditions in order to reasonably evaluate its performance. As a start in setting the specifications for fuel materials listed in Table 5–3, reactor grade quality material was accepted. However, the fabrication of the fuel indicated a need for further evaluation of such defects as seams, cracks, and internal porosity. Specific examples of these defects are being examined in the experimental fuel program. In an effort to determine the size and type of defect that is not acceptable it is necessary to irradiate fuels containing various sizes and types of defects. Eighteen rods of standard beta heat-treated fuel containing rejects have been assembled. These rods contain slugs that were rejected on the basis of (1) end cracks, (2) light seams, and (3) heavy seams. Their location in all rods is recorded in batch records. The batch numbers are marked on the fuel rods to permit identification of each of these reject slugs in hot-cell examination. Reject slugs of the alloy and oxide fuels will be assembled, irradiated, and examined in a similar manner.

Specifications of a typical SRE slug are shown in Fig. 5–4 and are listed below. It should be noted that both experimental and main fuel slugs

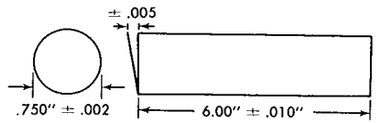

FIG. 5–4. SRE fuel slug specifications.

were derived from the same quality raw material and meet the same specifications.

DIMENSIONAL SPECIFICATIONS

End radius deburred, with no sharp corners.
All surfaces 250 root mean square.
Maximum single throw warp 0.003 inch per 6.000-inch length.
Ends to be square with centerline of part to ±0.005 inch.

MATERIAL QUALITY SPECIFICATIONS

Isotopic content: ±0.05 a/o U^{235}
Purity: See Table 5–3
Density (min.): Unalloyed 18.86 g/cm^3; U-Mo 18.45 g/cm^3; U-Zr 18.20 g/cm^3.
Grain size: Maximum of 0.21 mm.
Alloy content: ±0.1 percent of alloy element; from slug to slug and within one slug.
Metallurgical quality: Uniform microstructure, preferred orientation, less than standard grade alpha-rolled, beta heat-treated.
Surface, subsurface, and end imperfections: Seams or cold shuts longer than $\frac{1}{2}$ inch, wider than $\frac{1}{32}$ inch, or deeper than $\frac{1}{32}$ inch shall be rejected. Only three defects within a $\frac{1}{2}$-inch area on one piece are acceptable. Striations are rejectable only when in large quantity. Porosity or shrinkage cavities greater than $\frac{1}{32}$ inch deep or $\frac{1}{32}$ inch wide with two or more within a $\frac{1}{8}$-inch area on one slug are rejected. Cracks greater than $\frac{1}{32}$ inch in length are rejected.
Destructive tests: Representative samples will be destructively examined for specification verification. Machining defects beyond dimensional or other tolerances are rejected. Any macroscopic nonmetallic inclusions must be removed and the slug must pass all specifications after removal.

Note. The vendor has free choice to fabricate by any type or sequence of operations, provided the quality of the slugs meet the above specifications.

The available data indicate that unalloyed uranium will be limited to about 1000 Mwd/t exposure under full-power SRE conditions. This assumes 1200°F maximum central temperature. A lower central temperature would permit increased burnup. The experimental fuels are expected to substantially increase this burnup. Small-scale tests by Smith [4] at Argonne National Laboratory indicate the U-3 w/o Mo alloy to have potential for high-temperature conditions, and tests described later in this section indicate the possible future use of thorium-rich thorium-uranium alloy fuels. The U-10 w/o Mo fuel for the fast breeder reactor also appears attractive [5], but does not appear to be useful for thermal reactors because of high thermal neutron capture cross section.

Consideration of UO_2 fuel materials for SRE is based mainly on the encouraging results at high temperature and high burnup. The UO_2 atomic lattice structure is believed to provide space for the accumulation of fission gases and thus does not swell under reactor conditions. A total burnup of 20,000 Mwd/t has been achieved with UO_2 fuel [6]. Although attractive in some respects, oxide fuels also have some disadvantages, e.g., low uranium atom density (10.9 g/cm^3), and low thermal conductivity. At comparable total power output, the reactor core using oxide fuel is considerably larger than that for metal fuel, which results in difficult mechanical problems and higher capital costs. It is evident that choice of fuel material requires continual reappraisal of economic feasibility and technical feasibility.

The SRE experimental fuel program was purposely made very flexible, to accommodate new fuel materials and designs, and to take advantage of engineering changes and proposed theoretical improvements.

5–2.1 Thermocouple monitoring. Numerous thermocouples of stainless steel sheathed chromel-alumel wire are inserted in the fuel for temperature monitoring. The arrangement and location of these temperature monitors are shown in Fig. 5–5. There are both peripheral and center rod monitors. During the power runs to date, all the thermocouples have performed satisfactorily.

The shield plugs used for both the main and experimental fuels contain a conduit for the thermocouple wires that lead from the fuel element to the reactor floor. These shield plugs serve this function until the thermocouples are cut in the hot-cell disassembly; thereafter their function is that of a standard shield plug.

Allowance for growth of the fuel has been made in the thermocoupled fuel rods by drilling the hole for the thermocouple deeper than the thermocouple will actually extend. This prevents a buckling force from being exerted on the stiff thermocouple wire and consequent stress on the jacketing material due to longitudinal growth of the fuel. Fuel is permitted

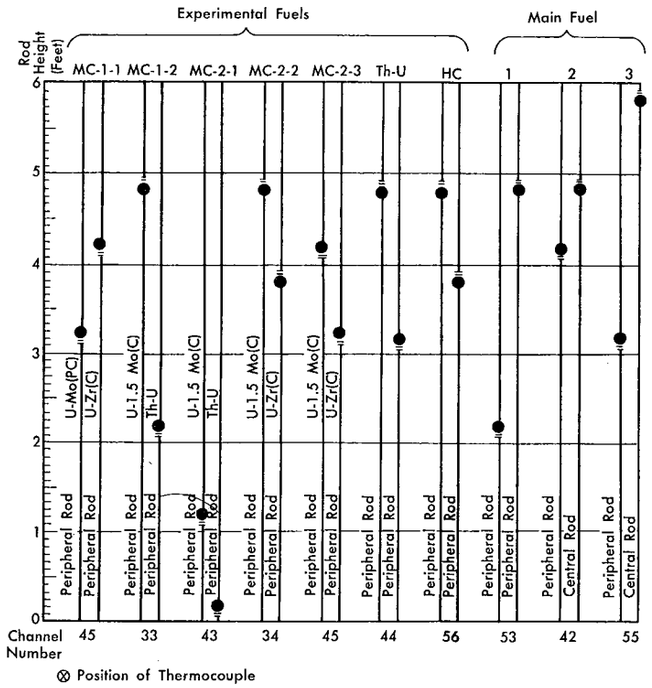

FIG. 5–5. Thermocouple distribution in the SRE.

to grow upward a maximum of 4 percent before it contacts the thermocouple. If radial growth of the fuel seizes the thermocouple, buckling strain is reduced by a coil wound in the top end of the sheathed thermocouple wire. A sleeve above the fuel slugs in the fuel element covers the coiled thermocouple and protects the 0.010-inch jacket material from distortion due to coil deformation.

The thermocouples in the fuel are also used to measure the temperature attained in the fuel-handling cask. In this manner the after-glow heating can be made a part of the thermal history of the fuel and provide data for future cask designs.

Locations of the thermocouples in the fuel rods are shown in Fig. 5–5. This arrangement is expected to yield a complete map of the temperature profiles in the SRE.

5–2.2 Radiation schedule. Because of the short potential life of the main SRE fuel, ~1000 Mwd/t, it is imperative to constantly review dimensional changes in the fuel materials. The earliest examination of

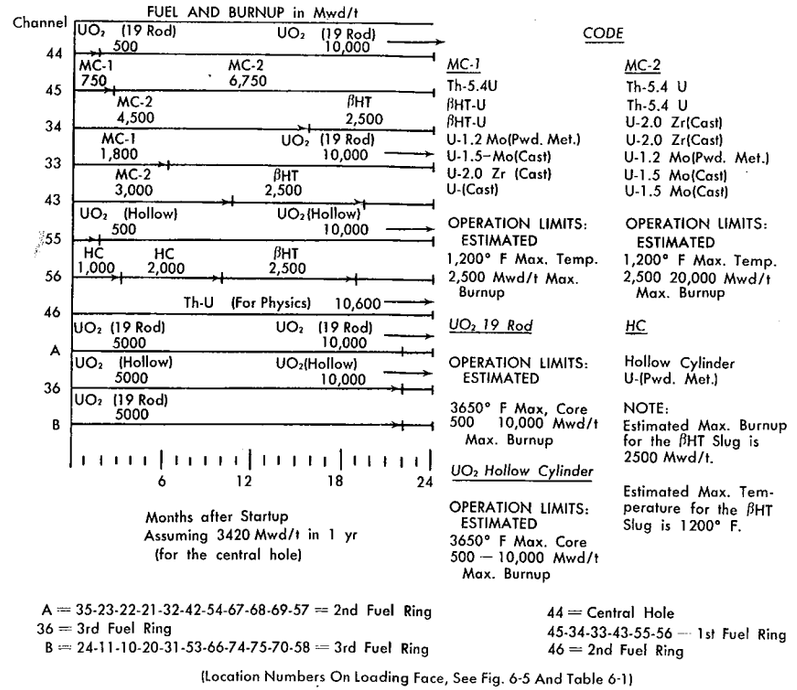

FIG. 5–6. SRE experimental fuel schedule.

the fuels will be made at 100 Mwd/t burnup, and examinations will be scheduled every 100 to 200 Mwd/t thereafter. The length of time required to attain a desired burnup in uranium base fuels is shown in Figs. 5–6 and 5–7.

The fuel-loading schedule was planned to allow insertion in the SRE of all of the experimental fuels in the first loading, after the SRE has come to nearly full power. The power was raised in the SRE by fairly small increments up to about 65 percent of full power. Subsequent increases in power were quite large over a short period. Insertion of the experimental fuel clusters during this later stage of power increase appears satisfactory.

5–2.3 Hot-cell examination. After removal from the reactor, the experimental elements will be cleaned of sodium and then transferred to the hot cell in the reactor building. The hot cell is so arranged that the fuel element can be lowered into it directly from the handling cask in the same manner that it would be lowered into the reactor or into fuel element storage cells.

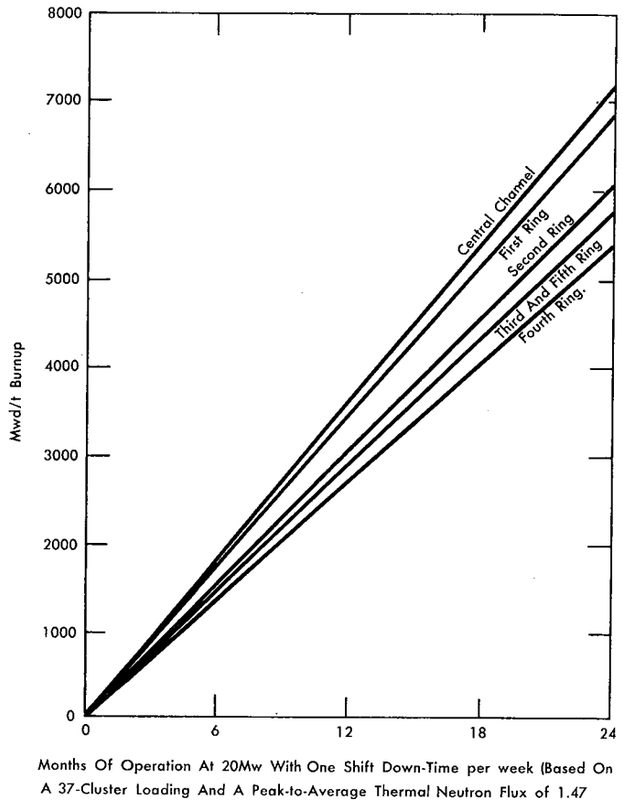

FIG. 5–7. Maximum attainable burnup of uranium-rich fuels in the SRE.

Postirradiation examination of both the experimental fuels and the standard fuels is done in a similar manner. Virtually all experimental fuel slugs are given an extensive examination, whereas only a fraction of the standard fuels are examined to an extent greater than a visual and dimensional check.

The complete examination proceeds as follows:

The fuel rods will be detached from the cluster spider in the hot cell and *decanned* under Ultrasene (a hydrocarbon solvent).

All the slugs in the rod are cleaned in an ultrasonic cleaner to remove NaK and other residue.

The slugs are divided into three categories: for visual and dimensional observation only; for visual, dimensional, and photographic observation only; and for visual, dimensional, photographic, and metallographic observation. Those in the last category will proceed as below; the others are examined and stored.

The slugs for metallographic examination have a wafer of fuel removed with a submerged abrasive *cutoff* wheel. This wafer is then mounted in a plastic or a metal mount.

The surface of the mounted wafer is then given a fine lap with a lapmaster machine and again cleaned ultrasonically before a final polish.

The sample is then etched either chemically or cathodically at the discretion of the metallographer.

The sample can then be examined with a metallograph and given a hardness test with a Tukon hardness machine, if desired.

Density measurements of the irradiated fuel are then made and samples and slugs are stored after examination.

It is expected that in this manner the experimental fuels may be evaluated and the most promising alloy and fuel configuration for power reactors determined.

5–3. MTR Irradiations of SRE Fuel

Only limited data were available on fuel material performance under SRE conditions of elevated surface temperature when reactor design commenced. To provide data on this problem, a series of MTR irradiations were initiated in which samples of SRE fuel materials were tested and examined.

Samples were individually sealed in NaK-filled capsules of the type shown in Fig. 5–8. The capsules were then welded end-to-end in series of either five or six to form an irradiation assembly.

The assemblies were placed in MTR reflector positions having unperturbed thermal neutron fluxes from 0.5 to 1.0×10^{14} neutrons/cm^2·sec. A burnup rate in these positions of about 0.025 to 0.05 percent of the total atoms per week of irradiation was obtained. The temperature gradient across the radius of the $\frac{3}{8}$-inch diameter by $1\frac{1}{2}$-inch long specimens ranged from 150 to 300°F.

Thermocouples were located at the axis of the specimens $\frac{1}{2}$ inch from the bottom end. In general, the central metal temperatures increased with irradiation at a rate of less than 30°F per week. Loss of thermal conductivity and loss of density of the samples appears to be related.

5–3.1 Procedure. The various specimens of SRE metallic fuel contained 10 percent enriched uranium. The 2 w/o zirconium-uranium specimens were cast, the 1.2 w/o molybdenum-uranium specimens were powder

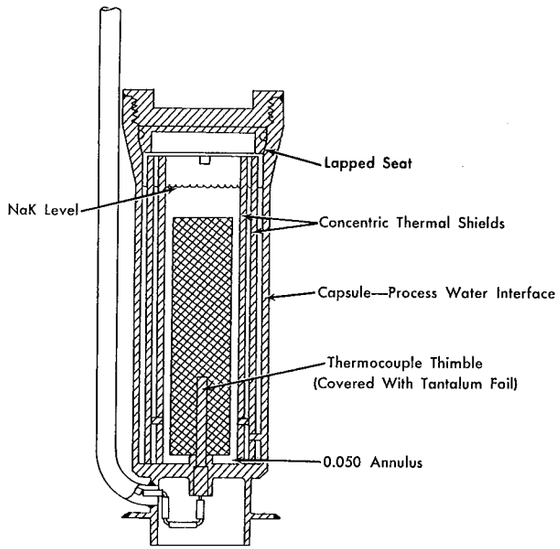

FIG. 5–8. Fuel slug irradiation capsule.

compacted, and the unalloyed specimens were alpha-rolled and beta heat-treated. These MTR-specimen fabrication techniques are identical to those used in fabricating the SRE fuels. Thermocouple thimbles support and locate the specimens so that the specimen is free to grow 0.100 inch radially and 0.376 inch longitudinally. Hot junctions of the thermocouples are $\frac{1}{2}$ inch above the bottom end of the specimens at the axis of the specimens. Thermocouple wires are conducted along the capsules to the top of the reactor and into a continuous recording six-point recorder.

The first assembly, NAA-15-1, was inserted in July, 1955. The peak temperature attained was only 400°F (rather than the expected 1200°F) and this assembly was discharged from the reactor at the end of the first cycle. Inaccuracy in predicting the flux required pointed out a need for monitoring the available neutron flux in a test hole before insertion of the experimental assembly. Therefore, monitor assemblies were built to closely simulate the neutron depression and perturbation of the NAA-15 assembly in order to locate a test hole with the calculated required flux (flux available at the axis, 1.2×10^{13}). NAA-15-2 was inserted in the new location and irradiated for one cycle (3 weeks). The temperature attained in the NAA-15-2 (~900°F) displayed the need for a flux about 50 percent higher to attain the desired 1200°F. Mechanical difficulties developed in the NAA-15-2 assembly when it was moved to a third location of higher flux and it was discharged to the MTR canal with about

0.07 percent burnup of total atoms attained. The next experimental assembly, the NAA-15-3, was then inserted directly into the third position and remained there for the following five MTR fuel cycles. Although the peak temperature (1050°F) was less than the desired 1200°F, it was not considered justifiable to endanger the assembly by moving it to a higher flux position. After less than 100 hours of operation, the thermocouple response was lost from capsule 4. After the first cycle, manipulation on another experiment inside the reactor tank accidentally caused a leak in the NAA-15-3 thermocouple chamber, and consequent loss of the remaining thermocouples. Since the experiment had already demonstrated its safety in this position, it was allowed to remain and the irradiation continued.

TABLE 5–4

RANGE OF TEMPERATURES IN NAA-15-3 DURING FIRST THREE WEEKS OF IRRADIATION

Capsule	Central temperatures recorded		
	Maximum, °F	Minimum, °F	Average, °F
1	1050	935	970
2	1035	930	960
3	960	865	910
4	910	900	900
5	790	710	750
6	640	570	600

During irradiation, peak temperature of the specimen is affected by the control-rod position, coolant flow, other experiments, etc. Table 5–4 illustrates the fluctuations experienced during the first cycle of irradiation of the NAA-15-3 (before loss of the thermocouples). Temperatures after this cycle may have been higher, due to a loss of conductivity in the fuel specimen, but no temperature is believed to have exceeded 1200°F.

At the end of the fifth cycle, the assembly was discharged to the canal. After four weeks' cooling time, the assembly was transferred to the SRE hot cell. This description is typical of the irradiation period for the subsequent tests. A total of five assemblies had been irradiated prior to startup of the SRE in mid-1957.

5–3.2 Results. Examination of the samples revealed an end effect that is not fully understood. Close examination indicates that this zone achieved a very high temperature, possibly melting. Figure 5–9 shows this end

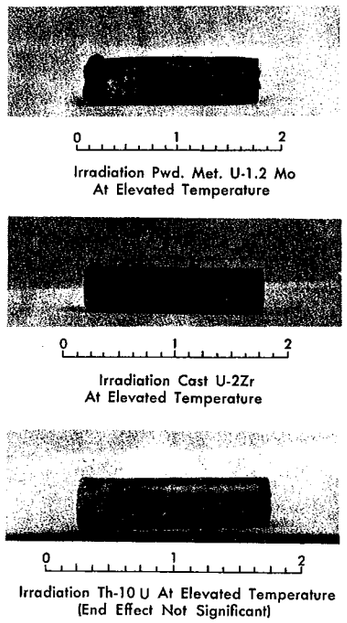

FIG. 5–9. Typical MTR irradiated fuel slugs.

effect on two typical samples. The U-1.2 Mo sample was irradiated to about 0.4 a/o (atomic percent) burnup with a maximum measured central metal temperature of 1050°F. The U-2 w/o Zr sample was irradiated to about 0.3 a/o burnup with a maximum measured central metal temperature of 640°F. Recalculation of the NaK level, using postirradiation measurements, did not reveal an inadequate NaK volume in the capsule. High neutron absorption of the tip of the specimen may be the reason for this end effect. The end effect is not as pronounced on the thorium-uranium samples, possibly because of superior high-temperature strength. Figure 5–9 also shows the appearance of a typical Th-10 U specimen after 0.3 a/o burnup of the total atoms with a maximum measured central temperature of 1230°F. All reported diameter measurements exclude the top end effects. The surfaces of all the irradiated specimens were fairly smooth. Sampling of the capsules for fission gases revealed only small quantities, and was generally inconclusive.

Table 5–5 lists the radiation conditions and the dimensional changes incurred as a result of the irradiation. These specimens appear to be representative of the sixteen samples measured.

TABLE 5–5

DIMENSIONAL CHANGES IN SAMPLE SRE FUEL

Specimen composition	Estimated burnup, a/o	Maximum meas. temp., °F	Maximum change in diameter	Maximum change in length	Increase in volume, %
U-1.2 w/o Mo	0.4	1050	+0.050	+0.094	35
U-1.2 w/o Mo	0.3	790	+0.037	+0.192	34
U-1.2 w/o Mo	0.2	1250	+0.029	+0.109	22
Th-U (10%)	0.3	1230	+0.005	+0.029	4.8
Th-U (10%)	0.3	1230	+0.003	+0.038	4.3

Th-U samples appear to be superior to the uranium base samples, but are nevertheless grossly affected by irradiation. The unalloyed uranium samples irradiated were alpha-rolled and beta heat-treated. Two of the unalloyed samples irradiated to 0.05 a/o burnup, with maximum measured central temperatures of 880°F, increased in volume 0.9 and 1.5 percent. These samples had slight diameter decreases and length increases respectively.

Based on the small number of samples tested the following conclusions may be drawn:

Thorium-10 w/o uranium alloy is less affected by irradiation at 1200°F central temperature than the uranium base alloys tested.

Dilute uranium alloys are subject to large dimensional changes under irradiation at high surface temperatures.

Dimensional changes appear to be strongly affected by the irradiation surface temperature.

Metallic fuel elements appear to have low burnup limitations at elevated surface temperatures, the exact limits depending on the fuel element design.

5–4. FUEL ELEMENT ASSEMBLY

Design of the SRE fuel element was derived from the fuel element configuration proposed during early design studies of the sodium-graphite type reactor. One of the features common to the several variations in the design of sodium-cooled, graphite-moderated reactors has been the concept of the fuel element as a replaceable assembly suspended from the top shield. The fuel element must have optimum nuclear and heat-transfer characteristics as well as the ability to meet the criteria of compat-

ibility of materials, stability of the composite element, and feasibility of fabrication procedures.

Auxiliary structures are required to bind the fuel rods into a fuel element. This hardware also serves to:

Connect the element to an upper shielding plug.
Guide the element into and out of coolant channels without *hangup*.
Regulate the amount and distribution of coolant flow through the element.
Permit each rod to expand individually.

In addition, the hardware is designed to allow assembly and disassembly of the fuel element by remote-controlled manipulators in a hot cell.

5–4.1 Fuel element configuration. The seven rods forming each cluster comprising an SRE fuel element are retained at each end. Vertical support is provided by the fixture at the top, while individual expansion of the rods is permitted by the fixture at the bottom end. Also at the bottom of the assembly is a locating guide and an orifice plate for controlling the flow of the sodium, as required for each particular fuel cluster. To prevent the rods from touching each other or the coolant tube, the six outside rods forming the cluster are spirally wrapped with an 0.091-inch diameter, stainless steel wire with a pitch of approximately 10 inches, with direction of wrap so arranged that adjacent rods are wrapped in opposite directions. To determine the temperature of the exit sodium from any coolant tube, a thermocouple is inserted down the inside of the stainless steel tube supporting the entire cluster from its plug in the top shield. The junction of this thermocouple is located just above the fixture at the top of the fuel element cluster.

The SRE is operated so that a maximum uranium metal temperature of approximately 1200°F is attained in each fuel element. This temperature is determined by the total power level of the reactor, the flow and temperature conditions in the sodium system, and by the selection of orifice plates for the fuel elements. During normal operation there is a pressure drop of 2.5 psi across the central fuel element and 1.5 psi across its orifice plate, making a total of approximately 4 psi. Sodium flow in this central tube is 5 ft/sec, corresponding to 17,500 lb/hr. Flow in a tube requiring the least cooling (near the outside of the core where the average thermal neutron flux is least) is 3 ft/sec. Nominal sodium outlet temperatures, with the 500°F inlet, are 908°F for the central tube and a maximum of 986°F for a tube in the lowest average neutron flux, giving a 950°F mixed mean temperature in the sodium pool. The maximum heat flux is about 340,000 Btu/ft^2·hr, yielding a heat transfer coefficient of approximately 10,000 Btu/ft^2·hr per °F. Approximate values of the peak-to-average heat flux are 1.35 for any channel and 1.63 for the entire reactor. Under these conditions, the central fuel element produces 650 kw, corresponding to 340 kw/kg of U^{235}.

5–4.2 Component description. SRE fuel enrichment selected was $2.75^{+0.05}_{-0.00}$ a/o U^{235}. An order was placed for 4300 kilograms of alpha-rolled, beta heat-treated material of this enrichment, which corresponded to approximately 5230 six-inch long slugs. Starting material was UF_6 from Oak Ridge, which was reduced to UF_4 and then to metal derbies. The resulting derbies were remelted and cast into ingots, which were cut into three sections. Each section was rolled into three rods which were heat treated by quenching from the beta phase and then machined to size. Members of the Atomics International metallurgical staff followed the operation, and obtained information on each step of the process for future reference. Each slug is stamped with six digits, using a system that makes it possible to trace the slug history back to the rod, ingot position, and to the batch of UF_6 from which it originated. A detailed record is kept of the location of each slug in the reactor and the conditions under which it is operated. A post-run metallurgical examination will assist in the attempt to establish the relationship of fuel performance and original metallurgical condition of the slugs. This will permit the establishment of realistic fuel material requirements for future reactors. (Refer to Fig. 5–4 for present fuel slug specifications.)

Based on the nature of service, the stainless steel jacket tubing had to be of the highest metallurgical quality, uniform in dimensions, and free from voids and nonmetallic inclusions. An 18-8 chrome-nickel stainless steel (Type 304) was selected as the clad material on the basis of its resistance to sodium corrosion, strength, availability, fabrication techniques, and acceptable nuclear properties in the relatively depressed thermal flux region adjacent to the fuel slugs.

Various manufacturers had indicated that welded and drawn tubing would be superior to seamless tubing for SRE requirements. It was considered that wall-thickness variations could be minimized by starting with flat strips. A minimum variation in wall thickness is especially important for thin-walled tubing, since a small variation in wall thickness represents an appreciable percentage of the total thickness. Also, welded and drawn tubing permitted examination of the skelp prior to welding; this examination would reveal any large defects present on the inner surface.

Rigid specifications were prepared before fabrication of the order. A requirement for minimum nonmetallic inclusions, similar to specifications used in selecting bearing grade steel, was established. Metallographic examination of samples submitted for nuclear tests determined whether *dirt* or inclusions were present in the starting material. Specifications also

included helium mass spectrograph testing and hydrostatic testing at pressures corresponding to just below yield point.

The tubing was redrawn from $1\frac{1}{2}$ inch OD by 0.065 inch walled stock with sufficient wall reduction to eliminate evidence of the weld. Redraw stock was made by inert gas shielded-arc automatic welding.

Positive clearance is required for insertion of a uranium slug into the tubing. This space acts as a thermal barrier and therefore a material of high thermal conductivity was selected to bond the fuel and jacket into a single metallurgical unit. The bonding material must be compatible with the slugs and cladding and also have acceptable nuclear properties. While both sodium and NaK satisfy these requirements, sodium is preferable from the standpoint of nuclear properties and thermal conductivity. However, the effect of the small quantity of bond metal is insignificant to the over-all neutron economy and temperature drop involved. Furthermore, the NaK, which is liquid at room temperature, led to simplified equipment and loading procedures, and was therefore chosen.

Type 304 stainless steel was also selected for all additional miscellaneous hardware in the fuel element assembly. This selection was based on the basic properties of Type 304 stainless steel and on the desirability of having material with uniform coefficient of expansion in all the structural parts of the fuel element assembly.

5–4.3 Rod loading equipment. Fuel-rod loading methods were explored by designing, fabricating, and testing an apparatus for assembly of a single rod. Techniques developed with the use of this single-rod loader were used as a basis for the design of a multirod loader.

Welds were made in the single-rod loader by rotating the end cap-to-tubing interface past a stationary electrode. Fuel slugs were contained in a revolving magazine and inserted in the jacket tubing after the addition of the bond. All moving shafts that penetrated the loading chamber were sealed with O-rings or bellows to permit operation in a vacuum or in an inert atmosphere.

Difficulties with the single-rod loader were encountered in heating slugs in the magazine, and in repeated positioning of the magazine with respect to the jacket tube to within the required 0.010 inch. In view of these problems and the fact that the single-rod loader was limited to a low production capacity, attention was directed towards the design of modified equipment in which several rods at a time could be loaded. The single-rod loader was retained for welding the variable size experimental fuel rods and for welding all SRE fuel rods that contained thermocouples.

Design of the multirod loader, Fig. 5–10, differed from that of the single-rod loader in several important respects. Most significant was the modification in welding fixtures, so that the weld electrode rotated around the

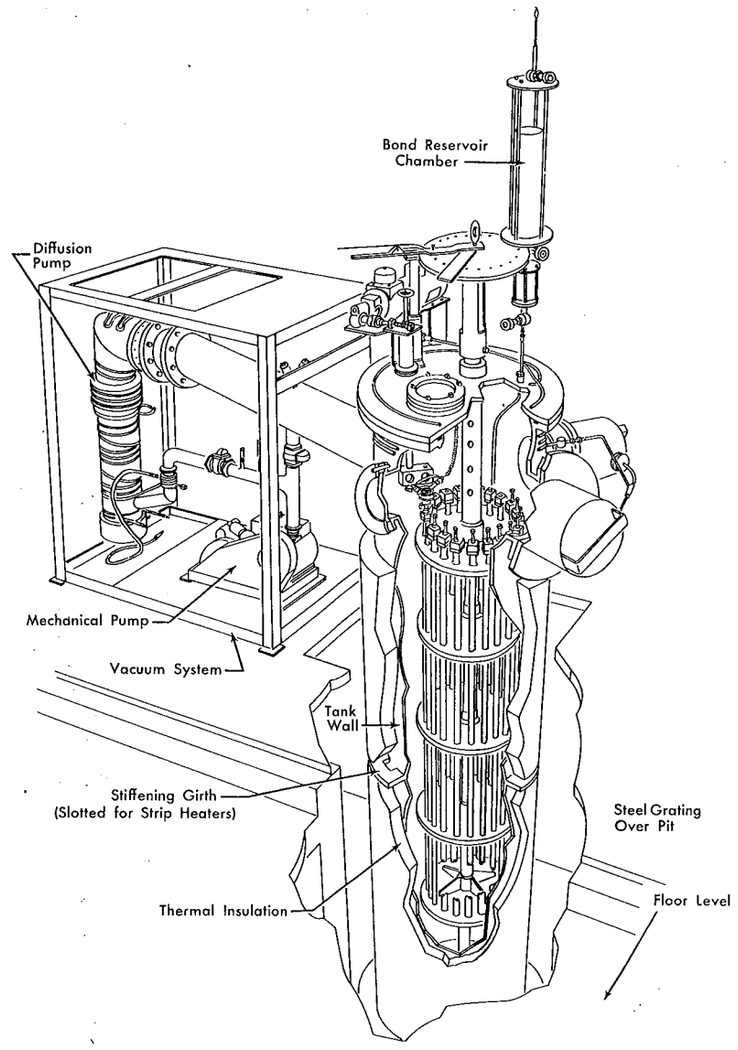

FIG. 5–10. Multirod loader.

tubing. This permitted simplified handling of the number of tubes which could be placed in a closely packed array, thus decreasing the volume to be evacuated and heated.

Based upon considerations of maximum production capacity, critical mass (if accidentally water moderated), weight, volume, and value of

material in each production load, it was decided to load 21 fuel rods (three fuel elements) at a time.

5–4.4 Rod fabrication procedure. Figure 5–11 is a flow diagram of the fuel-rod fabrication sequence procedure. All components were inspected for proper material and dimensions prior to delivery at the work area.

Stainless steel fuel-jacket tubing is first inspected with a Cyclograph* to reveal any subsurface defect, nonmetallic inclusion, or variation from specified wall thickness. A special cutting tool and lathe are used to trim the ends of the tube (no burrs or flaring) with the ends normal to the long axis. This cutting operation is conducted with care in order that the end caps will fit properly.

After one end is trimmed, the tubing is cleaned with acetone to remove all traces of surface grease. The end caps are also degreased in acetone just prior to use.

Twenty-one tubes are fitted with lower end caps by inserting the cap into the trimmed end of the tube until the welding flange is snug against the tube. The tubes are then placed in the multirod fuel loader, which is sealed and evacuated to less than 25 microns and then refilled with a mixture of 90 percent helium and 10 percent argon to atmospheric pressure. End caps are welded into the tubing by means of a welding device mounted on the tank lid. Upon removal from the loader, end caps are visually inspected and any poor welds are rejected. Each tube is evacuated and the weld and tubing walls are leak-checked with a helium mass-spectrometer leak detector. While some leakage through faulty welds has occasionally been found, at no time has there been any indication of leaks through the walls of the tubing. An attempt is made to repair a leaky weld, but if the weld cannot be made leaktight the end cap is removed by trimming the tube on a lathe just below the weld. A new bottom end cap is inserted and a new weld is made. In practice, it has rarely been found necessary to replace and reweld an end cap. Next, the tubes are cut to length and the upper end caps are turned on a lathe until they engage the tubing in a snug fit.

Twelve uranium slugs (the number required for one rod), which have been previously weighed, are visually inspected and their numbers recorded on a batch card. They are then placed in an acetone bath to remove any grease, dried in air, and electropolished. Several rinsing operations follow to remove all traces of the electropolish solution; in sequence the rinse baths are water, dilute ammonia, water, water again, and methyl alcohol.

The slugs are reweighed to estimate the quantity of material removed

* Distributed by the J. W. Dice Co., Englewood, N. J.

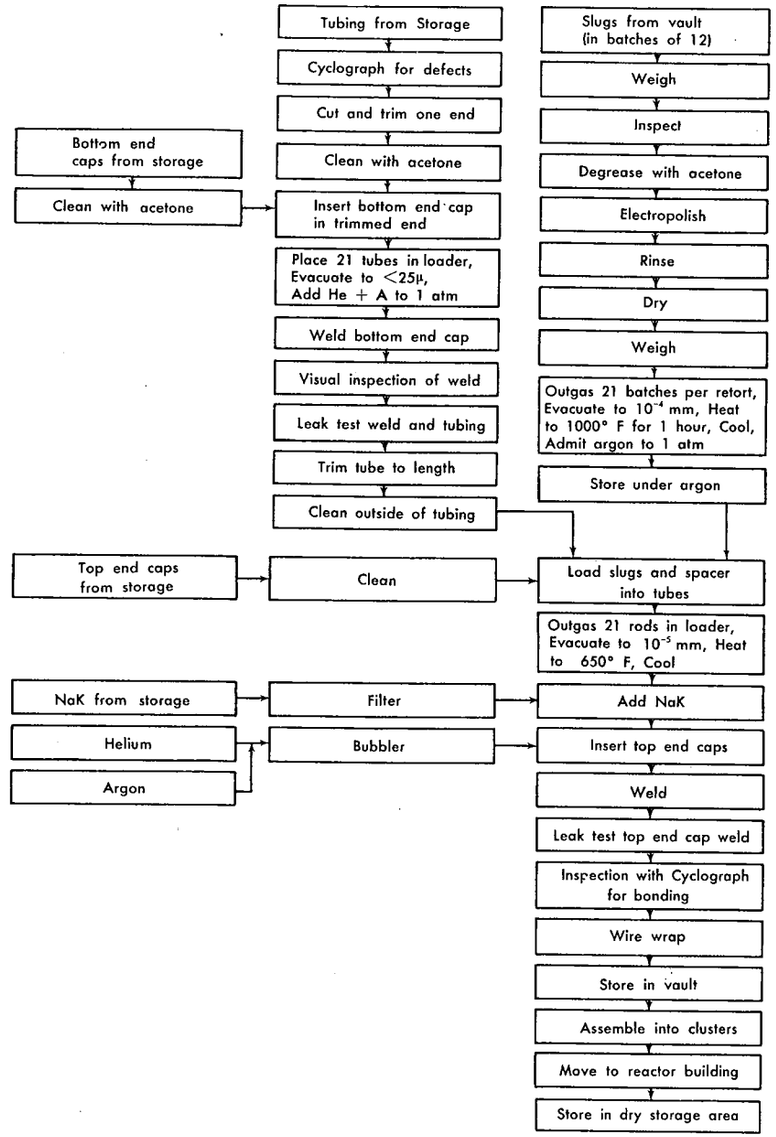

FIG. 5–11. Flow chart of SRE fuel-rod fabrication.

in the electropolishing bath. This information is utilized for accountability purposes and to prevent excessive buildup of material in the bath. This final weight is the reference weight for accountability of material in the fuel rod and for experimental information. Weighed slugs are immediately loaded into a rack and placed in a retort for vacuum outgassing. The retort is arranged to hold 252 slugs in 21 baskets of 12 slugs per basket. This arrangement has been determined to be a noncritical geometry. Slugs are outgassed by heating to 1000°F under a vacuum of less than 10^{-4} mm. After cooling, argon is admitted and the slugs are stored in the retort until required for use in the fuel-loading operation.

After outgassing, the slugs are loaded into the tubes by hand. Fuel-rod tubing is held at an angle such that the slugs slide in gently. The slugs are inserted in the same order as they are recorded on the batch card, and the number for each slug is checked off the batch card as the slug is added. Each tube containing 12 slugs is placed in the rack of the fuel loader as soon as it has been filled. A full rack of 21 fuel rods is placed in the loader along with the upper end caps for the tubes.

The fuel-loading machine is closed and evacuated to 10^{-5} mm. Outgassing is conducted by heating to a maximum temperature of 650°F at 10^{-5} mm of mercury or less. Then it is allowed to cool under vacuum to room temperature and a measured amount of filtered NaK is added to each fuel rod. The interior of the apparatus is returned to atmospheric pressure by filling with purified helium, thus permitting the use of glove ports in placing top end caps in the tubes. End caps are welded to the tubes and the rods are removed from the fuel loader. Top end cap welds are visually inspected, and the rods are leak-checked. Any leaks or damage are cause for rejection. A Cyclograph trace is made of each rod to determine the condition of the bond and the bond level. Completed fuel rods are stored in a fixed noncritical geometry to await assembly into the clusters. Outer fuel rods are wrapped with wire, using a special fixture to maintain the desired spacing between adjacent turns of the wire, and are assembled into clusters by hanging from the top hanger. After assembly of the orifice plate and lower guide the fuel element is lowered into a fixture which is used to check the straightness and diameter of the cluster to ensure proper fit in the reactor cooling channels. Assembled elements are then transferred to the reactor building, where the upper shield plug is lowered over each fuel element and connected to the element by a pin. The entire assembly is then lowered into a helium-filled dry storage cell until required for use in the reactor.

5–4.5 Testing. It is necessary to detect any flaws that might lead to failure in the physical structure of the fuel element before it is loaded into the reactor. Therefore, an inspection program was set up which included

tests on the slugs, jacket tubing, bonding, and end cap welds. Tests on assembled elements were also performed to obtain information for design improvements and on the expected behavior of the element under operating conditions. The inspection instruments used most extensively were the Cyclograph and the helium mass-spectrometer leak detector.

Uranium slugs were examined visually for surface defects such as cracks and seams, and dimensional checks were made for length, diameter, and straightness. A test for beta transformation was made with a Sperry Reflectoscope. It was estimated that the Reflectoscope could distinguish as little as 10 percent so-called alpha grains; all rods examined were full transformed. This was confirmed by microscopic examination of specimens, which revealed a uniform beta structure and exceedingly clean metal with a minimum number of inclusions.

Gamma graphs were made of the small groups of slugs which did not meet specifications (but which were accepted for test purposes) and of samples of comparative acceptable slugs. Using a 1-curie radium source, two exposures were made of each slug rotated about its longitudinal axis through 90-degree intervals. Defects in either the acceptable slugs or those with light seams could not be detected. However, some heavy seams and end-crack defects were apparent.

The thin-walled stainless steel tubing was checked for composition by chemical and spectrographic analysis. Metallographic analysis showed that the tubing was clean and had few stringers, oxides, or inclusions. The few inclusions present were primarily chromites (a mixture of iron oxide and chromium oxide).

Strauss tests were utilized to determine the presence of any areas of excessive carbide precipitation. Specimens of as-received tubing and tubing which had been heated in sodium for 100 hours at 800°F were subjected to immersion in a boiling solution (3 percent cupric sulphate, 10 percent sulphuric acid, and 87 percent distilled water) for 72 hours. No evidence of excessive carbide precipitation or intergranular corrosion was noted upon metallographic examination.

To determine whether heavily oxidized sodium at high temperature would cause pitting or selective attack, the following test was performed. Four specimens of tubing were sealed in a stainless steel capsule in contact with sodium which had been heavily oxidized. The capsule was maintained at 800°F for a total of 459 hours; it was opened after 100, 200, and 450 hours, at which time the specimens were washed in air and visually examined. None of these conditions contributed to any detectable localized surface attack.

Strength tests were performed on the jacket tubes at room temperatures. Eleven tensile specimens showed yield strengths ranging from 79,000 to 125,000 psi, and ultimate strengths ranging from 105,000 to 148,000 psi.

Elongation varied from 27 to 39 percent. Hydraulic strength tests indicated that the tubing would not burst until internal pressures from 2300 to 3100 psi were obtained.

Jacket tubes were checked for small defects and inclusions with the Cyclograph. After welding the bottom end cap to the tubing, the weld and the tubing were tested for submicroscopic pinholes by a helium mass-spectrometer leak detector.

Since this procedure could not be used to test the top-end cap weld for leakage after the rod was loaded, a special fixture was devised which allowed easy positioning of the fuel rod within a vacuum-tight test head. The fixture was connected to a helium leak detector and the region around the top end cap was evacuated. Leaks in the weld permitted the helium sealed inside the tube (at a pressure of 1 atmosphere) to pass through and enter the leak detector, producing a signal. Less than 5 percent of the loaded rods tested in this manner were rejected because of leaks.

Proof tests of the weld joints were conducted on prototype fuel rods. The tests were performed by applying a load sufficient to stress the weld joint without permanently deforming the thin-walled tubing. It was found that a tensile load of 700 pounds would not cause permanent deformation of the tubing, while a load of slightly over 1000 pounds would reduce the tubing diameter 0.001 inch. A tensile load of 2500 pounds was required to fracture the tubing. During these tests (to fracture) the tubing diameter decreased uniformly along its entire length.

Tensile tests were performed to determine the mode of failure and the ultimate strength of the weld securing the fuel-rod end-cap to the jacket tubing. Specimens were tested in air, at room temperature, at 1000°F, and at 1200°F. Failure occurred in the body of the tubing, indicating that the weld was stronger than the tubing.

The most important inspection tests undertaken were those for voids in the bond. Voids could cause localized overheating of the uranium. The maximum permissible void sizes for an SRE fuel rod are given in Table 5–6. Among the methods investigated for void detection were the Cyclograph,

TABLE 5–6

MAXIMUM PERMISSIBLE VOID SIZE, SRE FUEL-ROD BOND

Type of void	Maximum void size, inches
360 degree, circumferential	0.080
Axial, extending rod length	0.140
Square	0.34

autoradiography, radiography, temperature-sensitive paints, and infrared devices. The Cyclograph was selected for routine use.

Tests on the assembled element included handling, sodium soaking, cleaning, disassembling in the hot cell, and thermal cycling. Hydraulic studies and drop tests were also performed. Prototype fuel elements were fabricated and used in tests to establish handling and cleaning procedures. The fuel element was placed in a mockup section corresponding to a reactor coolant channel and soaked in static sodium at temperatures up to 1000°F for varying periods of time. Elements were then removed under an inert atmosphere into a cask and transferred to a cleaning cell.

Hydraulic studies were performed on prototype fuel elements using water at 180°F to approximate the Reynolds number expected for sodium in the SRE operating in the 500 to 800°F range. During these tests orifice plates were calibrated and pressure drop measurements across the fuel element were obtained. It was also established that vibration should cause no adverse effects. The coolant mixing studies were conducted later to establish that the center rod in the seven-rod element would be adequately cooled (Section 3–2).

During the operation of changing fuel in the SRE, a failure of the handling equipment could result in a fuel element dropping into the reactor. Under the worst conditions, the fuel element could fall approximately 24 feet before being stopped abruptly when the shielding plug reaches its normal operating position in the reactor top shield. If, at this time, the uranium slugs have sufficient kinetic energy to cause a rupture of the fuel jacket, slugs would fall into the plenum chamber beneath the reactor core. This would result in contaminating the coolant with fission products, as well as presenting a difficult recovery problem. A series of tests were performed to study the effects of accidentally dropping a fuel element. It was concluded that an accident resulting in a drop of as much as 12 feet would not cause rupture of the fuel jackets. The maximum possible drop of 24 feet could conceivably result in rupture of the jacket; however, only a few slugs should fall out, since the jacket tubing tends to retain the slugs because of a decrease in diameter.

References

1. A. H. Cottrell, *Creep of Alpha Uranium During Irradiation on Thermal Cycling*, Report AERE M/M-102, Gt. Brit. Atomic Energy Research Establishment.

2. S. Siegel, North American Aviation, Inc., and M. Finniston, United Kingdom, private communication.

3. J. H. Kittel and S. H. Paine, Effects of Irradiation on Powder Compacts of Uranium and Some Uranium-Base Alloys, in *Proceedings of the Second Nuclear Engineering and Science Conference*, Vol. 2, Advances in Nuclear Engineering. New York: Pergamon Press, 1957. (pp. 260–271)

4. J. H. Kittel and S. H. Paine, Effects of Irradiation on Fuel Materials, in *Proceedings of the Second International Conference on the Peaceful Uses of Atomic Energy*, Geneva, 1958.

5. W. N. McDaniel et al., Development of Core Elements for the Enrico Fermi Power Reactor in *Proceedings of the Second International Conference on the Peaceful Uses of Atomic Energy*, Geneva, 1958.

6. J. D. Eichenberg et al., *Effects of Irradiation on Bulk UO_2*, USAEC Report WAPD-183, Westinghouse Atomic Power Division, 1957.

CHAPTER 6

SRE COMPONENTS AND SYSTEMS

6-1. Reactor

6-1.1 Reactor core. The reactor core, Fig. 6–1, includes the moderator/reflector assemblies, fuel elements, control and safety rods, and containment for these assemblies.

Cavity liner, foundation, and biological shield. The core cavity liner is the outermost tank in the core cavity. This liner, 14 feet 8 inches in diameter and 23 feet high, was fabricated by welding from a commercial grade of carbon steel. The bottom of the tank is a 1-inch thick flanged tank head, and the shell was formed from $\frac{1}{4}$-inch plate material. Two box-type extensions on this liner form passages for coolant piping. Attached to these box-type extensions are circular entrances to the main and auxiliary galleries. These cylindrical gallery entrances accommodate gallery seal diaphragms providing a gas seal between the gallery and the reactor cavity.

The cavity liner is penetrated by four thimbles, which curve upward with entrances at the reactor floor level. These thimbles accommodate ion chambers and fission chambers, and permit these instruments to be located as near as possible to the core in its central plane when lowered from floor level (see Fig. 6–28).

The reactor foundation is a 4-foot thick reinforced concrete pad poured on a sandstone rock formation at the bottom of the cavity excavation. The cavity liner bottom and first course of shell plates were installed on anchor bolts located in the reinforced concrete foundation. A biological shield surrounds the cavity liner and extends from the concrete foundation up to the building floor. It is formed of reinforced concrete ~3 feet thick.

This shield and the foundation are cooled by circulating tetralin through pipes welded to the outside of the cavity liner (Fig. 6–2). There are 28 coolant pipes of 1-inch pipe size, connected in parallel circuits. These cooling circuits are designed to remove 150 Btu/ft^2·hr, of which 100 Btu/ft^2·hr is heat flowing out from the reactor core and thermal shield, and 50 Btu/ft^2·hr flows in from the concrete biological shield, generated by neutron and gamma heating. Thirty-nine thermocouples are located on the outside of the cavity liner in contact with the concrete biological shield to indicate temperatures in critical areas. Attention is concentrated on the area in the vicinity of the instrument thimbles, with five thermocouples placed in the vicinity of each of the four thimbles where they penetrate the cavity wall.

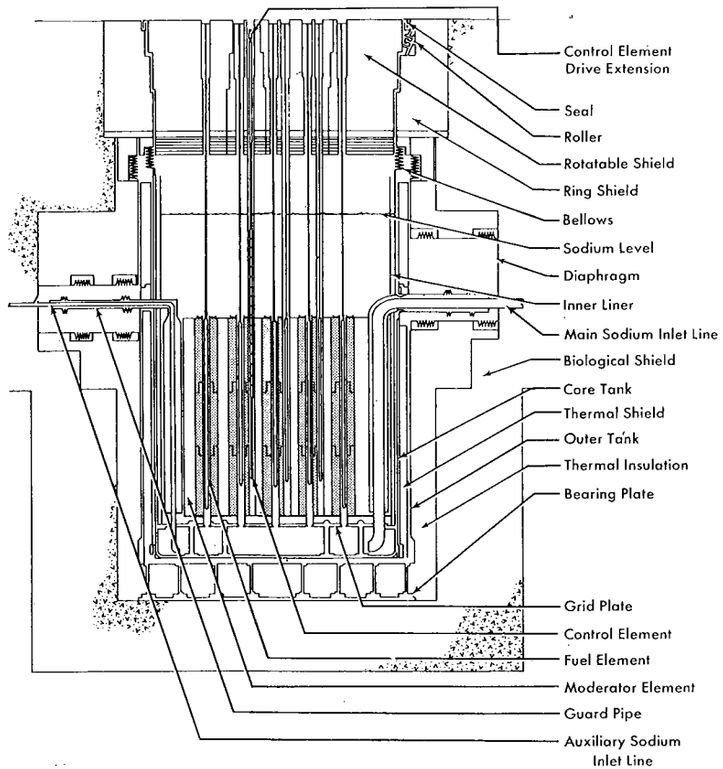

FIG. 6–1. Core cross section.

Insulation. Thermal insulation located immediately inside the cavity liner (Fig. 6–2) was selected on the basis of compatibility with molten sodium. The most satisfactory commercially available type insulation was found to be a calcined diatomaceous silica and asbestos block insulation. Each insulation block is 4 by 6 by 30 inches. Three courses of blocks, each 4 inches thick, were installed completely around the inside of the cavity liner, making a total insulation thickness of 12 inches.

Similar blocks were placed on the bottom of the cavity liner (Fig. 6–2). These blocks were trimmed to bring the surface of the insulation up to the top edge of the support cylinders. Since the compressive strength of the insulation is high, and the area under compression is large, the insulation could support the whole reactor in the unlikely event of a failure of structural supports. Vertical insulation blocks are fastened to the cavity wall with stainless-steel wires tied to clips previously welded on the

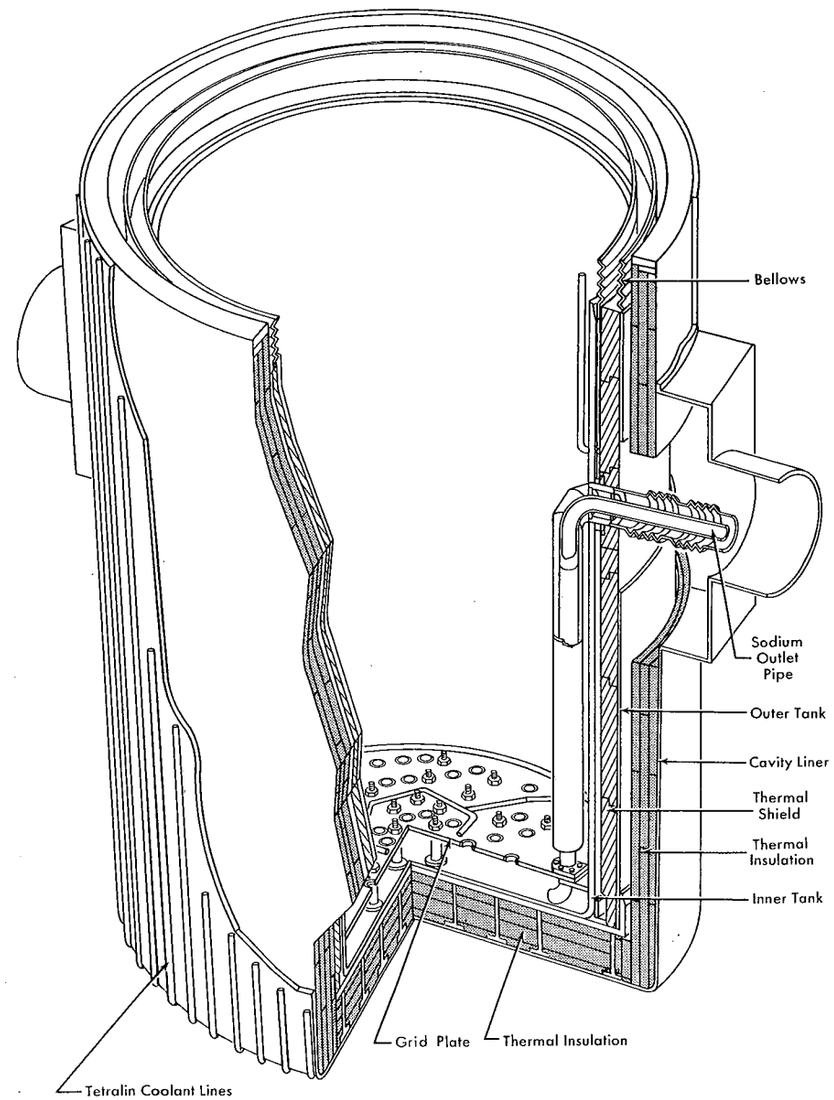

FIG. 6–2. Core containment cutaway.

cavity liner. To inhibit dusting, each block was coated with sodium silicate prior to installation.

At the top of the thermal insulation, in the corner formed by the cavity liner and core tank flange, a laminated, stepped ring of graphite was installed. Three courses of graphite make up this ring, with the top course radial width 12 inches, the center course 8 inches, and the bottom course 4 inches (Fig. 6–2). The ring was divided into 12 segments to facilitate fabrication and installation, the ends of each segment stepped to overlap when installed. This ring was installed to thermalize fast neutrons, in order to reduce streaming of neutrons and gamma rays which would otherwise occur through an unshielded crevice between the ring shield and the building floor.

Pipes, gas seal bellows, and gallery seal diaphragms were insulated with great care in order to maintain uniform temperature gradients. Insulation in these regions consisted of calcined diatomaceous block, wrapped and tied to the various components. Where this was impractical, a blanket-type, felted alumina and silica ceramic and fiber insulation was employed.

The insulation space atmosphere is nitrogen at 3 psig pressure.

Outer tank (see Fig. 6–2). Immediately inside the thermal shield is an open top vessel called the outer tank, fabricated of ASTM-A301 grade B steel (1% chromium—½% molybdenum). This tank is 12½-foot ID and 19 feet high, with a steel plate bottom 3 inches thick which serves as a thermal neutron shield below the reactor. This plate also provides support against the hydrostatic pressure existing in the lower plenum of the core tank and serves to support the thermal shield rings which are located in the annular space between the core tank and the outer tank. Both the upper and lower surface of the bottom plate were machined to true, flat surfaces after the plate was welded to a 15-inch high, 2-inch thick flange. This welded assembly was fully annealed prior to machining. The finished thickness of the bottom plate is 2⅜ inches. Succeeding courses of the outer tank were made up of ¼-inch thick material. Cleats for centering the thermal shielding and for centering and aligning the core tank were dowelled into place prior to welding the shell courses. Accurate placing of the cleats was assured by using a template which had been previously used for locating slots in the skirt of the core tank.

The support underneath the outer tank carries the total load of the core tank and its contents, the outer tank, and the thermal shield rings. It also resists the reaction produced by core and outer tank bellows when they are compressed by upward expansion of the tanks. This support is comprised of four concentric cylinders extending down to bearing plates fastened to the bottom of the cavity by means of anchor bolts extending into the concrete foundation. These bearing plates were precisely leveled by metal shims between the plates and the bottom of the cavity. The four

concentric cylinders are surrounded by thermal insulation, and have a wall thickness of ¼-inch except for the outermost cylinder, which is ½-inch thick.

This outermost cylinder serves to maintain the outer tank centered relative to the concrete foundation. Narrow flanges were welded to the outside surface of the cylinder at its bottom and top. These flanges have radial notches cut into the edges to fit around cleats welded to the bottom of both the outer tank and the outer bearing plates. This scheme locates the center point of the tank but permits free radial expansion of the tank bottom. This same principle of radial cleats and slots aligns the core tank with respect to the outer tank.

Loads on these support cylinders are 25,300 pounds on the inner cylinder, 50,900 pounds on the next cylinder, 75,300 pounds on the third cylinder and 243,600 pounds on the outermost cylinder. The maximum unit stress occurring in any of these cyclinders under the most unfavorable operating conditions amounts to less than 1500 psi, thus providing a safety factor of about 4.2. Thermocouples are attached to the outer tank and to the support cylinders. Leak detectors are installed near the bottom of the outer cylinder.

The top of the outer tank is sealed with an 18-inch high, four-convolution bellows.

A rectangular opening 32 by 42 inches, with its bottom edge at an elevation 11 feet 3⅝ inches above the floor of the core tank provides a passage for the auxiliary coolant pipes. A circular opening 66 inches in diameter is located opposite the auxiliary opening, to provide an area for the main coolant piping. The center of the circular hole is 14 feet ⅜ inches above the floor of the tank. Gallery seal bellows were attached to the outer tank after installation. Guard pipe to coolant-pipe seal bellows and the coolant pipe-to-gallery-diaphragm seal bellows are located within the gallery seal bellows.

Thermal shield (see Fig. 6–2). The side thermal shield is located in the annular space between the core tank and the outer tank. A bottom thermal shield is provided by the bottom of the outer tank, as noted above. The top thermal shield is an integral part in the loading face shield and will be described subsequently.

The side thermal shield is composed of seven cast SAE 1020 low-carbon steel rings. The finished size is 11 feet 6 inches ID and 12 feet 5 inches OD, as assembled. Each ring is about 35 inches high except for the top ring, which is 28⅞ inches high. The rings are stepped at the edges in order to mate when stacked. The total stacked height of the seven rings is 18 feet 10⅞ inches. The stack was centered at the bottom by a close fit of the bottom ring around core tank alignment cleats attached to the bottom of the outer tank. Cutouts were made in appropriate places in the rings to

permit passage of coolant pipes. Where cutouts were made, 2-inch thick steel plate collars were provided around pipes to complete the shielding and reduce gamma and neutron streaming.

Recesses are provided in the fourth shield ring opposite the fission chamber thimbles. Thickness of the thermal shield is reduced to 1 inch in these areas to reduce neutron attenuation and permit fission and ion chambers to function properly. In order to obtain data on thermal shield temperatures, two thermocouples are provided in holes drilled in the third ring from the bottom, opposite the center of the core.

The function of the thermal shield is to absorb gamma rays and thermal neutrons leaking from the reactor core, thus reducing heat generated in the concrete biological shield. The heat generation is calculated to be 3000 Btu/ft^2·hr. Ninety-seven percent of this heat will flow inward through the core tank wall to the sodium coolant, and the remaining 3 percent flows outward through thermal insulation to the cavity liner.

The annulus containing the thermal shield is maintained at an atmosphere of 3 psig of helium and has a net volume of 878 in^3/in of height. In the event of a leak within the core cavity, the sodium level in the reactor upper plenum will be lowered only 20 inches by filling this volume. A drain tube is provided. Helium was selected for this application because of its thermal conductivity, thus increasing the heat transfer from the thermal shield to the core tank.

Inner Tank. Design of the inner tank was predicated on the various conditions which it would be required to sustain: (a) a gas pressure of 3 psi over the top pool, to maintain a positive pressure at the coolant pump section, (b) hydraulic pressure loss through the core, (c) depth of coolant in the core tank.

The sum of all these pressures, combined with a margin for possible malfunction of gas relief valves for the space above the core, resulted in a tank design pressure of 14 psi.

Basic design conditions were heat generation, 20,000 kw; temperature rise in the reactor coolant, 460°F; maximum sodium outlet temperature, 1200°F.

The original reference dimensions of the reactor were core diameter, 10 feet; core length, 10 feet; fuel element spacing arrangement, 11-inch triangular spacing.

A requirement that no significant expansion of the core tank should take place due to creep under any conditions, including casualties, was set. It was therefore decided to establish 1500°F as the design temperature for this tank. Stresses of the magnitude permitted by the ASME Code [1] (allowable stress of 750 psi at 1500°F) would cause a negligible amount of creep for 10 years of continuous operation at 950°F.

Because of the safety requirements of the reactor and the imperfectly

known corrosion problems associated with liquid metal, it was necessary that weld joints be of the best quality. Welding procedures at AEC laboratories and other companies working with liquid metals were reviewed and a welding procedure was prepared. As a part of this program, welders were trained and all welds were closely inspected and tested to correlate weld quality with weld procedure and to improve both where possible. Prior to fabrication of SRE components these methods were incorporated into a process specification which established weld-joint preparation, welding material, welding procedures, and weld-joint inspection requirements.

In the design of reactor tank and components, weld-joint configurations were specified which would allow nondestructive testing and inspection and which would not include sharp re-entrant corners or notches for stress concentration. Where angle joints were necessary, generous fillets, carefully blended into the components being welded, were provided. No solution heat treatments were performed after welding because the sodium and sodium oxide circulated in the coolant system was not considered to be corrosive to the type of steel used in the tank. This was established on the basis of various tests performed at Atomics International and information published at that time.

The tank was fabricated of Type 304 stainless steel, in the form of a cylindrical, flat-bottomed, open-top vessel. It measures 11-feet ID, 18 ft $10\frac{3}{8}$ inches high, and has a $1\frac{1}{2}$-inch thick side wall and bottom. The requirements of the Rules for Construction of Unfired Pressure Vessels [1] were complied with for design and fabrication insofar as applicable. An efficiency of 90 percent was assumed for radiographically inspected weld joints. The flat bottom of the tank is a flanged head with an inside corner radius of $4\frac{1}{2}$ inches between the flange and the flat portion. The head thickness of $1\frac{1}{2}$ inches was selected for convenience in welding and for strength in the span subject to tank pressure between tank support pads. The moment applied to the corner radius resulting from reaction of a bellows seal at the tank top, and the weight of the shell, were determined to establish the adequacy of tank thickness from an allowable stress standpoint.

The vessel shell is formed of three courses of $1\frac{1}{2}$-inch thick plate material, two semicylindrical pieces making up one shell course. The bottom course is $55\frac{7}{8}$ inches high, the middle course 81 inches high, and the top course $81\frac{1}{4}$ inches high. The upper 4 inches of the top course is tapered from $1\frac{1}{2}$ inch to $\frac{1}{2}$ inch to facilitate welding to a $\frac{1}{2}$-inch thick top bellows nipple (Fig. 6–2). After the shell plates and bottom were formed, but prior to welding, they were inspected ultrasonically. A circumferential grid plate support, $1\frac{1}{2}$ inches deep by 5 inches wide is welded to the inside of the tank shell $18\frac{3}{4}$ inches above the bottom surface. A slotted $\frac{3}{4}$-inch steel

skirt is welded around the outside flange of the bottom tank head; the slots are used for alignment of the core tank. Three circular rows of pads (10-inch diameter) were welded to the outside of the bottom tank head to furnish bearing surface for core tank supports.

A row of pads (8-inch diameter) was welded inside the tank to correspond with the intermediate row of pads on the outside. The bottom head and first shell course assembly was stress relieved at 1350°F after completion of this operation. The assembly was machined so that the outside bottom pads provided a true flat bearing surface for the core tank, and the support ring provided a flat and parallel-to-the-bottom support for the grid plate. The inner 8-inch pads were also machined to a true and flat surface, and were bored and threaded to receive the grid plate supporting columns. The next two courses were then welded into position, and the required coolant pipes and nozzles were installed. A ring $2\frac{1}{4}$ inches wide by $\frac{3}{4}$ inches deep was welded inside the tank shell at an elevation 11 feet 11 inches above the bottom bearing surface to provide a support for the core tank liner.

Coolant inlet lines were arranged to enter the tank through the tank wall at an elevation somewhat above the top of the core, and to lead downward inside the tank vertically along the edge of the core to a plenum below the grid plate. It was necessary to provide thermal insulation around the inlet pipes to prevent undesirable heat transfer between the hot sodium pool and the cool inlet sodium. This was accomplished by making the inlet pipes double-walled and providing an annular helium gas filled space between the two walls. The attachment of the inner pipe to the outer pipe, in the vicinity of the grid plate, was a point of potentially high thermal stress in the event of sudden changes in coolant temperature. Thus, an attaching member was designed and installed in the shape of a cone to reduce heat transfer by making a longer metal path, and to provide flexibility in case of thermal shock.

To avoid anchoring the bottom end of the double-wall coolant inlet pipes, it was necessary to provide a flexible seal where these pipes penetrate the grid plate. A bellows at this point is not considered desirable because of inaccessibility, and therefore a double plate was designed and bolted to the grid plate to allow the inlet pipe to expand or contract vertically. This expansion is independent of the tank and allows lateral movement of the pipe with respect to the grid plate. The double plate is a sliding surface, and is not a perfect seal. However, all sliding surfaces were finished smooth and close tolerances were maintained to minimize leakage from the main coolant plenum to the moderator coolant plenum. Sliding test of Type 304 stainless steel in sodium, at the expected loading, were performed to ensure that neither seizing nor galling would occur. The cone arrangement previously described was again used at the top of the double-walled

pipe, with the small inner end of the cone fitting closely around a hard-surfaced sleeve welded to the inner pipe. This design allowed for a difference in expansion between the two pipes, yet provided a mechanical path for pipe reaction loads to be transmitted to the tank wall with very little deflection of either the inner or the outer pipe. The double pipe and cone arrangement is used in three places where incoming coolant is brought down inside the tank:

The main coolant inlet, a 6-inch diameter, schedule-40 pipe within a 10-inch diameter, $\frac{3}{8}$-inch wall guard pipe.

The auxiliary coolant inlet, a 2-inch diameter, schedule-40 pipe within a 10-inch diameter, $\frac{3}{8}$-inch wall guard pipe.

The moderator and reflector cell wall coolant inlet, a 2-inch diameter, schedule-40 pipe within a 4-inch, schedule-40 guard pipe.

Other pipes penetrating the tank wall, all at an elevation above the top of the core, are as follows:

The main coolant outlet, a 6-inch (nominal pipe size) nozzle.
The auxiliary coolant outlet, a 2-inch (nominal pipe size) nozzle.
The drain pipe, a 2-inch, schedule-40 pipe.
The vent pipe, a 2-inch, schedule-40 pipe.

Auxiliary inlet and outlet pipes are placed diametrically opposite the main coolant inlet and outlet. The auxiliary coolant outlet nozzle is placed 6 inches lower than the main coolant outlet nozzle, whose centerline is located $9\frac{1}{2}$ inches above the top of the core. This location was selected so that a break in the main primary piping system lowering the sodium pool level to that of the nozzle would still permit circulation of coolant through the core by the auxiliary system.

As a support for the moderator and reflector cans, and to separate the main coolant inlet plenum from the moderator/reflector wall coolant plenum, a perforated diaphragm called a grid plate was provided (Fig. 6–2). This grid plate is formed of $1\frac{1}{2}$-inch thick Type 304 stainless steel, 125 inches in diameter. Holes were bored on a precise 11-inch triangular spacing to receive and position the moderator and reflector can pedestals. These holes are cone-shaped on their top edges, with a smooth finish to provide a seal when mated with the spherical end of the pedestals. The grid plate was machined to a true, flat, smooth surface around the bottom edge where it rests upon the grid-plate support ring. Radial slots were provided to fit closely on studs threaded into the grid-plate support ring in order to hold down and center the grid plate.

Since the grid plate is a relatively thin membrane, further support is required to carry the load imposed by the core. This support is provided by 30 supporting columns, spaced in three circular rows coinciding with

the bearing pads welded on the bottom of the tank. Each column is equipped with a bearing pad at the bottom end; the intermediate row is welded to the bottom of the tank. The welded columns were provided so that an unusually high, lower-plenum pressure would not deflect the grid plate upward and raise the core. All columns extend through the grid plate and each column is provided with a threaded end to receive a nut on top of the grid plate. Washer-type shims are provided on a shoulder of each column, immediately under the grid plate, to correct for any irregularity in grid plate and tank bottom contour. A pointed dowel pressed into a hole in the grid plate is provided at one side of each pedestal hole. This dowel engaged a slot in the pedestal to ensure proper orientation of each moderator or reflector assembly when the core was installed.

Analysis indicated that temperature variations along the tank wall, resulting from sudden changes in reactor operation, would produce severe thermal stresses in the tank wall. A buffer zone of stagnant sodium $1\frac{1}{2}$ inches thick next to the tank wall was provided by installing a $\frac{1}{4}$-inch thick Type 304 stainless-steel liner all around inside the tank. This liner extends vertically from the top of the core tank to a point 2 feet above the grid plate. It is suitably pierced to accommodate piping and penetrations, with a clearance of approximately $\frac{1}{32}$ inch around each liner penetration. It is supported by the liner support ring previously noted.

A separate, self-centering cylinder is provided around the top edge of the core to center and support the top ends of the graphite assembly. This band, $\frac{1}{4}$ inch thick and 6 inches high, was manufactured from Type 405 stainless steel. It is supported and centered within the liner by means of dowels welded to its inside surface, projecting radially outward into holes drilled in the liner. Spacer plates on top of the moderator and reflector cans are clamped in position by 12 straight bars of Type 405 stainless steel mounted on the band. Two worm gears attached to the band with threaded studs are provided on each bar so that the bars may be adjusted radially to bear against the entire top of the core and properly align its position under the top shield.

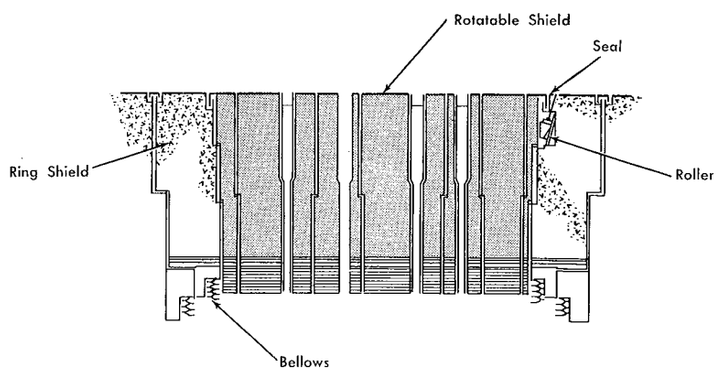

FIG. 6–3. Top shield plug.

A metal bellows located at the top of the core tank provides a gas seal and permits vertical expansion of the tank (Fig. 6–2). The bellows has the same inside diameter as the tank, has four convolutions, stands 18 inches high, and was fabricated from 0.093-inch thick Type 321 stainless steel sheet. It was welded at its bottom edge to the top of the core tank and at its top to a metal cylinder extending up to the bottom edge of the ring shield.

Thermocouples are located on the outside surface of the core tank, spaced vertically on the tank wall 75 degrees clockwise from the primary coolant inlet pipes. Other thermocouples are located on the main and auxiliary gallery side of the tank and the main inlet nozzle. Also, leak detectors are located near the bottom edge of the core tank.

Top shield plug. The top shield plug (Fig. 6–3) serves as both a biological shield for the top of the reactor cavity and as a gas seal for the atmosphere above the top sodium pool. The top shield is formed of two components, the loading face shield which covers the reactor core and a ring shield which covers the remainder of the reactor cavity.

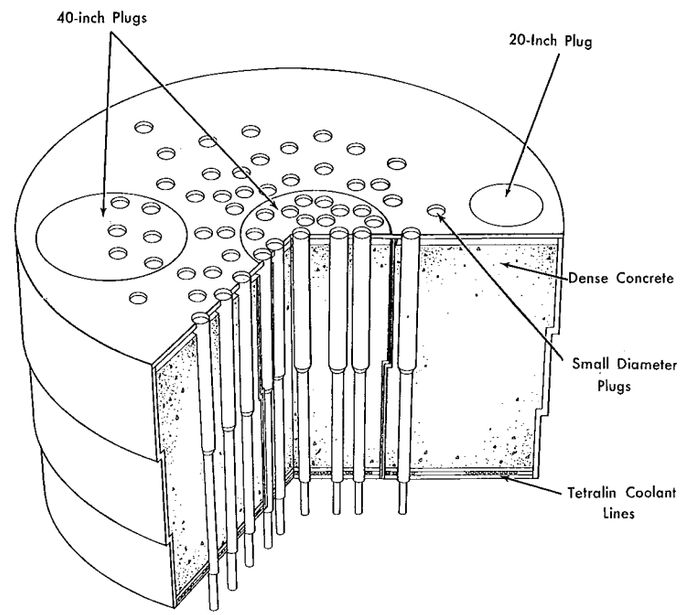

FIG. 6–4. Loading face shield.

Loading face shield. The loading face shield (Fig. 6–4) is a stepped plug, 11 feet $9\frac{3}{4}$ inches in diameter at the top, 10 feet $11\frac{1}{2}$ inches in diameter at the bottom, and $81\frac{1}{2}$ inches in over-all thickness. Two steps ~6 inches deep are located $24\frac{1}{4}$ inches and 49 inches from the top. These steps mate into corresponding steps on the inner surface of the ring shield to form a barrier to radiation streaming. The loading face shield is supported by the bottom step of the ring shield.

The top surface of the loading face shield is penetrated by eighty-one $4\frac{1}{2}$-inch diameter holes; 57 of these holes reduce to a minimum diameter of 3 inches, and 24 reduce to $3\frac{1}{2}$ inches, at the support shoulder located approximately 34 inches below the top surface of the loading face shield (see Fig. 6–5 and Table 6–1). One 20-inch hole and plug and two 40-inch holes with plugs are located to provide access for loading and removal of any moderator or reflector can.

The loading face shield may be rotated by lifting the shield 1 inch from its bearing surface. It is normally centered by means of three roller assemblies located on the inner face above the upper step of the ring shield. A gas seal between the rotatable loading face shield and the ring shield is provided by a lip-and-groove filled with low-melting (150°F) alloy. Calrod heaters are cast into this seal, to which portable electric leads may be attached when melting is required.

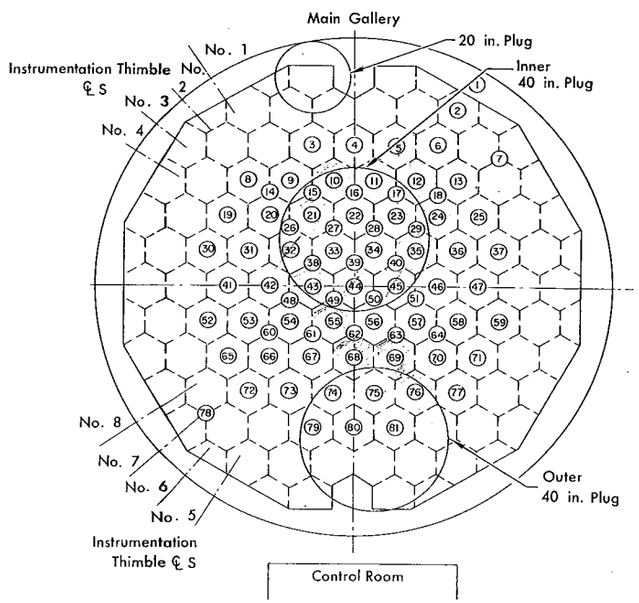

FIG. 6–5. Loading face top surface.

TABLE 6–1

SRE LOADING FACE

Element	Plug size, inches	No. required	Positions*
Fuel elements	3	31	10, 11, 20, 21, 22, 23, 31, 32, 33, 34, 35, 36, 42, 43, 44, 45, 46, 53, 54, 55, 56, 57, 58, 66, 67, 68, 69, 70, 74, 75
Safety rods	$3\frac{1}{2}$	4	27, 40, 48, 63
Control rods (one speed)	$3\frac{1}{2}$	2	28, 51
Control rods (two speed)	$3\frac{1}{2}$	2	38, 62
Source	$3\frac{1}{2}$	1	39
Dummy elements Center channel	3	13	2, 4, 6, 9, 12, 19, 25, 41, 47, 65, 71, 73, 76
Dummy elements Corner channels	$3\frac{1}{2}$	4	14, 18, 49, 50
Dummy elements Corner channels (temp. meas.)	$3\frac{1}{2}$	2	16, 61
Dummy elements Corner channels (temp. & press. meas.)	$3\frac{1}{2}$	2	60, 64
Plugs in top shield only	3	13	3, 5, 8, 13, 30, 37, 52, 59, 72, 77, 79, 80, 81
Plugs in top shield only	$3\frac{1}{2}$	2	15, 29
Plugs in top shield only (with leads from special moderator cans in 21 & 23)	$3\frac{1}{2}$	2	17, 26
Sodium level instruments	$3\frac{1}{2}$	2	7, 78
Special thimble (between core tank and core tank liner)	$3\frac{1}{2}$	1	1

* See Fig. 6–5.

All plugs in the loading face shield are stepped to prevent radiation streaming and to provide mechanical support. A gas seal for plugs in the loading face shield is made by two silicone rubber O-rings compressed between the plug and the casing near the top of the loading face shield, which is at substantially room temperature. A third gasket, depressed by a retaining ring, is incorporated in the top lip of each plug, so that this gasket may be maintained without the necessity of lifting the plug. The retaining ring is held in place by three screws and performs the additional function of positively locking the plugs in place after insertion in the loading face shield.

Calculations indicate that about 1000 Btu/ft^2·hr of heat is received by the underside of the loading face shield. About 85 percent of this heat is due to thermal radiation from the hot sodium pool, with the remainder generated by gamma and neutron capture. The radiative heat load passing into the shield is reduced by reflective insulation, formed by 13 stainless-steel sheets $\frac{1}{32}$-inch thick, and separated by a $\frac{3}{4}$-inch gap. This sheet assembly is suspended from the bottom of the shield. The reflective insulation assembly is not gastight, and some sodium condensation is expected. The assembly may be freed of sodium by shutting off the top shield cooling system and permitting the temperature to rise in the reflective insulation, thus melting condensed sodium and permitting it to drain back to the reactor through weep holes.

Cooling for the loading face shield is provided by a series of tubes embedded in the concrete biological shield material and in contact with the metal lower face of the shield. Tetralin is circulated through this tubing to maintain the maximum temperature of concrete below 150°F.

Materials for construction of the shell of the loading face shield were selected on the basis of thermal expansion characteristics. Consequently, the bottom shield plate and side walls were fabricated of Type 405 ferritic stainless steel, in order to obtain thermal expansion which would match the expansion of the concrete within the shield and reduce misalignment between shield plugs and core holes when the entire assembly was at operating temperatures. Steel casings serving as holes for the shield plugs are protected from excessive bending and shearing forces due to thermal expansion of the concrete, by annular sleeves. This permits expansion of the bottom plate without subjecting the casings to excessive shear loadings. The shell of the loading face shield was filled with magnetite ore when all fabrication operations had been performed and then grouted to form dense concrete. The finished loading face shield with plugs in place weighs approximately 82 tons.

The ring shield, which supports and surrounds the loading face shield, is 16 feet $5\frac{1}{2}$ inches OD at the top and 15 feet $11\frac{1}{2}$ inches at the bottom. A single 6-inch step at mid-height mates with a similar step in the cavity liner, and serves as a supporting shelf for the ring shield. The ring shield is $71\frac{1}{2}$ inches in over-all thickness. A gas seal between ring shield and cavity liner is provided by a low-melting (150°F) alloy similar to that provided for the loading face shield. A series of cooling coils was installed at the lower face of the ring shield, through which tetralin is circulated to maintain a temperature of less than 150°F.

The bottom seal plate and side walls of the ring shield were fabricated of Type 405 stainless steel. The bottom seal plate is $1\frac{1}{2}$ inches thick, on top of which a $1\frac{1}{2}$-inch thick layer of lead was poured. This lead layer contains the cooling coils. Immediately above the lead is a 1-inch plate of low-carbon steel which provides additional shielding for gammas and thermal neutrons. The ring shield was filled with magnetite ore and dense concrete grout, which provides the bulk of the necessary biological shielding.

6–1.2 Moderator and reflector elements. The graphite moderator and reflector elements are installed inside the core tank. Preventing contact with the sodium coolant is the principal problem associated with the graphite. Free contact would result in the absorption of sodium into void spaces in the graphite, which constitute approximately 27 percent of its volume. Since sodium is a neutron absorber, sodium absorption introduces a poison into the highest thermal neutron flux regions of the reactor, thus inducing prohibitively high neutron capture. Additionally, the transport of carbon from the graphite to cooler parts of the heat-transfer system would result in severe carburization of reactor and heat-transfer system structural material.

A large volume of metal is required for cladding the graphite logs in the SRE, and neutron economy would not permit the use of iron alloy in the moderator region. The cladding is formed of zirconium sheet fabricated into individual can assemblies, as shown in Fig. 6–6. A sheet 0.035 inch thick is used on the side panels of each hexagonal graphite column, and 0.10-inch thick zirconium stock is used for the bottom and top can heads. The distance across flats of each can assembly is slightly less than the 11-inch center to center spacing of the triangular fuel lattice. This reduction is sufficient to provide an average gap between cans of approximately 0.170 inch during normal operation. This gap forms a thin flat channel through which sodium may flow to remove heat generated within the graphite.

Each moderator/reflector assembly is bolted by zirconium studs to a supporting pedestal at the base of the can, and to a spacer plate at the top. Pedestals and spacer plates are fabricated from Type 405 stainless steel to minimize thermal expansion problems. The pedestal not only serves as a support for the can, but locates it in the lattice by fitting into

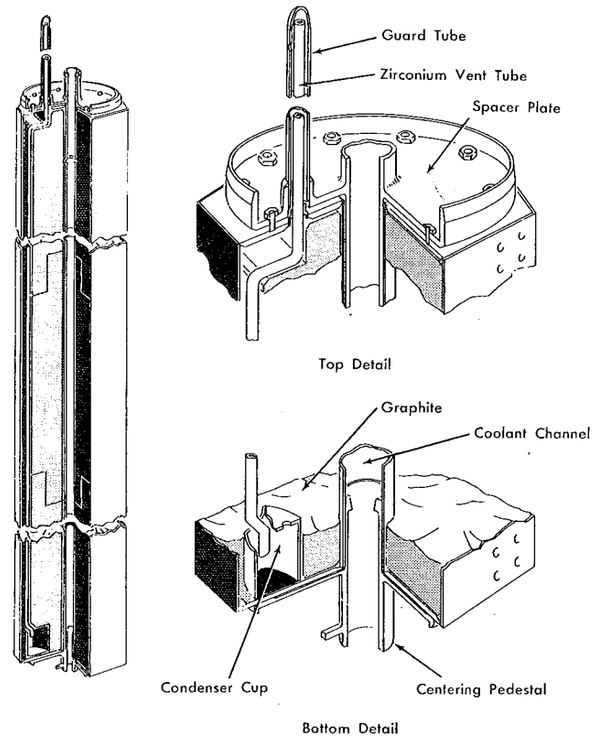

FIG. 6–6. Moderator can details.

an accurately located hole provided in the grid plate. The bottom of the pedestal is formed as a section of a sphere, which mates with a conical taper in the grid plate hole to form a seal. This seal was designed to prevent significant leakage into the plenum formed between the top of the grid plate and the bottom of the moderator cans.

Each moderator can pedestal has a circular channel along its axis which permits flow of sodium from the main lower plenum up through the coolant tube in the moderator can assembly. The top spacer plate serves as a lifting fixture for the entire assembly and as a means of lateral support for the cans. Spacer plates on adjacent cans nest together and are maintained in place by a clamping band around the periphery of the outer ring of cans. Each moderator can assembly in the core region is penetrated along its axis by a zirconium tube 2.80-inch ID and 0.035-inch wall thickness, welded to the bottom and top heads. Each tube normally contains a fuel element.

In event of reactor scram, sodium temperature in the coolant tube suddenly decreases, causing a contraction of the coolant tube relative to the outside walls of the can. This produces a deflection in both the bottom and top heads. The stresses thus produced have been calculated to be below the yield stress of zirconium, and mechanical flexure of test assemblies in sodium at operating temperatures has demonstrated that a life of at least 3000 scram temperature cycles may be expected.

Some of the moderator cans were modified from the regular hexagonal pattern of their cross section to provide a groove at two or three corners for the full length of the column. These grooves, when the cans are installed, form $3\frac{1}{2}$-inch diameter holes at the adjacent corners of three cans and provide space for control rods, safety rods, and special reactor accessory elements, such as the source element and a liquid level measuring device.

Reflector assemblies are generally similar to moderator assemblies except that no axial channels have been provided, and the outermost rows of reflector assemblies are canned in Type 304 stainless-steel sheet rather than zirconium.

To obtain an approximation to a cylinder for the core, some reflector cans were constructed as $\frac{1}{2}$ and $\frac{5}{6}$ hexagons. Eight different configurations were built, forming a duo-decagonal pattern. There are five different cross-sectional configurations of moderator cans included in the core, and the reflector portion of the core is made up of three different cross-sectional configurations of stainless-steel cells (Fig. 6–7).

There are a total of 119 cans in all. The odd shaped "G" type and "H" type cans facilitate mechanical support of the core from the vessel wall as well as provide a nearly cylindrical shape. An additional two "B" type moderator cans are provided with instrumentation tubes to obtain data on the effect of irradiation on the physical properties of graphite.

The moderator graphite was machined from 13-inch diameter logs of

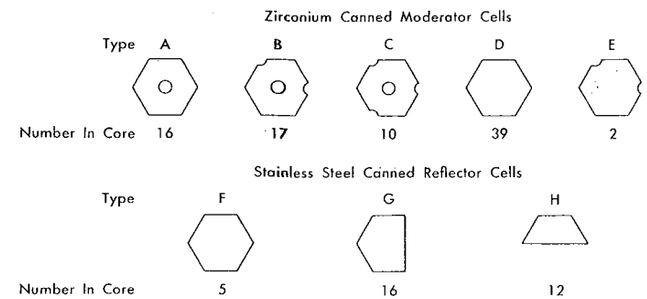

FIG. 6–7. Variations of the hexagonal shape used on moderator/reflector cans.

TSP reactor-grade graphite. This graphite was chlorine purified, twice reimpregnated, gas baked, and cooled in helium. Each moderator graphite column is assembled in three pieces connected with cylindrical graphite plugs for alignment. There are no special strength requirements on the graphite except that it must support its own weight and resist lateral earthquake acceleration while supported at the top and bottom ends.

The extent of outgassing from the graphite under radiation and temperature conditions expected in the reactor core was unknown when moderator can design was commenced. Consequently, it was considered necessary that provision be made for venting the moderator/reflector assembly in order that gas buildup would not bulge the cladding and distort coolant channels. A "snorkel" tube was attached to each can, running to the bottom of the moderator/reflector assembly and terminating just above a $2\frac{1}{2}$-inch deep by $2\frac{7}{8}$-inch diameter stainless steel cup. This $\frac{1}{4}$-inch zirconium snorkel tube projects above the can about 7 feet, so that it terminates in the gas atmosphere above the top pool. That portion of the tube which projects above the moderator can is protected by a $\frac{3}{4}$-inch stainless-steel guard tube. The purpose of the cup is to accumulate any condensed sodium vapor which may pass down the snorkel tube. The cup and lower end of the tube are approximately at inlet sodium temperature, and therefore condensation of vapor coming down the tube from above the pool (at reactor outlet temperature) could be expected to occur. The cup is sized to hold sodium condensed under operating conditions over a 20-year period. The snorkel tube is originally sealed with an alloy of lead, to permit initial evacuation and leak test of the moderator/reflector assemblies prior to their installation in the core. This alloy melts at 257°F, and thus permits free communication of pressure between the gas atmosphere above the top pool and the interior of moderator/reflector assemblies once the top pool has been brought up to a temperature above about 300°F.

Development and fabrication. In order to fabricate the moderator/reflector assemblies, it was necessary to develop suitable welding techniques for thin zirconium sheet. Although some welding development had been done at other sites, experience was limited to welding in glove boxes with atmospheric control. Because of the large bulk of moderator assemblies, this method appeared impractical. The welding development program included (a) choice of arc-welding process to be used and the detailed requirements of this choice, such as weld current, arc-voltage, inert gas flow rate, and electrode travel speed, and (b) the requirements and characteristics of an acceptable weld, including shape, color, shrinkage, porosity, hardness, tensile strength, and minimum bend radii.

Each zirconium can required six 10-foot long longitudinal seams. A special welding fixture, utilizing a reworked gun barrel, was fabricated for this purpose. A grooved copper backing bar, drilled along its centerline to allow inert gas flow, was mounted on top of the gun barrel. Pneumatically operated, copper-tipped, hold-down fingers provided firm uniform contact between the backing bar and zirconium sheet. An inert gas atmosphere was maintained on top of the weld by an extended trailer gas cup. Automatic welds made with this machine were excellent and free of distortion. They have 100 percent penetration and less than 0.005-inch sag. These welds were made with nonconsumable tungsten electrodes. Welds joining the can heads to the shield and coolant tubes were made by hand. Copper chill bars were employed so that each weld joint could be adequately cooled. Cooling rate was discovered to be a significant factor in minimizing contamination of the weld by oxygen and nitrogen. All welds were radiographed for porosity determination, cracks, and lack of penetration. Statistical samples were tested for tensile strength and minimum bend radii. The welding development program produced the following information:

Controlled atmosphere chambers were unnecessary.

A proper combination of chill and inert gas coverage produced welds softer and more ductile than the parent zirconium metal.

It was determined that color cannot be used as a basis for judging the quality of zirconium weld, although a weld having no metallic luster indicates excessive contamination producing hardening and embrittlement.

Porosity is primarily due to poor joint cleaning, and may be reduced by remelting the weld. (Tests have shown that as many as six remelts may be made without impairing the quality of the welded joint.)

6–1.3 Control elements. During the initial design phases of the SRE, it was concluded that the low system pressures permitted use of control element thimbles which would be essentially transparent to neutrons but would separate poison elements from flowing sodium. The advantages of this concept were considered to be:

Elimination of possible contamination of the coolant by corrosion of the poison material, and a wider choice of materials and lubricants in the control rods and mechanisms.

Elimination of dynamic seals operating in a sodium vapor atmosphere.

Probable reduction of problems connected with control-element maintenance. A plug-in unit capable of being completely removed in the fuel-handling cask appeared both possible and desirable.

Elimination of dynamic problems created by dropping a safety rod into an upward-flowing sodium coolant stream.

Heat is generated in the poison material of control rods that remain inserted in the reactor, and to prevent excessive temperature rises in the

poison material a relatively small clearance between poison rod and thimble is required. A test program to establish the maximum size of this clearance was instituted. These experiments, involving the use of electrically heated simulated control rods, indicated that a 0.038-inch diametrical clearance between poison rod and inner thimble wall would yield a maximum poison rod temperature of 1450°F.

A prime objective of the control and safety-rod program was to develop elements whose drives could be quickly and easily removed from the remainder of the mechanism (rod). Such designs required a major portion of the drives to be located below the loading face. Life testing of prototype rod units of this type under SRE temperature conditions indicated that this design would have a severely limited life. Size requirements, derived from the limited volume within the top shield available for drive mechanisms and the necessity for providing neutron and gamma shielding within the drive mechanism, forced compromises in traversing mechanism capabilities. These compromises resulted in a mechanism insufficiently rugged for regulating rod service but adequate for shim rods.

Consequently, control and safety mechanisms were devised in which all the drive and snubbing operations were accomplished above the shield. It is currently necessary to remove these somewhat heavy mechanisms, leaving the control and safety elements inserted in the reactor, prior to moving the fuel-handling cask over the reactor face.

The objective of an easily cleared reactor face is still most desirable, and promising development efforts to achieve this objective are now in progress. Absorption of shock loads by forming the safety-rod poison elements of crimped disks rather than solid cylinders appears to obviate the need for snubbing. Experimental determination of shielding required for gamma and neutron fluxes in the top shield during SRE operation indicates that a relaxation of space requirements is feasible.

The functional specifications to which the SRE control rods were designed are as follows:

Four control rods with a total of 7.8 percent reactivity control were required. All control rods should be capable of shim motion of 0.3 ft/min.

Two of these rods should also be capable of regulating motion of 3 ft/min within a total of 15 inches travel.

The poison rods must be able to operate in a dry helium atmosphere, within a thimble surrounded by sodium at a temperature varying from 500°F at the bottom to 950°F near the top. (The expected maximum heat generation in the poison rods, due to neutron capture, is 8.3 kw/ft.)

Rods are limited (by the fuel-handling cask) to maximum dimensions of $4\frac{1}{2}$ inches OD by $23\frac{1}{2}$ feet long.

One year of maintenance-free service is required.

Rod position must be continuously indicated at the control panel.

The thimble must be sealed to the top shield so as to prevent contamination of the reactor gas atmosphere.

Thimble. Each control rod is contained in a thimble that serves as a barrier between working mechanisms and sodium coolant. This $23\frac{1}{2}$-foot long, Type 304 stainless-steel thimble, supported on a step in the top shield, extends into the sodium pool to a point just below the active core. The lowest $8\frac{1}{2}$ feet of the thimble is located within the core and reflector volume and has a wall thickness of 0.049 inch. Immediately above the core section is a nominal $3\frac{1}{2}$-inch OD section approximately 12 feet in length with a $\frac{1}{8}$-inch thick wall. At the thimble support shoulder the thimble outside diameter is increased to $4\frac{1}{2}$ inches, with a $\frac{1}{4}$-inch thick wall.

Poison column. The poison columns are made up of a series of eighteen 4-inch long, $\frac{3}{8}$-inch thick, 2.484-inches OD boron-nickel alloy cylinders, mounted loosely on a *pull tube* (Fig. 6–8). Room temperature clearance between cylinders and thimble is 0.038 inch. The boron-nickel alloy contains the following constituents:

Element	*Percent*
Nickel	80–82
Chromium	10–12
Iron	4–5
Silicon	1.0 maximum
Boron	1.5–2
Carbon	0.7 maximum

Drive assembly. Each drive assembly is divided into two subassemblies; the support column assembly located above the loading face and the support rod assembly attached to the poison column within the thimble. The support column is a $9\frac{1}{2}$-foot long, 7-inch diameter tube flanged at both ends. The bottom flange bolts to the reactor face and the upper flange supports a drive motor assembly. Concentric with and enclosed within the support column is a $4\frac{1}{8}$-inch diameter guide tube. Diametrically opposed slots, 95 inches long and 0.657 inch wide, are milled through the wall of the guide tube. Roller cams, mounted in a carrier which contains the ball nut, ride in the slots, preventing the ball nut from rotating. A spring-loaded ball latch attached to the carrier automatically couples to the latch cup of the support rod assembly when the ball nut is at the extreme bottom of its travel. An 8-foot long, 0.25-inch lead, 1-inch OD screw drives the ball nut. The ball screw is driven by a ballbearing supported main shaft, the top of which is motor driven through a two-tooth clutch. The support rod assembly, which is below the reactor face, consists of four rods which are fastened to the poison column at their bottom ends and

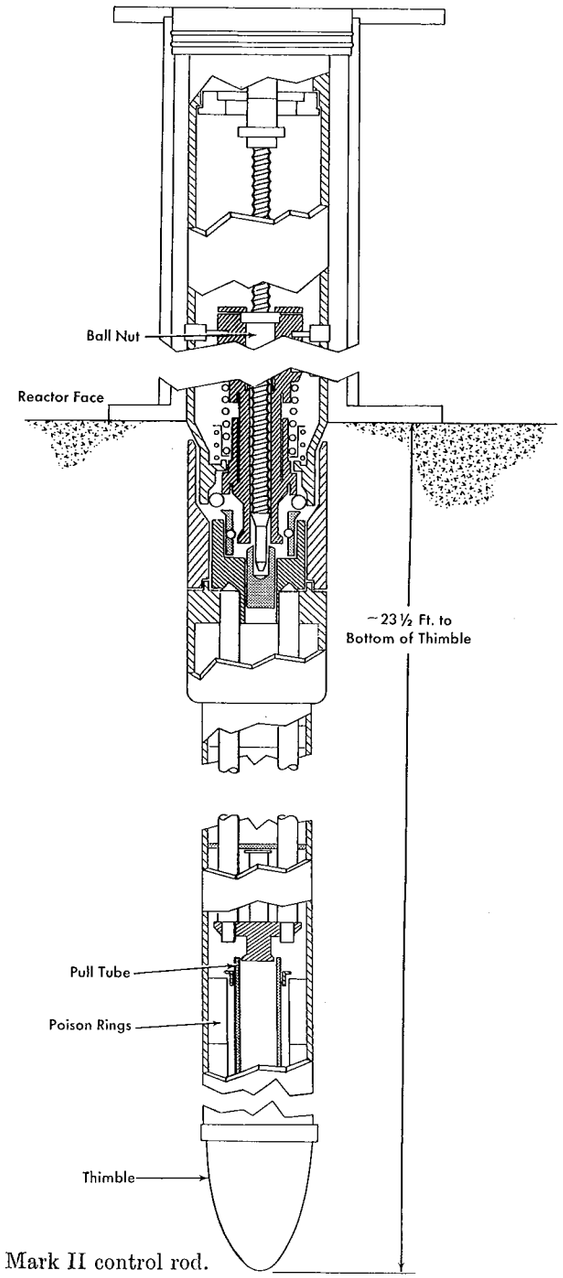

FIG. 6–8. Mark II control rod.

to a latch cup at their top ends. Powdered boron carbide sealed in a cylindrical can within the thimble serves as a radiation shield for the control rod.

Motion of the poison column is obtained through rotation of the lead screw, which drives the ball nut up or down within the guide tube. This motion is transmitted through the latch cup to the four-rod support assembly attached to the poison column. Control rods must be completely inserted into the core before the support column assembly is removed from the reactor face. Static O-ring seals maintain an inert atmosphere in the thimble. When the support column is removed from the reactor face the latch cup is sealed to the thimble by O-rings.

Two-speed drive motor assemblies. As previously noted, two of the control rods are arranged to have a regulating motion of 3 ft/min as well as a shim motion of 0.3 ft/min. The two output speeds required are obtained by driving a planetary gear system with either a 1200-rpm, constant-speed, three-phase, $\frac{1}{4}$-hp shimming motor or a 100-watt, 3600-rpm, variable-speed, two-phase servo regulating motor. One input shaft from each motor is provided. Shim speed is obtained by driving the planetary system sun gear through planet gears against a fixed ring gear held by a regulating side brake. Regulating speed is obtained by driving the ring gear through planet gears against the fixed sun gear held by a shim side brake.

The output shaft is coupled to the planet gears through a spring-loaded, ball-detent, torque-limiting clutch. In case of a malfunctioning rod, overtorque will cause this clutch to slip, thereby preventing further damage to rod or drive mechanism.

Regulating rod travel is limited to $\pm 7\frac{1}{2}$ inches beyond a position previously established by shim motor setting. A guided nut, traversing an Acme screw, driven from the regulating motor shaft activates limit switches at each end of a 15-inch rod travel. These switches de-energize the regulating motor, apply its brake, and energize a signal at the control console. The operator must then readjust shim rod positions. A double-ended selsyn transmitter is coupled to the Acme screw shaft through a worm gear speed reducer. A selsyn receiver indicates the regulating rod position on the reactor console. Worm gear ratio is such that the selsyn rotates less than 360 degrees for the full 15-inch regulating rod travel. A precision potentiometer is mounted on the selsyn shaft. This potentiometer forms part of a bridge circuit in the automatic neutron flux control circuitry.

A mechanical counter geared from the main drive shaft also indicates the position of the rod within $\frac{1}{16}$ of an inch. This counter is not remote reading, and must be observed from the reactor floor.

Single-speed drive motor. Although Mark I rods were not considered for the more rigorous service demanded of the regulating rods, two of the Mark I control rods are fitted for use as shim control only. The drives

are manually controlled single-speed assemblies which obtain the required low output speed by using double worm gear reducers. Clutches, coupling devices, counters, selsyn transmitters, and limit switch systems are identical to the corresponding components in the two-speed drive motor assemblies.

Control-rod tests. Because of the importance of reliability of control and safety-rod mechanisms to reactor operation, extensive service tests were performed to demonstrate the suitability of mechanisms for SRE service. As previously noted, these tests served their purpose in indicating that the Mark I or easily cleared reactor face control rods were not suitable for use as regulating rods as initially designed.

Life of the Mark I control rod was determined to be limited by the life of the ball-nut screw assembly operating at 1100°F. The operating life determined by prototype tests was 180 hours of motion at regulating speed, which is not considered adequate. The ground ball-nuts were operated with Haynes 25 alloy ground and annealed screws. These screw assemblies were run-in with hardened steel balls under a 3000-pound load, in an effort to work-harden the surfaces of the ball races. This running-in technique resulted in a maximum hardness of 29 Rc, although a minimum hardness of 40 Rc was considered necessary.

A rolled, Haynes-25 screw has subsequently been fabricated. Cold-work distortion extended to a maximum depth of 0.009 inch on the races. High-temperature tests at 1100°F indicated that hardness in the highly stressed area dropped from Rc 60 to Rc 54. Further heating resulted in continued softening of the races. Three additional specimens were rolled to $\frac{1}{4}$, $\frac{1}{2}$, and $\frac{3}{4}$ of full race depth, and were examined before and after heating. This work was undertaken to develop a fabricating technique that would not produce overworked races. These later samples exhibited the same characteristics as the previous one, and indicated that extreme working of the surface is not a function of rolling depth. It was concluded from this set of experiments that fabrication of ball-nut screws by grinding and rolling was impractical. Subsequently, fabricating screws by rolling and finish grinding was found to be practical.

Ball-nuts of sufficient hardness were developed. Annealed Haynes-25 slugs were cold upset (35 to 40%) and rough machined by tungsten carbide tools. The races were then finished by grinding.

Balls contributed to failure in some of the component tests. The Haynes-25 balls involved in two of three failures exhibited surface imperfections and variations in surface hardness. Soft areas covered an appreciable portion of the total ball surface. These soft areas were due to insufficient cold-work at the poles of the cup die in which they were upset. A hard area (Rc 50) was found at the equator of the balls. Balls fabricated using this technique were not used in production rods.

Cast Haynes Stellite No. 3 and No. 6 were investigated and judged to be more suitable than Haynes-25 balls. There was some question as to the ability of these materials to withstand the 1100°F temperature requirements without softening, but exposure of these materials to 1100°F demonstrated them to be adequate.

Poison material burnup. Heat-transfer experiments, using electrically heated models, determined necessary clearances between poison rings and the containing thimble. These tests determined the limiting temperature conditions to which poison rings should be subjected in service. Poison rings cycled to these extreme conditions exhibited a slight tendency to grow. This thermally induced increase in volume is small compared with that expected from swelling, and with distortion expected from the $B^{10}n\text{-}\alpha Li^{7}$ reaction.

6–1.4 Safety elements. The SRE contains four safety elements, located as shown in Fig. 6–5, which control an excess reactivity of about 5.7 percent. An easily cleared reactor face design of a safety rod was developed but not used in the SRE after the dry critical experiment as a result of environmental tests, to be described later. A modified design (Mark II) in which poison element retrieving, snubbing, and latching systems are located above the reactor face was found satisfactory, and is installed. The drive housing containing these mechanisms must be removed from the reactor loading face before the fuel-handling cask is free to move over the face. The poison element is fully inserted in the reactor core whenever the drive housing is removed.

Design considerations. As with the control rods, it was decided to avoid the difficulties accompanying the use of a sodium atmosphere seal around the safety rod by adopting the thimble arrangement, in which safety rods operate in a helium atmosphere. The safety rods must operate reliably at a temperature of 1100°F. Safety-rod design criteria were:

The poison column must fall into the reactor under the acceleration of gravity when an appropriate electric circuit is interrupted.

An electrical indication, used as an interlock, must be provided when the poison column is fully inserted in the reactor core.

Mechanisms must be provided to retrieve the poison column to a cocked position after a drop.

A means must be provided to release the poison column at any time during the retrieval from the reactor core.

Poison column position must be indicated during retrieval.

Limiting devices must be provided to protect the safety-rod mechanism from damage due to accidental overtravel.

Sufficient clearance must be provided to ensure against interference between poison column and thimble under any temperature conditions.

The rod must fail safe in any situation.

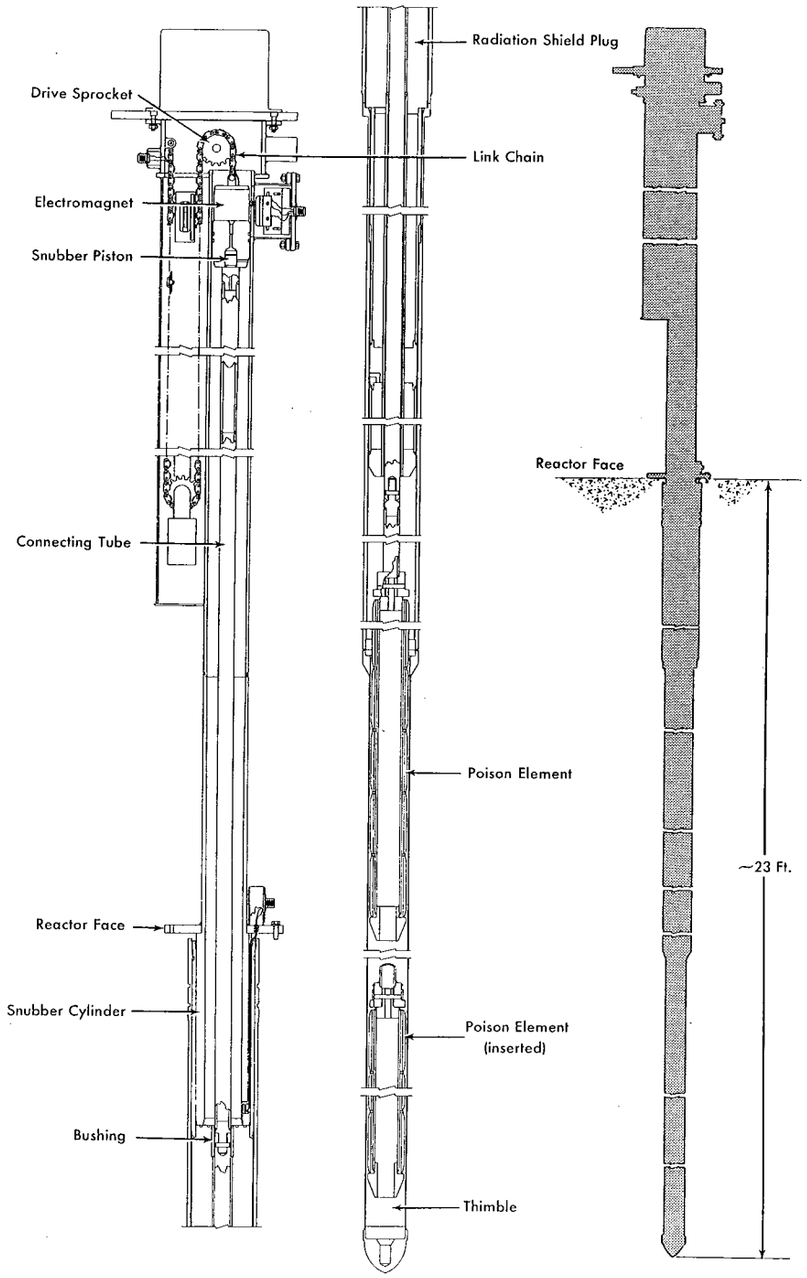

FIG. 6–9. Mark II safety rod.

Safety-rod description. The Mark II safety rod (Fig. 6–9) presently used in the SRE, avoids high-temperature problems by locating drive mechanisms in room temperature areas above the reactor face. An electric motor, reduction gears, a selsyn position indicator, drive sprockets, a link chain with attached electric leads, an electromagnet, and a snubber cylinder are located above the reactor face. A long connecting tube with a snubber system piston on the upper end, and poison elements on the lower end, a radiation shield plug, and a helium-tight thimble are located below the reactor face. An electromagnet connects the link chain to the piston on the connecting tube. De-energizing this magnet releases the poison rod to drop by gravity into the reactor core. Raising and lowering the poison element is accomplished by operating the link chain through the motor, drive gears, and the electromagnet linkage.

It is necessary to snub the falling rod gently as it approaches the bottom of its drop. Helium is trapped in the lower 18 inches of the snubber cylinder by the falling rod. Compression of helium occurs until the falling rod has expended its kinetic energy; the rod then bounces upward a small amount (less than 6 inches). Leakage of trapped gas from the snubber cylinder allows the rod to settle to its fully inserted position without excessive bouncing. Figure 6–10 shows rod position versus time during a drop from full height. The experimental curve shows the poison element within 2 inches of full insertion in 0.7 second. After two small bounces the rod is at rest, fully inserted 1.6 seconds after release. About 10 milliseconds is required for the electromagnet to release, with the remainder of the time employed in actual insertion of the poison element.

The prototype Mark II safety rod was dropped a total of 1400 times at temperatures up to 1100°F. The primary difficulty encountered was rapid wear of the bushing at the bottom of the snubber cylinder. Progressive wear soon permitted excessive gas leakage past the bushing, causing the piston to strike the bottom of the snubber cylinder. This difficulty was corrected by removing an azorized surface from the connecting tube, and

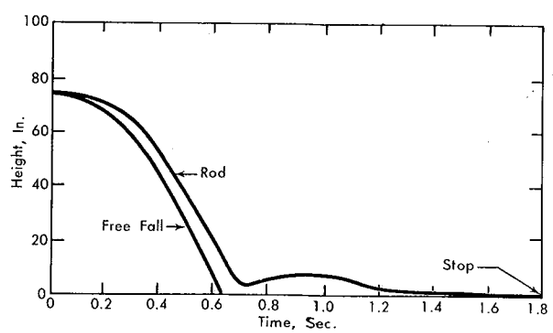

FIG. 6–10. Safety-rod drop, position versus time.

providing a hard brass wearing surface on the bushing. This material combination proved satisfactory.

Safety-rod testing. Material problems encountered during testing of the Mark I safety-rod prototype were identified, and advantage was taken of this experience to accelerate design and production of the Mark II rod finally used. Galling was experienced in latching mechanisms fabricated of Type 316 stainless steel lubricated with molybdenum disulphide. Silver plating the rubbing surfaces was attempted, but was not found suitable for extended use. A latch, flame-plated with tungsten carbide and lubricated with molybdenum disulphide, was found satisfactory, and showed negligible wear after 1200 cycles of operation at 1100°F.

Thimble difficulties were the prime cause of temporarily abandoning the Mark I design. Impact loads resulting from snubbing were transmitted through a section of the thimble which operated at about 950°F. Impact loads were sufficient to overstress the thimble at these temperatures, causing distortion and failure. Two thimble failures were experienced during prototype testing. (The snubber was located in this section of the thimble because of the thickness of radiation shielding calculated to be necessary above the snubbing system.) Actual radiation measurements indicate this thickness to be conservative, and offer the possibility of moving the snubbing mechanism into a cooler zone of the thimble. Replacement of the solid boron-nickel poison elements with crimped, stacked, washers offers an attractive means of reducing impact loading. Experimental tests indicate a reduction in impact loading of several orders of magnitude is possible due to the self-absorption of kinetic energy in the crimped-washer type elements.

6–1.5 Summary. Control-rod and safety-rod mechanisms now incorporated in the SRE are reliable in the service for which they were intended. They do, however, have the disadvantage that they must be removed prior to any refueling or maintenance operation requiring the use of the fuel-handling cask. Removal is accomplished using mechanical lifting and handling devices, but does create a bothersome delay when performing experimental physics measurements involving insertion or withdrawal of fuel elements from the reactor. Continued developmental work is expected to produce mechanisms which will render these delays unnecessary, and permit the expeditious refueling necessary to power reactors.

6–2. Sodium Systems

Sodium as a reactor heat-transfer fluid offers a number of advantages over more conventional fluids such as water. Its vapor pressure at temperature of interest in modern steam plants is quite low. At atmospheric pressure it boils at 1620°F. Although its heat capacity is less than that of water, its thermal conductivity is quite good and pure sodium exhibits very little tendency to corrode materials such as stainless steel and certain low-alloy steels.

Various disadvantages of sodium which must be overcome in a reactor design are its tendency to become radioactive, its chemical reactivity with oxygen, and its relatively low specific heat.

Significant properties of sodium are given in Table 6–2; for comparison, similar properties are listed for water.

Table 6–2

Comparison of Physical Properties of Sodium and Water at 600°F

	Sodium	Water
Thermal conductivity	$43.2 \frac{\text{Btu/ft}^2\cdot\text{hr}}{\text{°F/ft}}$	$0.275 \frac{\text{Btu/ft}^2\cdot\text{hr}}{\text{°F/ft}}$
Specific heat	0.316 Btu/lb·°F	1.45 Btu/lb·°F
Vapor pressure	$\sim 5 \times 10^{-5}$ mm Hg	1542.9 psi
Density	54.7 lb/ft^3	42.4 lb/ft^3

6–2.1 Heat-transfer system. The heat-removal system for the SRE is shown schematically in Fig. 6–11. Two primary, radioactive loops communicate through the reactor. Nonradioactive sodium is circulated in two independent secondary loops. The main coolant circuit, which consists of a primary and a secondary loop, is capable of removing up to 20 Mw of heat. The other primary and secondary loop make up the auxiliary circuit which is incorporated to provide up to 1 Mw heat-removal capacity. In case of failure in the main circuit, the auxiliary circuit acts as a standby to remove after-glow heat.

After a rapid shutdown of the reactor, convective flow in the main circuit is controlled by electromagnetic (E-M) eddy-current brakes. Eddy-current brakes are incorporated into a control system in such a way as to maintain the reactor outlet sodium temperature constant after a shutdown.

Moderator/reflector assemblies are cooled by sodium which enters the reactor through a branch line of the main circuit. Moderator/reflector outlet temperature is automatically maintained the same as fuel-channel outlet temperature. An E-M pump is used to control flow by controlling the pressure in the moderator can plenum between the grid plate and moderator can bottoms.

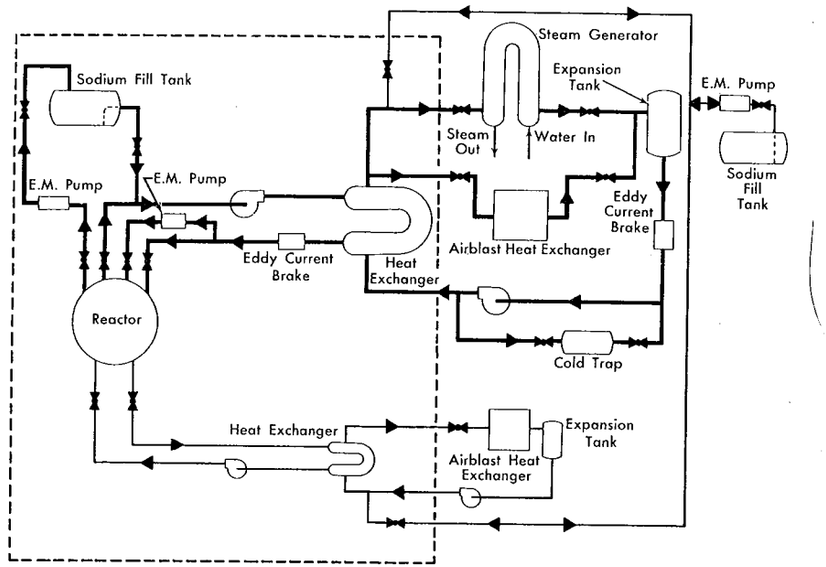

FIG. 6–11. SRE coolant system schematic (the area to the left enclosed by the dotted line represents the radioactive portion of the sodium system).

6–2.2 Sodium piping. Sodium piping for the heat-transfer loops is divided into four groups: main primary piping, auxiliary primary piping, main secondary piping, and auxiliary secondary piping. Except that main primary and auxiliary primary sodium communicate in the reactor vessel, all four systems may be operated independently. Both main primary and auxiliary primary piping are located below ground level. Steel-lined, concrete-shielded galleries are provided to house piping and other components.

All sodium piping in the heat-transfer loops is schedule-40 seamless, Type 304 stainless steel with welded joints. Where practicable, long radius elbows were used. To ensure against leaks, all welds were x-rayed and the entire piping system was leak-checked with a helium mass-spectrometer leak detector.

The main heat-transfer loops are 6-inch nominal pipe size. Two-inch piping is used in auxiliary heat-transfer loops. All sodium piping is insulated to reduce heat losses during circulation of sodium and to permit the pipe to be heated above the melting point of sodium (208°F). Depending upon the location of the piping and the pipe diameter, thicknesses of insulation up to 4 inches are used. In general, insulation in the secondary area, which is outdoors and subject to lower ambient temperature, is $\frac{1}{2}$-inch thicker than that in the primary piping galleries.

All sodium piping is traced by tubular electric resistance heaters, which are installed underneath the insulation adjacent to the piping. Power wattage input per unit length of piping is adjusted so that piping reaches an equilibrium temperature of about 350°F. This temperature is sufficiently above the melting point of sodium to minimize "cold spots" below sodium freezing temperature. Heater circuits are controlled manually by switches, with temperatures read from thermocouples placed on piping diametrically opposite from resistance heaters.

6–2.3 Sodium valves. The following types of valves are used in the heat-transfer systems:

Plug valves with frozen-sodium shaft seals are used as blocking valves in the main and auxiliary primary heat-transfer loops.

Globe valves with frozen-sodium shaft seals are used as throttling valves in the main secondary loop.

Bellows-sealed globe valves are used as throttle valves in branch lines and in the auxiliary secondary system.

The frozen-sodium shaft seal, used to prevent sodium leakage around the valve stem, is a gland through which tetralin can be circulated, thus freezing a narrow (~0.010 inch) annulus of sodium rising between the gland and the valve stem. This frozen seal takes the place of ordinary valve stem packing (Fig. 6–12). With a tetralin flow of 1 gpm at 90°F through this seal, temperature at the cold end of the shaft seal is about 100°F.

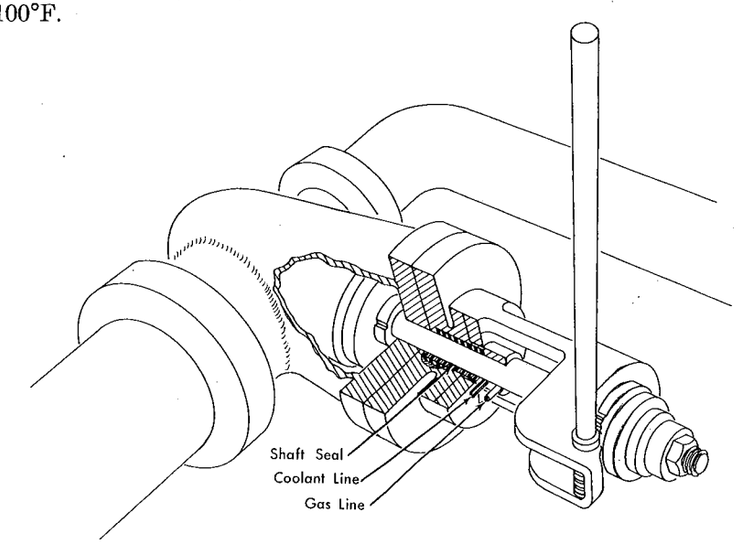

FIG. 6–12. SRE valve.

A second packing made of graphite-impregnated asbestos, located farther up the shaft from the frozen seal, serves as a backup seal and as a method for containing a helium atmosphere at the cool surface of the shaft freeze seal. This inert atmosphere prevents oxidation of sodium extruded through the shaft seal.

All valves located in the galleries are operated by means of manual valve actuators. These actuators are metal cables housed in flexible conduits and are turned from above the biological shield. A brass shear pin located at the upper (accessible) end prevents application of excess torque.

6–2.4 Eddy-current brakes. To control the amount of convective sodium flow following a normal or rapid shutdown of the reactor, eddy-current brakes are used in the main primary and main secondary sodium loops [2].

Each brake is a large electromagnet, the pole pieces of which straddle a flattened section of piping. The brake magnets are of mild-steel laminations, wound with glass-insulated No. 6 copper wire. No organic binders or insulating materials are used, since the main primary brake is located in an intense gamma-ray field.

An electronic control system is incorporated to adjust brake current automatically, receiving its signals from flowmeters and fuel-channel outlet thermocouples. Sodium flow is constrained by the brakes to maintain a constant temperature gradient across the reactor and across the main intermediate heat exchanger.

Some of the brake characteristics are as follows. At a current of 20 amperes, the magnetic flux across the pole pieces is 8030 gauss. The power requirement at this current is 2400 watts. For velocities below about 6 ft/sec the relationship between pressure drop across the brake and the average velocity of the sodium flowing through the brake throat is $\Delta P = 4.25V$ where P is in pounds per square inch and V is in feet per second. At higher sodium velocities the pressure drop does not increase quite so rapidly. As the velocity continues to increase, the pressure drop reaches a maximum and then begins to decline. Since the control range of the brake is in the region below a sodium flow of 20,000 lb/hr (or about 6 ft/sec), no difficulty is experienced in establishing the proper pressure drop to maintain the right amount of post-shutdown cooling.

6–2.5 Sodium pumps. Centrifugal pumps are used to circulate sodium through the reactor and the secondary systems. The pumps are mounted vertically within a casing. By unbolting a flange at the reactor floor and melting a casing freeze seal, it is possible to remove the entire pump assembly from the casing for maintenance. The main primary and auxiliary primary sodium pump casings extend downward through the concrete gamma shielding. Impellers for these two pumps are located in volutes within the main and auxiliary galleries respectively. Since it is not necessary to shield the casings for the main secondary and auxiliary secondary sodium pumps, these pumps are located above ground level.

Figure 6–13 is a cutaway view of one of the secondary sodium pumps. The primary pumps are similar except that the casing and drive shaft are lengthened to accommodate required shielding. Impeller diameter is $13\frac{1}{2}$ inches for the main pumps and 10 inches for the auxiliary pumps.

These pumps are modified hot oil process pumps with impeller and shaft made of Type 316 stainless steel. Other portions of the pump which come in contact with sodium are Type 304 stainless steel. Instead of packings to prevent leakage of sodium past the pump drive shaft into the pump casing, freeze seals are used.

The principle of operation of these freeze seals is the same as that for the freeze seals on the stems of the sodium valves. Two freeze seals are used to confine sodium in the SRE sodium pumps. Figure 6–14 shows a freeze seal around the impeller shaft and another on the pump casing. The latter freeze seal must be melted in order to remove the pump from the casing.

Thermocouples are provided to indicate the temperature of the frozen (top) end of both the shaft freeze seal and the case freeze seal. Should this temperature exceed 150°F, an alarm sounds in the control room. No automatic corrective action is taken, but tetralin flow is increased manually until the temperature is reduced.

To prevent oxidation of frozen sodium in the freeze seals, a helium atmosphere (slightly below system sodium pressure) is maintained within the pump casing at all times. This pressure will prevent sodium within the seal from creeping back into the flowing sodium stream. Should tetralin flow be interrupted, this pressure may be increased to a value higher than system pressure to prevent sodium from rising within the pump casing.

Shaft freeze seal cooling requirements depend upon sodium temperature and shaft speed. At a shaft speed of 500 rpm and a sodium temperature of 750°F, the required cooling load is 3.5 kw. This can be handled by a tetralin flow of 2 gpm at an inlet temperature of 90°F.

Sodium pumps are driven by DC motors which have variable speeds from 0 to 1500 rpm. The main primary pump motor is a 25-hp unit, the main secondary 50 hp, and the two auxiliary pump motors 5 hp each.

6–2.6 Miscellaneous components. *Freeze traps.* Freeze traps are used as a convenient method of introducing inert gases into the sodium piping or venting gases during filling of the loops. Each of these traps is a 4-foot

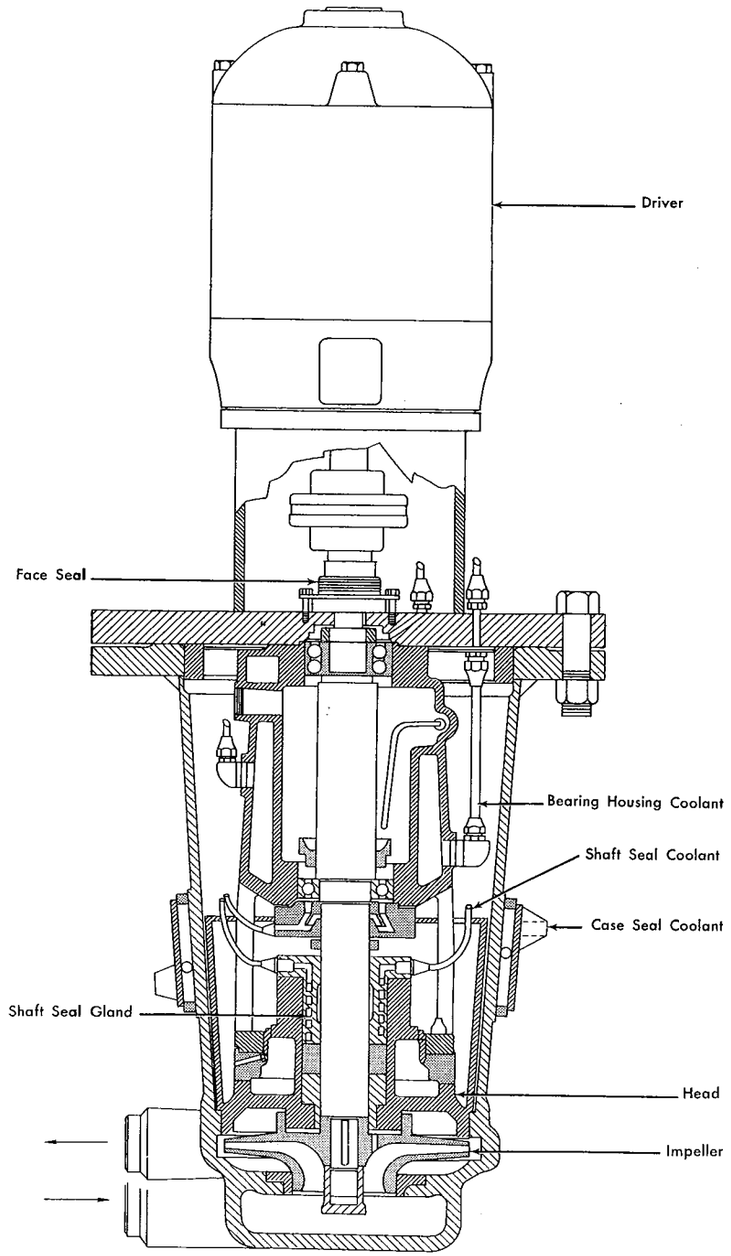

FIG. 6–13. SRE secondary sodium pump.

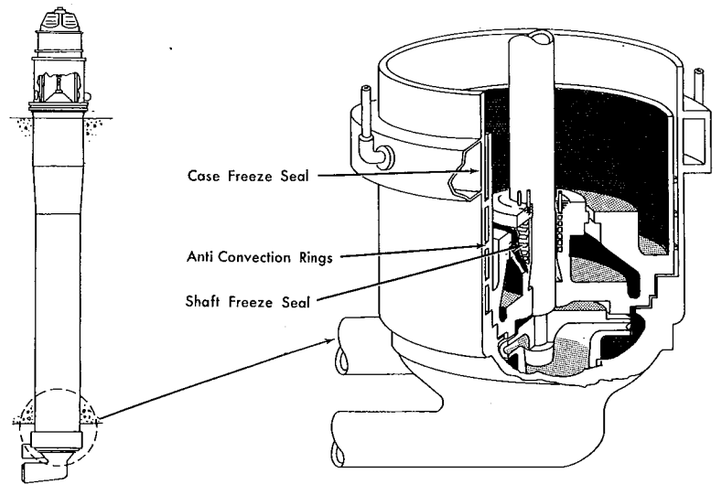

FIG. 6–14. SRE main sodium pump (cutaway of lower portion of pump, showing freeze seals).

length of $\frac{1}{4}$-inch diameter stainless-steel tubing wound into an 8-inch diameter helix. The helix is then cast into a cylinder of aluminum in the shape of a doughnut and encased in stainless steel. One end of the stainless-steel tube is connected to the sodium piping, the other to a vent line and a helium line. Convection cooling by the atmosphere keeps the freeze trap close to ambient temperature (80 to 120°F, depending upon location).

Sodium which enters the stainless-steel tubing and attempts to flow through the freeze trap solidifies. Heaters attached to the freeze trap enable the sodium to be melted when it is desired to introduce inert gas into the system.

Freeze traps are backed up by bellows-sealed valves, to prevent sodium from entering inert gas lines if the freeze traps should fail.

Vapor traps. In some locations, such as the tops of the expansion and fill tanks, vapor traps are used to prevent sodium vapor from diffusing into the inert gas supply line. These traps are small tanks packed with stainless-steel mesh. Vapor entering the trap condenses within the mesh, since the trap is not insulated. Strip heaters are provided to melt the condensed vapor. . Sodium condensate drains by gravity back to the fill or expansion tank which the vapor trap serves.

Vapor traps, like freeze traps, are backed up by bellows-sealed valves, to prevent sodium from passing upstream in event of trap failure.

Leak detectors. All sodium piping is traced by leak-detector cable. Each cable is composed of two conductors spaced $\frac{3}{8}$ inch apart by ceramic insulating leads. Leak-detector alarms and lights are registered in the control room. Action taken depends on the location of the leak. Leak detectors, to date, have not proved to be of great value in service, since numerous spurious leak alarms have been given.

Moderator coolant pump. A three-phase, linear induction E-M pump is installed in the moderator/reflector bypass line to control sodium flow to the moderator/reflector coolant plenum of the reactor. This flow control is necessary in order to assure that during steady-state operation of the reactor, as well as after a scram or slower shutdown, moderator coolant exit temperature is maintained at the average fuel-channel coolant exit temperature.

Sodium flow through the moderator cooling spaces between moderator cans is the sum of two incoming flows. One contributor is the leakage of sodium from the fuel-channel cooling plenum into the moderator cooling plenum. Each moderator can seals off a hole in the lower grid plate solely by virtue of its weight when submerged in sodium and some leakage past these seals is known to occur (Section 6–1). The other contributor is sodium introduced through the sodium line provided for that purpose, the moderator/reflector bypass line.

Depending upon orifice plate sizes in the fuel channels, leakage of sodium through the grid plate may be more or less than that required to maintain desirable moderator can coolant temperature. The moderator coolant pump is designed to maintain the appropriate pressure in the moderator coolant plenum to provide proper sodium flow.

A typical operating condition for this pump is as follows. With a core loading of 43 fuel elements the pump will be required to develop a pressure of about 20 psi to maintain a sodium flow of 10 gpm. Under these conditions the power requirement of the pump is approximately 10 kw.

An automatic electronic control system adjusts power to the pump in order to maintain a minimum difference between moderator coolant exit temperature and average fuel-channel coolant exit temperature.

6–2.7 Heat exchangers. *Main and auxiliary intermediate heat exchangers.* The main and auxiliary intermediate heat exchangers are counterflow liquid metal-to-liquid metal shell and tube heat exchangers, serving to isolate the radioactive primary sodium from the nonradioactive secondary sodium external heat removal circuit.

The main intermediate heat exchanger (Fig. 6–15) is a U-shaped shell mounted horizontally, with a slight pitch for gravity draining. It contains 316 single-wall seamless (Type 304, $\frac{3}{4}$-inch OD by 0.058-inch wall) tubes with a total area of 1155 square feet. The tubes terminate in a tube sheet

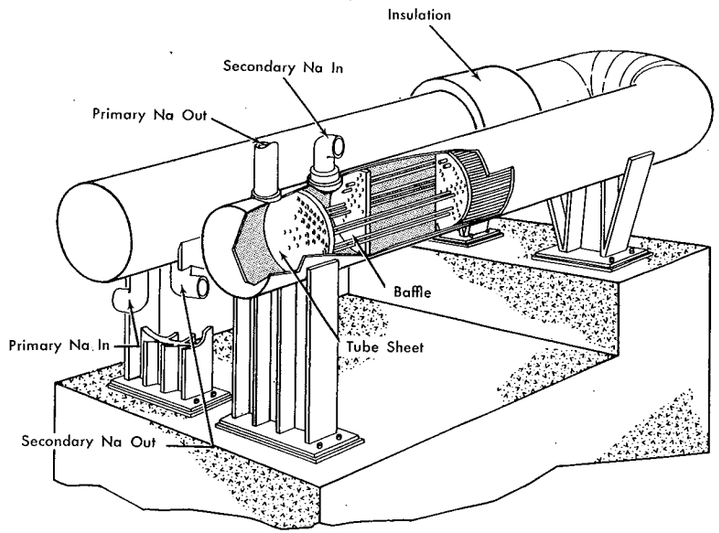

FIG. 6–15. Main sodium heat exchanger.

at each end. Primary sodium is in the tubes, the secondary sodium is in the shell. All joints sealing sodium are welded and, where possible, are 100 percent x-ray inspected. The U-type design is used to minimize thermal stresses due to tube expansion and to conserve space.

This unit is designed to exchange 20 Mw of heat with a logarithmic mean temperature difference of 60°F at a sodium flow of 485,000 lb/hr.

The auxiliary intermediate heat exchanger is similar to the main unit except for a reduction in size and the method of mounting. The exchanger is a U-shaped shell mounted vertically, resting on one side of the U. Thirty-eight $\frac{3}{4}$-inch tubes are contained within the shell. This exchanger is designed to transfer 1 Mw of heat with a mean temperature difference of 60°F at a sodium flow rate of 24,400 lb/hr.

Electrical strip heaters are installed on the shell to preheat shell and tubes to 350°F.

Maximum operating limits. The log mean temperature difference of the intermediate heat exchangers is specified as less than 60°F at full power. The sodium temperature change rates are limited to the following:

Normal startup

1 to 10 percent reactor power, 8°F/min.

10 to 100 percent reactor power; constant in primary, 1°F/min in secondary.

Normal shutdown

100 to 10 percent reactor power; constant in primary, 1°F/min in secondary.

10 to 1 percent reactor power, 8°F/min.

Emergency shutdown

100 to 10 percent reactor power; constant in primary, 60°F/min in secondary.

10 to 1 percent reactor power, 15°F/min.

Air-blast heat exchangers. Air-blast heat exchangers (Fig. 6–16) in the secondary system may be used to dissipate the reactor heat. They have U-shaped tube bundles installed in protective housing above motor-driven fans. Tubes are similar to those in the intermediate exchangers but have external Type 410 stainless-steel fins 2 inches in diameter, spaced 8 per inch. All tubes are connected in parallel from headers at one side of the

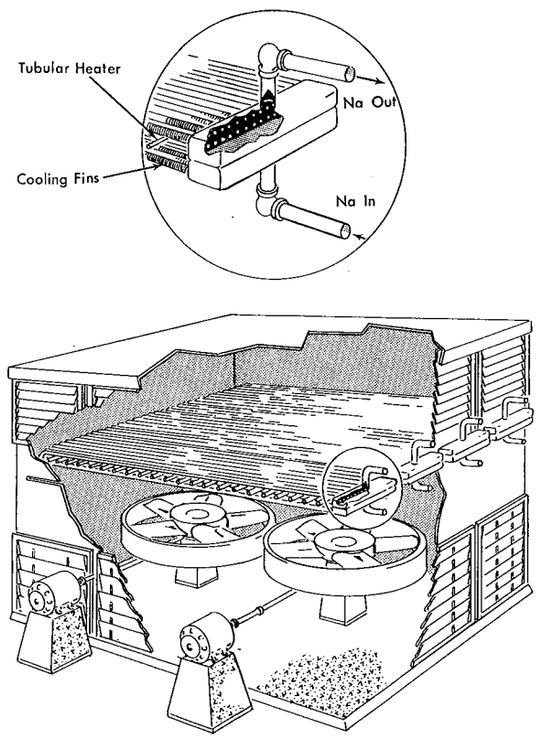

FIG. 6–16. Air-blast heat exchanger.

assembly. The direction of airflow is normal to the sodium flow. Mechanically operated louvers are installed above the tube bundles to assist in control of airflow. Tubular electric heaters are mounted below the tube bundles for preheating the system and for providing makeup heat during operation at low power. These heaters maintain a temperature of 350°F in the tubes during shutdown.

In the main air-blast heat exchanger there are 204 U-tubes $26\frac{1}{2}$ feet in length. They provide 23,600 square feet of heat-removal surface. At normal operating power with the estimated heat transfer coefficient of 8.3 Btu/ft^2·hr·°F, the exhaust air temperature is 277°F based on inlet air at 100°F. Below the tube bundles, two 11-foot diameter five-bladed fans are mounted, each driven by a 50-hp variable-speed DC motor. The auxiliary air-blast heat exchanger is similar in design, but has only 30 U-tubes 8 feet in length. It utilizes a 5-foot diameter fan driven by a 5-hp variable-speed DC motor. Air-blast exchangers can be operated in either of the following ways.

As the sodium temperature increases with power buildup the louvers are opened in proportion to the heat-rejection requirements. The temperature increase is held to 30°F/hr while increasing reactor power. When sodium outlet temperature reaches 440°F the automatic fan speed controller will start the fans at minimum speed. It is necessary to close the louvers somewhat during this phase to compensate for increased cooling caused by the fans. As sodium temperature increases, fan speed will increase to hold sodium outlet temperature constant. The louvers can now be opened slowly, allowing the fan speed controller to hold the temperature of the outlet sodium constant.

A second method of operation involves leaving the louvers closed until after the sodium reaches the control temperature. The fan speed is allowed to increase so that it is well within the control region before the louvers are opened. This results in a decrease of fan speed to compensate for the additional cooling when louvers are opened.

The procedure followed during shutdown is the reverse of that outlined above. As reactor power is decreased, the sodium outlet temperature decreases at a rate determined by flow and heat-rejection rates. Maximum rate of temperature change is held to 30°F/hr ($\frac{1}{2}$°F/min) during shutdown. The automatic fan speed controller reduces the fan speed as the reactor outlet sodium temperature decreases. During this period the louvers can be closed a little at a time to enable the fan speed controller to stay within range. For complete shutdown the fans are turned off and the louvers closed on the main air-blast heat exchanger. The auxiliary loop is used to exhaust the after-glow heat and is controlled to maintain the core temperature at the desired level. It is necessary to energize heaters during shutdown to maintain the sodium temperatures above 350°F.

The intermediate heat exchangers are mounted in the galleries at an elevation above the reactor core, whereas the air-blast exchangers are at an elevation approximately 40 feet above the intermediate heat exchanger. As a result, even without forced circulation by the pumps, it is possible to obtain cooling by natural convection in both primary loops and in both secondary loops. This arrangement constitutes a safety feature, since it is possible to remove a certain amount of after-glow heat from the reactor core under emergency conditions. It is estimated that with normal operating temperatures, as much as 2000 kw of heat can be removed by natural convection circulation within the complete main circuit, including cooling by air convection at the main secondary exchanger.

6–2.8 Process description. A schematic representation of the SRE heat-transfer system is shown in Fig. 6–11. Primary systems are filled, after being purged with helium, by closing the reactor sodium outlet valve and opening the valve in the system fill line connected to the primary fill tank. The main primary pump suction line is then allowed to fill by gravity. The pump is started and operated at its lowest speed, taking suction from the fill tank. Sodium flows through the entire main primary loop before flowing into the reactor core tank. Helium in the primary loop displaced by the sodium is vented through a freeze trap at the high point in the piping.

When the primary system has been filled, blocking valves are opened and the reactor is filled to a level 124 inches below floor level, providing a pool of sodium about 56 inches deep over the core. The auxiliary primary system is then filled by opening blocking valves and allowing helium to escape from the high point in the loop through a freeze trap. Freeze seals are established on the pumps by venting helium from the pump casings until sodium enters and seals off freeze-seal annuli.

Secondary systems are filled similarly. Helium gas is vented from the expansion tanks as the loop fills. An E-M induction pump is used to pump sodium from the secondary fill tank to the main secondary or auxiliary secondary systems, since gravity will not fill these systems because of their elevation. This pump is also reversible to allow for draining the loop. Pressure applied to the secondary fill tank accelerates the filling process.

Primary loops drain to the reactor core tank. To drain them it is necessary to reduce the level of sodium in the core tank to about 180 inches below floor level, which uncovers the inlet and outlet coolant nozzles. An E-M reactor drain pump is used to lower the level of sodium in the reactor core tank. It is possible to further drain the reactor to within a few inches of the bottom of the core tank through the reactor drain line, which extends to the bottom of the core tank. After the sodium has been drained back to the reactor core tank, both main primary and auxiliary primary loops may be isolated from the reactor by closing blocking valves.

In normal operation, the secondary loops are filled before filling the primary loops, since this allows sodium to enter the shell side of the intermediate heat exchangers.

Sodium flow in the main circuit, including the primary and secondary loops, may be varied between 485,000 and 24,000 lb/hr by changing the speed of the pumps. Similarly, the auxiliary circuit flow may be varied between 24,250 and 9750 lb/hr. At full power (20 Mw) the reactor outlet sodium temperature is 950°F and reactor inlet sodium temperature is 500°F. In the secondary loop the steam generator sodium inlet temperature (intermediate heat-exchanger outlet temperature) is 900°F. When the air-blast heat exchanger is being used to dissipate reactor heat, its inlet and outlet temperatures are the same as for the steam generator.

Valves in the main secondary loop permit sodium to be routed either to the main air-blast heat exchanger or to the steam generator. Normally sodium is drained from the air-blast heat exchanger when the steam generator is being used, and vice versa; either is capable of handling full reactor power output.

6–2.9 Sodium service system. Components and piping which contain sodium but which are not part of the reactor heat-removal system are considered to be the sodium service system. Where possible, components of the sodium service system are physically separated from the heat-transfer loops, to increase ease of maintenance, and permit more flexible operation. Items of this system are the sodium melt stations, fill tanks, cold traps, hot traps, and plugging meters, with associated system piping and valves.

Sodium melt stations. Sodium is supplied in 55-gallon drums. It must be melted under an inert atmosphere, passed through filters, and stored in the primary or secondary fill tank. Two melt stations are provided for this purpose. Each station incorporates the necessary helium and sodium piping to melt and drain a drum of sodium, electrical connections for drum heaters, and temperature read-out instruments to determine drum temperature.

Sodium fill tanks. Two Type 304 stainless-steel fill tanks are used to hold SRE sodium. The 20,000-pound capacity secondary fill tank supplies sodium to the nonradioactive loops. A 60,000-pound capacity primary fill tank supplies sodium to the radioactive loops, including the reactor. Both tanks are insulated and are equipped with strip heaters to maintain their temperatures at 350 to 400°F. Strip heater capacity is 14 kw on the primary fill tank and 4 kw on the secondary fill tank. Automatic temperature controllers are provided to maintain proper heater power.

Both tanks are used as reservoirs for filling and draining the primary and secondary sodium loops. The secondary systems are filled and drained through the same line. To fill, helium pressure on the secondary fill tank is increased and the valve in the fill and drain line is opened. A 480-volt, linear induction pump installed in the drain and fill line can also be used to speed up the process. Draining involves reversing the above procedure. In case of a leak which would render it impossible to pressurize the secondary loop, the E-M pump still makes it possible to drain the loop.

The reactor and primary sodium piping fill by gravity from the primary fill tank, which is contained in a shielded vault outside the reactor building. A drain line which reaches to the bottom of the reactor allows the reactor to be drained almost completely. This drain line, similar to the secondary drain and fill line, incorporates a 480-volt, linear induction pump. It is possible to drain all the primary sodium in about 6 hours.

In order to drain only the primary piping, it is merely necessary to drain the reactor sodium to a level just above the tops of the moderator cans, or about 180 inches below floor level.

Cold Traps. The presence of small amounts of oxygen in SRE sodium can be injurious to the zirconium in the reactor, as well as cause difficulties because of oxide precipitation at relatively cool points in the piping. Cold traps are used to keep the oxide content of the sodium low.

The main secondary loop cold trap is shown schematically in Fig. 6–17. Sodium, after passing through a regenerative heat exchanger cooled by exiting sodium, enters an inner tank which is packed with stainless-steel mesh. A cylindrical baffle inside the tank channels sodium upward through the outer annulus between the baffle and the tank, and then downward through the center cylinder. Enclosing the inner tank is a jacket to which toluene may be admitted from a toluene reservoir. A condenser, cooled by tetralin, is provided to condense the boiling toluene.

In operation, sodium entering the cold trap is cooled by the toluene in the cooling jacket. As it rises in the outer annulus of the inner tank its temperature drops to as low as 232°F (the boiling temperature of the toluene). As the sodium cools, oxides precipitate out of solution and remain in the stainless-steel mesh. It has been found experimentally that the amount of oxide remaining in the sodium stream depends on the minimum temperature of the sodium in the trap, which in turn depends on sodium and toluene flow rates.

As the oxide content of the sodium is reduced, sodium flow through the trap is also reduced to decrease the minimum sodium temperature in the trap. A typical operating condition for this type of trap is a sodium flow rate of ~960 lb/hr and a ΔT across the trap of 30°F. Under these conditions the trap is capable of reducing the oxide content of about 20,000 pounds of sodium to less than 10 parts per million as indicated by plugging meter determinations. The time required for this depends on the original

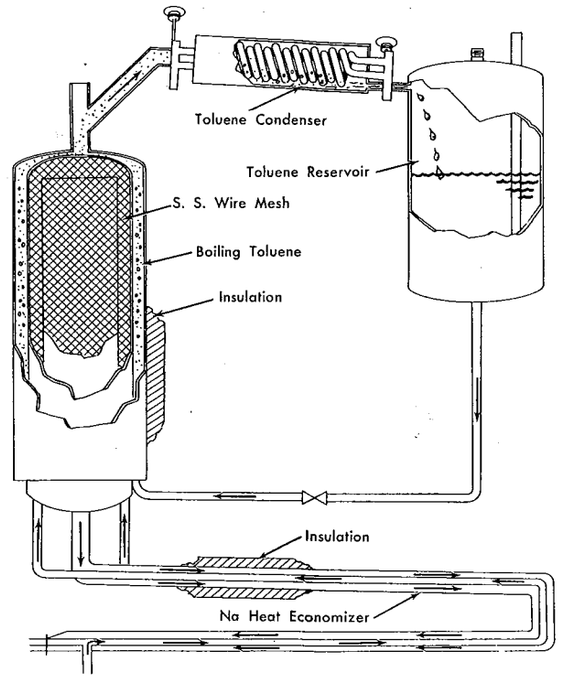

FIG. 6–17. SRE main secondary loop cold trap.

condition of the sodium, but is generally on the order of 24 hours, for sodium originally containing 30 ppm oxide.

The primary sodium system cold trap is located in a separate shielded vault and is connected into the primary system piping with flanges. When this trap has gathered sufficient oxide to prevent further sodium flow, it is removed and discarded. Although this disposable cold trap is about the same size as the main secondary cold trap, it differs in two ways. No regenerative heat exchanger is used and boiling toluene is replaced by a cooling jacket through which liquid tetralin is pumped.

Hot traps. Zirconium hot traps are provided for reducing the oxygen content of the sodium below that obtainable by the use of cold traps alone, removing any impurities in the sodium which would otherwise be absorbed by the zirconium sheathing on the graphite moderator cans. This is accomplished by selective absorption on a large, high-temperature zirconium surface.

Each of the two hot traps is a stainless-steel tank containing 4-mil-thick zirconium sheet, as shown in Fig. 6–18. Sodium enters the trap at the bottom and flows upward through the zirconium sheet element, which is

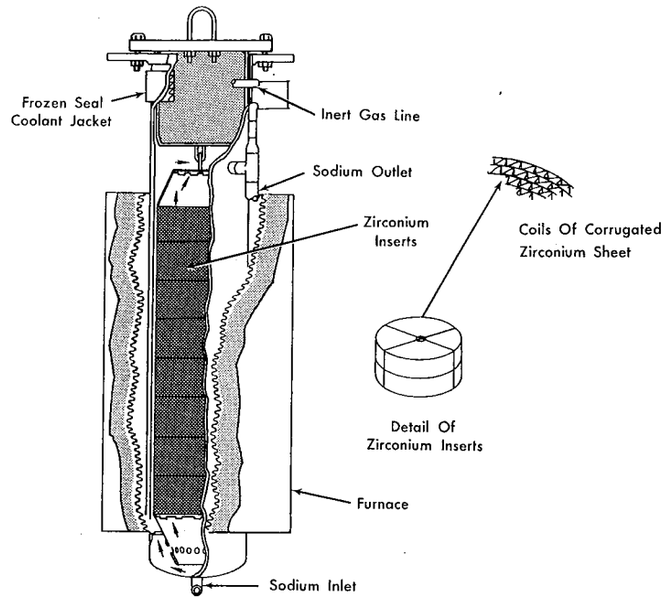

FIG. 6–18. SRE hot trap.

corrugated to allow for sodium flow. Each trap contains 240 pounds of zirconium, which gives a trapping surface area of about 350 square feet. A flange at the top of the hot-trap tank permits removal and replacement of the zirconium element. As further insurance against leakage of sodium, a tetralin cooling jacket is provided just below the flange to freeze any sodium that would rise beyond the removable plug which supports the zirconium element.

Heaters on the outside of the hot-trap tank raise the temperature of the sodium in the hot trap to higher than the hottest core zirconium. Typical operating conditions are: sodium flow 10,000 lb/hr, inlet temperature to regenerative heat exchanger 950°F, and hot-trap average temperature 1200°F.

The two hot traps are located along with the disposable cold trap in a shielded sodium service vault located exterior to the reactor building. Servicing of these components is accomplished by removing the vault shielding blocks with a portable crane. Access depends on the residual activity of the sodium.

Plugging meters. Plugging meters are used to obtain a measure of the oxide content of the sodium. Each plugging meter is composed of the

following: an economizer (regenerative heat exchanger), a cooler (cooled by tetralin), a plugging disk which is incorporated in a valve, and a heater.

As sodium enters the economizer, its temperature is reduced by sodium leaving the plugging meter. The tetralin cooler further reduces the sodium temperature. If sodium temperature has been reduced below the plugging temperature (the temperature at which oxides begin to precipitate out of solution) holes in the plugging disk begin to plug up. The plugging disk is formed by the disk of a bellows-sealed valve in which a number of holes are drilled to allow sodium to pass through the valve even when it is closed. The number of holes varies in the SRE plugging meters from 9 to 20, to ensure the proper pressure drop for a given flow rate. All holes are 0.040 inch in diameter.

After sodium passes through the plugging disk, it is heated by the regenerative heat exchanger and returned to the system. An electromagnetic flowmeter measures sodium flow and determines when plugging of the disk stops the flow.

To determine oxide concentration in sodium, the plugging valve is closed and tetralin cooling started in the cooler. A continuous record of sodium temperature and flow is kept. As the temperature of the sodium falls it reaches a value where the flow begins to drop. Flow is allowed to drop for about 1 minute; the cooling is then stopped and the plugging valve opened. This terminates the plugging run. Oxide content of the sodium is determined by reference to an oxide solubility curve which gives concentration as a function of temperature.

Plugging meters are provided in the main secondary system, auxiliary secondary system, and sodium service system. All plugging meters are identical except for the number of holes in the plugging valves.

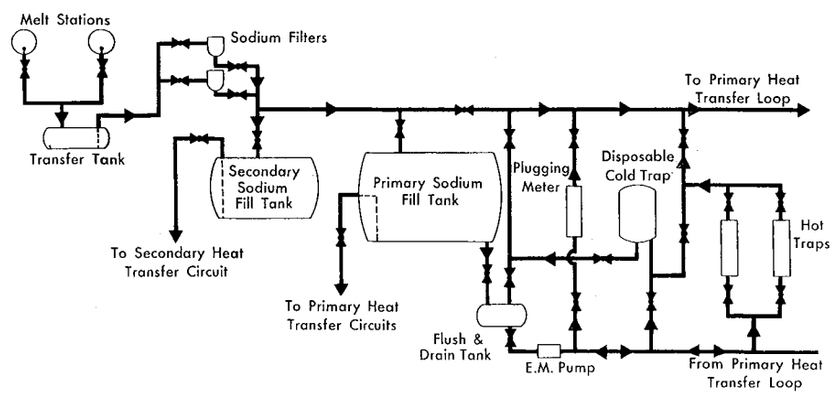

FIG. 6–19. Schematic of sodium service system.

Process description. Figure 6–19 shows schematically the ways in which sodium can be routed to the components which are located in the sodium service vault, the primary fill tank vault, and the sodium service building. The following flow paths may be used.

Sodium may be transferred from melt stations to the primary fill tank, the secondary fill tank, or the flush and drain tank.

Using the E-M pump, sodium may be circulated through the plugging meter, the cold trap, or the hot traps, via the flush and drain tank. Similarly, sodium may be circulated via the primary fill tank and the flush and drain tank.

Sodium may be circulated from the main primary or auxiliary primary heat-transfer loop through the plugging meter, the cold trap, or the hot traps.

6–3. Fuel-Handling System

6–3.1 Introduction. To remove any element from the reactor core it is necessary to use the shielded cask designed for this purpose (Fig. 6–20). It is carried on the 75-ton handling bridge and may be moved as required within the reactor room. To remove an element from the SRE, the fuel-handling cask is located over the plug of the element after electrical thermocouple connectors and the retaining ring with its gasket have been removed from the plug. A pneumatic mechanism within the cask forces a cylinder vertically downward to make an O-ring seal at the top of the plug casing. Following this, a large lead shield skirt is pneumatically lowered to the surface of the shield. A gas lock at the lower end of the cask, where the seal has been made to the casing, is then evacuated by means of a pump and purified helium is admitted to the 3 psig pressure existing in the core tank. A latch mechanism is lowered until it engages the top of the plug of the element to be removed. The direction of the motion is then reversed to raise the plug with its element up into the cask. A separate mechanism then rotates the entire lifting assembly to bring a new element into position over the center of the casing. The procedure is then reversed to lower the new element into place, disengage the latch, retract the lifting mechanism into the cask, close the opening between the lock and cask body, admit air into the lock, raise the shielding skirt, and break the seal made by the lock at the casing. The cask is then free to transport the irradiated element into the cleaning or storage facilities at the other end of the reactor room.

6–3.2 Cask design. *Cask carriage.* The cask carriage is mounted on rails located on a specially designed overhead bridge crane. This handling bridge is the means by which the cask is carried to all parts of the reactor

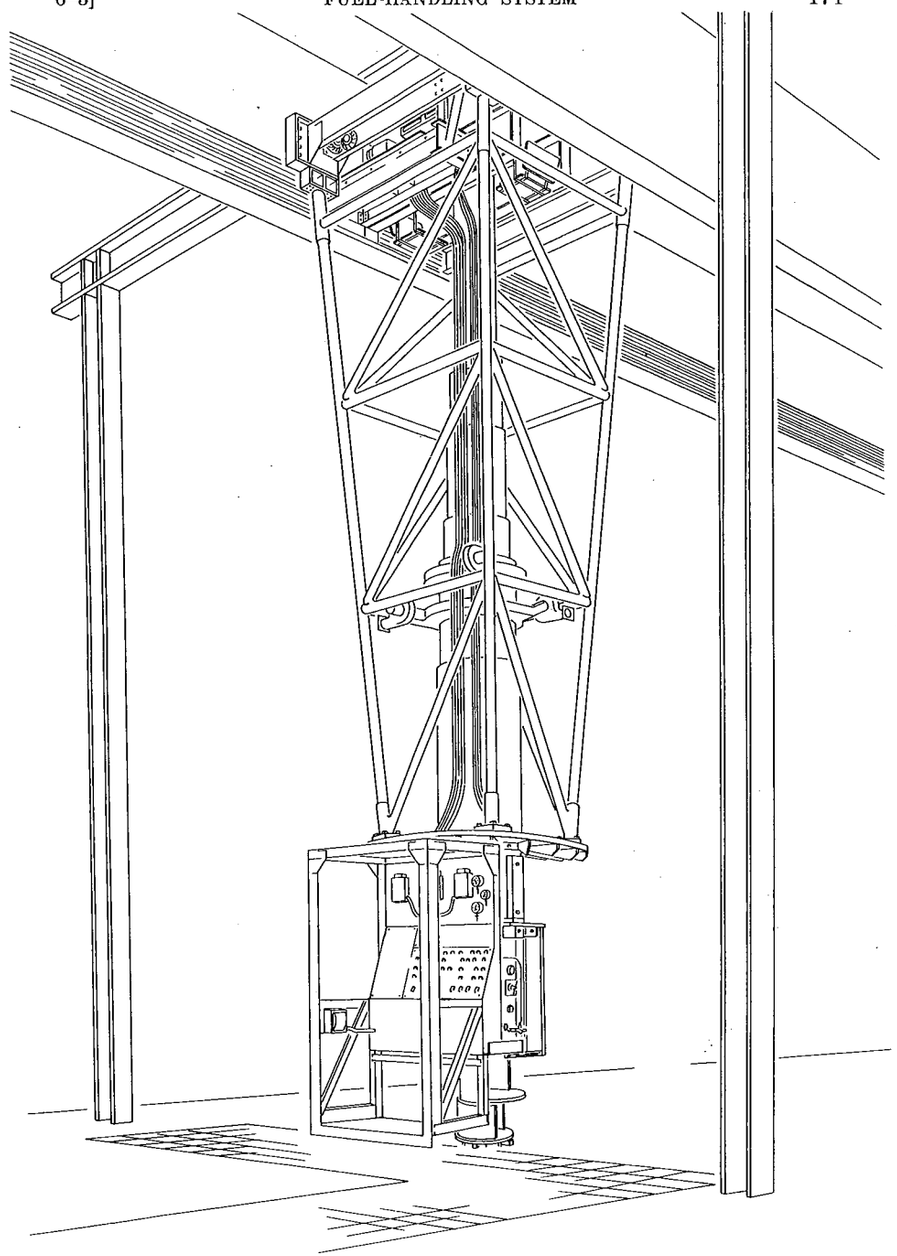

FIG. 6–20. Fuel-handling cask.

building floor. When not in use, the cask can be transferred from the handling bridge rails to a storage area on one side of the building. Matching storage rails and hinged transfer rails accomplish this transfer. The rail system is 35 feet above the reactor floor. Electric power is supplied to the carriage by sliding shoe contacts between the carriage and the bridge. When the cask is in the storage area the handling bridge is available for full use of the 75-ton crane mounted on the top bridge rails.

Body. The cask body is made of 16-inch diameter stainless-steel pipe, 35 feet long. The body, which supports all the weight of the shielding, is bolted to the underside of the carriage. A truss-type sway brace, also mounted to the carriage, is used to reduce the stresses and deflections of the cask body due to accelerations, while allowing it to lengthen due to temperature increase.

Shielding. Cask shielding consists of lead, 1 inch thick at the top, tapering to 9 inches thick at the lower body opposite the fuel. The operator is shielded by an additional 3 inches of lead placed at the control panel. All cracks in the assembled shielding are caulked with lead wool. The lead sections are held to the body with heavy box banding or bolted in place with steel bars, as appropriate to their location.

A 5-ton movable shield is located between the lower section of the cask and the floor. The entire shielding weighs 40 tons and the combined weight of the shield and cask is approximately 55 tons.

Cooling. Cask cooling is accomplished through a $\frac{3}{4}$-inch annulus between the steel cask body and the lead shield around it; air moving up through this annulus dissipates the heat transferred to the body from the hot fuel elements. Two blowers are placed about halfway up the side of the cask; one exhausts the air from the lower annulus and the other blows air to the upper annulus. This system keeps the cask from overheating and also reduces the thermal bending of the cask body caused by nonuniform heating.

Operator's platform. The operator's platform is mounted on the lower cask body approximately 18 inches above the reactor floor. Additional lead in front of, above, and below the operator affords adequate radiation protection. Mounted on this platform is a console that contains all the operating switches, indicating lights, load cell instruments, thermocouple instruments, and grapple position indicators.

Hoist mechanism. The hoist consists of a pair of endless, stainless-steel roller chains mounted on sprockets, which are in turn attached to turntables located at the top and bottom of the cask body. These turntables allow the internal hoisting mechanism to rotate 180 degrees about a vertical axis. The top and bottom turntables are joined by a torque-tube which rotates them in unison.

Top sprockets are driven by a gear-motor and a self-locking worm and

gear, so that loads on the hoist can still be supported even though motor and brake are removed. Between the worm and gear-motor is a slip clutch set at 700 pounds which limits the loads applied to the hoist chains. The normal hoisting load is about 550 pounds.

There are two hoists in the cask, one is used to hold the new fuel as the other is sealing the bottom of the cask, or removing used fuel from the reactor. Integrated with these hoists are the load cells and selsyn transmitters that indicate the load on the grapples and their vertical position.

Lifting mechanism. A lifting mechanism is attached to the two chains of the hoist assembly by a universal-type joint to ensure that the grapple remains vertical at all times. The grapple is designed to engage a lifting ring on the inside of the top of each fuel plug. Spring-loaded fingers are automatically engaged as the grapple is pushed into the top of the plug. These pneumatically actuated fingers can be released only when the grapple is in the down position and sealed in the gas-lock cylinder, to ensure against accidental release while in a raised position. Figure 6-21 is a detailed drawing of the lower section of the SRE cask.

Gas lock. The gas lock is lowered from the bottom of the cask body to the reactor face by three pneumatic cylinders, and seals into a special fitting previously mounted around the fuel plug to be removed from the reactor. After the gas lock is sealed, the air in it is evacuated and replaced with helium before any fuel transfers take place. This assures a continuous helium atmosphere from the reactor through the fuel cask. During transportation of fuel, the helium atmosphere within the cask is maintained by using the unloaded grapple to plug the port in the bottom of the cask.

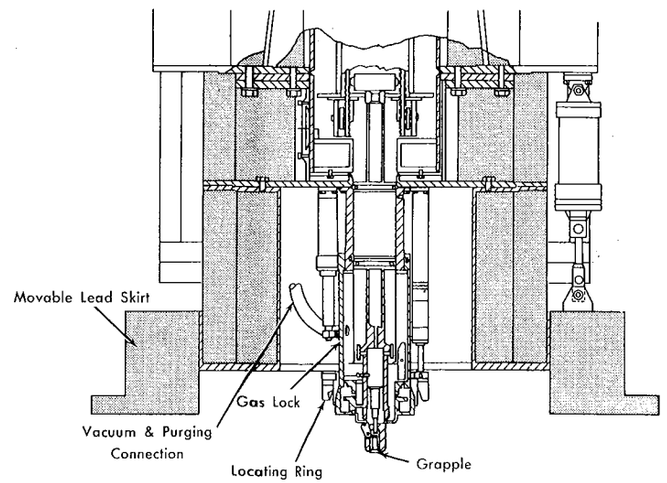

FIG. 6-21. Lower section of fuel-handling cask.

6–3.3 Cask operation. Before the fuel cask is used to remove an element from the reactor or fuel storage, the hold-down ring of the fuel plug is removed and the cask index ring is put in place. A lifting ring and retaining snap ring are placed in the top of the plug and the cask is moved to position by the slow-speed drive. Initial positioning of the cask over a plug is done visually with the aid of another man on the reactor floor. After the cask is visually indexed over the selected element and index ring, the operator performs the following operations.

As the cask is moved slowly to final position, the microswitch trip levers contact two points 90 degrees apart on the cask index ring. Exact position, within $\pm\frac{1}{8}$ inch, is indicated on the cask control panel. The cask must be properly indexed before the remainder of the sealing operations can be completed.

The gas seal may then be lowered. Three solenoid-operated, 2-inch pneumatic cylinders raise and lower the gas-lock sleeve assembly which seals to the index ring. Lights on the panel indicate the "up" and "down" positions.

Actuating a switch on the control panel lowers the pickup device from its "travel" position to its "down" position. A microswitch stops its downward motion and an interlock is completed that allows the vacuum buggy to be operated. This vacuum system will not operate unless the grapple plug is in the "down" position to hold down the fuel plug assembly during evacuation. In case the down switch fails, an override switch (emergency vacuum buggy) allows power to the vacuum buggy.

The shielded vacuum buggy is then used to evacuate the gas interlock. The vacuum buggy consists of a vacuum pump and shielded discharge tank. All valves on the buggy are of the solenoid type, operated from a separate pendant. When evacuation is completed the buggy inlet valve is closed, along with the cask vacuum valve switch. Helium is admitted until the pressure is 3 psig.

The removable shield is lowered by the following sequence:

Three 5-inch pneumatic cylinders lift the shield slightly off its locking pins. A switch actuates other pneumatic cylinders to remove the three pins holding up the shield. Another switch actuates a solenoid valve in the orificed exhaust lines from the shield-lifting pneumatic cylinders, causing the shield to descend slowly to its lowest position.

A switch engages the lift motor lowering the pickup device to engage the plug from which the fuel element hangs. Reversing this switch causes the lift motor to raise the pickup device and fuel element until a photo-cell light beam is no longer interrupted, at which point the motor is stopped by a photocell switch. This switch is installed to stop the pickup in the "travel" position when a plug or element is not attached. Before lifting a fuel element both blowers must be on.

When both pickup devices are in the "up" position, an interlock is completed that permits the internal cask mechanism to be rotated 180 degrees. This rotation puts the new fuel element in position for lowering. An interlock is made which allows only the pickup device over the hole at the bottom of the cask to be lowered. A microswitch shuts off the hoist motor and turns on a panel light when the pickup device is in the "down" position and has lowered the new element into the core.

A switch (grapple release solenoid) actuates a solenoid valve controlling the flow of helium to a piston in the pickup device, when in the "down" position. Pressure on this piston causes the grapple to release the plug. The proper hoist motor lifts the pickup device detached from the fuel element. The photocell switch previously mentioned stops the pickup device in the "cask travel position," at which point the cask interior is sealed from the gas lock by the piston on the pickup device. An interlock is completed that permits the gas lock to be lifted.

If for some reason a fuel plug is still hanging on the pickup device, the fuel plug denoting switch will so indicate by a light on the panel, and an interlock level prevents the seal from being lifted. The load cell also indicates the presence of an unreleased load. The pickup device will have to be lowered again to the bottom of its travel and again released and sequenced to its travel position as mentioned above.

A switch actuates a solenoid valve which raises the movable shield to its up position. Another switch actuates a solenoid valve which activates three pistons which push three lock pins in place. Lights indicate the locked position.

The cask bridge and traverse motors cannot operate unless the seal, index, and movable shield are in the "up" position. The plug hold-down rings must be replaced.

An emergency blower is available in the event of power failure while an irradiated fuel element is within the cask. If, due to mechanical failure, the hoist motors do not operate, it is possible to remove the dust cover from the cask hoist assembly and then, by removing a lock ring, free the hoist slip clutches. This will allow manual lowering of a fuel element if it is deemed necessary. A special override switch on the cask traverse motor permits emergency operation when the index head, seal, and shield are down. An emergency grapple release is provided in case of malfunction of the pressure operated release device.

The steps taken and time required to remove a fuel element are given in Table 6–3.

6–3.4 Fuel storage cells. There are 99 fuel storage cells, located in the west end of the reactor building. The cells are steel tubes, 4 inches in diameter and 21 feet 6 inches in length, recessed below floor level with the

TABLE 6–3

FUEL ELEMENT REMOVAL

(Assuming that the dummy plug is in the cask and the cask contains a helium atmosphere, the following steps are required to remove and replace a fuel element.)

Step	Minutes
1. Translate cask over process tube, center, and lower gas lock	2
2. Evacuate and flush gas lock	3
3. Lower grapple plug and engage fuel element	1
4. Hoist spent fuel element into cask	3
5. Traverse grapple plugs in cask	1
6. Lower dummy plug (or new fuel element) into process tube	3
7. Release, raise grapple plug to seal cask, raise gas lock, move over wash cell	2
8. Evacuate gas lock and wash cell, flush, and let down to 2 psig helium	4
9. Raise grapple plug	3
10. Traverse plugs in the cask	1
11. Lower fuel element into wash cell	3
12. Release, raise plug, move cask away	2
Subtotal	28
After washing, drying, and pump down	
13. Replace cask over wash cell, center, lower gas lock, flush, and lower grapple plug to engage element	6
14. Raise element into cask	3
15. Traverse grapple plugs in cask	1
16. Lower empty grapple plug to seal cask	3
17. Raise gas lock, move over process tube, center, seal, evacuate, flush, lower grapple plug	4
18. Raise dummy, plug into cask	3
19. Traverse grapple plugs in cask	1
20. Lower fuel element into process tube	3
21. Release, raise plug to seal cask, raise gas lock, and move away	2
Subtotal	26
Total	54

access at floor level. The access is designed to form a seal with the O-ring on the fuel plugs or control rod thimbles. Three of these cells are isolated from the others, and are designated for new fuel storage. The remaining 96 form a rectangular lattice 6 cells wide and 16 cells long. Eighty of the cells are cooled by tetralin circulating through a pipe welded to the outside of the tube. The coolant line passes down one side of the tube and up again on the diametrically opposite side. The new cells and 16 of the others are not cooled. An inert atmosphere is established in the cells by an auxiliary cask designed specifically for this purpose.

6–3.5 Fuel storage cell evacuation cask. This cask is used in evacuating air from the fuel storage cells and loading them with a helium atmosphere. With a fuel assembly, control-rod thimble, or dummy plug in the storage cell, the cask is lowered over the cell with the bridge crane. A sleeve projection on the bottom of the cask is received by the sleeve at the top of storage cell. An O-ring near the bottom of the cask sleeve projection forms a seal between mating surfaces of the two sleeves. A hoisting grapple with a ball extrusion pickup lifts the plug in the storage cell by a peripheral ring in the top of the plug. Lifting force is supplied by a hydraulic cylinder powered by a hydraulic hand pump on the side of the cask. The cask can elevate the plug approximately 1 foot.

A valved port on the side of the cask permits evacuation and helium loading of the cask. With the plug elevated, the storage cell atmosphere is common with that of the cask, and can be evacuated and helium-loaded in a like manner. Evacuation is accomplished with a portable vacuum pump, and helium is loaded from a portable helium supply bottle. A compound gauge on the cask indicates up to 30-inch Hg vacuum and 30-inch Hg pressure.

6–3.6 Fuel-cleaning facilities. Three cleaning cells are located adjacent to the fuel storage cells. They are designed to wash sodium from the fuel elements, control rod thimbles, etc., with water under an inert atmosphere. Gas liberated from the sodium water reaction is passed to the radioactive-gas vent system. Wash water from the cells is passed to the liquid-waste system.

Cleaning cells. Each cleaning cell consists of two concentric steel shells, a 24-inch galvanized steel outer shell, and a 4-inch stainless-steel fuel-cleaning cell. The top end of the inner shell is designed to receive and seal with O-rings on shield plug assemblies and thimbles. The annulus between the two shells is filled with water to a height of 10 feet to serve as heat sink for gamma heat generated in the fuel and the heat of reaction from sodium and water in the cleaning cell. Liquid-level indicators indicate the level of water in the cooling annulus of the cells.

A drain line in the bottom of the outer cell serves to drain both cells. An O-ring on a protruding outlet on the bottom of the inner shell seals the annular area from the drain when the inner shell is in position, and the drain then serves the inner shell only. When the inner shell is raised sufficiently to break this O-ring seal, the water from the annular area can drain. Valves on the drain lines from the three cells are located in a pit in the east wall of the hot-cell service area. Valve stem extensions to the reactor floor level just inside the west wall of the reactor building permit operation of the drain valves from that point. Drainage of the water from the annular area must be done in batches, not exceeding the capacity of the sump tank (150 gallons). Liquid-level alarms signal the loss of water in the drain lines, indicating that the cell has been drained.

Effluent from the fuel-cleaning cells and liquids collected by floor drains in the hot cells flow by gravity to a sump tank, a part of the liquid waste system complex.

6–3.7 SRE hot cells. The SRE hot cells are located in a basement area of the reactor building. The cells are designed to afford examination facilities for the evaluation of primary SRE, experimental SGR, and breeder fuels. Their physical location allows direct transfer of fuel from the reactor to the cells via the fuel-handling cask. This feature dictated that the cells be built below the level of the reactor building floor, with the transfer point within reach of the main crane. The fuel-handling cask retracts a fuel element from the reactor, replaces it with a new one, and then inserts the used element into the cleaning cell, where the sodium is removed. Then the cask picks up the clean element and moves it into a storage cell for radioactive and thermal cooling. After a proper cooling period, the element is picked up by the cask, which moves over the access port in the primary hot cell roof, retracts the plug, and inserts the fuel element into the hot cell.

SRE hot cells function primarily as tools for critical metallurgical examination of fuel material irradiated in the SRE, and as such are not general-purpose cells. Since they are the only cells presently available at the reactor site, it is expected that they will be used for other experiments as well, but such is not their designed function.

Figure 6–22, which is a plan view of the cell area, will help to explain and orient the design. The cells separate the space into an operating area and a service area and are connected by a small change room. Personnel access is via a stairway entering from the reactor building floor in a small cupola which is installed to aid ventilation control. Equipment access is by way of 7 by 7-foot hatchways in the roof of both the operating and service areas.

General-purpose manipulation is accomplished with ANL Model 8

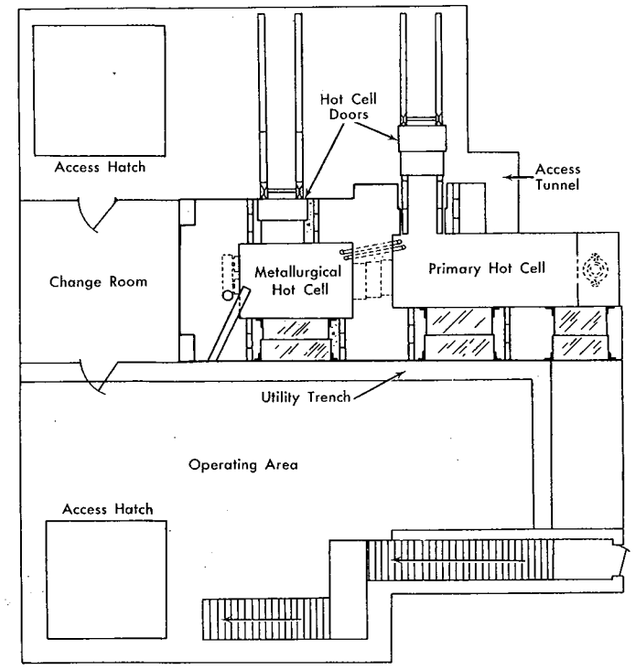

FIG. 6–22. Plan view of SRE hot-cell area.

manipulators at each operating station, plus a small ½-ton bridge crane in the primary cell only. All equipment is designed to operate remotely with fixed-manipulative techniques aided by these general-purpose tools.

The element is inserted into the cell and is left hanging with the bottom extending into a well below the cell floor and the top at eye-level in front of the first window. In this position, the element may be visually examined and photographed. In disassembly, the outer six rods are freed from their upper holding spider by backing off the locking nut above the positioning fins with a pneumatic wrench, raising the fin assembly, and grappling each rod in turn with a special hook attached to the crane. The rod is then lifted slightly, moved radially outward, and lifted clear of the lower spider. The center rod is also removable, but this is an infrequent operation, because of the lower burnup experienced by this rod. Each rod is then separately photographed, visually examined, and measured for distortion.

When a particular rod is selected for detailed slug examination, it must be cut open and the fuel slugs removed. First, a grinder cuts the wire wrap

at each end of the rod and the wire is removed by means of master-slave manipulators. The rod is then placed in the de-canner and an abrasive saw slits the jacket tube longitudinally. Care must be used to remove the slugs from the tube without damaging the fuel slug. After the tube is slit open, the slugs are removed and placed in an alcohol bath to clean off the NaK. The clean slugs may then be photographed and measured.

A slug selected for metallographic examination is then sectioned in the area of interest by an abrasive saw. Slices $\frac{1}{8}$ inch thick are cut from the slug, cleaned in an ultrasonic cleaner, and placed in a metal specimen mount. (The mount permits electrical and thermal contact with the specimen, practically zero outgassing in vacuum up to 300°F, magnetic handling, and almost no edge-rounding during grinding and polishing.) The specimen is then placed in a turret holder on a lapping machine and lapped down to undisturbed metal by an Oak Ridge National Laboratory (ORNL) technique. Another cleaning in the ultrasonic cleaner is followed by two polishing steps accomplished with ORNL designed equipment. After polishing, the specimen is etched chemically, electrochemically, or cathodically, as the metallurgist desires.

There is a shielded, remotely operated Bausch and Lomb research metallograph placed outside the metallurgical hot cell and communicating with the interior via a tunnel through the wall. The design and operation of this equipment follows closely that employed by Argonne National Laboratory except that, for this cell, shielding provisions are greater. A Tukon micro-hardness tester, suitably shielded and remotely operated, is also placed outside the metallurgical hot cell; communication with the cell is via the same tunnel. These two pieces of equipment, augmented by density measurements and Rockwell hardness tests, will furnish most of the data required for the studies contemplated on SRE and SGR fuels.

The primary cell was designed to afford gamma attenuation down to 0.7 mr/hr at the operating face from a source consisting of 1×10^6 curies of irradiated SRE fuel material after 10 days' cooling; the requirement was 42 inches of magnetite concrete. The metallurgical cell is constructed of 36 inches of magnetite concrete, since it need handle only small specimens a few at a time.

The cells are heavy concrete (3.7 density) sheathed inside and out with $\frac{3}{16}$-inch mild-steel plate to facilitate mounting of equipment. All surfaces are painted with Amercoat 74 (a 3-component, epoxy, catalyzed system), using a 5-coat application. Ventilation is accomplished in a conventional manner: filtered air is drawn into the cell, discharged through prefilters and absolute filters, and finally out through a short stack. Standby blowers and connection to the reactor emergency battery power supply provide adequate provision for power or equipment failure.

Cell windows are all-glass dry type made up of a combination of 3.3 density nonbrowning glass in proper proportions so that the average density matches that of the concrete. The lights were cast as thick as possible to cut down the number of interfaces, thus reducing light loss. The glass is enclosed in a tight "can" which inserts as a package into the cell wall. The advantages of this type of window are: lower cost than $ZnBr_2$ or oil-filled all-glass, no maintenance due to clouding or precipitation of liquid media, and no necessity for a liquid-tight can.

Use of both sodium-vapor and mercury-vapor lighting gives excellent light transmittance and results in good visibility within the cells.

6–4. Auxiliary Systems

The reactor services described in this section include those supporting systems serving the reactor to provide radioactive-waste disposal, cooling, and inert atmosphere for the reactor, its auxiliaries, or other service systems.

6–4.1 Inert gas system. All pipes, tanks, and mechanical equipment which contain sodium, and the galleries in which they exist, within the confines of the reactor area have an inert atmosphere maintained in voids not occupied by sodium. In addition, all auxiliary units (casks, storage cells, etc.) into which items coated with sodium are placed have an inert atmosphere established before receiving the sodium-coated item. All units exposed to a neutron flux which contain voids that do, or may at a later time, communicate with reactor room atmosphere have an inert atmosphere. Nitrogen, because it is more economical than helium, is used in the galleries that have a large volume and are not exposed to a high neutron flux. Helium serves all neutron flux areas, or areas that at some time will communicate with the atmosphere of a unit which is exposed to a high flux.

6–4.2 Helium system. The helium system (Fig. 6–23) is comprised of a supply, piping, and the necessary equipment needed to establish a helium atmosphere in the units listed in Table 6–4.

The helium supply, located outside the reactor building, consists of 80 helium bottles manifolded into two groups of 40 bottles each. The volume available through each manifold is approximately three times that of the primary sodium system. The two manifold systems are connected in parallel, and valved to permit use of one group at a time. A pressure control station in each of the manifolds reduces the pressure from 2300 psi (under full tank conditions) to 50 psi in the manifolds.

NaK bubblers. Helium from the supply tank passes through NaK absorption columns and into the low-pressure storage tank. Five cylindri-

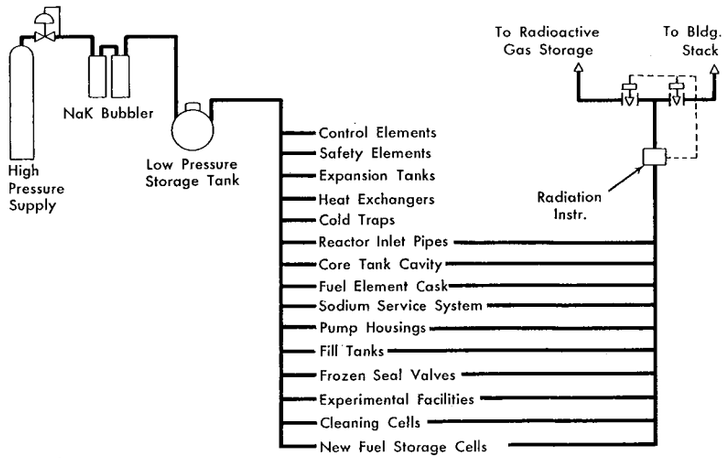

FIG. 6–23. Helium system.

cal tanks, connected in series, make up the NaK bubbler system. The second and fourth tanks are filled with the eutectic alloy of sodium and potassium, and the first, third, and fifth tanks contain stainless-steel wool which removes NaK vapor from the gas stream and prevents NaK from backing up into the upstream helium line in the event of a reverse pressure surge. There is also a check valve downstream from the bubbler to prevent reverse flow in case the pressure is lost at the supply tank.

Helium flows through a pipe to the bottom of the first tank, up through the stainless-steel wool to a pipe which carries it to the bottom of the second tank, where it bubbles up through the sodium-potassium into the third tank, etc. Oxygen present in the helium combines with the NaK to form oxides which are disentrained from the gas stream by the stainless-steel wool fibers.

Helium storage and distribution. A 35-cubic foot, low-pressure storage tank serves as a surge tank to minimize pressure fluctuations arising from sudden changes in helium demand. The helium distribution system, comprised of several parallel supply headers, feeds a group of parallel branch circuits which in turn supply the individual units requiring a helium atmosphere. The units they serve are listed in Table 6–4. Prior to filling the system with sodium, all components and piping are swept with helium to remove air.

6–4.3 Nitrogen system. The nitrogen system (Fig. 6–24) is comprised of the necessary equipment and piping to establish an inert atmosphere in the units listed in Table 6–5.

TABLE 6–4

COMPONENTS SERVED BY THE HELIUM SYSTEM

1. Fuel element cask service, at cask service area; future moderator cask service
2. Cleaning cells; new fuel storage cells service connection in fuel storage cell area
3. Main primary block valves
4. Main primary double wall pipes
5. Reactor atmosphere
6. Reactor control rods
7. Reactor safety rods
8. Service connection at reactor
9. Auxiliary primary block valves
10. Auxiliary primary double wall pipe
11. Primary fill tank atmosphere
12. Disposal cold trap; flush and drain tank drain line; sodium line from disposable cold trap; sodium flush line to disposable cold trap
13. Main primary cold trap; main primary line at main intermediate heat exchanger; main secondary line at intermediate heat exchanger
14. Mass transfer assembly in main primary system
15. Main primary sodium pump casing
16. Auxiliary primary sodium pump casing
17. Auxiliary primary cold trap; auxiliary primary line at auxiliary intermediate heat exchanger; auxiliary secondary line at auxiliary intermediate heat exchanger; drain and fill line at auxiliary intermediate heat exchanger
18. Sodium drums; sodium transfer line at melt station
19. Secondary sodium fill tank atmosphere
20. Main secondary sodium pump casing
21. Main secondary expansion tank atmosphere; main secondary cold trap
22. Auxiliary secondary sodium pump casing
23. Auxiliary secondary expansion tank atmosphere; auxiliary secondary plugging meter piping
24. Reactor drain line
25. Core tank cavity atmosphere

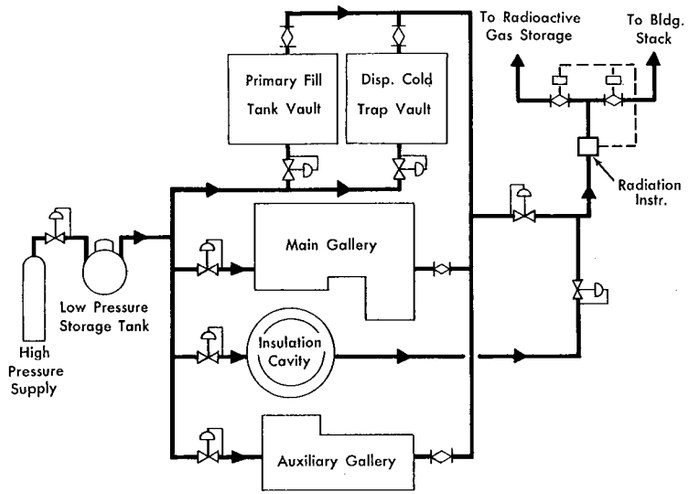

FIG. 6–24. Nitrogen system.

The nitrogen supply is also located outside the reactor building, in close proximity to the helium supply system. Supply for normal operating conditions consists of 20 nitrogen bottles manifolded into two groups of 10 bottles each. Provisions exist for connecting a nitrogen trailer to the manifold when a large quantity of gas is required for purging the system. Normal supply source is intended only to replace the leakage from the system and the amount vented as a result of "breathing" when the system is alternately heated and cooled.

A pressure-control station in each of the supply manifolds reduces the pressure from 2300 psi to 50 psi. A low-pressure alarm in the high-pressure side of the control valve in either manifold sounds an alarm in the control room when the pressure drops below 150 psi.

TABLE 6–5

NITROGEN SYSTEM LOCATIONS AND VOLUME

Space	Volume, ft^3
Main primary system gallery	5683
Auxiliary primary system gallery	776
Primary fill tank vault	2660
Disposable cold trap vault	2097
Insulation cavity	1373

Storage and distribution. A 35-cubic foot, low-pressure storage tank serves as a surge tank to minimize pressure fluctuations.

The nitrogen distribution system is comprised of several parallel supply headers. Each header feeds a group of parallel branch circuits which supply the individual areas requiring a nitrogen atomsphere. The system is arranged to provide a pressure-control manifold for each of the areas served, as shown in Table 6–5. Each of the areas listed in the table is served by a pressure-control station. In the adjacent piping downstream from each control station there is a flow indicator and pressure indicator, and a pressure relief valve connected to the reactor vent system.

Gases from the area containing a nitrogen atmosphere, with the exception of the reactor insulation cavity, intercommunicate through a parallel vent header system. Two tributaties, one collecting from the main primary and main auxiliary galleries, and one from the primary fill tank vault and disposable cold trap vault, vent through a common line. Gases from each tributary pass through a radioactive dust filter station and past a radiation-detection instrument. This instrument operates solenoid valves which divert gases to the reactor building stack or to the decay tanks if they are radioactive. They may be released to the vent system through a common pressure-control station if the pressure exceeds 1.5 psig.

Each radioactive dust filter station has two types of filtering media, a coarse section to remove the major part of the dust, and a CWS section to remove fine particles. Each filter is installed with a pair of blocking valves and a bypass valve. Purging of the nitrogen is performed after the galleries, vaults, and insulation cavity are sealed for operational testing of the sodium systems.

6–4.4 Organic cooling system. A circulating organic (tetralin) cooling system (Fig. 6–25) removes heat from the concrete surrounding the reactor and from reactor components. The establishment and maintenance of sodium freeze seals is also accomplished by this tetralin system. Tetralin (tetrahydronapthalene) is a hydrocarbon with a low cross section for thermal neutrons, which makes it an ideal coolant in circuits exposed to a neutron flux. It boils at 403°F and its vapor pressure is 1 millimeter at 100°F.

The tetralin coolant system consists of cooling circuits serving structural and mechanical units of the reactor, reactor auxiliaries, and reactor service systems. The supply tank, pumps, and evaporative coolers are located approximately 50 feet north of the reactor building.

The 500-gallon tetralin supply tank, which is approximately one-half of the system requirements, serves primarily as an expansion tank and to supply a suction head for the pumps. System filling is accomplished via the tank, through a filter. This tank is vented to the atmosphere through a flame arrestor to prevent flashback. Strainers installed at various loca-

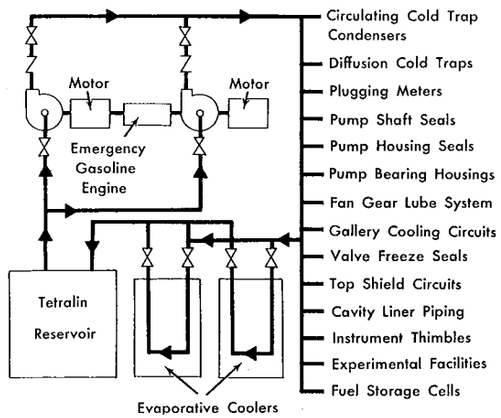

FIG. 6-25. Organic cooling system.

tions in the system filter out particulate matter that could be circulated through a neutron flux and become activated. A 1-inch bypass line passes the tetralin through a dessicant, activated alumina, to remove water.

Pumps. There are two constant-speed tetralin pumps rated at 370 gpm and 61 psi differential pressure. Each pump is capable of supplying the entire tetralin distribution system, with 15 percent reserve.

Each pump is normally driven by a 440-volt, 20-hp, constant-speed electric motor. Upon failure of the main power supply to the pump motors, the pump motor that is operating is automatically switched to the emergency power system. If the pump or pump motor that is operating suffers mechanical or electrical failure, as indicated by a low-pressure alarm, switching to the other pump and engine is accomplished manually by the operator in the control room. A gasoline engine located between the two pumps is coupled to the spare pump for use if the emergency power system should fail to start or cease to function. Each pump is equipped with a "Y" type strainer in the 6-inch inlet pipe and a check valve in the 6-inch discharge pipe, and can be isolated by a pair of gate valves. Switches for the pump motors are located on a panel in the control room.

Evaporative coolers. There are two evaporative coolers each with sufficient cooling capacity to decrease the temperature of 200 gpm of tetralin from 125 to 95°F. Both coolers will be operated during normal operation of the reactor. Failure and subsequent removal from service of one cooler will decrease the tetralin flow and raise the temperature approximately 15°F. Loss of water to the coolers decreases their efficiency by 93 percent.

Each cooler is equipped with a water reservoir and a recirculating pump. Water is pumped from the reservoir under the cooling columns to the top

of the cooling columns, and the amount not evaporated drips back into the reservoir. Each cooler has 106-gallon water reservoir in which the water level is maintained by a self-contained float-type level control, actuating a valve in the water makeup line. An overflow drain is provided to prevent flooding the tetralin equipment area. Water from the reservoir is dumped to the drain (at a rate equal to one-third the circulation rate) to blow down salts.

Each cooler has a 6 gpm recirculating water pump, and both the pump line and the pump bypass line from the water makeup line have a check valve. A check valve in the makeup line controls the pressure lower than the discharge pressure from the pump. During normal operation, the flow is through the pump, and the pressure supplied by the pump retains the check valve in the bypass line in the closed position, preventing reverse flow in the bypass line. If a pump fails, pressure in the bypass line exceeds that in the pump line and closes the check valve in the pump line, preventing reverse flow. Water is then supplied to the cooling coils from the water storage tank by gravity.

Each evaporative cooler has a one-speed 10,500 cfm air fan, located above the cooler, which draws air vertically upward across the tubes.

Distribution system. The tetralin distribution system is comprised of several parallel supply and return headers. Each pair of headers feeds a group of parallel branch circuits which serve the following individual structural or process units requiring cooling.

Freeze seals and bearing housing for the four centrifugal pumps in the heat-transfer circuits.
Freeze seals for main and auxiliary primary systems blocking valves, and moderator/reflector inlet valve.
Top shield, which consists of loading face, plugs, and ring shield.
Diffusion cold traps.
Condensers for circulating type cold traps.
Coolers for plugging meters.
Main and auxiliary gallery atmosphere cooling tubes.
Reactor nuclear instrumentation thimbles.
Core cavity liner.
Mass-transfer assembly freeze seals.
Freeze section in pipe for secondary system drain valves.
Fuel storage cells.
Hot trap freeze seals.

Flow and temperature are read on a panel in the control room. There is a temperature indicator and a flow indicator (read locally) incorporated into each cooling circuit. A bypass line around these indicators permits them to be isolated for maintenance purposes.

6–4.5 Liquid-waste system. The liquid-waste system (Fig. 6–26) permits storage of effluent from the fuel-cleaning cells and liquid collected by floor drains in the hot cells. The liquid waste flows by gravity to the sump tank in a pit on the north side of the hot-cell service area.

The sump tank is located 35 feet below reactor building floor level in a waterproof pit on the north side of the hot-cell service area. The pit is accessible from the top at ground level or through a manhole in the north wall of the hot-cell service area. The sump tank is made of stainless steel, and has a capacity of 150 gallons. Its primary function is to collect drainage from the fuel-cleaning cells. In addition, it collects condensate from the floor drains in the hot cell. Gases are prevented from backing up into the cleaning cells and hot cells by traps built into associated piping. A valve in the hot-cell drain line, upstream from the sump tank vault, has an extension permitting operation from the hot-cell floor level. Liquid pumped from the sump tank is prevented from returning by a check valve on the discharge line from the pump.

A differential manometer, located at the fuel-cleaning control panel, measures the liquid level in the sump tank, and the radiation level is indicated in the control room. Liquid waste is pumped from the sump tank to a selected one of ten holdup tanks located 100 feet north of the reactor building. After sufficient decay time the waste passes by nitrogen pressure and gravity to either of two liquid-waste storage tanks located 30 feet east of the holdup tank.

Holdup-tank station. The holdup-tank station is made up of ten 80-gallon tanks located in two adjacent concrete vaults on a hillside 400 feet north of the reactor building. Liquid pumped from the sump tank to this station may be routed to various tanks by manually operated valves. This station

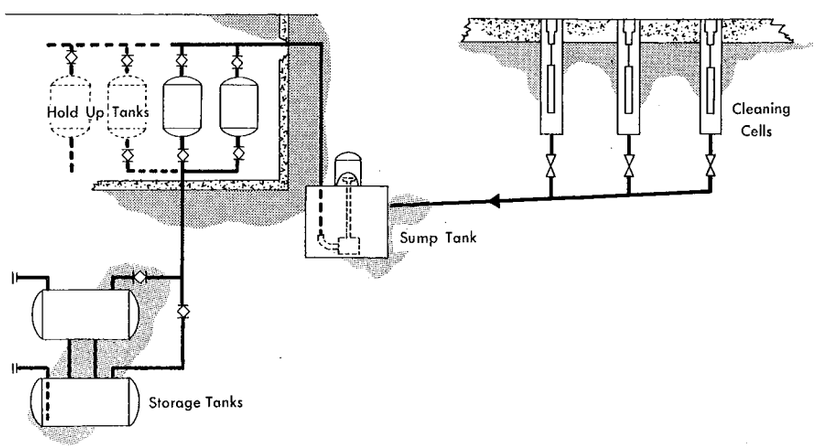

FIG. 6–26. Liquid-waste system.

serves as a check point to permit sampling and analysis for radioactivity. Each tank can be drained by gravity to either of two liquid-waste storage tanks located immediately south of the holdup tanks. All valves at the station have an extension through the concrete shielding to permit operation from outside the vaults. Each tank has a pump-out connection extending to the bottom of the tank for emergency use. Floor drains from each vault permit drainage to the liquid-waste storage tanks. Valved water connections on the headers to each bank of five tanks permit flushing either into a holdup tank, or to the sump tank.

Each tank can vent through a check valve to a header common to four other tanks. Each header is connected to the radioactive vent gas system through a relief valve set at 2 psi. A manually operated valve in a bypass around each relief valve is normally open. The relief valves operate only if the manual valve is closed. A three-way valve on each header permits the vent line from the sump tank to be opened to either or both headers. In addition, these same three-way valves permit purging with nitrogen through the holdup tanks to facilitate representative sampling.

Liquid level in each holdup tank is indicated on the liquid-waste storage control panel by a Levelometer. Before any radioactive liquid is transferred to the radioactive liquid-waste storage tanks, a sample of the liquid is analyzed by the health physics group to determine if its activity is low enough for transfer.

Liquid-waste storage tanks. There are two 5000-gallon liquid-waste storage tanks buried in the ground immediately south of the liquid-waste holdup tanks. A manually operated valve at the entrance to each tank has an extended stem permitting operation from ground level. Each tank is vented to atmosphere and has a pump-out connection extending to the bottom of the tank, through which sampling can be effected. A concrete basin provides a secondary containment for these tanks. The liquid level of the tanks is indicated on the liquid-waste storage control board. The radiation level of the tanks is determined by analysis of a sample.

6–4.6 Gaseous-waste system. A schematic diagram of the SRE gaseous-waste system is shown in Fig. 6–27.

Nonradioactive gas disposal. Gases with no detectable radioactivity are routed by the radiation controller through solenoid valves in the vent system to the reactor building ventilation exhaust. Any activity level would be monitored by a recorder in the control room. The collected gases are mixed with the hot-cell exhaust and blown to the atmosphere.

Radioactive gas handling. Radioactive gases are routed to a compressor suction tank by the radiation monitor station. The gases are pulled from the suction tank by two compressors and moved to any one of four 350 cubic foot capacity decay tanks. The four tanks have a combined capacity

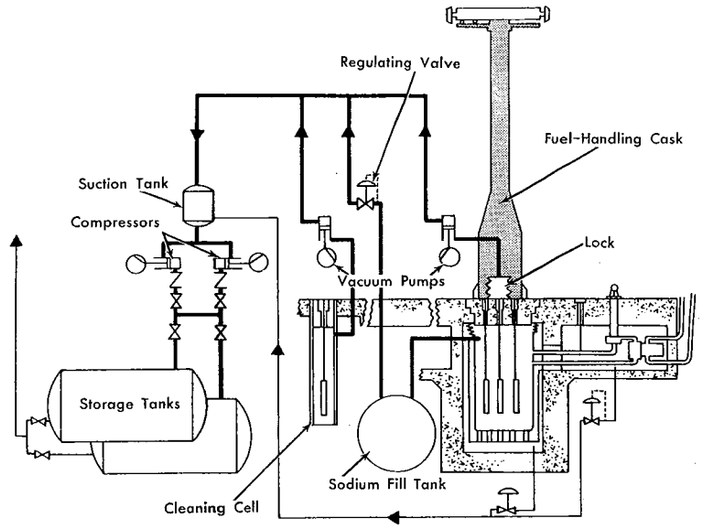

FIG. 6–27. Gaseous-waste system.

of 10,800 scf of gas at 100 psig. The two radioactive vent gas compressors are located in a concrete vault on a hillside 170 feet north of the reactor building. Each compressor is rated at 20 scfm with a suction pressure of 10.7 psia and a discharge pressure of 113.7 psia.

When analysis of a gas sample taken from a decay tank shows that sufficient decay has occurred, the tank can be vented to the building exhaust by a manually operated valve. These gases are first filtered to remove any particulate matter. Under no conditions will the concentration of radioactive gases at the building exhaust be permitted to exceed the maximum permissible concentrations listed in the Code of Federal Regulations. A radiation recorder-controller in the ventilation exhaust stack actuates a safety valve to stop the flow of gas from the decay tank if any activity is observed.

A helium-supply station comprised of two 225 scf helium bottles is connected to the system at the compressor suction tank and at the suction and discharge sides of the compressor to permit purging of the system.

The 100-cubic foot suction tank is located on a hillside 100 feet north of the reactor building, and is buried under earth for shielding purposes. There is a pair of dehydrators connected in parallel on the line between the suction tank and the compressors. The relative humidity of gas passing through the dehydrators will be reduced to approximately 16 percent at 80°F. The pressure of gas in the suction tank is indicated locally and in

the control room. If the pressure exceeds 14 psia an alarm is actuated in the reactor control room.

6–5 INSTRUMENTATION

6–5.1 Nuclear and reactor control instruments. Eight thermal neutron detectors located in the thimbles at the periphery of the outer tank provide neutron flux level signals for controlling the reactor. Figure 6–28 shows the position of the instrument tubes with relation to the reactor core tank. There are four tubes, capped at their lower ends, on each side of the reactor. They permit access for two fission counters and six ionization chambers.

The two fission counters provide neutron level signals for duplicate channels during startup operation. Two compensated ionization chambers provide neutron level signals for duplicate reactor period channels, two uncompensated ionization chambers provide neutron signals for duplicate high neutron level safety channels, one compensated ionization chamber provides a neutron level signal for automatic neutron servo control, and the remaining compensated ionization chamber provides a neutron level signal for the neutron flux level channel. The six ionization chambers

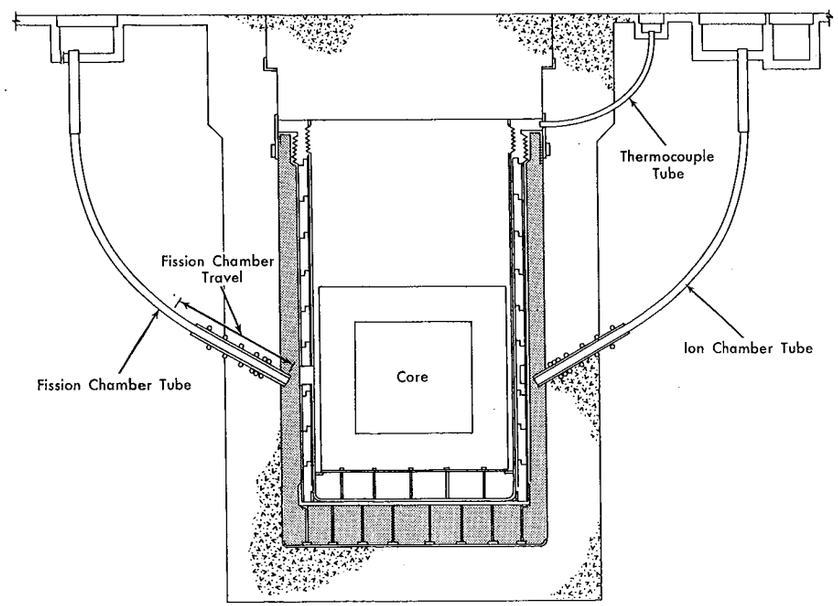

FIG. 6–28. Instrumentation tubes providing access to the reactor core.

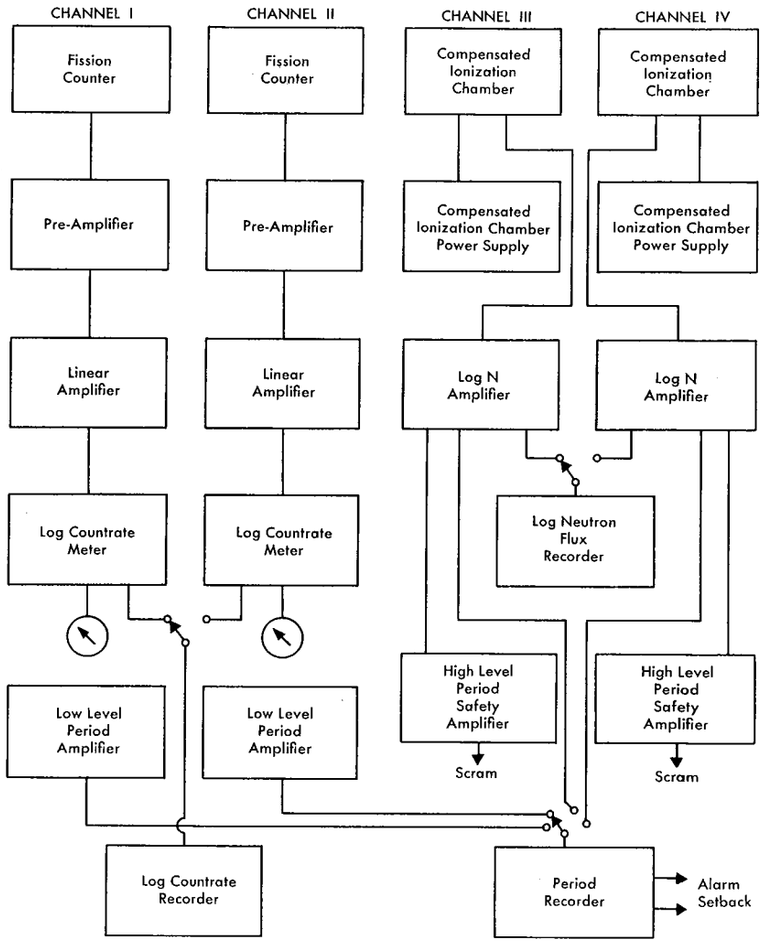

FIG. 6–29. SRE nuclear instrumentation, channel I–IV.

remain fully inserted in the thimbles during high power operation. The two fission chambers are used primarily for startup operation and are retracted by motors as the reactor power increases.

Counters (Fig. 6–29) are used during reactor startup to indicate multiplication of neutrons in the count rate region. Each of the two channels consists of a fission counter, a preamplifier, a high-gain linear amplifier, a log count rate meter, a low-level period amplifier, and appropriate recording equipment.

Each startup fission counter rides in a four-wheeled cart which is raised and lowered in the thimble by a motor. A synchro position indicator on the control console follows a transmitter which is also driven by the motor. A light on the control console indicates when the fission counter is completely inserted, and limit switches shut off the motor. The fission counters will measure neutron flux levels from 1 to 10^5 n/cm^2·sec. The sensitivity is 0.7 count/n/cm^2. The output is indicated on meters on the control console, and recorded by a four-decade logarithmic strip chart recorder.

The function of the log N period channels (Fig. 6–29) is to measure reactor period in the period region, and provide signals for a reactor scram in the event of a short period. The period trip circuit is bypassed when the reactor is operating in the power region. Each of the two period channels consists of a compensated ionization chamber, a compensated ionization chamber power supply, a log N amplifier, a high-level period amplifier, and appropriate recording equipment.

The compensated ionization chambers will measure 10^4 to 10^{10} n/cm^2·sec in the presence of 10^5 r/hr of gamma radiation. The sensitivity is 4×10^{-14} ampere per unit flux. The output of the logarithmic amplifier is recorded by a six-decade logarithmic strip chart recorder, and the period is recorded by a strip chart recorder with a chart calibrated 30-∞-3 seconds.

Each of the two neutron level safety channels (Fig. 6–30) is comprised

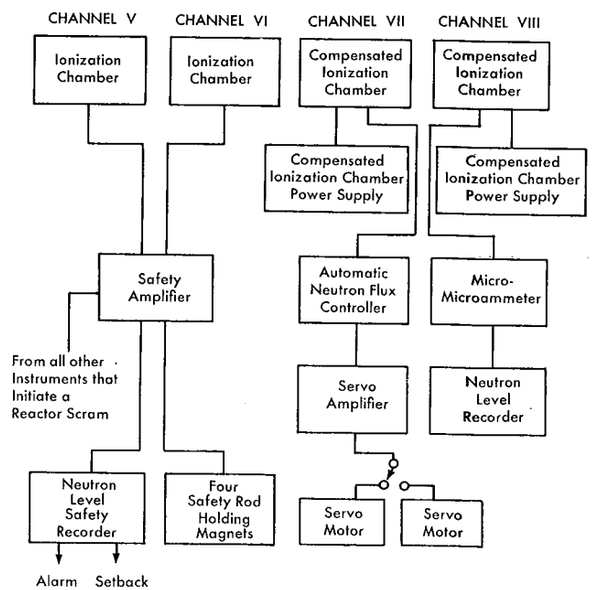

FIG. 6–30. SRE nuclear instrumentation, channel V–VIII.

of an uncompensated ionization chamber and a safety trip amplifier. The uncompensated ionization chambers will measure 10^5 to 10^9 n/cm^2·sec. The sensitivity is 10^{-13} ampere per unit flux. The ionization current is used to actuate a sensitive relay and to trip a holding current amplifier in the event of abnormal high neutron flux. Other conditions that initiate a reactor scram provide signals to trip the holding current amplifier.

The neutron level control channel for automatic neutron flux control (Fig. 6–30) consists of a compensated ionization chamber, a high-voltage supply, a potentiometer indicator with control slidewire, and a position adjusting type servo amplifier. Steady-state neutron flux is maintained by three-mode action: proportional band, rate, and reset action. This prevents overshooting or oscillation of the control rod and also prevents the neutron flux from settling off of the control point. The control set point can be automatically programmed to control the rate of change in reactor temperature when reactor power is changing. The controller is flexible for receiving signals from temperature, steam pressure, etc., for other automatic control applications.

The neutron flux level channel (Fig. 6–30) consists of a compensated ionization chamber with a high-voltage power supply, a micro-microammeter, and a flux level recorder. The micro-microammeter is a vibrating capacitor type stable DC amplifier, and is used to give a linear indication of neutron flux over several decades. The DC amplifier has a maximum sensitivity of 10^{-11} ampere and a maximum current reading of 10^{-3} ampere. The amplifier output is displayed on a meter on the control console and provides a signal for a linear strip chart recorder.

6–5.2 Reactor safety system. The reactor safety system is designed to give protection for the reactor equipment in case of accidents or malfunction of reactor components. A high degree of inherent safety is designed into the reactor; however, a system which will shut down the reactor fast enough to prevent large temperature excursions that might damage reactor components is also required. Safety rods and control circuits in the SRE are designed to respond within milliseconds to any abnormal condition requiring a scram, and to reduce the reactor to a subcritical condition when such a signal is received.

Following a reactor scram, four boron safety rods with a total worth of approximately 5.7 percent $\Delta K/K$ are released from holding magnets and inserted in the reactor core by gravity. The safety-rod holding magnet is raised and lowered by a three-phase synchronous motor with an electric brake which prevents excessive coasting. A synchro-transmitter coupled to the safety-rod drive mechanism transmits the position of the rod to a synchro indicator on the main control console.

A double-pole double-throw (spring return to neutral) switch on the main control console may be used to raise or lower the safety rod by energizing the motor starter. All four safety rods can be raised or lowered simultaneously by a switch on the main control console. Electric interlocks prevent raising any safety rod if any control rod is removed from its down position; however, the safety rod is always free to be inserted into the reactor by the chain drive mechanism. In the event the reactor is scrammed, electric interlocks prevent raising the safety rods until the scram condition is corrected. Micro-limit switches actuated by the safety rods at the extreme limits of travel remove power to the motor drive. A green light on the control console indicates when each safety rod is completely inserted in the reactor and a red light indicates when each safety rod is completely withdrawn.

The safety amplifier includes four holding-coil amplifiers which provide plate current for energizing the four safety-rod holding coils. In a normal condition, the reactor scram loop circuit is closed, applying a positive bias to the input of each holding-coil amplifier. Plate current conduction through the amplifiers energizes all holding cells.

Thyrite varisters are installed across the holding magnets to limit inductive surge overload voltage to a safe value when the inductive current is interrupted by a reactor scram. This does not increase the time constant.

The curve in Fig. 6–31 represents the safety-rod response time from the instant that current is removed from the holding magnet until the safety rod is at its lower limit.

Table 6–6 gives the response time of the measuring instrumentation for the various conditions that initiate a reactor scram. The total time to reduce the reactor from full power to zero power is the sum of the response time of the measuring instrumentation and the safety-rod drop time;

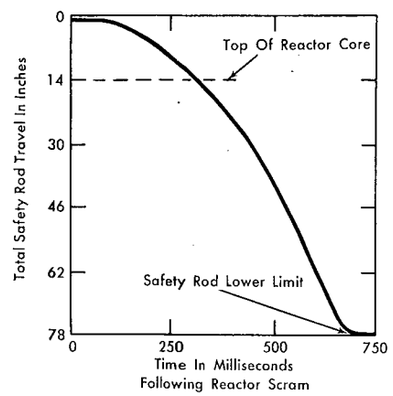

FIG. 6–31. Safety-rod response time following release from holding magnet.

TABLE 6–6

RESPONSE TIME OF SRE SAFETY INSTRUMENTATION

Conditions that initiate a reactor scram	Response time of the measuring circuit
Short reactor period (<5 seconds)	200 milliseconds (measured as the time derivative of reactor power using an Rc differentiating network)
High reactor power (>125% full power)	20 milliseconds (measured by neutron detectors and fast response DC amplifiers) *Note:* Total time was 490 milliseconds to reduce reactor power from full power to 1% power
High fuel-channel temperature (>110% of temperature at full power)	3.4 seconds (measured by thermocouples at the outlet of the fuel channels)
Abnormal sodium flow in the cooling system (±15% deviation from control setting)	2.6 seconds (measured by comparing the control setting with magnetic flowmeters and sodium pump speed)
Total loss of feedwater through the steam generator	9 seconds (measured by a pressure gauge at the discharge of the feedwater pump) *Note:* An 8-second time delay is built in the circuit to allow time to start the standby feedwater pump

however, it must be noted that there is a 99 percent reduction in power when 20 inches of the four safety rods are in the reactor core.

The following conditions will prevent reactor startup or initiate a reactor scram:

Reactor period. Scram contacts are provided by a plate current relay in the output stage of the period amplifier. The interlocks are bypassed when operating in the power region.

Neutron level. Scram contacts are provided by a plate current relay in the safety amplifier.

Fuel-channel temperature. Scram contacts are provided by three temperature-indicating controllers (Article 6-5.7).

Earthquake. Scram contacts are provided by a pendulum-type earthquake switch.

Manual. Scram contacts are provided by a momentary pushbutton switch on the main control console.

Electrical power failure. Scram contacts are provided by a time-delay relay which is energized by normal power. The delay is adjustable, 0 to 10 seconds.

Sodium flow. Scram contacts are provided by a relay in the pump control circuit.

Main air-blast heat exchanger. Scram contacts are provided by a relay in the fan-control circuit. This scram condition will be bypassed when the heat is removed by the steam generator.

Loss of feedwater. Scram contacts are provided by a pressure switch in the feedwater line between the discharge side of the feedwater pump and the boiler. This scram condition will be bypassed when the heat is removed by the air-blast heat exchanger.

Main secondary cold leg temperature. Scram contacts are provided by a Brown strip chart temperature recorder (Article 6–5.7).

In the event there is a false scram originating at the reactor loading face shield (such as a safety rod being jarred loose from the holding magnet), the sodium pumps are shut off, and the magnetic brakes are energized into operation. The following conditions will initiate a reactor setback: reactor period, neutron level, and fuel-channel temperature. In the event one or more of the above conditions becomes abnormal and exceeds the operating limits, all four control rods are driven into the reactor at shim speed. The rod insertion continues only until the condition initiating the setback is corrected. Any correcting action on the sodium pumps to keep the fuel-channel sodium exit temperature constant is performed by the operator.

In the event one or more of the conditions listed in Table 6–7 becomes abnormal and exceeds the operating limits, an alarm is given by the annunciator alarm system. The alarm can be reset by a switch on the main control console. A window is lighted on the annunciator chassis indicating the cause of the alarm, and can be reset only after the condition causing the alarm is corrected. An alarm does not automatically insert safety or control rods into the reactor, but serves as a command to the operator to take corrective action. The annunciator alarm units are installed in the panels in the control room.

The over-all safety system is designed for a "fail-safe" condition. In the event a relay opens, a tube burns out, etc., a warning is given by the annunciator alarm system identifying the area in which the part is defective. In some cases a defective part will scram the reactor; however, all

TABLE 6–7

SRE OPERATIONAL DATA

Reactor Scrams, Setbacks, and Alarms

	Scram	Setback	Alarm
1. Manual	×	×	
2. Earthquake	×		
3. Electrical power failure	After 2 sec delay		
4. Reactor period	<5 sec	<10 sec	<20 sec
5. Neutron level	>125% NF	>115% NF	>105% NF
6. Main primary sodium flow	90% set flow rate		<95% set flow rate
7. Main secondary sodium flow	<90% set flow rate		<95% set flow rate
8. Fuel-channel temperature	>1040°F	>1000°F	>980°F
9. Loss of the main air-blast fans	<85% set fan speed		<90% set fan speed
10. Loss of either air-blast fan	<80% set fan speed		<90% set fan speed
11. Loss of feedwater	<600 psi plus 8-sec delay		<600 psi
12. Main secondary cold leg temperature	>550°F		>500°F or <400°F
13. Main primary hot leg temperature			>1000°F
14. Main primary cold leg temperature			>550°F or <450°F
15. Low tetralin flow			<300 gpm
16. Auxiliary primary hot leg temperature			>1000°F
17. Auxiliary primary cold leg temperature			>500°F or <450°F
18. Auxiliary secondary cold leg temperature			>490°F or <400°F

TABLE 6–7 (*Continued*)

	Scram	Setback	Alarm
19. Auxiliary primary sodium flow			<70% set flow
20. Auxiliary secondary sodium flow			<70% set flow
21. Freeze seal temperatures			>180°F
22. Sodium pump bearing temperatures			>150°F
23. Helium pressure in the reactor tank			>5 psi or <2½ psi
24. Dummy fuel-channel temperatures			>1050°F
25. Discharge pressure from primary sodium pump			>27.5 psi
26. Reactor sodium level			<4 ft 3 in. above main sodium outlet
27. Reactor core tank temperature			>1000°F
28. Sodium leak			×
29. Helium gas supply			<125 psi
30. Tetralin supply level			<36 in.
31. Evaporator cooler flow			<5 gpm
32. Vent system pressure			>120 psi
33. Sodium level in the main secondary expansion tank			>65 in. or <40 in.
34. Sodium level in the main auxiliary expansion tank			>12.5 in. or <7.5 in.
35. High radiation background (stack)			$>5 \times 10^{-7}$ μc

TABLE 6–7 (*Continued*)

	Scram	Setback	Alarm
36. Concrete shield temperature			>150°F
37. Fission and ion chamber B supply failure			×
38. Electronic component failure			×
39. Helium pressure in the core tank cavity			>5 psi <2½ psi
40. Helium pressure in the primary fill tank			>5 psi <2½ psi
41. Main primary pump helium casing pressure			<9 psi
42. Main secondary pump helium casing pressure			<9 psi
43. Auxiliary primary pump helium casing pressure			<9 psi
44. Auxiliary secondary pump helium casing pressure			<9 psi
45. Nitrogen gas supply			<125 psi
46. Insulation cavity nitrogen pressure			>5 psi <2½ psi
47. Compressor suction tank			>14 psia
48. Steam generator sodium exit temperature			>490°F or <400°F
49. Mercury pressure in the steam generator			>400 psi <300 psi
50. Throttle valve between the steam generator and turbine			Closed

components were selected for a high degree of reliability, and an attempt has been made to minimize the possibility of false scrams. Induction motors are used for the safety and control rods so that no accident can make the motors run in excess of synchronous speed, eliminating the danger of too-rapid withdrawal of rods.

6–5.3 Reactor control system. The neutron level system is designed to start up and shut down the reactor as well as to maintain a satisfactorily accurate regulation of the neutron flux over the required range of operating levels. Startup and shutdown are accomplished manually; operation at a given power level may be accomplished manually or by using the automatic servo-control system.

Power output of the reactor is determined by the position of four boron control rods with a worth of approximately 7.8 percent $\Delta K/K$. The drive mechanism for the control rods utilizes a ball screw principle. All four control rods can be inserted or withdrawn at a rate of 0.3 ft/min by a 208-volt, three-phase, $\frac{1}{4}$-hp motor.

A double-pole double-throw (spring return to neutral) switch on the main control console is used to raise or lower an individual control rod by energizing the motor starter. All four control rods can be raised or lowered simultaneously by a switch on the control console. Interlocks prevent raising any control rod if any safety rod is removed from its up position; however, the control rod is always free to be inserted into the reactor. In the event the reactor is scrammed, interlocks prevent raising the control rods until the scram condition is corrected. Micro-limit switches actuated by each control rod at the extreme limits of travel remove power to the motor drive. A green light on the control console indicates when the control rod is completely inserted into the reactor, and a red light indicates when the control rod is completely withdrawn. A synchro-transmitter coupled to the control rod drive transmits the position of the control rod to a synchro-indicator on the control console.

Two control rods are used only as shim rods and are designed to insert positive and negative reactivity at the slow rate of 0.3 ft/min. The other two control rods are used both as shim rods and as regulating rods, and are designed for fine reactivity control as well as for shim motion. These two rods are moved at a rate of 3.75 ft/min during both automatic servo control and manual operation when regulating.

Regulating motion is provided by a 115-volt, two-phase, $\frac{1}{7}$-hp motor. A manual-automatic switch on the control console selects either manual or automatic operation of the rods provided with regulating motion. Regulating rods may be operated individually or simultaneously during manual operation; however, during automatic servo operation only one rod is regulated. Micro-limit switches shut off the motor drive when the

rod exceeds its designed length of regulating travel ($\pm 7\frac{1}{2}$ inches). In servo control a warning buzzer indicates when the regulating rod has exceeded its limits of travel, and control automatically reverts to manual operation. Interlocks prevent the automatic servo control from functioning if the error signal is excessive when the selector switch is turned to automatic. This interlock prevents the servo motor from withdrawing the rods at a rate which would cause a fast increase in power or period. A switch on the control console changes the range of the rod position synchro-indicators to provide vernier scales over 15 inches of rod travel when the regulating rods are driven by the fast motor.

6–5.4 Magnetic brake control system. The function of the control system for the magnetic brakes and throttle valve is to program sodium flow decay to match reactor power decay so as to maintain system temperatures following a reactor scram. Thermal convection flow following a reactor scram is excessive, and requires temperature control by reducing sodium flow with magnet brakes and a throttle valve. Fuel exit temperature is controlled by providing a thermocouple temperature signal to a temperature controller and servo amplifier. The servo amplifier controls a motor-operated rheostat which regulates current in a magnetic brake installed in the primary cold leg. Deviation of the fuel exit temperature is corrected by action of the brake on the sodium flow. The primary cold leg temperature and secondary hot leg temperature are controlled by a brake and throttle valve in the secondary cold leg. The secondary cold leg temperature is maintained by reduced feedwater through the steam generator.

6–5.5 Relation of instruments to reactor startup and operation. The operation cycle of the SRE consists of four stages: precritical, the approach to critical, the rise to operating power, and operation in the power region.

Precritical operation consists of checking and calibrating nuclear and control instrumentation each time the reactor is subcritical. Figure 6–32 gives the relationship of neutron flux level to instruments during the approach to critical, the rise to operating power, and operation in the power region. Figure 6–33 shows the ranges covered by the various instruments used to measure the neutron density of the reactor. SRE operational data for scrams, setbacks, and alarms are given in Table 6–7.

6–5.6 Remote radiation monitoring system. The radiation monitoring system was designed to perform the following functions:

Measure and record the radiation levels in the tank vaults.

Measure and record the radiation levels in the radioactive vent system and provide signals for controlling solenoid valves in the vent lines.

Measure and record the radiation levels in the reactor building for personnel safety.

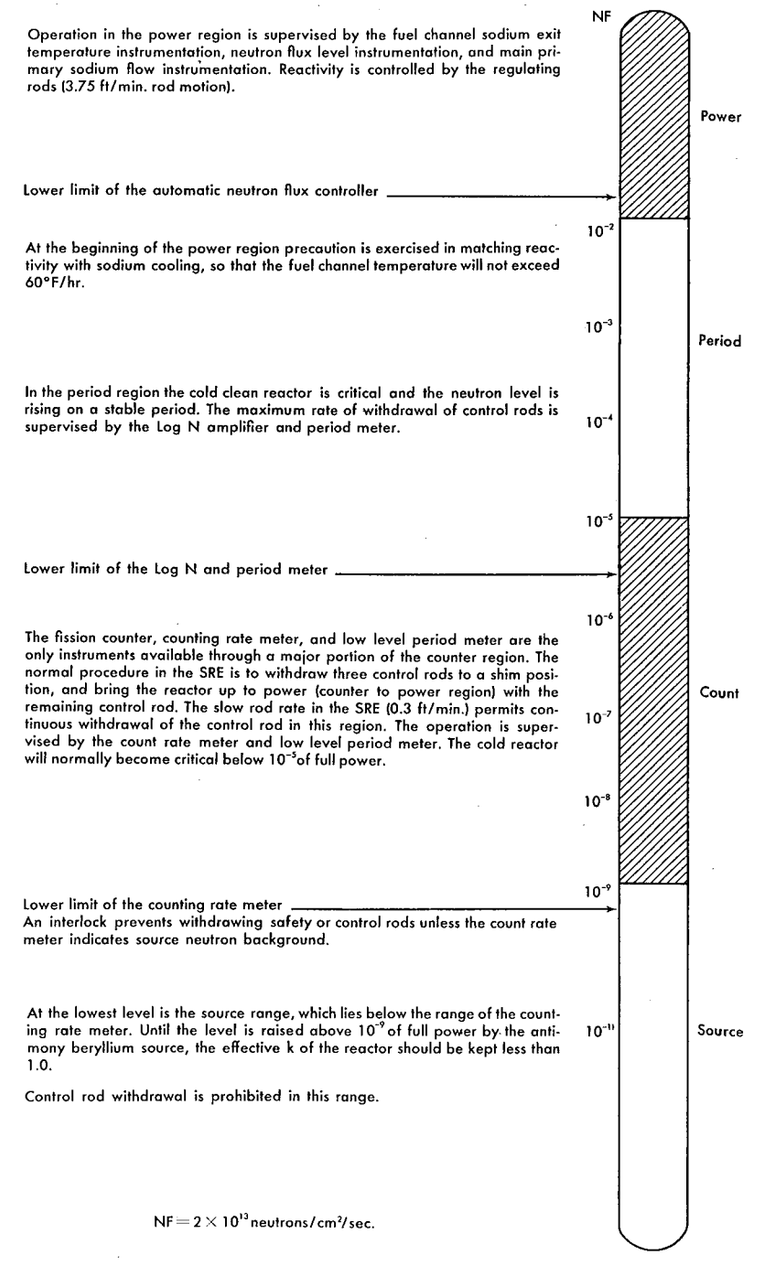

FIG. 6–32. Relation of neutron flux level to instrumentation and control.

Power, Watts	Thermal Neutron Flux at Neutron Detector nv/cm²/sec.	Ionization Chamber Current, Amperes
2×10^8	2.5×10^{10}	10^{-3}
2×10^7	2.5×10^9	10^{-4}
2×10^6	2.5×10^8	10^{-5}
2×10^5	2.5×10^7	10^{-6}
2×10^4	2.5×10^6	10^{-7}
2×10^3	2.5×10^5	10^{-8}
2×10^2	2.5×10^4	10^{-9}
20	2.5×10^3	10^{-10}
2	250	10^{-11}
.02	25	10^{-12}
0.02	2	10^{-13}

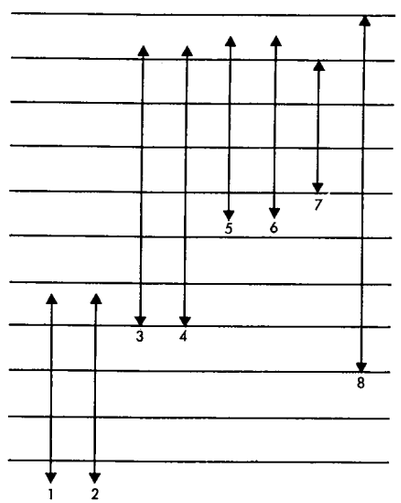

1. Fission Counter Count Rate Channel
2. Fission Counter Count Rate Channel
3. Comp. Ionization Chamber Log N Period Channel
4. Comp. Ionization Chamber Log N Period Channel
5. Ionization Chamber Safety Trip Channel
6. Ionization Chamber Safety Trip Channel
7. Comp. Ionization Chamber Automatic Neutron Flux Control
8. Comp. Ionization Chamber Electrometer Channel

FIG. 6–33. Ranges of nuclear instrumentation.

A Neher-White ionization chamber and Geiger-Mueller (G-M) tube are used for detecting gamma and beta radiation. This detector consists of an ionization chamber and a preamplifier encased in a stainless-steel cylinder. The detectors used for measuring beta activity in the radioactive vent system have an open cylinder at one end to provide maximum sensitivity. Each preamplifier is connected to a log count rate meter in the control room, calibrated in mr/hr, which provides contacts for the annunciator alarm system. A multipoint recorder records the output from the count rate meters. Radiation monitors in the radioactive vent system provide control signals for solenoid valves in the vent lines. These solenoid valves direct the off-gases to the vent stack or to the holdup decay tanks, as appropriate. A radiation monitor at the outlet of the decay tanks prevents releasing off-gases from the decay tanks to the stack until the activity decays to permissible levels.

A stack monitor, which is a backup for the decay tank ionization

chambers, prevents releasing off-gases from the decay tanks to the vent stack in the event the activity exceeds the permissible tolerances. The stack monitor consists of two G-M tubes installed in a cylinder located in a lead shield. Gases from the stack are pumped through the cylinder at a constant rate to provide true measurement of the dosage rate.

The nitrogen atmosphere in the piping galleries is circulated through a dehumidifier unit and returned to the galleries. Three G-M tubes installed in the headers at the outlet of the piping galleries between the piping galleries and the dehumidifier are coupled to a preamplifier and a count rate meter. These count rate meters provide control signals for closing valves in the header lines in the event the radiation levels exceed permissible tolerances.

Other monitoring methods intended for personnel safety include constant air monitors, hand and foot counters, counter room equipment, and portable survey instruments. In the event the gross gamma activity in the reactor building air exceeds the permissible tolerances the building vent system is closed. Table 6–8 lists the radiation detectors and ranges.

6–5.7 Process control instruments. Textbooks generally refer to instrumentation in research reactor coolant systems as secondary or auxiliary instrumentation. In the nuclear power reactor program this type of instrumentation is as vital to the over-all control of the reactor as are the nuclear instruments, and in the SRE it will be referred to as "process control instrumentation." A description of the various components of this instrumentation follows.

Temperature measurements are classified into three groups: (1) preheating of the sodium piping, (2) obtaining stress and heat transfer data, and (3) process control. The sodium piping temperatures are monitored by thermocouples attached to the piping. The second group consists of thermocouples embedded or attached to the structural steel and concrete biological shielding which surrounds the reactor core tank. The third group consists of thermocouples installed in the fuel element hangar rods at the outlet of the fuel channels, and in thermocouple wells in the sodium systems. Thermocouples which require fast response time are welded to the walls of the thermocouple wells.

To determine the temperatures in the sodium stream cooling the moderator, two corner channels receive special elements containing thermocouples with their junctions at various elevations within the core. Each temperature-measuring element consists of a column of beryllium cylinders suspended on a stainless-steel tube extending down from a plug in the top shield. Thermocouples do not contact the liquid sodium.

Plant temperatures are measured with iron-constantan and chromel-alumel thermocouples. The reference junctions are located in the re-

TABLE 6-8

RADIATION DETECTORS AND RANGES

Radiation detector and location	Count rate meter ranges	Readout instrument
N. W. ionization chamber Disposable cold trap vault	0.01 to 10^4 r/hr	Strip chart multipoint recorder
N. W. ionization chamber Primary fill tank vault	0.01 to 10^4 r/hr	
N. W. ionization chamber Radioactive sump tank	0.1 to 100 mr/hr	
N. W. ionization chamber Reactor loading face shield	0.1 to 100 mr/hr	
N. W. ionization chamber Cleaning cell area	0.1 to 100 mr/hr	
N. W. ionization chamber Control room	0.1 to 100 mr/hr	
N. W. ionization chambers Five locations in the radioactive vent system	0.1 to 100 mr/hr	
G-M tube Stack monitor	0.1 to 10,000 cps	Strip chart recorder
G-M tube Main gallery outlet header	1 to 500 cps	
G-M tube Auxiliary gallery outlet header	1 to 500 cps	
G-M tube Sodium service vault outlet header	1 to 500 cps	

corders and indicators. Standard iron-constantan and chromel-alumel lead wire is used between the reference junction and thermocouple. Chromel-alumel thermocouples were selected for areas where the temperature exceeds 800°F.

Seventeen magnetic flowmeters, ranging in size from 1 to 6 inches, are used in the sodium systems. Sodium flow in the piping, in the presence of a strong magnetic field, produces a voltage which is proportional to the flow rate. Leads are welded to the piping to measure the millivolt signal. Shielded wire is required for the signal leads between the magnetic flowmeter and readout instrument. Null-balance, potentiometer type recorders and indicators were selected for the readout instruments to eliminate errors introduced by the IR drop in the signal leads.

Leak-detector wires trace all sodium piping, tanks, and heat exchangers that are located in inaccessible vaults. The leak-detector wires are run in pairs along the bottom of the various sodium containers. In the event of a sodium leak the wire tracings are shorted, which sounds an alarm in the control room and sodium service room. A light identifies the location of the sodium leak.

Two types of sodium pressure transducers are used. A bellows-actuated differential transformer type is used in the primary radioactive sodium loops and a pneumatic force balance type is used in the secondary non-radioactive sodium loops. Electrical transducers were selected for the primary sodium loops to eliminate circulating filtered air in potential radioactive areas.

To determine the oxygen concentration in the sodium cooling system, the sodium is sampled from the main sodium streams and circulated through a plugging meter at 1 gpm. The sodium is cooled before it passes a plugging valve. Plugging occurs at the valve at a temperature that is related to the oxygen concentration in the sodium. Once the plugging temperature is obtained, the oxygen concentration in the sodium is read from a calibration curve of Na_2O versus temperature.

Three types of electromagnetic coil assemblies are used to determine the liquid sodium level in the tanks: the long or continuous type gauge, short alarm coils, and the precision or probe type coils.

Stainless steel Type 304 thimbles were welded into the tank and piping assemblies during the fabrication of the tanks. Level gauges are installed in the thimbles, and the sodium level is sensed, electromagnetically, through the walls of the stainless-steel thimbles. This method allows replacing or changing level gauges without exposing the sodium vapor and cover gas to air. The solenoid coils used for detecting the level are inside the cover can and do not extend all the way to the junction box. The coils are designed and tested for operation up to 1200°F. The coil impedance is a function of the sodium level. The current is held constant; therefore

the voltage is directly proportional to the sodium level. Sodium level calibration curves were established at several different sodium temperatures.

An alarm coil set consists of two coils in a bridge. One coil is temperature compensated and the other is the sensing coil. The lower set of coils is the low-level alarm set and the upper set of coils the high-level alarm set. An abnormal sodium level changes the impedance of the detector coil and the bridge is unbalanced. The contact meter relay provides a signal for the annunciator alarm system.

Precision probe coil assemblies have a chassis which contains a 1000-cycle power supply, the detector circuit, and indicating meter with controls. The probe consists of the coil head and an extension tube of sufficient length to allow the plug connection to be made outside the high-temperature region. The probe head is capable of withstanding continuous duty at 400°F and intermittent duty up to 1200°F. The probe is inserted in a thimble in the tank to be measured. As the probe approaches the sodium level the coil impedance changes and the bridge circuit is unbalanced. A DC ammeter indicates an unbalanced bridge circuit. The accuracy of the precision probe coil is $\pm\frac{1}{16}$ inch of level over the range from room temperature to 1200°F. Accuracy is independent of the thickness or number of layers of stainless steel between the probe and the sodium, and is independent of range of level to be measured.

Pressure transducers for the tetralin and inert gas systems are composed of a bellows which actuates a precision potentiometer in one leg of a bridge circuit. A change in the displacement of the bellows will unbalance the bridge circuit and produce a meter indication which is proportional to the pressure. The measuring element for the tetralin pump discharge header flow is a differential bellows which is linked to an electromechanical metametering transmitter of the impulse duration type. The value of the measured variable is transmitted to an indicator in the control room as a function of time rather than an electrical magnitude.

Pressure switches consisting of a diaphragm and a micro-switch are installed in the helium and nitrogen gas systems. The switches actuate an alarm in the control room in the event of abnormal pressures.

Differential pressure gauges are used to measure level in the tanks in the radioactive liquid-waste systems. There are over 200 local instruments on the piping and vessels in the SRE, such as thermometer temperature indicators, bourdon pressure gauges, sight-glass flow indicators, etc., which are not read out on instrument panels.

An electrolytic hygrometer unit is installed in the header lines between the piping galleries and the dehumidifier to measure the moisture concentration of nitrogen in the piping galleries. This hygrometer measures the dewpoints of nitrogen down to one part water in one million parts of air. The output of the hygrometer is recorded by a strip chart recorder.

Samples of the nitrogen atmosphere in the piping galleries are analyzed

TABLE 6–9

INTERCOMMUNICATION BETWEEN THE EDISON STEAM-GENERATING FACILITY AND THE SRE

Edison steam-generating facility		SRE
Metering transformer at the turbine generator output	→	Kilowatt meter $EI \times \cos\theta$ Range: 0 to 10,000 kw
Bellows-actuated pressure transducer Steam pressure in the steam generator	→	Steam pressure gauge Range: 0 to 1000 psi
Flow transmitter Feedwater flow	→	Feedwater flow indicator Range: 0 to 100,000 lb/hr
Iron-constantan thermocouple Steam-generator sodium exit temperature	→	Strip chart temperature recorder Range: 0 to 800°F
Sodium flow indicator Range: 0 to 1800 gpm	←	*Electromagnetic flow meter* Main secondary sodium loop
Neutron flux level indicator Range: 10^6 to 10^9 DC	←	*Ionization chamber* DC amplifier

by a continuous oxygen analyzer. The oxygen concentration can be determined down to 1 percent.

Table 6–9 lists information that is transmitted between the Edison steam generating facility and the SRE.

6–5.8 SRE electrical distribution system. Reliability, continuity of power for vital equipment, and limited maintenance were criteria for electrical distribution system design. The SRE facility receives electrical power from a 3000 kva substation, which is tied directly into the Santa Susana 60-Mw Chatsworth distribution center, located one mile east of the SRE site. The SRE substation is located on a transformer pad at the southeast corner of the SRE building and consists of six transformers which provide 480 volts three-phase at 1000 kva, and 240 volts three-phase at 300 kva. Switch gear located in the SRE electrical distribution room provides heavy-duty air circuit breakers for the distribution of all normal and emergency power. The 440-volt bus provides power for all the reactor services, and the 240-volt bus is used primarily for electrical heaters on the piping and vessels.

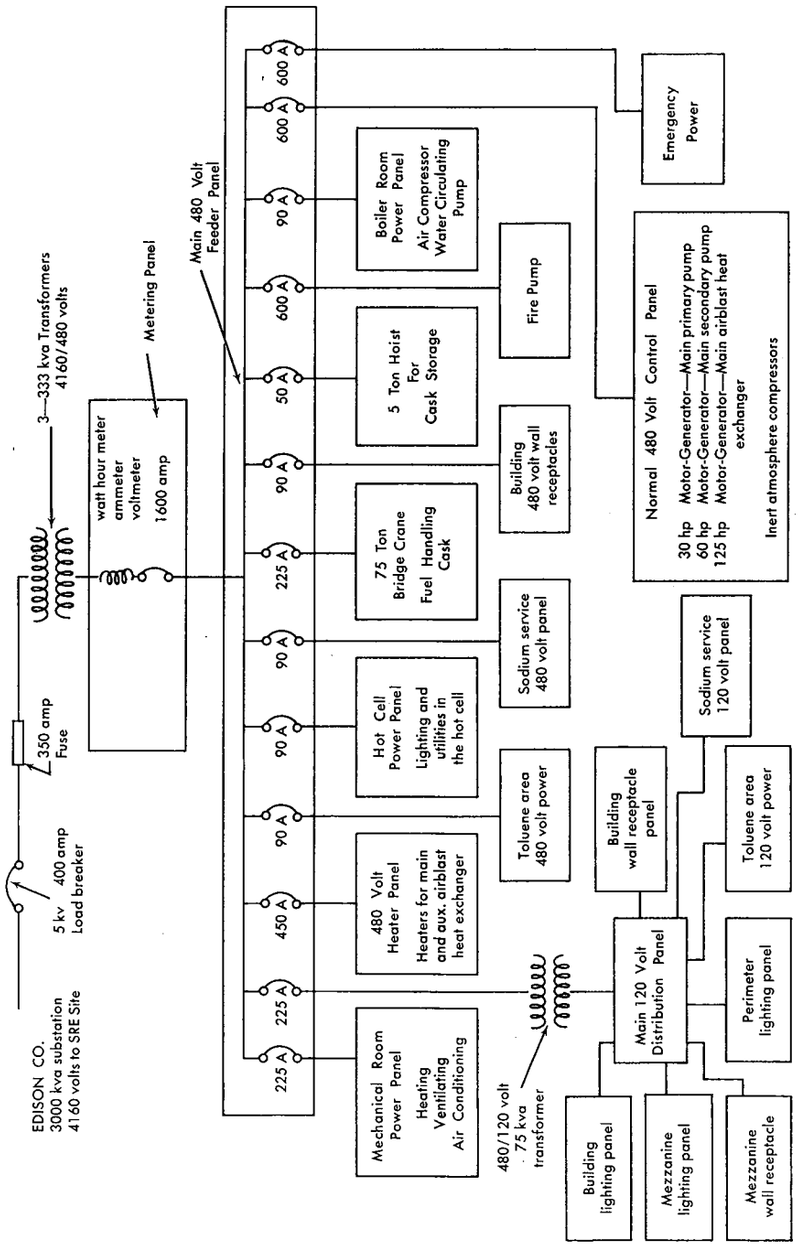

FIG. 6–34. Block diagram of 480-volt distribution circuit.

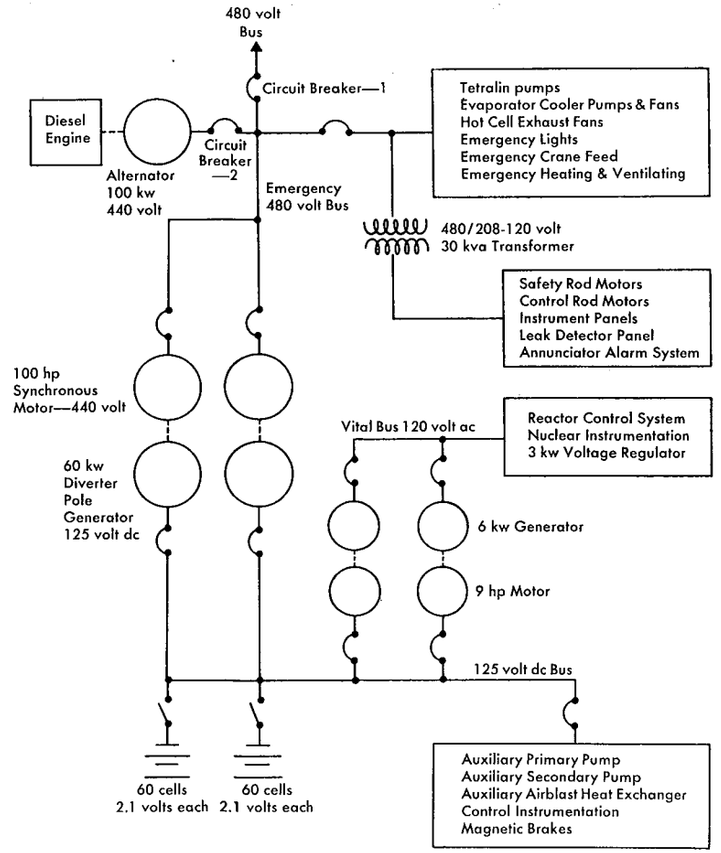

FIG. 6–35. Emergency electrical power system diagram.

Figure 6–34 is a block diagram of the 480-volt distribution circuit. The 240-volt and 480-volt circuits are delta-connected, with no grounds. The main 120-volt circuit is wye-connected with center ground.

The reactor control system and equipment in the sodium systems require uninterrupted electrical power. An emergency electrical power system (Fig. 6–35) which operates automatically is provided to supply emergency power when a loss of power from the 3000 kva substation occurs. This system provides power for a 480-volt emergency power bus. A battery-charging motor-generator set is supplied by normal power and runs continuously. This unit float charges 120 wet-cell batteries and supplies 125 volts DC. When normal power is lost:

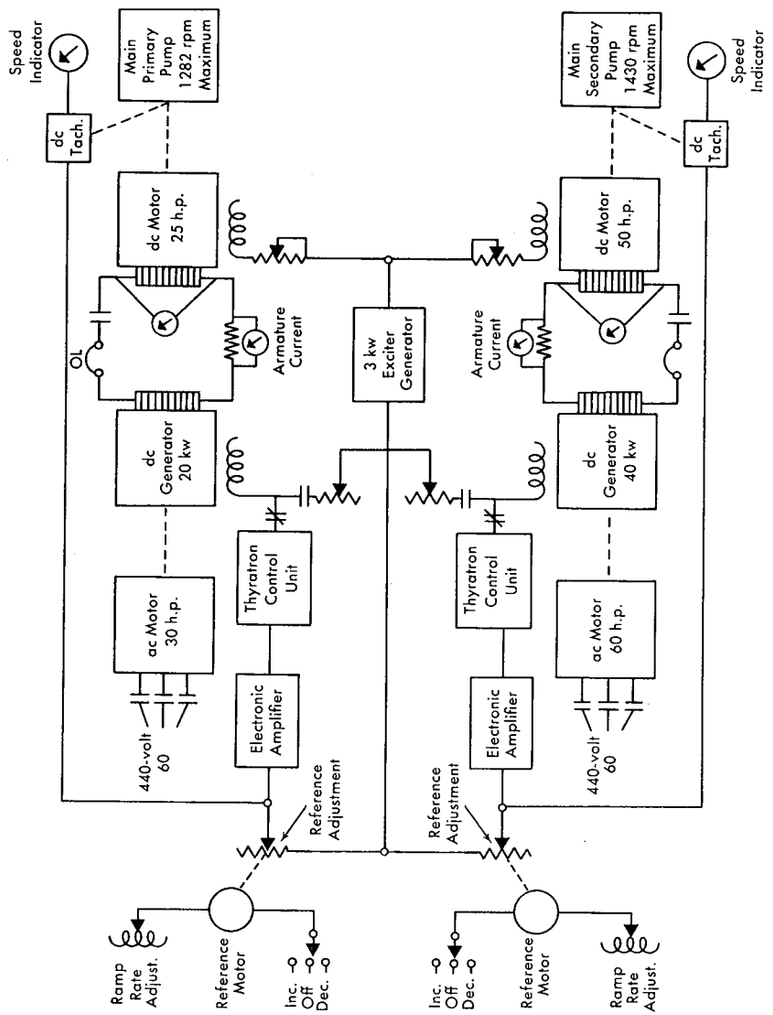

Fig. 6–36. Main sodium pump drive system.

A relay which is supplied by the 480-volt bus drops out at 80 percent of the bus voltage and opens CB-1 (see Fig. 6–35).

The diverter pole generator and synchronous motor changes to a battery-driven motor alternator supplying emergency 480-volt power. This changeover occurs within 0.2 seconds.

The diesel alternator starts up, and when it is running at the proper voltage and frequency, it is synchronized either manually or automatically with the battery-driven alternator. A circuit breaker on the line from the diesel alternator, which is normally open, closes, and the diesel engine alternator supplies the emergency load. This changeover occurs within a few seconds.

The motor alternator reverts back to a motor-generator battery charger.

When normal power returns and synchronizes with emergency power, CB-1 closes after a delay. The delay is adjustable from 1 to 10 seconds, to ensure that normal power has returned permanently. CB-2 opens, and the diesel engine alternator shuts off.

A DC control panel located in the electrical distribution room contains all the controls for the emergency power system.

A vital bus is provided for the nuclear instrumentation and reactor safety circuits. This bus is free of power transients which could cause erratic operation of instrumentation and false scrams. A 120-volt AC generator is constantly driven by a DC motor supplied by the 125-volt DC bus. A frequency control and a voltage regulator provide stable uninterrupted power which is free of power transients.

During periods when the reactor is down, the sodium is kept fluid by electrical heaters on piping and vessels. There are over 500 electrical resistance-type heaters on the piping and tanks in the SRE as follows: strip heaters on the tanks, immersion heaters in the primary fill, secondary fill, and reactor core tanks, and tubular heaters on the piping. The spacing and the length of the heaters installed on the piping and tanks are designed to give uniform heating over the entire heated area. Sufficient electrical heaters are installed on all the piping and tanks so that the heaters can be operated at 50 percent rated capacity or less to meet the normal heat requirements, thus extending heater life. Heater switches are grouped for convenience, and each group of heaters is controlled by circuit-breaker type switches.

Immersion heaters in the reactor core tank are controlled by powerstats. Iron-constantan thermocouples are installed on the piping and tanks to provide an indication of the preheating temperatures. Null balance-type readout instruments are used for indicating the preheating operation.

Main primary and main secondary sodium pumps (Fig. 6–36) are driven

by DC motors with constant field excitation and DC generators to provide adjustable armature voltage. An adjustable DC reference voltage is compared with the signal voltage from a DC tachometer-generator, which is coupled to the motor drive.

The reference voltage is varied by a motor-driven rheostat, controlled by a switch on the control console. The error signal is amplified by an electronic amplifier which controls a thyratron control unit that regulates the excitation current for the DC generator field. The excitation determines the output voltage of the generator, and hence the speed of the DC shunt motor which drives the pump. The thyratron control unit provides a motor speed ratio of 20 to 1. If there is a failure of the electronic amplifier and thyratron control unit, generator field excitation current can be regulated manually by a motor-driven rheostat. Power for this rheostat is supplied by the exciter generator.

The motor for the reference adjust is operated at a speed determined by a ramp rate control on the control console. Speed can be adjusted from 5 to 30 percent a minute. As the error between the control set point and the tachometer-generator is reduced to less than 5 percent, the speed of the motor is reduced linearly in accordance with the amount of error. This provides built-in rate action to prevent the pump speed from overshooting the control set point.

Auxiliary primary and auxiliary secondary sodium pumps are driven by DC motors with constant armature voltage and adjustable field excitation current. The field excitation current is adjusted by rheostats on the main control console, which provide motor speed ratios of 3.5 to 1. Both sodium pumps are operated separately.

Main air-blast heat exchanger fans are driven by two DC motors with constant field excitation and a DC generator to provide adjustable armature voltage. Speed of the fans can be controlled by manual operation or by automatic servo control. Manual operation is provided by two pushbutton switches on the control console. The switches operate a motor-driven potentiometer, which adjusts a reference potential that is compared with a feedback signal voltage from the DC generator. The error signal is amplified by an electronic amplifier which controls a thyratron control unit that regulates excitation current for the DC generator field. This excitation determines the output voltage of the generator, and hence the speed of the DC shunt motors which drive the fans.

The two air-blast fans can be operated simultaneously or separately. A switch on the control console selects fan No. 1, fan No. 2, or both fans. If there is a failure in the electronic DC supply, excitation voltage can be supplied by the exciter generator. A manually operated rheostat located in the power distribution room is provided to operate the fans under emergency conditions.

A switch on the control console selects either manual or automatic servo operation. A thermocouple installed at the outlet of the heat exchanger supplies a signal voltage to a temperature indicator and servo amplifier which regulates the fan speed to hold the sodium exit temperature constant at a preselected value. If an error signal exists between the control set point and the thermocouple output, the servo amplifier operates the motor-operated potentiometer to readjust the generator field excitation to provide the proper motor speed. The motor-operated potentiometer provides a motor speed ratio of 20 to 1. Resistors and contactors are provided for dynamic braking of the motors.

The auxiliary air-blast fan is driven by a DC motor with constant armature voltage and adjustable field excitation current. Speed of the fan can be controlled by manual operation or by automatic control. Manual operation is provided by two pushbutton switches on the control console. The switches operate a motor-operated rheostat which adjusts the excitation current for the DC motor field. A thermocouple installed at the outlet of the auxiliary air-blast heat exchanger provides a signal voltage to a temperature indicator-controller. This controller regulates the fan speed to hold the sodium exit temperature constant at a preselected value. If an error signal exists between the control set point and the thermocouple

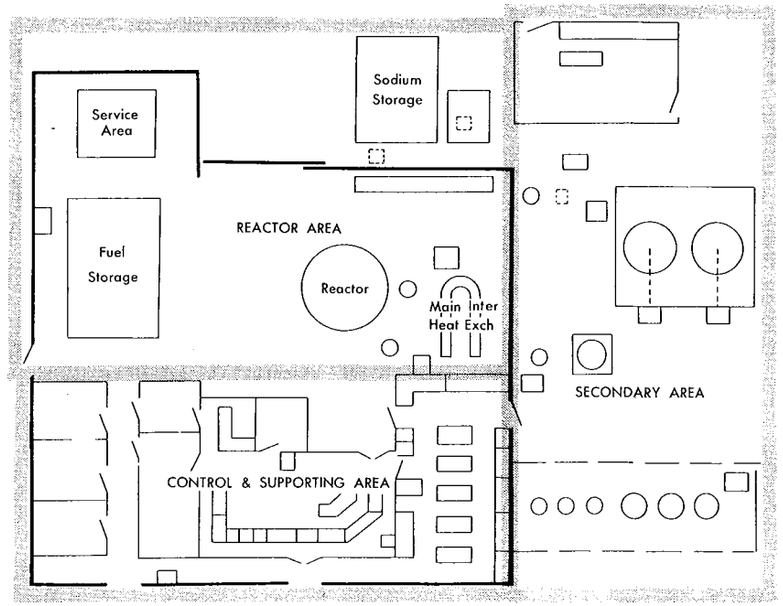

FIG. 6–37. Floor plan of reactor building.

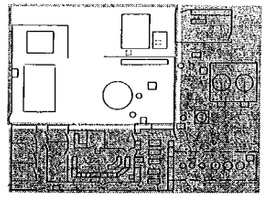

REACTOR AREA

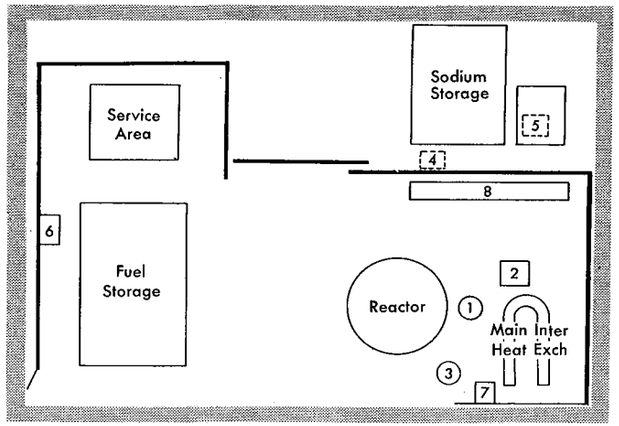

1 Main Primary Pump Motor
2 Main Primary Magnetic Brake
3 Auxiliary Primary Pump Motor
4 Reactor Drain EM Pump
5 Cold Trap Flush EM Pump
6 Liquid Waste Panel
7 Auxiliary Primary Temperature Panel
8 Magnetic Brake Panel

FIG. 6–37(a). Reactor area.

output, the controller operates the motor-operated rheostat to readjust motor field excitation current to provide the proper motor speed. The motor-operated rheostat provides a motor speed ratio of 3 to 1.

6–5.9 Control centers. The reactor control room is normally the center for maintaining control over the reactor operations. However, other panels

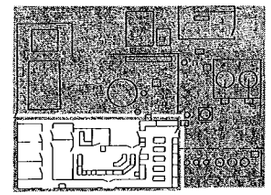

CONTROL & SUPPORTING AREA

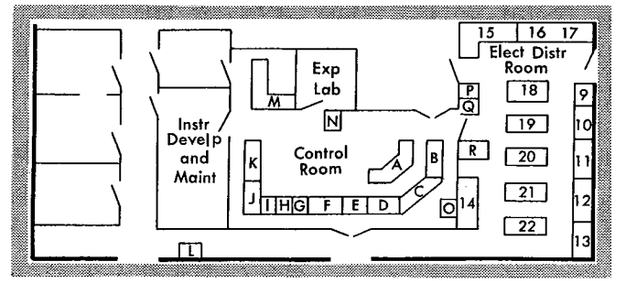

A Control Console
B Recorders
C Recorders
D Recorders
E Recorders
F Sodium Process Instruments
G Pre-Heat Panel
H Inert Gas Panel
I Tetralin Panel
J Radiation Panel
K Nuclear Panel
L Hand and Foot Counter
M Load Forcing and Load Following
N Edison Panel
O Relay Panel
P Sodium Flow Off-Normal Panel
Q Auxiliary Pump Motor and Fan Control Panel
R Main Pump Motor Control Panel

9 480V Metering Panel
10 480V Main Feeder Panel
11 Normal 480V Distribution Panel
12 Emergency Power Distribution Panel
13 Building Lighting Panel
14 DC Control Panel
15 240V Distribution and Heater Panel
16 240V Metering Panel
17 480V Heater Control Panel
18 125 HP MG Set for Main Fans
19 30 HP MG Set for Main Primary Pump
20 60 HP MG Set for Main Secondary Pump
21 100 HP Motor-Generator Battery Charger No. 1
22 100 HP Motor-Generator Battery Charger No. 2

FIG. 6–37(b). Control and supporting area.

are located in the high bay and other areas for maintaining the reactor auxiliary operations. All plant alarms are given in the control room, either denoting an abnormal operating condition, a reactor setback, or a reactor shutdown. Figure 6–37 is an elementary drawing of the SRE building showing the location of the instrument and electrical panels.

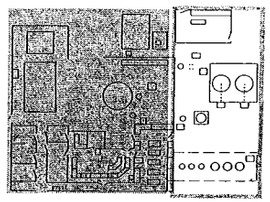

SECONDARY AREA

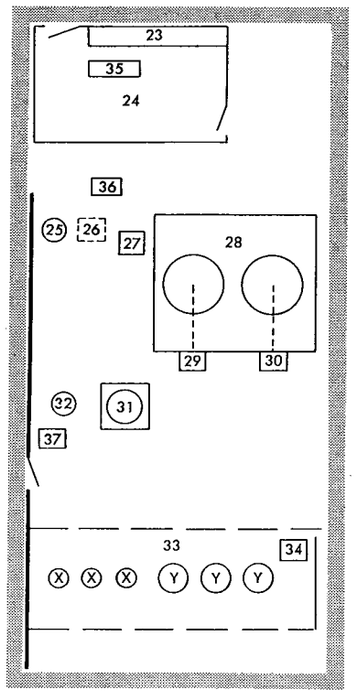

23	Control Panel
24	Sodium Service Building
25	Main Secondary Pump Motor
26	Secondary Fill and Drain EM Pump
27	Main Secondary Magnetic Brake
28	Main Airblast Heat Exchanger Fans
29	Airblast Fan Motor
30	Airblast Fan Motor
31	Auxiliary Airblast Heat Exchanger Fans
32	Auxiliary Secondary Pump Motor
33	Transformer Pad
34	5 KV Load Breaker
35	Sodium Service Panel
36	Main Secondary Cold Trap Panel
37	Auxiliary Secondary Panel
XXX	Three 100 KVA 4160/240V Transformers
YYY	Three 333 KVA 4160/480V Transformers

FIG. 6–37(c). Secondary area.

REFERENCES

1. *Boiler and Pressure Vessel Code.* New York: The American Society of Mechanical Engineers.

2. R. S. BAKER, *Calculation of Developed Pressure and Fluid Power in Linear Poly-Phase Induction Liquid Metal Pumps,* Mine Safety Appliance Corp., No. 48, 1956.

CHAPTER 7

INSTALLATION AND OPERATION OF SRE

7–1. SITE

The SRE facility is located in a small valley at the northwest edge of North American's Field Laboratory in the Santa Susana Mountains, approximately 30 miles northwest of downtown Los Angeles, California. The area was selected because of desirable drainage control, remoteness from other activities, and feasibility of extending existing utilities to the new construction. Meteorological studies also indicated that in case of accident the radius of fallout of the airborne contaminate would probably be confined to uninhabited areas.

The valley in which the SRE is located is approximately 400 by 600 feet. This small area allows positive control of surface drainage. Drainage design was based on a storm intensity of "once in 50 years." The drainage system consists of perimeter trenches which carry the water to a small earth-fill holdup dam at the foot of the valley. This dam allows positive control of drainage water before release to the inhabited area which lies northwest of the site.

7–1.1 Buildings. The SRE building consists of three basic areas; the high-bay reactor area of approximately 5630 square feet, the low-bay operations and support area of approximately 7990 square feet on two floors, and the hot-cell basement area of approximately 1520 square feet.

The structure, in general, is of permanent construction consisting of concrete basement, hot-cell and gallery areas, a structural steel superstructure, $5\frac{1}{2}$-inch thick tilt-up concrete exterior wall panels, a $2\frac{1}{2}$-inch thick poured gypsum roof with built-up roofing, and interior wood stud and plaster (or gypsum lath) partitions. A concrete block boiler house is contiguous on the south, and a similar concrete block structure houses the hot-cell ventilation equipment on the west.

High bay. The high bay contains the reactor and its associated galleries, fuel and moderator storage and cleaning area, hot-cell loading area, and the cask storage area. The total area is approximately 102 feet long by 46 feet wide by 50 feet high. Height of the structure was dictated by the length of the fuel-handling cask plus clearances for the 75-ton transfer

crane which serves the entire area. Width was dictated by the necessity for sufficient clearance and access to the galleries of the primary system. Framing in this area is structural steel bents with separate column supports for the 75-ton crane. All column footings are carried to bedrock to minimize differential settlement. The floors are 8-inch thick reinforced concrete, with the exception of the area immediately adjacent to the reactor, and are designed for heavy truck loadings. Truck access to the high-bay area is through a 16 by 20 foot sliding door on the north wall of the building. Illumination consists of color-corrected mercury vapor lights.

Low bay. The low-bay area contains offices, emergency power battery system, and the heat and vent room on the mezzanine floor. Control room, electrical equipment room, instrument storage and maintenance room, change room, and lavatories occupy the first floor. Mezzanine construction is wood frame with the exception of the battery room and heat and vent room, which are provided with open-web steel joints and a 2-inch thick poured concrete floor.

Hot cells. The hot-cell area is located in a 21-foot deep basement in the west portion of the high-bay area. Operating philosophy dictated the location of the cells relative to main floor level. Fuel elements may be drawn up into the fuel-handling cask and discharged directly into the top of the hot cells. The area contains the hot cells, operating area, service area, and a change room. Cell configuration is in two portions, the primary cell and the metallurgical cell. Specifications of construction related to radiological shielding are detailed in Section 6–3. Entry to the cells is by shield doors on the service area side.

Electrical equipment room. The electrical equipment room contains the 480-volt distribution board, 480-volt emergency switchgear, 480-volt normal switchgear, 240-volt distribution switchgear, 240-volt heater panels, 480-volt heater panels for the air-blast heat exchanger, emergency control panels, M-G set and control for main air-blast fans, M-G sets for primary and secondary pumps, control panels for auxiliary pumps and auxiliary air-blast fan, two M-G sets for battery charging and emergency power, and lighting transformers and panels. The various electrical panels are connected with the other areas and outdoor equipment by means of underground transite conduits, which lead into the service trenches of the electrical room. The transite conduit was laid in runs on a prepoured concrete base. After the runs had been laid the conduit was encased in concrete.

Fire protection. Fire protection is provided in the control room by a one-shot CO_2 system. All instrumentation leads are fed by conduits in open trenches from the reactor area to the control room panelboards. Windows in the control room allow the operator to observe the entire high-bay reactor area.

7–1.2 Utilities. *Water supply.* Water supply is a deep well located approximately 2000 feet east of the site. A 4-inch line carries water from the well to a 50,000-gallon storage tank located on a hill approximately 125 feet above the floor of the SRE building. A 4-inch line from the tank provides water distribution to the complex. The tank also serves two 2000 gpm fire pumps, which in turn feed an 8-inch main, providing distribution to five fire hydrants in the area. Supply to the tank is controlled by a single pole float which starts and stops the well pump. As a safety measure a 10-inch bypass line around the well connects the SRE to the main loop of the Propulsion Field Laboratory providing a million-gallon storage. The system requires water from the main loop only if the well is unable to furnish an adequate supply.

Sewage. Domestic sewage is handled by a septic tank and leach field system. Drainage from the hot-cell area is carried to a sump where, as a precautionary measure, it is monitored before release to the domestic sewage system. Industrial radioactive wastes are pumped directly to liquid holdup tanks for decay in the waste disposal area.

Substation power. Power is provided from a substation on the site, whose capacity is 1000 kva at 4160/480 volts and 300 kva at 4160/240 volts. This power is taken from a commercial station approximately 1 mile east of the site. A second substation at the site has a capacity of 300 kva at 4160/120-208 and 600 kva at 4160/480 volts.

7–2. Steam Electric Facilities

The steam plant is an outdoor installation consisting of a 7500-kw turbine generator, supplied with steam from a once-through, liquid-metal to water steam generator. A plant capacity slightly in excess of the rated reactor output was selected in order to benefit by the economic and delivery time advantages of purchasing standard equipment, and to provide for any possible increase in reactor output resulting from experimentation or design margins in the reactor and its appurtenant equipment.

The turbine generator is of the package type, mounted on and supported by a 7000-square foot two-pass surface condenser, and is complete with air cooler, oil cooler, and throttle valve. The steam conditions at the throttle are 600 psig and 825°F. Two stages of extraction are utilized; one in a Cockrane tray type deaerating heater, and the second in a closed feedwater heater.

The steam generator receives nonradioactive sodium at 900°F and returns it at 440°F. Constant steam temperature is achieved by means of an attemperator.

A steam bypass, which discharges directly into the condenser, has been provided around the turbine to facilitate stabilizing steam conditions

with the reactor prior to admitting steam to the turbine. Twin mixed-bed demineralizers, each with a polishing capacity equal to 30 percent of the full condensate flow have been provided to ensure a high purity of water to the steam generator. An induced-draft cooling tower supplies cooling water to the condenser.

The electric power-producing facilities of the sodium reactor experiment contain many standard components which will not be detailed in this description. There are three areas of components which are unique to this system installation and differ from components which might be found in any conventional fossil-fuel fired electric power-producing steam plant of this capacity: the steam generator, the water conditioning plant, and the interconnections between the reactor and the steam plant.

7–2.1 Steam generator (Fig. 7–1). The steam generator is a liquid-sodium to water, once-through type heat exchanger with a mercury monitoring system. The generator is a U-tube unit with sodium flowing on the shell side and water flowing on the tube side. The tubes are double-walled, with mercury in the annular space between the inner and outer tubes. Tube dimensions are as follows:

Straight tubes: Outer tube—$\frac{11}{16}$-inch OD by 0.054-inch wall thickness
Inside tube—$\frac{1}{2}$-inch OD by 0.050-inch wall thickness

At the U-bends: Outer tube—$\frac{7}{8}$-inch OD by 0.069-inch wall thickness
Inside tube—$\frac{1}{2}$-inch OD by 0.050-inch wall thickness

The increased diameter at the U-bend is to accommodate differential

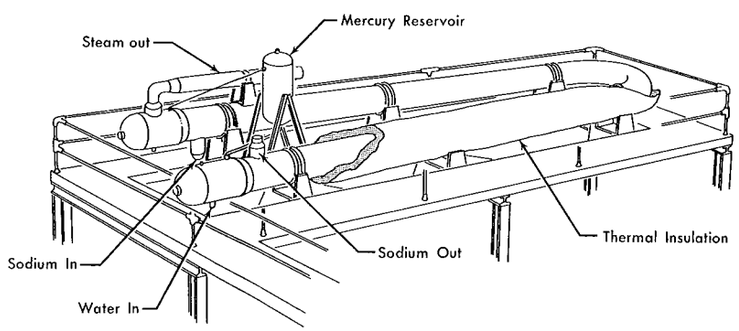

FIG. 7–1. SRE steam generator.

expansion. Tubes are spaced in a triangular pattern $1\frac{1}{8}$ inch center to center. The centerline length of the steam generator is 86 feet, with a shell diameter of 19 inches. The entire assembly is constructed of Type 304 stainless steel.

In the event of tube failure, provisions have been made to identify the faulty tube prior to removing the heat-exchanger heads. If an outer tube failure is suspected (a description of the monitoring system is included later in this section), positive determination and tube identification can be made after draining and cooling by pressurizing the shell side with helium gas and then sniffing with a probe inserted through the removable plugs around the tube-sheet periphery. Each hole is indexed with a definite row of tubes. If an inner tube failure is suspected similar investigation can be made at the outer tube sheet through a $4\frac{1}{2}$-inch removable plug in the heat-exchanger head.

The steam generator is designed to remove 30 Mw of heat from the reactor under either of the conditions given in Table 7–1. While the reactor heat removal rate will be nominally 20 Mw, the steam generator has been designed for 30 Mw of reactor heat to provide for possible greater heat removal rates in the course of the experimental program.

Attemperator. To limit steam temperature during normal operation to 825°F, a spray type attemperator is installed in the outlet steam piping. Boiler feedwater is introduced into the steam via a venturi section within the attemperator. The attemperator will maintain 825°F steam temperature under Condition A (Table 7–1), ranging from the estimated 30-Mw maximum heat load output of the reactor down to a minimum of 2 Mw. In addition, it is designed to maintain 825°F steam temperature when operating at the higher sodium temperature conditions under Condition B

TABLE 7–1

OPERATING CONDITIONS

	Condition A*	Condition B†
Heat load (max. 30 Mw)	102.39×10^6 Btu/hr	102.39×10^6 Btu/hr
Sodium inlet temperature	900°F	1140°F
Sodium outlet temperature	440°F	670°F
Steam pressure at attemperator outlet	600 psig	600 psig
Steam temperature	825°F	825°F
Feedwater temperature	297°F	297°F

* Planned sodium temperatures for initial operation.
† Higher sodium temperatures which may be used experimentally at a later date.

TABLE 7–2

OPERATING CONDITION (30-MW LOAD FOR 297°F FEEDWATER)

	Condition C	Condition D
Heat load	102.39×10^6 Btu/hr	102.39×10^6 Btu/hr
Sodium inlet temperature	900°F	1140°F
Sodium outlet temperature	440°F	670°F
Steam generator output	88,700 lb stm/hr	77,700 lb stm/hr
Attemperator output	0	11,000 lb stm/hr
Total steam output	88,700 lb stm/hr	88,700 lb stm/hr
Steam temperature maintained at turbine inlet	825°F	825°F

throughout the entire load range. The amount of attemperation and output of the steam generator at 30-Mw load for 297°F feedwater is given in Table 7–2.

The pressure drop through the steam side of the generator when producing 88,700 pounds of steam per hour at 620 psia and 825°F is estimated to be 52 psi. The pressure drop through the steam side of the attemperator will not exceed 6.5 psi under any conditions. The amount of attemperation is controlled by the flow of feedwater through an air-operated valve located at the ground level below the steam generator. This valve may be controlled manually or automatically from the control house. Two safety valves are mounted on the attemperator housing above the steam generator. The total relieving capacity of these valves is greater than the maximum steam generator output; note Table 7–2.

Hot-water preheating system. Since sodium solidifies at 208°F, it is essential that the steam generator be preheated before filling with sodium. Heating is required also to maintain sodium temperature well above 208°F during brief shutdown periods or when draining of the system may be necessary. An electrically heated hot-water recirculation system has been provided for this purpose. Since liquid sodium will be introduced at 350°F, the preheating system has been designed for this temperature.

An expansion tank with vent and gas supply provides a nitrogen pressure of 165 psig to the preheat loop to permit raising the water temperature to 350°F without steaming. It consists of an expansion tank approximately 12 inches in diameter and 2 feet 7 inches high, connected at the bottom directly to the preheating loop and at the top to a vent valve outlet and the inert gas supply. The nitrogen pressure on the tank is adjusted through a pressure regulating valve.

The heater for the hot-water preheating system consists of a 6-inch diameter pipe 7 feet $5\frac{1}{4}$ inches long. The assembly is mounted vertically with electrical-resistance type heaters attached to the bottom flange. Water is brought in through a side connection at the top and moves downward to the discharge at the bottom flange of the assembly. The heater is rated at 75 kw and is equipped with a selector switch for either a partial output of 25 kw or the full output of 75 kw.

Monitoring system. A monitoring system is utilized to detect leaks within the steam generator. Mercury fills the space between the inner and outer tube, providing a barrier between the sodium on the shell side and water on the tube side. The mercury annulus is pressurized by a nitrogen source at 190 psia under Condition C and 450 psia under Condition D (Table 7–2). This mercury pressure is intermediate to the water side pressure of 620 psia and sodium side pressure of 35 psia. Under all steady-state operating conditions, a tube leak between the water side and the annulus will be detected by a pressure rise, while a leak between the sodium side and the annulus will result in a pressure drop. The annulus pressure is recorded and is equipped with high- and low-pressure alarms. A cutaway illustrating the mercury barrier is shown in Fig. 7–2.

Supplementing this pressure monitoring device, a sight-level gauge glass is provided on the mercury expansion tank and, in addition, a mercury vapor detector continuously monitors the exhaust of the steam jet air ejectors. Five tons of mercury are used in this system. An expansion tank located above the steam generator and connected to the nitrogen gas supply provides reservoir and pressure medium for the monitoring fluid.

The once-through, liquid-sodium to water steam generator is, to the best

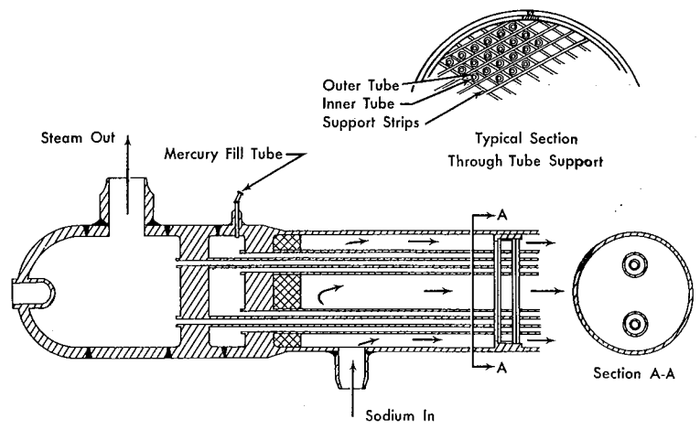

FIG. 7–2. Simplified section of SRE steam generator.

of our knowledge, the first of its kind to be placed in operation in this country. Since a knowledge of thermal distribution is desirable, 70 thermocouples have been located throughout the generator shell. Since initial operation, an additional 25 thermocouples have been added to the water inlet and steam outlet heads. A 126-point monitor recorder is located in the control house for recording these temperatures, as well as sodium supply and return line temperatures.

Main steam bypass. A main steam bypass provides a means for building up and stabilizing steam conditions with the reactor, prior to opening the turbine throttle valve. This is accomplished by directing the steam through a pressure-reducing desuperheater and discharging into the condenser.

During the startup procedure, water at a temperature of 350°F is circulated through the hot-water preheating system (see above). Following this first operation, as sodium and steam temperatures are increased, steam is directed into the main steam bypass. When approximately 3 Mw of heat is diverted in this manner, the turbine throttle valve is opened and the heat load is shifted to the turbine.

The main steam bypass can also act as a stabilizer should it become necessary to suddenly shut the turbine valve; up to a maximum of 4 Mw of heat energy may be diverted through the main steam bypass, thus permitting reactor setback operation in place of a scram operation.

7–2.2 Water conditioning. *Water preparation plant.* Since the steam generator is the once-through type, where water is heated and evaporated to complete dryness while passing through the unit, solids may either deposit on the heating surfaces or carry over and form sludge on the turbine blades. The equipment manufacturer has recommended that the following feedwater conditions be maintained:

pH	9.5 to 9.6
Fe	0.01 ppm
Cl	0.10 ppm
Solids	0.5 ppm (maximum)
O_2	less than 0.005 ppm

In order to supply high quality makeup water and to maintain the total solids in the feedwater within the prescribed limits, a water conditioning plant has been installed. The water for the experimental station is drawn from several deep wells and although these well waters are quite clear and practically colorless, they contain appreciable amounts of dissolved mineral matter. The total hardnesses range from 16.5 to 25 gpg and total solids range from about 28 to 29 gpg. Because of this high solid content, it was decided to demineralize both the makeup water and the water used to rinse the mixed-bed demineralizers after regeneration.

Since these raw waters have from 13 to 21 gpg of bicarbonate hardness, it was deemed prudent to remove the carbon dioxide (formed from the bicarbonate in the demineralization process) mechanically instead of chemically, in order to lower the operating costs. Therefore, a hydrogen cation exchanger was installed for the first stage of the demineralization process so as to remove about two-thirds of the cations and furnish a mixed effluent which is neutral or slightly acid. This effluent is degasified in a vacuum degasifier and then passed through a mixed-bed demineralizing unit (Fig. 7–3).

An automatic pushbutton filter 30 inches in diameter and 5 feet high is installed before the hydrogen cation exchanger. This pressure filter contains crushed and graded anthracite as the filter medium. The flow of 15 gpm is at a rate of 3 gpm/ft^2, and removal of the occasional traces of turbidity encountered is accomplished without the aid of a coagulant.

A single unit hydrogen cation exchanger of the pressure type, 30 inches in diameter and 9 feet high, is employed. It is rubber-lined and contains a bed of cation resins 55 inches in depth. Clear, filtered water is separated into two streams, so that $\frac{2}{3}$ of the water passes through the hydrogen cation exchanger and $\frac{1}{3}$ is bypassed around the exchanger to be mixed with its effluent. The bicarbonate in the bypassed $\frac{1}{3}$ thus neutralizes the acids in the hydrogen cation-exchanger effluent. For the most economical operating conditions in the mixed-bed demineralizers, the water should be neutral or slightly acid.

The neutralized water is next passed downward through the vacuum degasifier (1 foot in diameter by 21 inches high), which is mounted on a

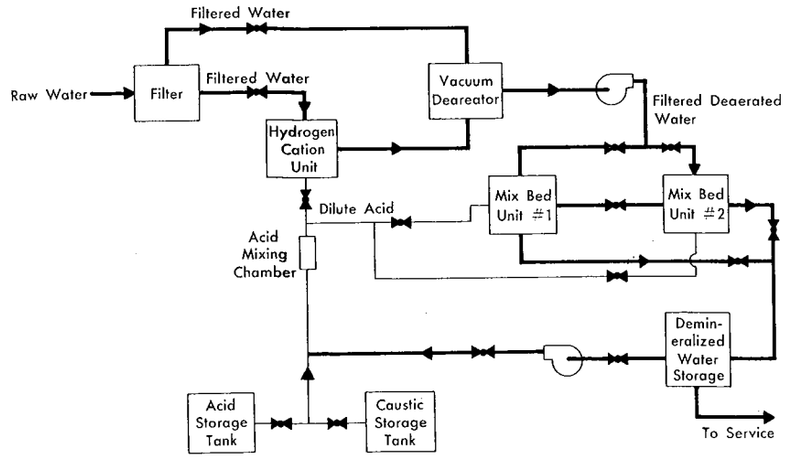

FIG. 7–3. SRE water-conditioning system flow diagram.

rubber-liner and packed with Raschig rings. A vacuum pump exhausts the liberated carbon dioxide to the atmosphere. The degasified water is refiltered and then demineralized in passing through the mixed-bed units to the 15,000-gallon storage tank. The refiltering is done in twin filters, made up of honeycomb fiber filter tubes in stainless-steel shells. Each will handle full rated flow.

A portion of the condensate from the condensate pump discharge may be polished through the mixed-bed units and returned to the condenser or, by proper valving, the mixed-bed unit can be placed in series with the feedwater line for initial operation on low loads. The design capacity of the polishing system is 50 gpm which is equivalent to 50 percent of condensate flow at rated reactor plant output of 6000 kw.

The mixed-bed demineralizers are of the pushbutton automatic type, and the rubber-lined shells are 42 inches in diameter by 6 feet high. Each unit has a normal design flow rate of 58 gpm; they are operated in parallel. The operation of the two units is staggered so that only one unit at a time requires regeneration. During a regenerating period, the mixed-bed unit in service will handle a total flow as high as 65 gpm: 50 gpm for polishing condensate and 15 gpm makeup to storage, if required. An electrical signal informs the operator when a mixed-bed unit run needs regeneration, and at the push of a button all the operations of separating the cation and anion resins, regenerating and rinsing the separated beds, mixing them, and returning the unit to service are done automatically.

A controlled backwash which lifts the lighter granules of the anion exchanger above the heavier cation exchangers separates the beds, and leaves the anion resin bed on top of a bed of cation resins. The cation exchanger is regenerated with a sulfuric-acid solution and the anion exchanger with a caustic-soda solution. The soluble by-products are then rinsed to waste. The resins are mixed by blowing air up through them, after which any air above the bed is displaced by water and the unit is automatically returned to service. Since only one of the two mixed-bed units is regenerated at a time and either can carry full load, the condensate polishing service is uninterrupted. When the single hydrogen cation unit is regenerated, the 15,000-gallon storage tank floating on the line is ample for this and all other normal demineralized water requirements.

An extremely high degree of demineralization is obtained. Mixed-bed demineralizers were chosen because of their ability to demineralize water more effectively than any other type of equipment. This is due to the fact that the mixed-bed demineralizers offer the advantages of series operation of a battery consisting of an exceedingly large number of alternating hydrogen cation and strongly basic anion-exchanger granules.

The capacity of each mixed-bed unit is 8900 gallons of pretreated well water between regenerations, therefore the gross plant capacity is 17,800 gallons. Since each mixed-bed demineralizer requires 4600 gallons of demineralized water per regeneration, the water plant produces a total net output of 8600 gallons.

Chemical treatment of feedwater. The steam generator imposes critical and difficult limits on any chemical treatment program. Two factors are of prime importance: (1) since the unit is essentially a once-through operation, total dissolved solids in the feedwater must be at an absolute minimum, and (2) since the unit is of stainless-steel construction, it is generally agreed that chlorides and oxygen content must be held to very low values. In view of the total dissolved solids limitation, it is obvious that chemical treatment must contribute no dissolved solids to the feedwater. On this basis, experience dictated the use of hydrazine as an oxygen scavenger and morpholine as an agent to elevate pH. The hydrazine and morpholine are fed, together, into the deaerator discharge.

Suitable conductivity equipment provides a high degree of monitoring to detect inleakage of solids due to condenser leakage, poor quality makeup, or other improper conditions. A great deal of effort is being expended in setting up and maintaining an intensive analytical program that will provide a large accumulation of data. The station is equipped with a small but complete chemical laboratory for water control analysis.

7–2.3 Interconnections between reactor and steam plant. A low-pressure switch is activated if the steam plant loses feedwater pressure, and in turn actuates an alarm on the annunciator panel of the reactor control board. If pressure is not regained within 8 seconds, a time-delay relay automatically shuts down the reactor.

The SRE sodium flowmeter, which records the proportionate sodium flow to the steam generator, is interconnected with the steam-plant control board.

The following steam-plant operational information is displayed in the SRE control room:

Kilowatt output (indicating).
Steam pressure (indicating).
Feedwater flow (indicating).
Sodium temperature at outlet of steam generator.
Indicating lights showing position of sodium valves in the piping to the steam generator.
Alarm from low feedwater pressure, in conjunction with scram signal.
Alarm from high or low sodium temperature at outlet of steam generator.
Alarm from turbine throttle valve trip.
Alarm from high or low pressure of monitoring fluid in the steam generator.

The following SRE information is displayed in the steam-station control room:

Neutron flux level (expressed in percent power).
Alarm from reactor scram.
Alarm from reactor setback.
Sodium temperatures (from steam-plant measuring devices).
Temperature at steam-generator inlet, indicated and recorded.
Temperature at steam-generator outlet, indicated and recorded, with high- and low-temperature alarms broadcast on the annunciator panel.

7–3. Reactor Operation

7–3.1 Operating philosophy. The SRE, although designed and built as an experimental reactor to permit the evaluation of graphite as a moderator and sodium as a coolant, is of most interest to the general public as an integral plant capable of producing electricity. Much of the design and initial operating philosophy was conservative, based upon the premise that this was a new reactor concept. This is reflected, for example, in the provision of a separate heat-transfer loop capable of removing after-glow heat following a full-power scram (5 percent of full power output), and in the fast drive rate of the regulating motion on the control rods (3.75 ft/min). It is significant to note after brief operating experience that the stability and ease of operation of this reactor concept make it unnecessary to have a fast control rod drive to correct for transients, and that after-glow heat is adequately dissipated by convection flow in the main primary loop.

Low-enrichment metallic uranium fuel was used for the first loading in an effort to minimize fuel cost, increase stability of the reactor, and reduce heat flux density. The latter permits lower operating pressures by requiring less coolant flow to be forced past a given unit of core area. Use of this fuel also imposes some operating restrictions. Alpha-rolled, beta heat-treated uranium has temperature limitations, since the alpha-to-beta phase transition (1235°F) imposes serious distortions on the fuel elements. The large amounts of fuel required make it desirable from a fabrication standpoint to form the fuel into larger elements (for the SRE, each fuel slug is $\frac{3}{4}$ inch in diameter by 6 inches long). From a heat release point of view, the larger diameter configuration increases the ratio of center-temperature to surface-temperature, since the transfer of heat to the coolant can take place only at the surface. From this is obtained an operational requirement to maintain the coolant stream at sufficiently low temperatures to retain fuel center-temperatures below 1200°F.

The unique characteristics of graphite and sodium make it possible to

operate with coolant temperatures up to 1000°F for use in production of high-quality steam. The characteristics of sodium facilitate heat transfer between primary (radioactive) and secondary (nonradioactive) sodium in the intermediate heat exchanger, and from secondary sodium to steam production in the steam generator, with modest size equipment and small temperature drops from one loop to the next. These characteristics also permit the reactor and heat-transfer loops to be operated at low pressures (the gas blanket over the sodium plenum above the reactor core is maintained at 3 psi).

An operating requirement, to maintain the oxygen concentration of sodium as low as possible (<10 ppm, Section 4–1), stems from the zirconium moderator cladding. When the oxide content of the sodium is determined (by plugging meter measurements) to be excessive, cold traps and hot traps are employed.

Sodium has a low neutron absorption cross section by comparison with other suitable liquid metals, but under the fluxes imposed on sodium in the SRE core, the primary sodium reaches a saturation of 0.3 curie/gram. Consequently, operating personnel cannot enter the primary pipe galleries until the activity has been removed by draining the sodium from the system, and sufficient decay of residual sodium activity has occurred. If there has been no mass transfer (no appreciable amount has been detected to date), entrance to the gallery can be made after 14 days of decay from saturation activity, provided the loops are drained to the fill tank.

There is considerable advantage in utilizing the high heat-transfer capacity of sodium and high-temperature systems, but the distribution and rates of change of temperatures in relation to resultant stresses must be taken into account in order to minimize the possibility of such stresses. From the experience and data gained in this area by operating the SRE, future reactors can be designed without critical focal points for thermal stresses.

7–3.2 Operating parameters. *Over-all parameters.* The SRE has a thermal power rating of 20 Mw and produces 6 Mw of electrical energy, giving an over-all efficiency of 30 percent at full power.

Heat-transfer loop parameters. Primary sodium enters the core at 500°F, circulates up through the core at rates up to 1080 gpm, and leaves at 950°F. It is cooled in passing through the tube side of the intermediate heat exchanger.

Secondary sodium circulates at rates up to 1080 gpm, picks up heat from the primary sodium by entering the shell of the intermediate heat exchanger at 440°F, and leaves at 900°F. It enters the shell of the once-through steam generator at 900°F and exits at 440°F, liberating heat energy in generating superheated steam. Feedwater flowing at 60,200 lb/hr

enters the tube side at 285°F and steam leaves at 825°F and 600 psi, having 335°F superheat.

To develop a sodium flow rate of 1080 gpm in the heat-transfer loops, the centrifugal pumps operate at 1000 rpm. Hydraulic balancing of the pump impellers provides a sodium pressure against the shaft freeze seal that is almost independent of pump speed and discharge pressure. This feature makes it easy to maintain a positive seal between the stationary seal body and the rotating shaft. Figure 7–4 shows discharge pressure versus pump speed, and seal pressure versus pump speed.

The primary pump speed control is manual and pump speeds can be increased or decreased at rates up to 200 rpm/min. The secondary pump can be operated manually in a like manner, or can be "slaved" to follow the primary pump speed.

Electromagnetic eddy-current brakes in the main primary and main secondary sodium loops, by adding varying amounts of impedance, permit control of the flow at any rate for any pump speed; by imposing a current

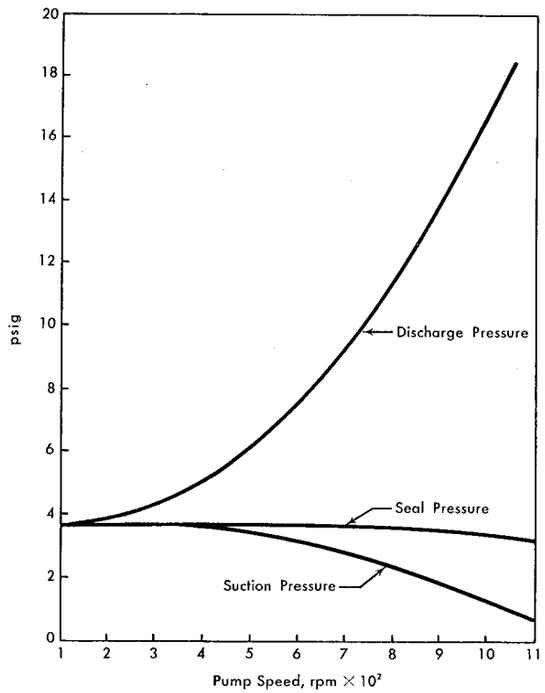

FIG. 7–4. Main primary pump pressure versus rpm.

of 23 amperes to the brake, the flow can be reduced from 100 to 18 percent in 5 seconds with the pump running at 1000 rpm. If the pump motors are de-energized simultaneously with the application of the current to the brake, the flow will be reduced to 0.5 percent in 4 seconds. Figure 7–5 shows the effect of the brakes on sodium flow for the simultaneous action.

7–3.3 Operating procedures. Prior to operating a power reactor, as in any other power plant, it is necessary to establish a fuel inventory. The fuel supply for a projected operating period is loaded into the reactor core at the beginning of the period and the rate of usage determined by operating level. After a predetermined depletion, any number or all of the fuel elements may be replaced without losing the inert gas atmosphere of the reactor tank. Details of fuel handling are described in Section 6–3.

Startup. With sodium in the heat-transfer loops circulating at 350°F isothermal, and with the fuel loading complete, the reactor complex is ready to operate. The sequence of operations in startup of a reactor electric plant is very similar to the startup of a fossil-fuel-fired boiler plant. The heat source is activated, heat is transferred, steam is generated, the turbine is rolled, and the electric generator is put on the line. The startup procedure for the SRE is governed not only by the necessity of high-quality steam for the turbine, but also by the capacity of the condenser to handle

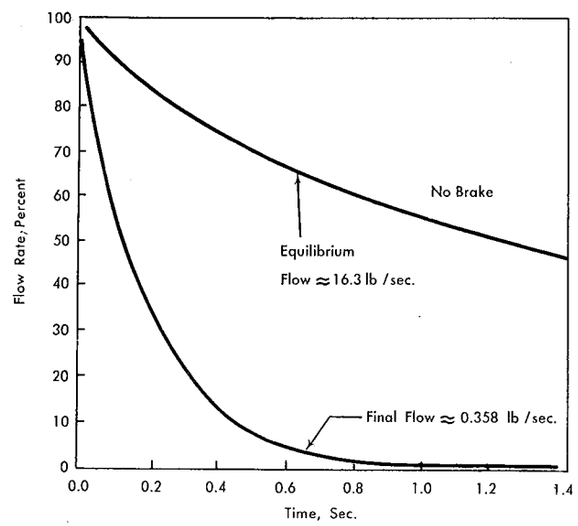

FIG. 7–5. Primary system flow decay (assumes no contribution from pump rotor after $t = 0$; also assumes instantaneous application of 20-ampere coil current to eddy-current brake).

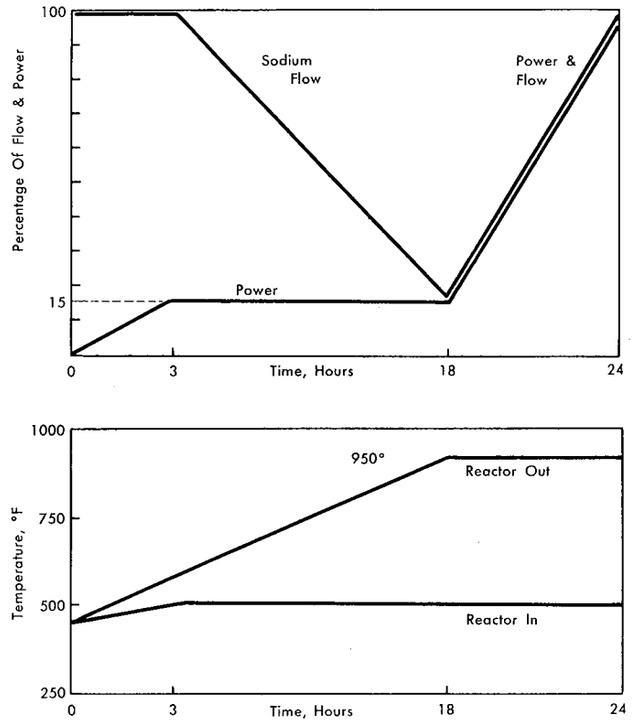

FIG. 7–6. Typical cold-start procedure for the SRE.

no more than 15 percent of rated plant steam capacity. On this basis, the typical cold startup procedure is as follows (Fig. 7–6):

Check all "interlocks satisfied" circuits.
Establish 100 percent sodium flow.
Increase reactor power to establish 500°F isothermal (as near as possible) conditions in the primary and secondary loops.
Increase reactor power to 15 percent, maintaining reactor inlet at 500°F.
Reduce sodium flow to establish full temperature gradient across the reactor.
Raise reactor power and flow together to maintain full temperature gradient until full power is reached.

Following a scram from full temperature gradient, the gradient can be held by utilizing the eddy-current brakes in the main heat-transfer loops.

Under these conditions, a restart can be effected much more readily than a cold start by proceeding in the following manner:

With the eddy-current brakes set, raise pump speed to 25 percent.
Raise reactor power. The eddy-current brake control will increase flow to maintain the temperature gradient.
Raise pump speed and reactor power together to maintain reactor temperature gradient up to full power.

Steady-state operation. The control system for the SRE electric plant complex was designed for, and limits operation to, a load forcing procedure. On this basis, the steady-state operation of the reactor is comprised of neutron regulation. Interlock circuits protect the reactor and steam plant in the event the steam-electric plant cannot follow the reactor, but the responsibility for following reactor power fluctuations lies in the steam-plant control system.

Steady-state neutron regulation can be easily maintained by manipulation of a rod control switch. The rod is withdrawn approximately 1.5 inches per day, with fractional adjustments made every hour. Automatic controls for this purpose require only 2 minutes' operation in 17 hours, as measured by timing devices, to maintain the reactor at steady-state power conditions.

Shutdown. Shutdown of the reactor may be effected by planned manual programming, i.e., driving in the control rods, and following the decrease in power with flow decreases to program the temperature decrease desired. It may also be initiated by any one of five scram contacts in the automatic emergency shutdown control system. In this case the flow programming automatically maintains constant inlet temperature to the reactor. The sources of scram initiation and their set points are given in Table 7–3.

TABLE 7–3

SCRAM INITIATION SOURCE AND SET POINTS

Conditions	Scram set points
Short reactor period	<5 seconds
High reactor power	>125% full power
High fuel-channel temperature	110% of full temperature at full power
Abnormal sodium flow in the heat-transfer systems	±15% deviation from control setting
Loss of feedwater through steam generator	<600 psi feedwater pressure

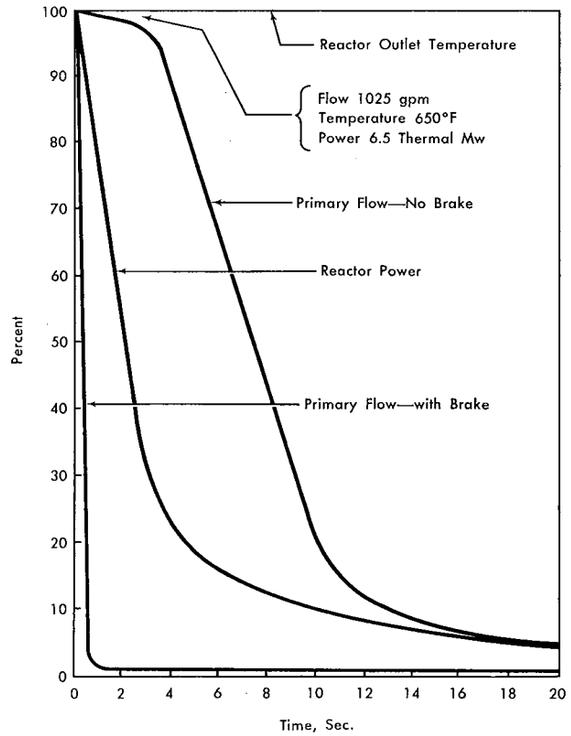

FIG. 7–7. Post-scram sodium flow from 150°F ΔT.

Upon receipt of a scram signal, the automatic control system will release the safety rods, remove power to the sodium pumps, activate the eddy-current brakes in the main primary and main secondary heat-transfer loops, and maintain temperatures throughout the reactor and heat-transfer systems. If the fuel-channel outlet temperatures go above or below preset values, the eddy-current brakes will establish an appropriate flow. Figure 7–7 shows post-scram parameters.

7–3.4 Engineering evaluation. Operating experience with the SRE has in general verified the design concepts and validated the designed parameters. Some of the equipment was modified or replaced after the initial startup, as discussed in Section 7–4, following.

Experience and observations. A comparison of calculated and measured number of fuel elements for dry and wet criticality follows:

	Dry	*Wet*
Measured	22.2	32.7
Calculated	21.1	28.4

The close comparison of calculated to measured values for dry criticality are encouraging, but a single set of data cannot be considered to validate the two-group calculation methods employed, especially since they are recognized to be only accurate to 20 percent.

The fabrication and accurate location of multiple moderator cans used in the SRE has proved to be feasible. Orientation and alignment of 119 cans was such that the largest deviation between fuel element centers in the cans and fuel shield plugs in the loading face, some 20 feet above, was $\frac{1}{16}$ inch, making fuel alignment during reactor loading very easy.

Mechanical, centrifugal impeller pumps, with frozen sodium seals to isolate the pump casing, provide a feasible method of circulating sodium in the reactor heat-transfer systems. Properly hydraulically balanced pumps of this type have operated in the SRE systems for many thousands of hours with only the slightest indication of small sliverlike extrusions past the rotating shaft freeze seals. Prior to proper hydraulic balancing, some of these seals had failed. To maintain a free-turning shaft seal under fluctuating pressure conditions is difficult, but this condition is rarely evident when the reactor is at power.

Sodium is an effective heat-transfer fluid because of its physical properties. Properly handled, it poses no pronounced operational problems. Two hundred barrels of sodium have been melted, transferred, and circulated for well over a year in the SRE systems. One pint of sodium that was lost from one of the 200 barrels at the melt station dripped into a catch pan containing vermiculite and no fire was observed.

There has been no indication of leakage from pipes or vessels. It has been difficult, however, to re-establish flow in some small service lines (less than 2 inches in diameter) in which sodium was allowed to stagnate at a temperature below that of the bulk sodium flowing in the intersecting main lines. Thermal expansion, resulting from raising the temperature of sodium between two solid plugs in a small line, has ruptured bellows on bellows-seal valves. One such rupture permitted more than 1 gallon of sodium to be lost in the pipe gallery, but because of the inert gas atmosphere in the gallery (less than 1 percent oxygen in nitrogen), only a slight amount of slow oxidation took place, with no indications of fire. Piping systems have been simplified and the number of valves minimized in SRE sodium systems; this simplification is recommended for future sodium systems.

Some concern was expressed over the galling of control-rod drive ball-nut mechanism surfaces that was observed in component tests with con-

tinuous operation at elevated temperatures. However, since the control-rod drive mechanism operates only approximately 2 minutes in 17 hours to maintain constant power operation, the galling action observed in the tests would not result for 5 to 10 years of operation.

Reactor core temperature distribution. During the design stages it was recognized that minimizing temperature gradients was an area of concern in a high-temperature sodium system.

For initial power runs, fuel elements were installed with uniform orifices to provide a reference base. The radial temperature gradient was pronounced; temperature was high at the core center in accordance with the flux distribution curve. From data obtained during the first power run, orifice plates were resized to compensate for the power distribution, and two succeeding runs, one with a 130°F and one with 150°F gradient across the reactor, were made. Figure 7–8 shows the comparison of the radial temperature distribution under the three conditions. With the new

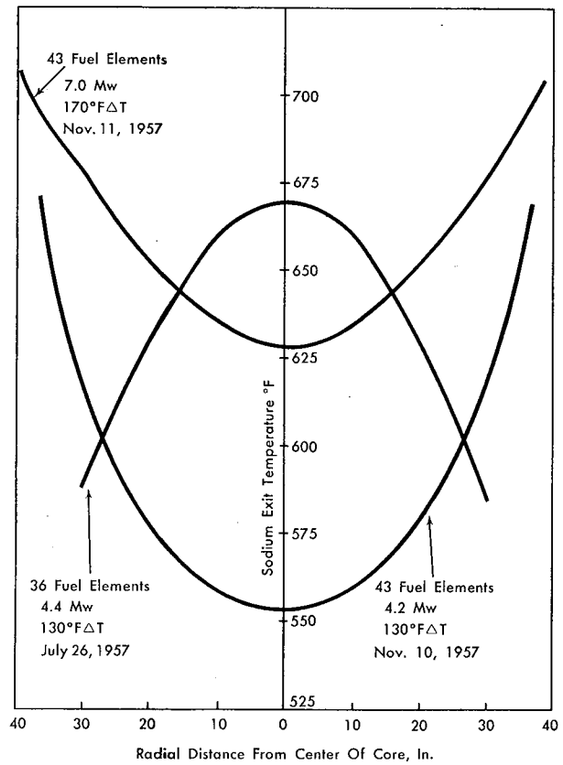

FIG. 7–8. Sodium output temperature versus radial distance.

orifice plates, the temperature is almost uniform across the diameter of the core as the reactor power is elevated.

Temperature profiles taken along the vertical surface of the moderator element sheaths indicated excess cooling of this surface, resulting in a pronounced temperature gradient at the top of the can. This condition was determined to originate with leakage past the grid plate from the fuel-channel coolant plenum. Installation of a bidirectional electromagnetic pump in the line to the moderator coolant plenum permitting control of coolant to the moderator cans, resulted in a more gradual temperature gradient at the top of the cans.

Systems analysis during the design of the reactor had predicted the possibility of excessive convection flow, and disclosed that the design features of the core tank outlet nozzle and the moderator can heads made them vulnerable to thermal stress. This was found to be a transient problem following scrams. It resulted from convection flow after the reactor power was removed, when cold sodium came in contact with surfaces still at elevated temperatures. Installation of eddy-current brakes in the main primary and main secondary loops reduces the flow of sodium when the reactor is scrammed to maintain the temperatures of the various parts of the system.

Intermediate heat-exchanger temperature distribution. Excess log mean temperature differences observed on the main intermediate heat exchanger during the first power runs reflected inefficiency of the unit and excessive thermal stresses at the tube sheets. Sixty thermocouples were installed along the length and around the girth of the heat-exchanger shell. The steady-state longitudinal temperature distribution along the shell is shown in Fig. 7–9. The temperature gradient is uniform along the straight legs of the exchanger and is practically zero around the bend, indicating no heat transfer through the bend section. Examination of heat-exchanger construction prints disclosed a wide gap between the tube bundle and the shell on the bend, and since this section is not baffled, the shell-side sodium bypasses the tubes.

Transient temperature data taken on the heat exchanger indicated very marked stratification. Following a scram from 135°F inlet-outlet difference on the heat exchanger, a 90°F gradient develops from top to bottom on the cross section of the shell leg. This stratification is shown by the temperature curves in Fig. 7–10.

No modifications to this heat exchanger were made, but the information gained is being used to develop improved sodium heat exchangers.

Reactor temperature coefficient of reactivity. The steady-state (over-all) temperature coefficient of reactivity has been demonstrated to decrease as the temperature is elevated; it is positive up to at least 750°F ($d\rho/dT = 8 \times 10^{-6}$/°F at 500°F and 2×10^{-6}/°F at 750°F). This factor provides a small net gain in reactivity and accompanying extension of operating

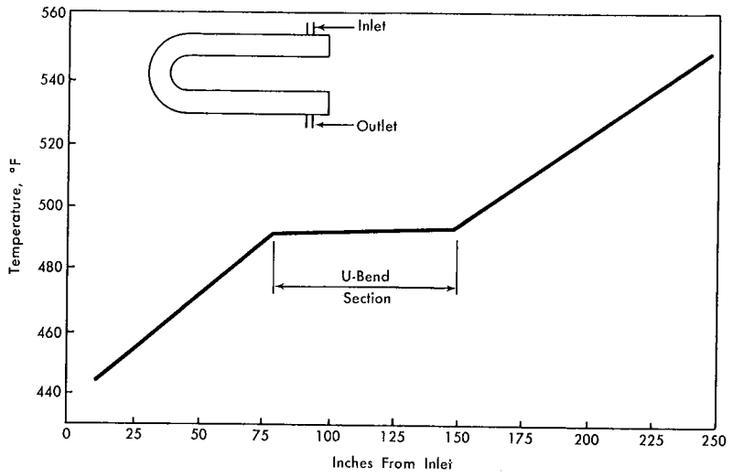

FIG. 7–9. Main intermediate heat-exchanger temperatures during steady-state operations.

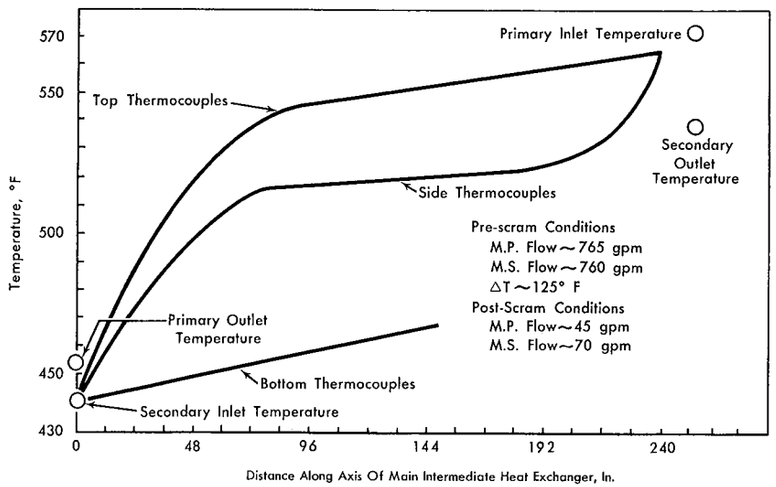

FIG. 7–10. Main intermediate heat-exchanger shell temperatures 18 minutes after scram (Nov. 20, 1957).

time. It involves no hazard, since the time constant associated with this coefficient is approximately 3 minutes. The fuel-temperature coefficient is negative and amounts to -7.1×10^{-6}/°F. The time constant associated with this coefficient is approximately 2 seconds; consequently the negative coefficient controls the reactivity on short-time temperature fluctuations. The strong, fast-acting negative coefficient, combined with the fact that the fuel temperature exceeds coolant temperature under power conditions, explains the observed extreme stability exhibited by the reactor during power runs.

7–4. PREOPERATIONAL TESTING

Preoperational (functional) testing of the components comprising the reactor, its service systems, and auxiliaries was started while the construction crews were still working on the installation of equipment. The most significant observations are tabulated by system or major component below. In general, the problems were those encountered in the startup of more common types of industrial plants; i.e., malfunction of hardware and electrical components.

7–4.1 Inert gas systems. Excessive leakage from joints and connectors was alleviated by isolating the leaks and repairing them. Foreign material in the pipes has caused malfunction (failure to seat) of some of the valves in these systems. No leakage is measurable from the reactor tank; however, a 1 ft^3/hr leak has been measured from the insulation cavity and from the thermal barrier cavities through the core cavity liner below floor level.

The nitrogen leakage rate from the galleries is 3 ft^3/min at 1 inch H_2O. The path of the major part of this flow is through the concrete walls, primarily adjacent to the gasket seal framework. Painting the concrete area adjacent to these channels with "scotch cast" reduced this leakage from 730 ft^3/min at the same pressures.

7–4.2 Tetralin systems. The system was filled and circulation started on January 14, 1957. Rework and repairs were made on numerous leaks at threaded pipe and sweat copper tubing joints. Foreign material in the pipes made cleaning the strainer chambers mandatory several times during initial operation of the system. It was necessary to replace the gasoline engine supplied for emergency pumping during power outage, and to install automatic controls to start the engine in the prescribed time limits. The system is currently functioning properly.

7–4.3 Sodium systems. Valve operators for sodium valves at the reactor floor level required rework to permit free operation. One valve in the main secondary fill and drain line would not seal tight enough for

helium and was replaced. The new valve and some others in similar installations do not currently make a tight seal against sodium. Consideration is being given to a freeze-off backup for these valves.

Binding of wear ring surfaces of the sodium pumps was observed. The tolerances were relieved by removal of 0.025 inch from the diameter of the wear ring. The main secondary pump was shimmed at the top flange to improve alignment.

Minor alterations to the electrical heaters on the piping permitted heating to temperatures above 350°F. Heaters were installed on the valve bodies to eliminate the possibility of freezing sodium in the valves.

7–4.4 Fuel-handling cask. Several modifications have been made to improve the operating characteristics of the cask. New gears and gear suspensions and heavier motors were installed on the grapple hoist drive. An improved cask-position indexing system was installed. Several circuit changes were made to improve integrity and function of the control system. The interlock drive mechanism and internal protection sleeve were modified to eliminate hangup.

7–4.5 Reactor. All moderator cans fit the close tolerances to which they were designed. Two were slightly damaged (scratched) during installation and were replaced. The original (Mark I) safety rods were replaced with an improved design (Mark II). A large number of reactor plugs were reduced slightly in diameter to improve clearances. Numerous changes in control circuitry have been effected.

7–4.6 Sodium instrumentation. *Sodium-level instrumentation.* The absolute accuracy of the sodium-level gauges is 1 to 4 percent, depending on the application and the tank in the SRE being measured. Performance of the main secondary expansion tank sodium-level gauge has been erratic; however, no defects have been detected in the components. Failures have been encountered in the connector to the reactor portable search coil.

High impedance grounds in signal leads to the sodium-level alarm coils have caused erratic operation of the sodium-level alarm system. This is being corrected by installing noninterlocking isolated meter relays. Precision sodium-level search coils with an accuracy of 1 percent have been fabricated for use as standards in calibrating the sodium-level instrumentation.

Sodium flowmeters. The Atomics International designed and fabricated magnetic flowmeters have performed satisfactorily. During initial filling of the sodium loops, the flowmeter indication was not representative of the pump speed. This was attributed to insufficient wetting of the walls of the flowmeter pipes; after wetting, satisfactory flow conditions were indicated.

The statistical noise recorded by the main primary and main secondary sodium flow recorders is approximately 3 percent of designed flow at full power.

All magnetic flowmeters on the 2-inch (and smaller) lines were removed after installation, and the magnetic flux was measured with a precision magnetic flux meter to establish calibration curves. Careless handling of the magnets during installation caused the flux to change as much as 25 percent.

Defective installation of the signal leads to the magnetic flowmeters has caused erratic operation in the flow recorders. The main sodium flow recorders were modified to provide thermal power integration and sodium flow off-normal scram circuits. Scales on the main primary and main secondary flow recorders were expanded.

Sodium-temperature instrumentation. Thermocouple wire and temperature readout instrumentation installed in the SRE was designed for an industrial application and has not provided the accuracy desired in the research and development program. The average accuracy of the sodium-temperature instrumentation is about 1 to 2 percent. This has presented a problem during the heat-balance performance tests.

Several iron-constantan thermocouples have been lost due to defective installation and corrosion in the exposed areas. Terminal junctions between the thermocouples and readout temperature indicators introduced errors in temperatures which have been eliminated by careful rework of conductors and junctions. Several bearing and freeze-seal thermocouples on the sodium pumps have been damaged and have required repair.

The temperature readout instrumentation has been modified to provide the following:

Thermal power integration.
Expanded temperature scales.
Scram, setback, and alarm contacts.
Range changes.
Up-scale and down-scale burnouts.

The bearing and freeze-seal and fuel-channel thermocouple scanners do not meet specifications and will not scan at the rate of 4 points per second. The bearing and freeze-seal scanner will be modified to reduce the scanning rate, and the fuel-channel scanner has been eliminated from the system.

Sodium leak detection. Although no sodium leaks in the tanks and piping have been encountered to date, many false alarms have been given by the sodium leak-detection instruments. This is attributed to shorts between the sodium leak tracings and the sodium piping, and to defective installation. This problem has also been encountered at other reactor installations that use sodium as a coolant.

Sodium-pressure instrumentation. Electrical sodium-pressure instrumentation has operated satisfactorily. Zero drift has been encountered with pneumatic sodium pressure instrumentation. The orifice on pneumatic pressure transmitters and pilot valves was redesigned to reduce zero drift in the main and auxiliary secondary sodium pump suction and discharge pressures. Filters were installed in all pneumatic air lines, and the air lines were all changed in secondary areas to reduce damage by corrosion and foreign materials. The main primary pump discharge pressure instrumentation was modified to provide high-pressure alarms.

7–4.7 Nuclear instrumentation. The nuclear instrumentation, which was modified extensively to adapt commercial instruments to the SRE reactor concept, has performed satisfactorily. Neutron flux distribution appears to be uniform at the instrument thimbles, and the neutron detectors have the sensitivity specified by the vendor. The reactor has not been operated at high power long enough to determine the effect of the neutron flux on the U^{235} fission chambers, nor to adjust the gamma compensating voltages on the ionization chamber. Double-shielded signal wire was required in all nuclear channels to improve the signal-to-noise ratio.

Count-rate channels. Period amplifiers in the count-rate channels, which were modified and used during the fuel-loading program, have proved to be ineffective because of neutron statistical noise, and they have been eliminated from the SRE safety system.

Linear amplifiers were modified for use with the count-rate meters and fission chambers. The count-rate meters were modified to adapt to the period amplifiers and count-rate recorder.

Lead shielding was installed on the fission chambers to improve neutron-to-gamma signal ratio.

The counter balances and fission-chamber drive systems (within instrument thimbles) had to be completely reworked to provide ease of operation over pulleys.

Log N and period channels. Time constants have been modified in the log N and period channels to eliminate false alarms caused by neutron statistical noise and voltage transients from the line power. Voltage regulation for the log N period channels has been modified to decrease line power transients and reduce false period scrams.

The period and log N recorders have been modified to provide setback and alarm circuits. Log N and period amplifiers have been modified to adapt to the period recorders.

Neutron flux safety channels. Fission ionization chambers required modifications to adapt to the safety amplifiers. The safety amplifier required modifications to adapt to the Mark I and Mark II safety rods to provide one- and four-rod reactor scrams, and to provide a high impedance input for measuring currents of low magnitude during loading.

A separate power supply was fabricated to supply sufficient current for the Mark II safety-rod holding coils.

The neutron flux safety level recorder was modified to provide setback and alarm contacts.

Neutron flux control channel. The automatic neutron flux control system performs satisfactorily. Several modifications were required on the PAT flux controller and regulating rod feedback currents to provide proper gain, proportional band, rate, and reset action. A remote set-point adjustment for the automatic neutron flux controller will be installed on the control console.

Radiation monitoring instruments. Ionization chambers have not performed satisfactorily. Component failures have made the system inoperative several times. Electrometer tubes have failed, requiring replacement of the Neher-White chamber. The Jordan chambers in the radioactive vent system required modification to change the windows from gamma to beta detectors. The linear count-rate meter required modifications to adapt to the stack monitor and stack monitor recorder. The beta detector at the outlet of the decay holdup tanks was removed from the system. Additional gamma detectors will be installed in the high-bay area and control room.

7–4.8 Reactor control and safety system. *Safety rods.* Mechanical and electrical failures in the Mark I safety rod caused a delay in the SRE fuel-loading program. The latching mechanism failed several times, and galling between the safety rod and thimble required removing the safety rods for repairs. Tolerances in the limit switches were too small and caused failures in the control circuits and drive mechanisms.

Mark II safety rods. The Mark I safety rods were replaced with the Mark II safety rods, which have performed satisfactorily but required the following modifications:

Signal leads to the magnets were changed from solid wire to flexible stranded wire. Gaskets were changed on the flanges to prevent helium leaks. Counterbalance and pulley and chain were modified to eliminate false scrams.

Reactor safety and control circuits. The circuits have been modified to provide the following:

One-safety-rod reactor scram.
Four-safety-rod reactor scram.
Motorized control-rod setback.
Safety and control-rod interlocks.
Sodium pump interlocks.
Adaptation of the circuits for the Mark II safety rods.

Additional instrumentation circuits have been added to the annunciator alarm system.

7–4.9 Electrical distribution system. *Heaters.* Heaters on the piping and vessels have been changed extensively from the original design concept to provide a uniform distribution of heat during the preheating operation, and to supply required heat when the reactor is not operating. Additional heaters have been added to the valves, pumps, heat exchangers, piping, and tanks. Titon heaters have been replaced with tubular heaters on the sodium pumps.

In every sodium system the heaters have required recircuiting from series connections to parallel connections to provide uniform distribution of heat along the piping and across the tanks. A panel with 20 variacs was fabricated to control the reactor immersion heaters during the reactor core preheating program.

Many heaters have burned out or become defective because of hot spots and defective installations. The heaters will be repaired when it is feasible to remove the insulation on the piping. Spare heaters were included on the piping, so that significant delays have not resulted. Overload breakers to all the heater circuits were underrated and constantly tripped out during the preheating operation. Circuit breakers with a higher rating have been installed in several systems. Clamshell heaters on the plugging meter loops have been replaced by tubular heaters.

7–4.10 Main primary and secondary pump control. The sodium pump controls of the main primary and secondary systems, as originally delivered and installed, were found to be inadequate for the following reasons:

Excessive dead band.
Ramp rates not constant.
Possibility of excessive hunting, with resultant wear of mechanical regulating system.
No possibility for the detection of unsafe operating conditions.

It was decided to install an electronic speed-control system. In addition to these control circuits, an *off-normal* safety system has been developed which initiates alarm signals whenever flow or speed depart by more than 15 percent from the set values and also will scram the reactor whenever these parameters depart by more than 10 percent of the set values.

7–5. Chronological History of SRE Preoperational and Operational Testing

February 1, 1957 to April 1, 1957

Construction effort phased out as reactor neared completion.

February 20, 1957

Sodium melting was started and the sodium stored in the secondary and primary fill tanks. No difficulties were encountered. The melting time

was about 2 hours per barrel and the transfer of approximately 200 barrels of sodium was completed with loss of only 1 pint of sodium from one barrel. Sodium dropped into a vermiculite filled drip pan. There were no fires.

March 11, 1957

The antimony-beryllium neutron source was assembled and installed in the reactor.

March 12, 1957

The auxiliary secondary sodium loop was filled without incident.

March 22, 1957

Filled main secondary sodium system and started circulation without incident.

March 23, 1957

Dry ambient subcritical experiment (Phase II) was performed. Extrapolation of the inverse multiplication curve with 18 elements indicated criticality would be reached with 22+ elements.

April 19, 1957

Filled reactor and primary loops with sodium and started circulation without incident.

April 25, 1957

Criticality was achieved at 1219 with 33 fuel elements in the core, three control rods fully withdrawn, and the fourth at 62 inches. Criticality was maintained for 10 minutes. The count rate increased from 350 to 1000 counts/sec and held at 1000 for 2 minutes. Activity of sodium in the galleries increased to a maximum of 6 times background. The thirty-fourth fuel element was added to facilitate control-rod calibration.

April 29, 1957 to May 17, 1957

The shaft freeze-seal of the main primary pump was lost, causing partial filling of the pump casing with 600 pounds of sodium. The pump was cleaned and an extension was added to the lower case seal; heaters were installed in the upper portion of the housing to permit melting of sodium in event of another seal failure; a sodium leak detector was installed.

May 4, 1957 to May 10, 1957

Due to a hoisting failure, a fuel element was dropped into a wash cell. The wash cell and 4 fuel rods were damaged. Of 13 damaged fuel slugs, 12 were repairable.

May 25, 1957

The worth of Th-U fuel element was determined. Sodium flow characteristics were investigated.

June 8, 1957

Sodium systems were drained, and gallery shield blocks were set. The systems were refilled and cold trapped. Sodium valve operators were modified. Galleries were purged in preparation for the initial power test.

July 5, 1957

An isothermal test of the sodium system at 670°F was conducted, using electrical heaters.

Nuclear measurements demonstrated that the temperature coefficient of reactivity was positive, but decreased with increasing temperature throughout the range of measurements. In particular, the coefficient $d\rho/dt$, was 0.0033 at 400°F and 0.00017 at 670°F.

July 9, 1957

Preparations for the initial power generation run of the SRE-Edison complex started July 9, 1957, when the steam generator was filled with sodium. The reactor was operated at a thermal power of $2\frac{1}{4}$ Mw with a 50°F rise in sodium temperature (395°F inlet, 445°F outlet).

The reactor was scrammed July 11, 1957 to evaluate thermal transients. The reactor was then brought to a 60°F ΔT (outlet 510°F, inlet 450°F) and the Edison turbine was started. At 1247, July 12, 1957, the turbine generator was placed on the Southern California Edison grid. Power was increased to 6.7 Mw thermal, giving 1.7 Mw electrical, with a 150°F temperature rise across the reactor. The run was terminated July 15, 1957 with a planned scram. Reactor power, sodium flow, and temperature decay curves are shown in Fig. 7–11.

July 25, 1957

The second power test was conducted July 25 and 26, 1957. This run was at a lower power and of shorter duration than the initial test. This run was terminated with a planned scram from 130°F ΔT across the reactor.

Power production summary:

	July 14	*July 26*
Reactor inlet temperature, °F	481	475
Reactor outlet temperature, °F	631	605
Primary sodium flow, gpm	1000	780
Thermal power, Mw	6.5	4
Electrical power, Mw	1.7	1
Electrical energy for run, Mw-hours	59.8	18.4

August 5, 1957

Beginning the first week in August, sodium pump impellers were removed for rework. Rework consisted of enlarging and increasing the

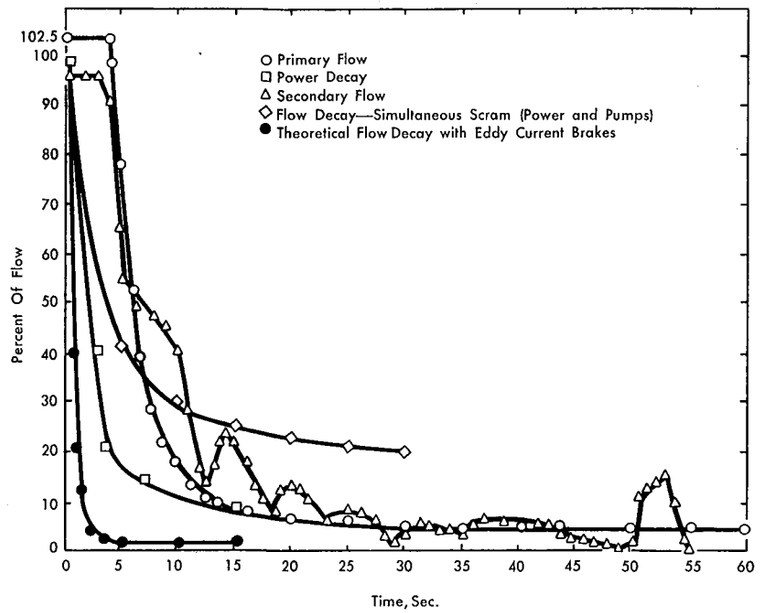

FIG. 7–11. Planned scram of SRE (July 15, 1957).

number of weep holes, as indicated by hydraulic tests. Additional thermocouples and tetralin freeze-seal circuits were also added.

August 7, 1957

A throttle valve in the auxiliary secondary sodium system was added.

August 30, 1957

Grid-plate leakage tests were conducted.

The 20-inch plug was removed for a moderator can inspection. Photographs of the tops of the moderator cans showed that none were out of place.

September 7, 1957

In order to improve temperature distribution in the reactor, orifice plates on the fuel elements were changed.

September 24, 1957

Three center-channel dummy elements were found to be stuck in the moderator cans and, at first, could not be removed with the fuel-handling cask. These dummy elements were raised until they supported the mod-

erator can weight. After a short hanging period, the moderator can slipped down and dummy elements were then free to be removed. The tips of the dummy elements were later modified to permit more sodium washing action, thus preventing oxide accumulation. This modification has proved successful.

September 25, 1957

It had been discovered during the orifice plate changing program that the fuel element in RH-57 had broken from its hanger rod. The fuel cluster had separated into its individual rod components and rods were removed individually under an argon atmosphere. The rods were later opened, and uranium slugs were counted, weighed, and identified as a check that all of the element was removed from the reactor.

October 7, 1957

The disposable cold trap became ineffective, due to oxide plugging, and was removed from the cold-trap vault. A new filter element was fabricated and the entire assembly reinstalled.

October 31, 1957

Completed loading to 33 fuel elements.

November 1, 1957

An attempt to obtain criticality was unsuccessful at the 33-element loading and an additional fuel element was loaded into the reactor core.

November 2, 1957

Criticality was obtained with a reactor loading of 34 fuel elements. The difference in critical loading from that obtained on April 22, 1957 was due to 7 core channels being filled with sodium rather than graphite dummy elements.

Completed loading reactor core to 37 fuel elements.

November 5, 1957

The reactor was made critical with a loading of 43 fuel elements.

November 6, 1957

A comparison check of all control rods, using 10 different configurations, was completed. In the time available only a one-point check was obtained for each configuration. With the configurations used, each control rod appeared to be of equal value. A calibration of No. 3 control rod was completed.

November 8, 1957

Activities were directed toward the SRE Dedication program for Thursday, 14 November 1957. The reactor was successfully operated and the Edison turbine generator was on line as outlined by the following comments:

November 9, 1957—At 0645 the sodium exit temperature was 560°F with 80°F ΔT across the steam generator. The turbine started at 0735 and went on the line at 0928 with 200-kw output. By 1200 there was 130°F ΔT; the reactor was on automatic control; thermal power 4 Mw; electrical output 0.7 Mw.

November 10, 1957—Small changes in pump speeds more nearly equalized main intermediate heat-exchanger temperatures and resulted in a higher steam temperature. The readings for the 24-hour period indicated 4.2 Mw thermal power and 0.8 Mw electrical output.

November 11, 1957—During day shift the ΔT was increased to 155°F; electrical output increased to 1.1 Mw. During second shift the ΔT was maintained at 150°F; thermal power 6.01 Mw; electrical output 1.5 Mw.

November 12, 1957—By 0700 electrical output was stable at 2 Mw; thermal power 7.0 Mw; reactor ΔT 170°F. This condition was maintained for the remainder of the 24-hour period.

November 13, 1957—Reactor and turbine operations for the 24-hour period continued as outlined for November 12, 1957.

November 14, 1957—Continued 2-Mw electrical output during the SRE Dedication program. Beginning second shift the thermal power was reduced to 4.5 Mw, electrical output approximately 0.8 Mw.

November 15, 1957—The reactor continued at 4.5 Mw thermal; electrical output 0.8 Mw; ΔT 130°F for the 24-hour period.

November 17, 1957

Fuel clusters in 11 different hot and cold channels were rotated 90, 180, 270, and 360 degrees and the fuel exit temperatures were measured in each channel. None of these temperatures changed more than 4°F, with the exception of channel No. 65. This channel was originally running hot and its exit temperature decreased 10.7°F after the 180-degree rotation of the fuel.

November 20, 1957

The reactor was shut down with a planned one-rod scram. Integrated power for this run was 1654.09 Mw-hours.

December 1, 1957

Wet critical was obtained on December 1, 1957, with approximately 33.5 fuel clusters at a sodium temperature of approximately 415°F. The SRE was again made critical on December 2, 1957, with approximately

33.2 fuel clusters at a sodium temperature of 360°F. This value is in good agreement with the value for wet critical obtained on April 25, 1957. The higher fuel requirement for criticality obtained on December 2 is primarily attributed to 6 fuel channels filled with sodium, rather than graphite dummy elements as was the case in the April and the November measurements.

December 15, 1957

Both primary cold traps and the disposable cold trap became ineffective.

January 7, 1958

Assembly of the first convective flow control eddy-current brake was begun.

January 10, 1958

Main primary gallery shield blocks were removed, to permit installation of the eddy-current brake.

January 14, 1958

Pile-oscillator mechanisms were completed and preliminary experiments in the reactor were undertaken. Danger coefficient measurements of the rotary oscillator mechanism showed the mechanism to be worth about 2 fuel rods. The peak-to-peak reactivity excursion was found to be about $1.9 \times 10^{-4}\ \Delta K$. Experiments to determine the zero-power transfer function of oscillation were performed with frequencies ranging from 1 to 0.001 cps. By use of another mechanism, the No. 1 control rod was oscillated in a sinusoidal manner at a frequency of 0.05 cps ($\frac{1}{2}$-inch peak-to-peak linear travel of the control rod). The purpose of this test was to obtain a control-rod calibration utilizing the pile-oscillator technique.

The first loop tests of the eddy-current brake were completed and preliminary results indicate performance characteristics better than had been expected.

January 17, 1958

The reactor was shut down in preparation for an extensive system modification program.

January 21, 1958

The main primary cold trap, which is not accessible during reactor operation, was removed from the system, as it had become ineffective.

February 4, 1958

The auxiliary primary cold trap and plugging meter were removed from the system. All cold trapping of primary sodium will be done in the disposable cold trap.

February 12, 1958

Installation of the eddy-current brake in the main primary gallery was

completed. Completion of the remaining mechanical operations (application of heaters, thermocouples, insulation, etc.) followed.

March 6, 1958

Fuel-channel coolant exit temperatures for the power runs in November were plotted. The flow per fuel channel was calculated and the power per fuel channel was determined. The power distribution thus obtained showed that the neutron flux distribution was now flatter than the initial distribution.

March 8, 1958

The moderator coolant flow control pump piping was completed; heaters, thermocouples, and leak detectors were installed and the discharge line was insulated. A flowmeter was located near the middle of the discharge line.

March 29, 1958

All modification work inside the main and auxiliary galleries was completed, including checkout of electrical and instrument circuits.

April 5, 1958

The secondary system was filled completely and sodium was circulated April 6, 1958. The secondary sodium cold trap was put into operation April 6, 1958. On April 9, 1958 the main secondary sodium plugging temperature was 220°F, with a bulk temperature of 310°F.

April 6, 1958

Preheating of the primary sodium system and core tank began. The sodium level probe coil was positioned in the core for the filling operation. The core and primary system filling was completed April 11, 1958.

April 10, 1958

Both eddy-current brakes were checked out at full current and appeared to be operating quite satisfactorily.

April 11, 1958

A brief investigation was made of the effect of various modes of operation of the two eddy-current brakes on main intermediate heat-exchanger tube-sheet stresses. It appears that a stress reversal can be induced with both pumps operating at full rpm and both brakes activated at 20 amperes. A more accurate and thorough study will be made in the near future.

April 12, 1958

Flow was established through the primary cold trap. Sodium throughput averaged 40 gpm with a constant ΔT of 20°F. Flow began to decrease

noticeably on second shift April 13, 1958. Cold trapping was discontinued on April 14. Total oxide in the system was more than sufficient for saturation of the cold trap at its operating temperature (375°F). The trap was removed and inspected. Inspection revealed a 2-inch thick plug of oxides in the mesh at the top of the center tube, with little oxide in the sodium annulus. The trap was cleaned and modified to give more filtration area in the center tube.

April 13, 1958

A liquid nitrogen system replaced the bottled-gas nitrogen supply previously used.

April 17, 1958

Tests of transients which occur during transfer of the vital power from normal sources to the battery and diesel units were completed. These tests proved to be satisfactory, since no transients were observed in the reactor instrumentation and control circuitry.

April 24, 1958

The reactor core was loaded with 34 fuel elements and safety and shim rod drives were installed and checked. The same configuration of core elements was maintained as in previous 34 fuel element loadings. Criticality was obtained at approximately 1725, April 24, 1958. A difference of less than 0.013 percent $\Delta k/k$ between this check and that of December 1, 1957, was observed.

April 28, 1958

The reactor was fully loaded with 43 fuel elements. Criticality was obtained. Control-rod calibrations completed April 30, 1958 indicated an excess reactivity of 3.67 percent $\Delta k/k$ at a sodium temperature of 357°F. Preliminary results from the control-rod calibration tests indicate a total worth of 7.83 percent $\Delta k/k$ for the 4 control rods. Shadowing effects were not considered. The worth of the control rods are established as:

Control rod No. 1, 2.11%; control rod No. 2, 1.83%; control rod No. 3, 2.15%; and control rod No. 4, 1.74%.

Sodium flow through the main primary cold trap began to diminish April 27. The cold trap was removed, inspected, cleaned, and reinstalled. Inspection of the removed filter indicated that the trap was operating satisfactorily. Cold trapping of the primary was resumed.

May 3, 1958

The reactor was operated to obtain relative reactivity measurements on a Th-U element.

A scram test was conducted at a 65°F ΔT, since Southern California Edison was limited by the 1120-gpm flow in the secondary system.

May 6, 1958

The gallery dehumidification system was put into operation. Approximately 10 gallons of condensate were collected in the first 2 hours.

May 7, 1958

Reactivity of a Th-U fuel cluster containing 7.6 percent uranium enriched to 93 percent U^{235} was measured relative to the standard fuel cluster in channel No. 45.

May 9, 1958

Scram tests from temperature gradients of 65°F and 150°F were performed to evaluate the performance of the eddy-current brakes installed in the main primary and main secondary systems. In both tests the reactor gradient was maintained following the scram. During these tests 33 channels of fast recording equipment recorded the variables of interest. Final results of these tests are awaiting completion of the data analyses.

May 10, 1958

The reactor was restarted and leveled off at 200 kw thermal. Plugging temperature in the main primary system was 330°F, with a bulk temperature of 355°F. The cold trap was valved off May 12 with a plugging temperature of 264°F and a bulk temperature of 405°F.

May 12, 1958

Beginning this date, reactor power and ΔT were increased for a planned 300°F ΔT scram. At steady-state, just prior to the planned scram, the reactor was 15.3 Mw thermal; 4.1 Mw electrical; ΔT 284°F. The reactor was scrammed at 2030, May 12, 1958. It was decided not to reach a 300°F ΔT because of unequal temperatures in some fuel channels.

May 13 to May 19, 1958

Orifice plates of 5 fuel elements were changed to correct unequal temperature distribution. The fuel elements were replaced in the reactor.

Auxiliary system sodium pumps were removed for inspection and repair. The auxiliary primary pump case contained a large amount of sodium (~10 pounds). Pumps were cleaned, repaired, and replaced by May 19, 1958.

The primary sodium plugging temperature on May 16 was 212°F, with a bulk temperature of 345°F.

May 21, 1958

Full reactor power (20 Mw thermal) was reached at 2130. Sustained full-power operation was commenced, interrupted only for examination of experimental fuels, reactor experiments, etc.